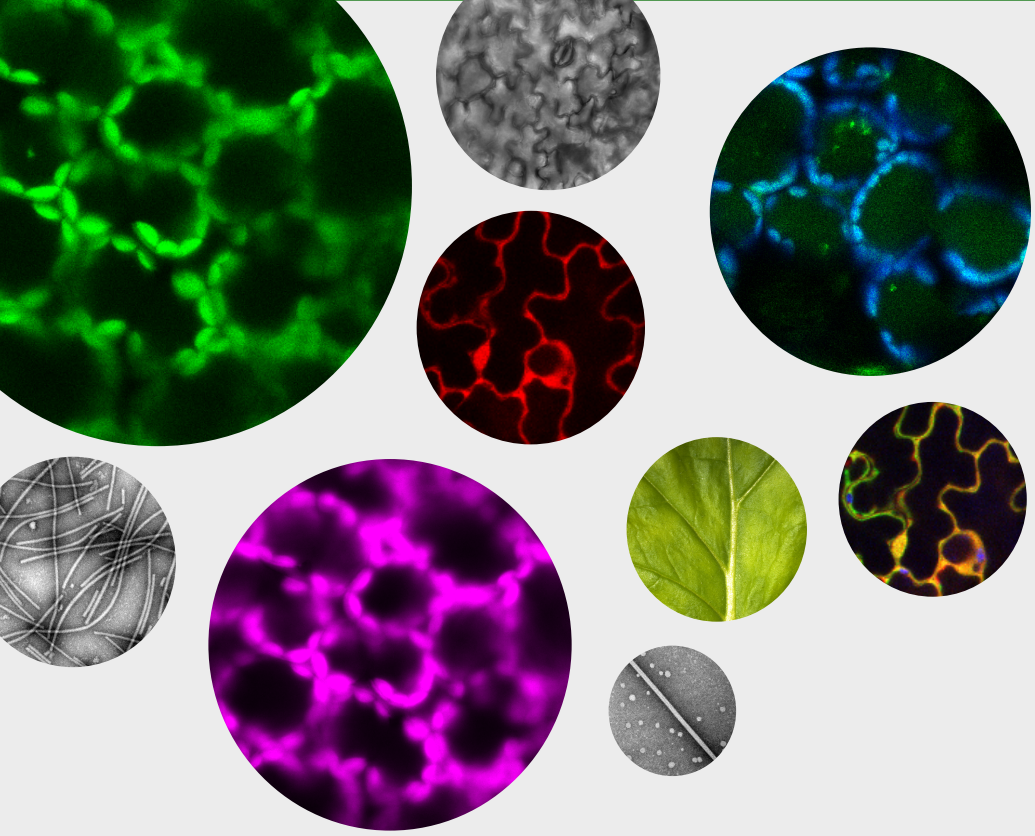

PLANT-BASED PRODUCTION OF METABOLITES AND NANOPARTICLES USING POTYVIRUS VECTORS

PhD Thesis

Mari Carmen Martí Botella

Supervisor: Dr. José Antonio Daròs

Valencia, June 2022

UNIVERSITAT POLITÈCNICA DE VALÈNCIA

PhD in Biotechnology

PLANT-BASED PRODUCTION OF METABOLITES AND NANOPARTICLES USING POTYVIRUS VECTORS

Mari Carmen Martí Botella

Supervisor: Dr. José Antonio Daròs Arnau

Valencia, June 2022

D. José Antonio Daròs Arnau, Doctor en Ciencias Biológicas por la Universitat de València y Profesor de Investigación del Consejo Superior de Investigaciones Científicas (CSIC) en el Instituto de Biología Molecular y Celular de Plantas (IBMCP), centro mixto del CSIC y Universitat Politècnica de València,

CERTIFICA:

Que Dña. Mari Carmen Martí Botella, Graduada en Biología por la Universidad de Alicante (UA), ha realizado bajo su dirección el trabajo con título "Plant-based production of metabolites and nanoparticles using potyvirus vectors" que presenta para optar al grado de Doctora en Biotecnología por la Universitat Politècnica de València.

Y para que así conste a los efectos oportunos, firma el presente certificado en Valencia a 13 de junio de 2022.

JOSE ANTONIO| DAROS|ARNAU

Firmado digitalmente por JOSE ANTONIO| DAROS|ARNAU
Fecha: 2022.06.13 09:29:06 +02'00'

D. José Antonio Daròs Arnau

“The most important thing is to never stop questioning. Curiosity has its own reason for existing”

Albert Einstein

"Nothing in life is to be feared, it is only to be understood. Now is the time to understand more, so that we may fear less”

Marie Curie

TABLE OF CONTENTS

SUMMARY

Modern plant biotechnology and molecular farming aim to convert plants into sustainable 'biofactories' to produce valuable compounds as proteins, metabolites or nanoparticles of pharmaceutical or industrial interest. Plant viruses, obligate intracellular parasites, constitute a major cause of plant diseases inducing devastating crop losses. Despite their minimal genomes, they have the ability to hijack the host cell machinery to produce high amounts of their own viral proteins. From this property arose the idea of repurposing plant viruses from foes to friends into tools for plant biotechnology as transient expression vectors and scaffolds for nanomaterials.

Carotenoids are relevant metabolites based on their nutritional and health-promoting properties. Animals cannot synthesize carotenoids and thus rely on their diets to supply them. The first goal of this work was to manipulate the carotenoid biosynthesis pathway to produce highly appreciated saffron apocarotenoids, the products of carotenoid cleavage. For this purpose, a vector derived from *Tobacco etch virus* (TEV; genus *Potyvirus*, family *Potyviridae*) was engineered to express specific carotenoid cleavage dioxygenase (CCD) enzymes from *Crocus sativus* and *Buddleja davidii*. Metabolic analyses of infected tissues demonstrated that, after only two weeks, remarkable amounts of crocins and picrocrocin in adult *Nicotiana benthamiana* plants were reached. The sole virus-driven expression of *C. sativus* CsCCD2L resulted in an accumulation of 0.2% of crocins and 0.8% of picrocrocin in leaf dry weight (DW). Co-expression of CsCCD2L with another carotenogenic enzyme, such as *Pantoea ananatis* phytoene synthase (PaCrtB), using the same viral vector increased crocin accumulation to 0.35%. Although these amounts are still far from those accumulating in natural sources, such as saffron stigma, this virus-driven system represents the first heterologous system able to produce crocins.

Phenolic compounds represent another broad group of plant secondary metabolites that are highly appreciated for their the health promoting and chemical properties. Curcuminoids are polyphenols with high antioxidant activity that are naturally found in turmeric (*Curcuma longa*) rhizome. The second goal of this work was to establish a system for the heterologous production of curcuminoids in *N.*

benthamiana using viral vectors. To this aim, a double-virus vector system, based on TEV and *Potato virus X* (PVX; genus *Potexvirus*, family *Alphaflexiviridae*), able to co-express different biosynthetic enzymes in the same cells was developed. This system was used to express *C. longa* diketide-CoA synthase 1 (DCS1) and curcumin synthase 3 (CURS3) in *N. benthamiana* plants. Metabolic analysis confirmed the successful production of curcuminoids. Curcumin quantification indicated that sequential inoculation of both viral vectors was more efficient than co-inoculation (6.5 ± 0.6 versus 1.9 ± 0.3 µg/g dry weight, DW, respectively). Co-expression of DCS1 and CURS3 was next analysed using a single viral vector derived from TEV (TEVΔN-DCS1-CURS3). This resulted in a more efficient approach as it led to a 2-fold increase in curcumin accumulation (11.7 ± 1.5 µg/g DW). A time-course analysis using the TEVΔN-DCS1-CURS3 vector showed that a maximum accumulation of 22 ± 4 µg/g DW was achieved at 11 days post-inoculation.

Viral nanoparticles (VNPs) have also attracted attention in biotechnology for their potential use as building blocks for novel materials in nanotechnology and medicine. Nanobodies are the variable domains of heavy-chain (VHH) camelid antibodies that have sparked interest as therapeutic molecules due to their simple structure, small size and high specificity. The last goal of this work was to produce genetically encoded VNPs decorated with a nanobody. *Zucchini yellow mosaic virus* (ZYMV; genus *Potyvirus*, family *Potyviridae*) and TEV were used as scaffolds to produce VNPs decorated with a nanobody against the green fluorescent protein in zucchini (*Cucurbita pepo*) and *N. benthamiana* plants, respectively. Inclusion of a picornavirus 2A splicing peptide between the fused proteins was necessary in ZYMV-derived VNPs, resulting in a mixed population of unmodified and decorated coat proteins, but not in those derived from TEV. Assembly and binding functionality of both VNPs against GFP was confirmed.

Altogether, the work presented in this thesis contribute to the concept that plant viruses, conveniently manipulated, can turn into powerful tools in plant biotechnology and molecular farming.

RESUMEN

La biotecnología de plantas actual y la así llamada agricultura molecular aspiran a convertir las plantas en “biofábricas” sostenibles para producir compuestos de valor como proteínas, metabolitos o nanopartículas de interés farmacéutico o industrial. Los virus de plantas, parásitos intracelulares obligados, constituyen una de las principales causas de enfermedades vegetales induciendo pérdidas devastadoras en los cultivos. A pesar de sus genomas mínimos, tienen la capacidad de secuestrar la maquinaria celular del huésped para producir cantidades elevadas de sus propias proteínas virales. Esta propiedad dio lugar a que surgiera la idea de reconvertir los virus de plantas de enemigos a amigos en herramientas para la biotecnología de plantas como vectores de expresión transitoria y andamios para nanomateriales.

Los carotenoides son metabolitos relevantes debido a sus propiedades nutricionales y beneficiosas para la salud. Los animales no pueden sintetizar carotenoides y, por lo tanto, dependen de su ingesta a través de la dieta para obtenerlos. El primer objetivo de este trabajo fue manipular la ruta de biosíntesis de carotenoides para producir los muy apreciados apocarotenoides de azafrán, siendo estos los productos de la escisión de carotenoides. Para este propósito, se diseñó un vector derivado del virus del grabado del tabaco (TEV; género *Potyvirus*, familia *Potyviridae*) manipulado para expresar unas enzimas específicas, dioxigenasas de escisión de carotenoides (CCD) de *Crocus sativus* y *Buddleja davidii*. Los análisis metabólicos de los tejidos infectados demostraron que, después de sólo dos semanas, se alcanzaron cantidades notables de crocinas y picrocrocina en plantas adultas de *Nicotiana benthamiana*. Solamente la expresión de CsCCD2L de *C. sativus* impulsada por virus dio como resultado una acumulación en hoja de 0.2% de crocinas y 0.8% de picrocrocina en peso seco. La coexpresión de CsCCD2L con otra enzima carotenogénica, como la fitoeno sintasa de *Pantoea ananatis* (PaCrtB), usando el mismo vector viral aumentó la acumulación de crocinas al 0.35%. Aunque estas cantidades todavía están lejos de las que se acumulan en fuentes naturales, como el estigma del azafrán, este sistema mediado por virus representa el primer sistema heterólogo capaz de producir crocinas.

Los compuestos fenólicos representan otro amplio grupo de metabolitos secundarios en plantas, muy apreciados también por sus propiedades químicas y promotoras de la salud. Los curcuminoides son polifenoles con alta actividad antioxidante que se encuentran naturalmente en el rizoma de la cúrcuma (*Curcuma longa*). El segundo objetivo de este trabajo fue establecer un sistema para la producción heteróloga de curcuminoides en *N. benthamiana* utilizando vectores virales. Para ello, se desarrolló un sistema viral doble, basado en TEV y en el virus X de la patata (PVX; género *Potexvirus*, familia *Alphaflexiviridae*), capaz de coexpresar diferentes enzimas biosintéticas en las mismas células. Este sistema se usó para expresar la dicétido-CoA sintasa 1 (DCS1) y la curcumina sintasa 3 (CURS3) de *C. longa* en plantas de *N. benthamiana*. El análisis metabólico confirmó la producción exitosa de curcuminoides. La cuantificación de curcumina indicó que la inoculación secuencial de ambos vectores virales era más eficiente que la coinoculación (6.5 ± 0.6 frente a 1.9 ± 0.3 µg/g de peso seco, respectivamente). Posteriormente se analizó la coexpresión de DCS1 y CURS3 usando un solo vector viral derivado de TEV (TEVΔN-DCS1-CURS3). Esto dio como resultado una producción más eficiente, ya que condujo a un aumento del doble en la acumulación de curcumina (11.7 ± 1.5 µg/g peso seco). Un análisis temporal utilizando el vector TEVΔN-DCS1-CURS3 mostró que se lograba una acumulación máxima de 22 ± 4 µg/g peso seco a los 11 días tras la inoculación.

Las nanopartículas virales (VNP) también han atraído la atención en biotecnología por su uso potencial como componentes básicos para nuevos materiales en nanotecnología y medicina. Los nanoanticuerpos son los dominios variables de los anticuerpos de camélidos de sólo cadena pesada (VHH) que han ganado interés como moléculas terapéuticas debido a su estructura simple, tamaño pequeño y alta especificidad. El último objetivo de este trabajo fue producir VNPs decoradas con un nanoanticuerpo codificadas genéticamente. El virus del mosaico amarillo del calabacín (ZYMV; género *Potyvirus*, familia *Potyviridae*) y TEV se utilizaron como andamios para producir VNPs decoradas con un nanoanticuerpo contra la proteína verde fluorescente en plantas de calabacín (*Cucurbita pepo*) y *N. benthamiana*, respectivamente. La inclusión de un péptido de procesamiento 2A de picornavirus entre las proteínas fusionadas fue necesaria en las VNP derivadas de ZYMV, lo que resultó en una población de proteínas de cubierta mixta no modificadas y decoradas, pero no en las

derivadas de TEV. Se confirmó funcionalmente el ensamblaje y unión de ambas VNPs contra GFP.

En conjunto, el trabajo presentado en esta tesis contribuye al concepto de que los virus de plantas, convenientemente manipulados, pueden convertirse en poderosas herramientas en biotecnología vegetal y agricultura molecular.

RESUM

La biotecnologia de plantes actual i la anomenada agricultura molecular aspiren a convertir les plantes en "biofàbriques" sostenibles per a produir compostos de valor com a proteïnes, metabòlits o nanopartícules d'interès farmacèutic o industrial. Els virus de plantes, paràsits intracel·lulars obligats, constitueixen una de les principals causes de malalties vegetals induint pèrdues devastadores en els cultius. Malgrat els seus genomes mínims, tenen la capacitat de segrestar la maquinària cel·lular de l'hoste per a produir quantitats elevades de les seues pròpies proteïnes virals. Aquesta propietat va donar lloc al fet que sorgira la idea de reconvertir els virus de plantes d'enemics a amics en eines per la biotecnologia de plantes com a vectors d'expressió transitòria i bastides per a nanomaterials.

Els carotenoides són metabòlits rellevants a causa de les seues propietats nutricionals i beneficioses per a la salut. Els animals no poden sintetitzar carotenoides i, per tant, depenen de la seua ingesta a través de la dieta per a obtindre'ls. El primer objectiu d'aquest treball va ser manipular la ruta de biosíntesi de carotenoides per a produir els valuosos apocarotenoides de safrà, sent aquests els productes de l'escissió de carotenoides. Per a aquest propòsit, es va dissenyar un vector derivat del virus del gravat del tabac (TEV; gènere *Potyvirus*, família *Potyviridae*) manipulat per a expressar uns enzims específics, dioxigenases d'escissió de carotenoides (CCD) de *Crocus sativus* i *Buddleja davidii*. Les anàlisis metabòliques dels teixits infectats van demostrar que, després de només dues setmanes, es van aconseguir quantitats notables de crocines i picrocrocina en plantes adultes de *Nicotiana benthamiana*. Solament l'expressió de CsCCD2L de *C. sativus* mediada per virus va donar com a resultat una

acumulació en fulla de 0.2% de crocines i 0.8% de picrocrocina en pes sec. La coexpressió de CsCCD2L amb un altre enzim carotenogènic, com la fitoé sintasa de *Pantoea ananatis* (PaCrtB), usant el mateix vector viral va augmentar l'acumulació de crocines al 0.35%. Encara que aquestes quantitats estan lluny de les que s'acumulen en fonts naturals, com l'estigma del safrà, aquest sistema mediat per virus representa el primer sistema heteròleg capaç de produir crocines.

Els compostos fenòlics representen un altre ampli grup de metabòlits secundaris en plantes, molt valuosos també per les seues propietats químiques i promotores de la salut. Els curcuminoides són polifenols amb alta activitat antioxidant que es troben naturalment en el rizoma de la cúrcuma (*Curcuma longa*). El segon objectiu d'aquest treball va ser establir un sistema per a la producció heteròloga de curcuminoides en *N. benthamiana* utilitzant vectors virals. Per a això, es va desenvolupar un sistema viral doble, basat en TEV i en el virus X de la creïlla (PVX; gènere *Potexvirus*, família *Alphaflexiviridae*), capaç de coexpressar diferents enzims biosintètics en les mateixes cèl·lules. Aquest sistema es va usar per a expressar la dicétid-CoA sintasa 1 (DCS1) i la curcumina sintasa 3 (CURS3) de *C. longa* en plantes de *N. benthamiana*. L'anàlisi metabòlica va confirmar la producció reeixida de curcuminoides. La quantificació de curcumina va indicar que la inoculació seqüencial de tots dos vectors virals va ser més eficient que la coinoculació (6.5 ± 0.6 enfront de 1.9 ± 0.3 µg/g de pes sec, respectivament). Posteriorment es va analitzar la coexpresió de DCS1 i CURS3 usant un sol vector viral derivat de TEV (TEVΔN-DCS1-CURS3). Això va donar com a resultat un enfocament més eficient, ja que va conduir a un augment del doble en l'acumulació de curcumina (11.7 ± 1.5 µg/g pes sec). Una anàlisi al llarg del temps utilitzant el vector TEVΔN-DCS1-CURS3 va mostrar que s'aconseguia una acumulació màxima de 22 ± 4 µg/g pes sec als 11 dies després de la inoculació.

Les nanopartícules virals (VNP) també han atret l'atenció en biotecnologia pel seu ús potencial com a components bàsics per a nous materials en nanotecnologia i medicina. Els nanoanticossos són els dominis variables dels anticossos de camèlids de només cadena pesada (VHH) que han guanyat interès com a molècules terapèutiques a causa de la seua estructura simple, grandària xicoteta i alta especificitat. L'últim objectiu d'aquest treball va ser produir VNPs decorades amb un nanoanticos codificades genèticament. El virus del mosaic groc de la carabasseta

(ZYMV; gènere *Potyvirus*, família *Potyviridae*) i TEV es van utilitzar com a bastides per a produir VNPs decorades amb un nanocos contra la proteïna verda fluorescent en plantes de carabasseta (*Cucurbita pepo*) i *N. benthamiana*, respectivament. La inclusió d'un pèptid d'entroncament 2A de picornavirus entre les proteïnes fusionades va ser necessària en les VNP derivades de ZYMV, la qual cosa va resultar en una població de proteïnes de coberta mixta de no modificades i decorades, però no en les derivades de TEV. Es va confirmar la funcionalitat d'assemblatge i unió de totes dues VNPs contra GFP.

En conjunt, el treball presentat en aquesta tesi contribueix al concepte que els virus de plantes, convenientment manipulats, poden convertir-se en poderoses eines en biotecnologia vegetal i agricultura molecular.

ABBREVIATIONS

Ab, antibody

bp, base pair

CaMV, cauliflower mosaic virus

CCD, carotenoid cleavage dioxygenase

CCoAOMT-1, caffeoyl-coenzyme A (CoA)/5-hydroxyferuloyl-CoA 3/5-O methyltransferase

cDNA, complementary DNA

CHO, Chinese hamster ovary cells

COVID-19, coronavirus disease 2019

CMV, cucumber mosaic virus

CP, coat protein

CPMV, cowpea mosaic virus

CRISPR, clustered regularly interspaced short palindromic repeats

crtB, *Pantonea ananatis* phytoene synthase

crtE, geranylgeranyl diphosphate synthase

crtI, phytoene desaturase

crtY, lycopene β-cyclase

CURS3, curcumin synthase 3

DCS1, diketide-CoA synthase 1

DNA, desoxyribonucleic acid

dpi, days post-inoculation

DW, dry weight

eGFP, enhanced green fluorescent protein

GFP, green fluorescent protein

GOI, gene of interest

GMO, genetically modified organism

GMP, good manufacturing practice

HCAbs, heavy-chain antibodies

HIV, human immunodeficiency virus

HPLC-DAD-HRMS, high performance liquid chromatography-diode array detector-high resolution mass spectrometry

ICTV, International Committee on Taxonomy of Viruses

Ig, immunoglobulin

LSCM, laser scanning confocal microscopy

mAb, monoclonal antibody

MP, movement protein

NIaPro, nuclear inclusion a protease

NIb, nuclear inclusion b

nt, nucleotide

ORF, open reading frame

PCR, polymerase chain reaction

PDS, phytoene desaturase

PPV, plum pox virus

PSY, phytoene synthase

PVX, potato virus X

PVY, potato virus Y

RNA, ribonucleic acid

ROS, reactive oxygen species

RT-PCR, reverse transcription-polymerase chain reaction

SARS-CoV-2, severe acute respiratory syndrome coronavirus 2

SDS-PAGE, sodium dodecyl sulfate-polyacrylamide gel electrophoresis

ssRNA, single stranded RNA

ssRNA-, single stranded negative-sense RNA

ssRNA+, single stranded positive-sense RNA

T-DNA, transferred DNA

TEM, transmission electron microscope

TEV, tobacco etch virus

TEVΔN, NIb deleted TEV

TGB, triple gene block

TMV, tobacco mosaic virus

TuMV, turnip mosaic virus

UGT, uridine diphosphate (UDP)-glucosyltransferase

UTR, untranslated region

VHH, variable antigen-binding domain

VIGE, virus-induced genome editing

VNP, virus nanoparticle

VLP, virus-like particle

VPg, viral protein genome-linked

wt, wild-type

ZEP, zeaxanthin epoxydase

ZYMV, zucchini yellow mosaic virus

INTRODUCTION

MOLECULAR FARMING

Plants are crucial in almost all ecosystems, making up around 80% of all biomass on Earth, providing humans and other animals food, oxygen and shelter. In addition, plants play key roles as feedstock, building materials, clothing, fuel, and as source of bioactive compounds for medicinal use (Jose et al., 2019). As a result of the modern plant biotechnology and genetic engineering, a great variety of techniques have been used to develop crop plants with desired traits by introducing foreign genes or silencing the expression of others endogenous to the plants. The focus was mainly on (1) agronomic traits to obtain resistance to herbicides, abiotic (salt, cold and drought) or biotic (insects, fungi, bacteria, viruses) stresses, improving yield, nutritional quality or nutrient use efficiency; (2) bioenergy; and (3) molecular farming, the production of valuable proteins or novel metabolites of pharmaceutical or industrial interest (Jose et al., 2019; Kumar et al., 2020; Majer et al., 2017; Mohammadinejad et al., 2019; Xu et al., 2012).

For the last 30 years, plants have been used as heterologous expression platforms or 'biofactories' for the synthesis of valuable compounds (Tschofen et al., 2016). This approach relatively recent is known as plant molecular farming (Mohammadinejad et al., 2019). The target compound (e.g. recombinant proteins or metabolites) is either extracted and purified or used as part of a crude extract, whereas the plant is merely a host (Ma et al., 2003; Sack et al., 2015; Tschofen et al., 2016), which is either discarded at the end of the process or can be further used as a separate side-product for other purposes (Buyel, 2019). Since the first pioneering studies (Ma et al., 2003), plant molecular farming have gained support and interest within the scientific community exploring the heterologous production of different molecules in improved and diverse host systems (Fischer et al., 2012; Molina-Hidalgo et al., 2021; Sainsbury, 2020; Tschofen et al., 2016). So far, the industry is concentrated on well-established manufacturing platforms based on bacteria (*Escherichia coli*) yeast (*Pichia pastoris*), insect and mammalian cell cultures as the Chinese hamster ovary (CHO) cell lines (Fischer and Buyel, 2020; Shanmugaraj et al., 2020). Plant-based systems represent exceptional renewable sources for the sustainable production of valuable compounds, with many well documented advantages, emerging as an attractive

alternative over conventional expression platforms (Table 1) (Shanmugaraj et al., 2020; Xu et al., 2012).

Table 1. Comparison of heterologous biofactory systems used for the production of recombinant proteins and metabolites. Adapted from Shanmugaraj et al. (2020), Ma et al. (2003), and Fisher and Buyel (2020).

Expression System	Advantages	Disadvantages
Bacteria	Easy to manipulate Low cost High expression Quick Ease to scale-up Established regulatory procedures and approval	Improper folding Lack of post-transcriptional modifications Contamination risks (endotoxin accumulation) Low product quality
Yeast	Rapid growth and scalable Easy to manipulate Medium cost Ease to scale-up Simple and inexpensive media requirements and culture conditions Post-translational modifications Low contamination risk	Difficulty in cell disruption due to complex cell walls Limited glycosylation capacity Hyperglycosylation of proteins
Mammalian Cells	Proper folding and authentic post-translational modifications Very high product quality Existing regulatory approval	High production cost Expensive media and culture condition Long production timescale Very low scale-up capacity High contamination risks (viruses, prions and oncogenic DNA)
Insect Cells	High expression levels Ability to produce complex proteins Proper folding and post-translational modifications	High cost and time-consuming Expensive media and culture conditions
Plants	Optimized growth conditions Very low cost Rapid (for transient expression) Very high scalability Free of pathogens and bacterial toxins High product quality Post-translational modifications similar to mammalian cells	Regulatory compliance Limited glycosylation capacity Long production timescale (only for transgenic plants)
Plant-cell Suspensions	Medium production timescale Low contamination risk High product quality	Medium cost (in between mammalian cells and transformed plants) Low scale-up capacity

First, it faces lower costs and ease of cultivation. Plants possess exceptional biosynthetic capacity and require only simple media and sunlight to produce large amount of biomass. Moreover, certain plants such as tobacco (*Nicotiana tabacum* and *N. benthamiana),* considered as a molecular biology workhorse of the plant world, can

be grown in high density in a matter of weeks (Fischer and Buyel, 2020; Peyret and Lomonossoff, 2015) even as hydroponics or vertical farming (Diego-Martin et al., 2020; Fischer and Buyel, 2020). Second, the technology is scalable for harvesting and processing plants on a large scale. Third, plants have lower contamination risks with animal pathogens or toxins. Fourth, plants can implement eukaryotic post-translational modifications, required for the recombinant protein functional activity (Fischer and Buyel, 2020; Mohammadinejad et al., 2019; Peyret and Lomonossoff, 2015; Sack et al., 2015; Shanmugaraj et al., 2020). Fifth, plant-made products can be targeted to a particular tissue or cellular compartment in which they are more stable (Tschofen et al., 2016). Sixth, when the plant tissue is used directly as food (e.g., edible vaccines), purification requirements can be ignored, thus reducing most of the costs (Daniell et al., 2001), which is an important advantage in developing countries (Sack et al., 2015). Rapid advancements in plant molecular farming in the recent decade have alleviated their initial drawbacks regarding low yields and downstream processing, making possible that plants are now more attractive manufacturing systems. Nevertheless, as conventional expression systems are well characterized and established in an industrial setting, plant molecular farming adoption by industry is still hindered (Buyel, 2019; Shanmugaraj et al., 2020). This is mainly due to the most challenging and economical critical step, isolation and purification in downstream processing of the target product, reaching up to 80% of the total process costs (Fischer et al., 2012; Fischer and Buyel, 2020).

The expression modalities used for the production of heterologous compound in plants can be stable (either nuclear or plastid) or transient (Shanmugaraj et al., 2020) (Figure 1). The soil gram-negative phytopathogen bacteria *Agrobacterium tumefaciens* naturally infects wounds in plants, causing crown gall disease with tumour formation on roots. A major breakthrough was the use of engineered *A. tumefaciens* as an unprecedented tool for plant genetic transformation (Figure 2) (Chilton et al., 1977). Plant stable transformation is the traditional strategy of genetic manipulation and considered initially in plant molecular farming and plant metabolic engineering approaches. It involves the stably introduction of a transgene into the plant genome obtaining lines of genetically transformed plants. This is a time-consuming and resource-intensive process (Shanmugaraj et al., 2020). Furthermore, the full

implementation of transgenic plants is constrained due to the negative public perception and the potential risk of gene escape.

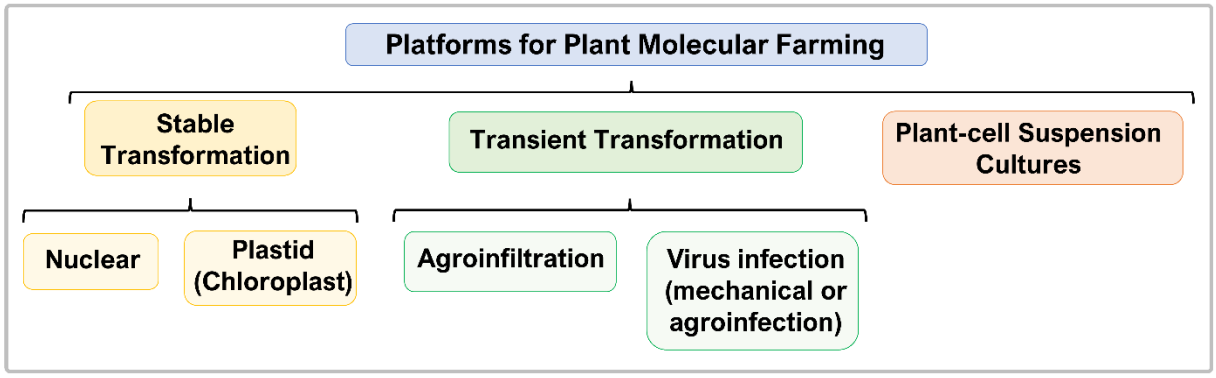

Figure 1. Plant transformation approaches employed in plant molecular farming to produce heterologous compounds of interest. Adapted from Shanmugaraj et al. (2020) and Mohammadinejad et al. (2019).

In contrast to stable transformation, transient expression in plants appear as a solution to obtain the product in just a matter of days, reducing dramatically the time-line in plant molecular farming (Fischer and Buyel, 2020; Majer et al., 2017; Peyret and Lomonossoff, 2015). Transient expression systems do not involve transgenic plants as the target gene is expressed for only a few days before the plant colapses or the construct is cleared. This strategy is ideal to rapidly screen different constructs for stable transformation, as well as for situations where a rapid response is needed such as emerging pandemic diseases (Mohammadinejad et al., 2019). Transient expression can be achieved through (1) infiltration with *A. tumefaciens* carrying a recombinant Ti plasmid (agroinfiltration); (2) mechanical inoculation with recombinant viral vectors; or (3) agroinfiltration with Ti plasmids carrying viral vectors (agroinfection) (Gleba et al., 2004; Mohammadinejad et al., 2019; Molina-Hidalgo et al., 2021; Peyret and Lomonossoff, 2015).

Products from plants range from antibodies, vaccines, therapeutic proteins, enzymes, growth factors, research or diagnosis reagents to cosmetic ingredients (Fischer and Buyel, 2020) or biomaterials (Mohammadinejad et al., 2019). To reach the market, non-pharma products have an easier route due a regulatory burden to meet the strict criteria enforced for the current good manufacturing practice (GMP) conditions, as well as lower costs in terms of downstream processing (Capell et al., 2020; Fischer and Buyel, 2020; Tschofen et al., 2016). Veterinary pharmaceuticals have

gained much attention (Topp et al., 2016) and have a lower regulatory burden compared to those for human use (Mohammadinejad et al., 2019; Shanmugaraj et al., 2020). Although the majority of the approved recombinant biopharmaceuticals are produced in mammalian cell lines (Shanmugaraj et al., 2020), those from plant platforms gradually make their way into the market. In this sense the first pharmaceutical plant-based product was released in 2012, 'Elelyso' by Protalix Biotherapeutics for the treatment of Gaucher disease (Capell et al., 2020; Margolin et al., 2020; Shanmugaraj et al., 2020; Tschofen et al., 2016). Since then, numerous plant-produced human therapeutic proteins are being currently tested in clinical trials and close to commercialization (Tsekoa et al., 2020).

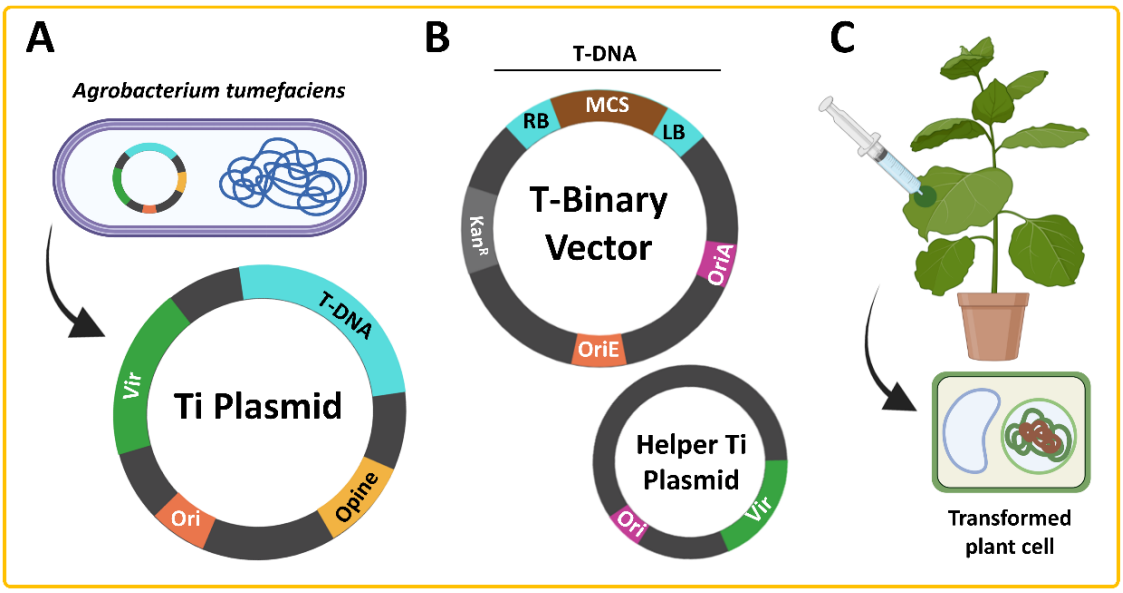

Figure 2. Plant transformation by means of *Agrobacterium tumefaciens*. **(A)** Wild type *A. tumefaciens* harbours a tumour-inducing (Ti) plasmid that contains two elements: (1) the transfer-DNA (T-DNA), a virulent DNA molecule delivered from these bacteria into the host plant genome, and (2) the virulence (vir) region. **(B)** Adaptation of *A. tumefaciens* as a tool for plant genetic transformation. The Ti plasmid was mutated, where the tumour-controlling genes in the T-DNA from the Ti-plasmid were replaced by a multiple cloning site (MCS) for the insertion of heterologous sequences. This 'disarmed' plasmid was known as a 'binary vector', containing also a selectable marker (such as a kanamycin resistance gene), and replication origin in *E. coli* and *A. tumefaciens* (OriE and OriA, respectively). Right and left borders from the T-DNA are also indicated (RB and LB). The *vir* genes were placed on one plasmid which could act as genetic background, the so called ''helper Ti-plasmid'. **(C)** Agroinfiltration consists in the massive delivery of an *A. tumefaciens* suspension culture to the intercellular space of plant leaves, either by negative pressure using a needle-less syringe or applying vacuum.

Much effort is being done to boost plant molecular farming, as with two major H2020 projects, Pharma-Factory and Newcotiana, using a non-food crop as tobacco as a preferred species (Capell et al., 2020; Molina-Hidalgo et al., 2021; Shanmugaraj et al., 2020). In fact, several companies are already specialized in the development of plant-derived proteins as diagnostic reagents, namely Agrenvec (Spain), Diamante (Italy), ORF Genetics (Iceland) or Ventria Bioscience/Invitria (USA). As for pharmaceuticals, Medicago (Quebec, Canada) stands out for the production of virus-like particles (VLPs) as vaccine candidates for the seasonal influenza H1N1 in phase III clinical trials (Fischer and Buyel, 2020). VLPs are self-assembled structures from native viruses that mimic their morphology but are unable to replicate as they lack the infectious viral genome (Marsian and Lomonossoff, 2016). From the identification of the circulating influenza pandemic strain to the obtention of the vaccine, it takes only three weeks, that is a 4-8 fold reduction of the time over the traditional egg-based method (Sainsbury, 2020).

Globalization and climate change urges a technology which allows quick responses to emerging pathogens in epidemic or pandemic threats with vaccines candidates or diagnostic reagents (Capell et al., 2020; Sainsbury, 2020). Plant molecular farming offers a rapid, scalable and flexible production in plants with transient expression to address these challenges. This was proven during the Ebola outbreak in 2014 with the production of an experimental drug ZMapp, an antibody cocktail to treat humans made in tobacco plants. Other studies have focused on diseases which pose a major public health threat in low- and middle-income countries, where local production is needed, with a vaccine candidate against West Nile virus (WNV), associated with encephalitis outbreaks in humans and horses (Stander et al., 2021).

More recently, the current human pandemic of coronavirus disease 2019 (COVID-19), caused by a novel coronavirus known as severe acute respiratory syndrome coronavirus 2 (SARS-CoV-2), has forced governments to introduce emergency containment measures to slow down the spread of the disease. This outbreak has revealed the strengths and the weaknesses of the world capacity to respond to a global health crisis. In this sense it has been become evident a dramatic shortage in the diagnostic reagents for the COVID-19 control (SARS-CoV-2 RNA,

proteins, antibodies, vaccines and antiviral drugs) and the means to produce them (Capell et al., 2020). On the positive side, scientific data and information have been shared at an unprecedented speed fuelled by the preprint phenomena, and this has considerably strengthened our ability to develop new technology-based solutions (Diego-Martin et al., 2020). Among the scientific community, plant molecular farming researchers have addressed their knowledge on transient expression for the easy, rapid and scalable obtention of scarce products to fight against COVID-19 (Capell et al., 2020). In detail, several studies have proved how plants can be excellent platforms or biofactories for the local manufacturing of reagents. For example, in a matter of weeks and in a framework of an academic laboratory, different recombinant monoclonal antibodies against SARS-CoV-2, as well as the recombinant nucleoprotein (N) and the receptor binding domain (RBD) of the SARS-CoV-2 spike (S) protein were produced in *N. benthamiana* (Diego-Martin et al., 2020). Medicago, along with other enterprises as Kentucky BioProcessing (USA) and iBio (USA) joined the global race for developing potential plant-based vaccines for COVID-19 (Shanmugaraj et al., 2020).

Despite not supplanting the current manufacturing systems, plant-based products are expected to experience a dramatic growth in the near future (Mohammadinejad et al., 2019), as they are rapidly emerging into the marketplace and have been demonstrated to be effective, safe and inexpensive (Hefferon, 2017; Tsekoa et al., 2020). In particular, the conversion of non-food crops as *Nicotiana* genus into efficient and improved biofactories is expected to be a strong asset in the development of a sustainable bioeconomy (Mohammadinejad et al., 2019; Molina-Hidalgo et al., 2021). In order to make affordable, it has been proposed the development of widespread infrastructures which would serve regular production needs in normal times but could be rapidly re-purposed to strategic manufacturing in times of crisis (Diego-Martin et al., 2020). The technology of plant-based transient expression has demonstrated that is able to meet requirements for both human and animal health (Sainsbury, 2020).

METABOLIC ENGINEERING

Plants play a key role in relation to our health through our diets, providing necessary macronutrients for energy and growth as well as essential vitamins, minerals, fibre and phytonutrients. A massive variety of secondary metabolites (more than 200,000) are produced by plants, essential for survival, reproduction and defence (Mohammadinejad et al., 2019). Many of them are valuable antioxidants, generated to counter oxidative stress from reactive oxygen species (ROS) formation (Nowicka et al., 2021). For centuries plants have been used to prevent and cure diseases (Ma et al., 2003), based on the presence of these bioactive compounds (de Araújo et al., 2021). In recent years, there is increasing evidence that the consumption of fresh fruit and vegetables reduces the risk of developing major chronic diseases, such as obesity and type-2 diabetes and certain types of cancer (Martin and Li, 2017).

There is an increasing demand for natural compounds as colourants, dyes, cosmetics (Zia-ul-haq, 2021), as well as therapeutics (Arya et al., 2020). These are considered more stable, less toxic, having fewer side effects and cheaper than their synthetic counterparts, which are produced from toxic reagents and expensive machinery (Arya et al., 2020; Ashrafizadeh et al., 2020; Chouhan et al., 2017; Islam et al., 2021). A better understanding of plant biosynthetic pathways is leaning the industry towards their isolation and heterologous production (Mohammadinejad et al., 2019; Prasad et al., 2014; Rodrigues et al., 2015). Metabolic engineering can be defined as the use of genetic engineering to modify the metabolism of an organism in order to increase the production of valuable chemicals for health, food, energy, materials and others. It can involve the optimization of existing biosynthetic pathways or the introduction new components to them, mostly performed on bacteria, yeast or plants (Otero-Muras and Carbonell, 2021). In this sense, the improvement of the nutritional value of crops is a global challenge. Biofortification or enhanced concentrations of phytonutrients and vitamins can be addressed through conventional breeding (Zheng et al., 2021; Zhu et al., 2017) or with the help of plant biotechnology and genetic engineering (Martin and Li, 2017). Nevertheless, after decades it is still challenging the commercialization of genetically modified (GM) crops as a food source since the presence of foreign DNA, with complicated regulatory requirements and sometimes

low public acceptance (Zheng et al., 2021). Clustered regularly interspaced short palindromic repeats (CRISPR)-based precise genome-editing has emerged as a transgene-free promising tool to develop new crops biofortified, more productive and resistant to pests (Jones and Naidu, 2019; Kaur et al., 2020; Mäkinen, 2020; Zaidi et al., 2020). In particular, since the first genetically modified food in 1994, the Flavr Savr tomato expected to have a longer shelf life, many promising examples of biotech crops have been conducted (Figure 3) (Bawa and Anilakumar, 2013). Plant metabolic engineering still requires a deep understanding of the complex metabolic pathways in order to identify a set of target genes required to improve or to strengthen the metabolic flux to produce the precursors of target compounds by enhancing or silencing some reactions (Couto et al., 2017; Fresquet-Corrales et al., 2017; Grützner et al., 2021; Polturak et al., 2017; Zhu et al., 2017).

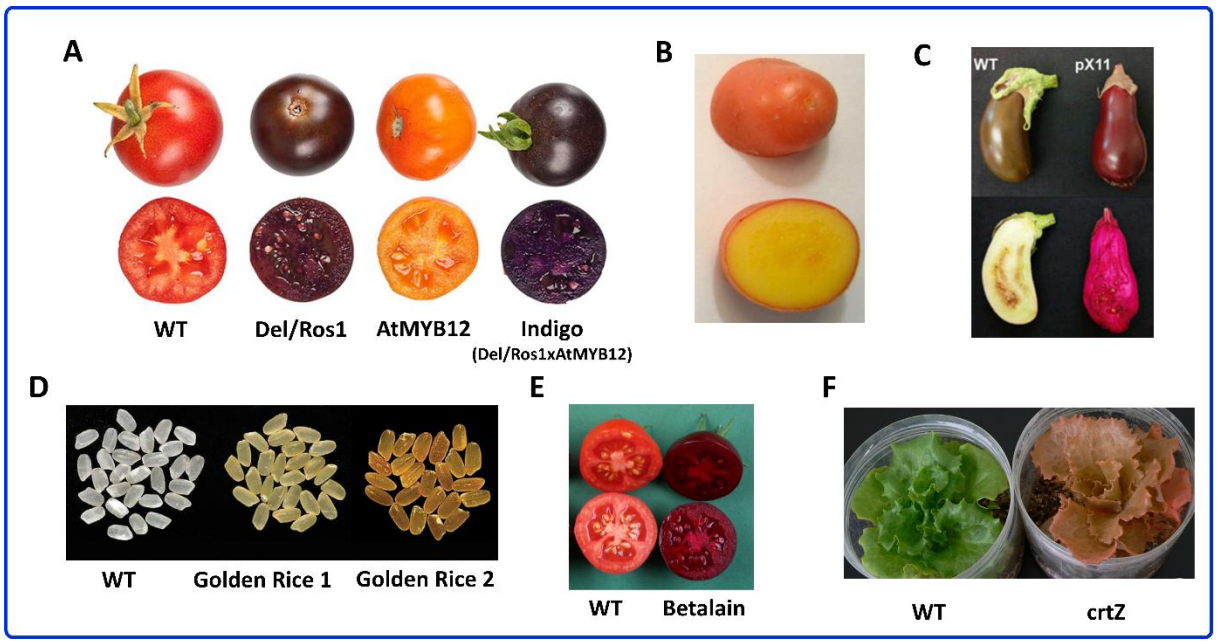

Figure 3. Some examples of biotech crops, such as **(A)** tomato with anthocyanins (Zhang et al., 2015), **(B)** potato enriched with carotenoids (Diretto et al., 2007), **(C)** eggplant accumulating betalain (Polturak et al., 2017), **(D)** Golden Rice enriched with pro-vitamin A (Paine et al., 2005), **(E)** tomato with betalain (Grützner et al., 2021), **(F)** transformed lettuce for astaxanthin accumulation (Harada et al., 2014).

The inadequate consumption of vitamins or minerals leads to a 'hidden hunger', also referred to as micronutrient deficiency. This disorder affects more than 2 billion people globally and can have devastating effects, especially in poor populations, causing various diseases such as blindness, anaemia, growth retardation, birth

deffects, and poor development of mental health (Kaur et al., 2020; Zhu et al., 2017). As a consequence, over the last few years, enormous financial and social effort has been taken in biofortification of staple crops with vitamin A, iron (Das et al., 2020), zinc, iodine and folate (Blancquaert et al., 2015; Das et al., 2020; Martin and Li, 2017). Several successful cases were reported, just to mention some, β-carotene-enriched ‘‘Golden Rice’’ (Paine et al., 2005) or oranges (Martin and Li, 2017) with carotenoid enrichment, as well as ‘‘Purple Tomatoes’’ (Butelli et al., 2008) with a higher content of anthocyanins. Prior to see in detail more successful examples of biofortified plants, the major classes of metabolites targeted by metabolic engineering, as carotenoids and polyphenols, will be reviewed.

Carotenoids are compounds derived from isoprene units with more than 750 different chemical structures (Arias et al., 2021), being the second most abundant natural compounds that occur in nature after chlorophylls (Zia-ul-haq, 2021). The majority of the carotenoids are pigments produced by all photosynthetic organisms (including plants, algae and cyanobacteria), as well as some non-photosynthetic archaea, bacteria, fungi and few animals. In plants, carotenoids can be considered as both primary (essential) and secondary (specialized) metabolites (Torres-Montilla and Rodriguez-Concepcion, 2021). Essential for photosynthesis to harvest light, photoprotection and also as phytohormone precursors (Arias et al., 2021). As specialized metabolites, carotenoids act as communication attracting insects for pollination and luring animals for seed dispersal with yellow, orange to red colours of fruits and flowers (Bonet et al., 2016). Broadly, based on their molecular composition, carotenoids can be classified in carotenes, made up only of carbon and hydrogen (α-carotene, β-carotene, lycopene, etc.), and xanthophylls that also contain oxygen (lutein, zeaxanthin, astaxanthin, etc.) (Arias et al., 2021; Torres-Montilla and Rodriguez-Concepcion, 2021). Plant carotenoid biosynthesis occurs in plastids, specifically in chloroplasts of green leaves and stems, and in chromoplasts of coloured flowers, vegetables, fruits and roots (Kang et al., 2017; Martin and Li, 2017). The carotenoid biosynthetic pathway in plants has been thoroughly studied (Figure 4) (Arias et al., 2021; Torres-Montilla and Rodriguez-Concepcion, 2021).

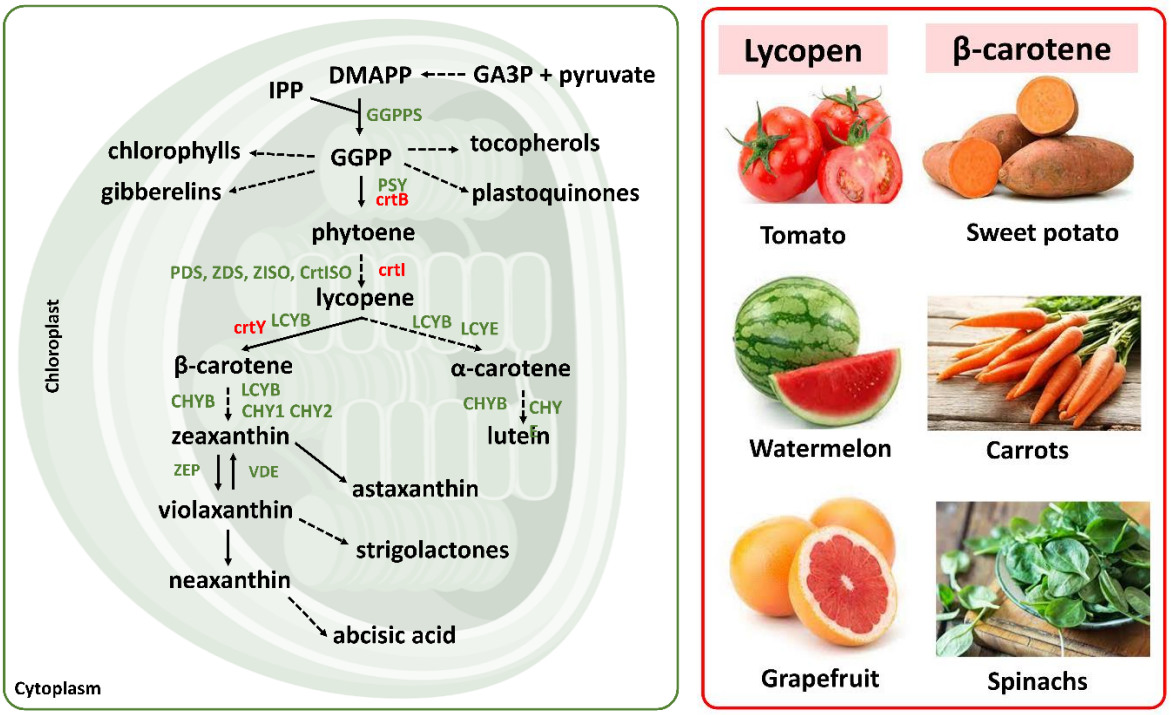

Figure 4. Plant carotenoid pathway. **(Left panel)** Carotenoids derive from the methylerythritol 4-phosphate (MEP) pathway; three isopentenyl diphosphate (IPP) and one dimethylallyl diphosphate (DMAPP) are condensed in plastids catalysed by geranylgeranyl diphosphate (GGPP) synthase to form GGPP. Then two molecules of GGPP are condensed to the non-colored carotenoid phytoene, by the enzyme phytoene synthase (PSY) in the first bottleneck reaction. Different enzymes catalyse the sequential desaturation and isomerization reactions to obtain lycopene, leading to either and lutein from α-carotene, or on the other branch and zeaxanthin, violaxanthin and neoxanthin from β-carotene. Plant enzymes in green, bacterial in red. Glyceraldehyde-3-phosphate (GA3P), phytoene desaturase (PDS), ζ-carotene desaturase (ZDS), ζ-carotene isomerase (ZISO), carotene isomerase (CrtISO), lycopene epsilon cyclase (LCYE), lycopene beta cyclase (LCYB), α-carotene ε-ling hydroxylase (CHYE), non-heme carotene hydroxylases (CHY1, CHY2), zeaxanthin epoxidase (ZEP), violaxanthin de-epoxidase (VDE). **(Right panel)** Examples of some foods rich in carotenoids as lycopene or β-carotene.

Animals, in general, cannot synthesize these nutritional and health-promoting molecules *de novo* (excluding some aphids or spider mites) and thus rely on their diet to supply them, particularly β-carotene, as vitamin A precursors in their diet (Zheng et al., 2021). Besides important antioxidants and scavengers of ROS in biological membranes, carotenoids are precursors of retinoids, including vitamin A. Deficiency in this vitamin is caused by insufficient intake of pro-vitamin A (β-carotene) (Kaur et al., 2020), common in low-income countries which rely on grain or tuber staple crops (Zheng et al., 2021). When carotenoids are ingested, being β-carotene the best precursor of vitamin A, each metabolite produces two retinal (rhodopsin) molecules, a visual pigment in the eye, which can be further reduced to retinol or directly oxidized

to retinoic acid, crucial to sustain human health and required for cell development, growth and differentiation or embryo development (Arias et al., 2021; Kang et al., 2017). Therefore, a carotenoid-enriched diet protects from age-related diseases (Zheng et al., 2021), and decreases the risk of developing others such as macular degeneration, atheromas, cognitive malfunctioning, as well as some types of cancer.

Consequently, due to the importance of carotenoids for human (and animal) health and their economic value for the industry, in the past two decades extensive efforts have been made worldwide to improve the carotenoid nutritional value of plant-based food or crops, as rice, tomato, cassava or maize (Arias et al., 2021; Kaur et al., 2020; Torres-Montilla and Rodriguez-Concepcion, 2021). The well-known 'Golden Rice' was an important breakthrough. A biosynthetic pathway was established in rice by inserting genes coding for a phytoene synthase (PSY) gene from daffodil, as well as a phytoene desaturase (PDS, named crtI in prokariotes) and lycopene cyclase (LCY) from the bacteria *Pantoea ananatis* (previously called *Erwinia uredovora*), which resulted in a yellow endosperm (Ye and Beyer, 2000). Later studies showed that LCY was not required (Das et al., 2020; Tian et al., 2019) and the daffodil PSY was replaced by its maize homolog, developing 'Golden Rice 2' and increasing the pro-vitamin A content by 23-fold, with a maximum of 37 µg carotenoids/g in rice endosperm (Paine et al., 2005). Other examples of carotenoid enrichment include potatoes with yellow flesh, named as 'Golden Potatoes', transformed with a bacterial mini-pathway of three genes encoding the phytoene synthase (crtB), crtI and lycopene β-cyclase (crtY) enzymes from *P. ananatis*, accumulating more than 3,000 fold β-carotene over a non-transformed control (Diretto et al., 2007). More recently, other genes from carrot (DcPSY2 and DcLCYB1) have been investigated to improve the nutritional value of tomatoes or apples showing a significant 2-fold increase in their carotenoid content (Arias et al., 2021; Diretto et al., 2007).

Apocarotenoids (Figure 5) are cleavage molecules from carotenoids, generally obtained from the enzymatic breakdown of β-carotene, lycopene, and zeaxanthin. The carbon skeleton of this carotenoids is shortened by the removal of fragments from one or both ends by the action of carotenoid cleavage dioxygenases (CCDs). More than one hundred apocarotenoids have been reported, acting as pigments, plant hormones (abscisic acid or strigolactones), defence compounds, retinoids (retinol or vitamin A),

volatiles (aroma of some flowers, wine or tea) or repellents (Kang et al., 2017). The highest sources of apocarotenoids are saffron (*Crocus sativus*) flower stigmas and waxy seed arils of achiote (*Bixa orellana*) (Frusciante et al., 2022). Saffron, is one of the most expensive species worldwide composed of dried stigmas from flowers picked manually may reach up to 2,000-10,000 €/kg. The glycosylated derivatives, crocins and picrocrocin, are the responsible for the colour and sour taste of the saffron spice, respectively. These are the result from the cleavage of zeaxanthin by a specific plastid-localized CCD enzyme (CCD2) (Demurtas et al., 2018; Torres-Montilla and Rodriguez-Concepcion, 2021). The saffron market has risen due to its high medicinal value as anti-inflammatory, analgesic, anti-cancer, anti-diabetic, cardio protective, anti-depressant or anti-convulsant properties, as well as beneficial effects on Alzheimer's disease or nervous system disorders (Zia-ul-haq, 2021).

Figure 5. Apocarotenoid natural sources **(A, B, C)** and some examples of transgenic approaches in plants to produce them **(D, E, F)**. **(A)** Saffron stigmas from *Crocus sativus* accumulate high amounts of crocins. **(B)** Seeds from achiote (*Bixa orellana*) also accumulate high amount of crocins. **(C)** Green algae *Haematococcus pluvialis* and yeast *Xanthophyllomyces dendrorhous* (in less extent) are the main industrial source of astaxanthin. **(D)** Tomato with crocins from chiote (Frusciante et al., 2022). **(E)** Maize kernels (Liu et al., 2021) and **(F)** tobacco plants (Agrawal et al., 2022) accumulating astaxanthin.

Astaxanthin is another carotenoid produced by certain microalgae, believed to be the world strongest natural antioxidant, as its antioxidant activity is 10 times greater

than those of β-carotene, zeaxanthin, lutein, and canthaxanthin. It is a red carotenoid commercialized mainly for colouring the aquaculture products, mainly salmonid fish and shrimps. Astaxanthin has important role in detoxifications and immunizing. It also has anticancer potentials and is used in cosmetic, pharmaceutical and nutraceutical products (Nogueira et al., 2019). The algae *Haematococcus pluvialis* is the main natural source of astaxanthin (Zia-ul-haq, 2021). Using metabolic engineering, tobacco plants (Mann et al., 2000), tomato fruits (Huang et al., 2013), lettuce (Harada et al., 2014) or mayze (Liu et al., 2021) were engineered to produce astaxanthin.

Phenolic compounds or polyphenols are a broad and heterogenous group of secondary metabolites (more than 8,000) biosynthesized from several pathways as the pentose phosphate, shikimate and the phenylpropanoid (de Araújo et al., 2021). They are efficient antioxidants since their phenolic groups can accept an electron, disrupting chain oxidation reactions in cellular components (Pandey and Rizvi, 2009). They are involved in defence as signalling molecules to protect plants against oxidative stress and ultraviolet radiation or pathogens, as well as in attracting pollinators and animals to disperse seeds due to their colours or flavours (de Araújo et al., 2021). Fruits as grapes, apples, cherries or berries contain a particularly high content of phenolic compounds (200-300 mg/100 g). They are also abundant in cloves, beans, onions, spinach, chocolate or beverages as coffee or tea (de Araújo et al., 2021; Pandey and Rizvi, 2009). Interest in polyphenol phytonutrients is increasing predominantly due to their therapeutic effects and beneficial effects on human health, protecting against the development of several human chronic diseases such as diabetes, obesity, cardiovascular diseases, osteoporosis, certain types of cancer and neurodegenerative diseases such as Parkinson or Alzheimer (de Araújo et al., 2021; Martin and Li, 2017; Pandey and Rizvi, 2009). They can also be used in food, cosmetic or textile industries as natural dyes, in the preservation of foods and its packaging, as prebiotic ingredients due to their colouring, antioxidant and antimicrobial properties (Figure 6) (Albuquerque et al., 2021; de Araújo et al., 2021).

According to their structure, the major classes of polyphenols are phenolic acids, flavonoids, tannins, lignans and stilbenes (resveratrol). Other polyphenols include the subclass of curcuminoids (Albuquerque et al., 2021; Islam et al., 2021; Pandey and Rizvi, 2009). Flavonoids constitute the most studied group with more than

4,000 molecules known to date, divided into six subclasses: anthocyanins, flavonols (such as quercetin and kaempferol), flavones, flavanones, flavanols (such as catechins and epicatechins) and isoflavones (Pandey and Rizvi, 2009).

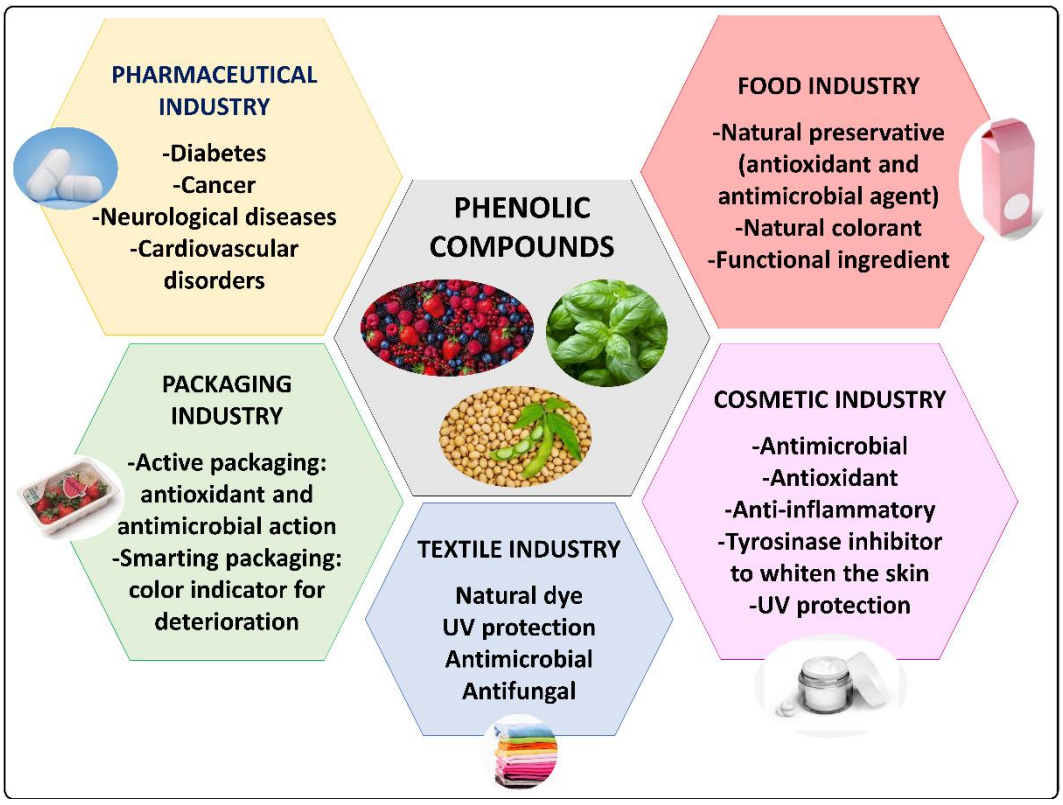

Figura 6. Industrial applications of phenolic compounds. Adapted from Albuquerque et al. (2021).

Within flavonoids, a great number of projects have focused their attention on anthocyanins as powerful antioxidants (Liu et al., 2018). They are brightly coloured polyphenols providing pink, red, purple and blue colours to fruits and vegetables such as blackberries, blueberries, red cabbages and aubergines. To improve the flavonoid accumulation, as previously mentioned, genes which encode enzymes directly involved in the biosynthetic pathway can be expressed. In parallel, regulatory genes as those coding for transcription factors can be also modified to control the expression of biosynthetic genes and increase upstream precursors (Fresquet-Corrales et al., 2017; Liu et al., 2018). Several biofortification approaches have targeted anthocyanins and succeeded its production. A pair of transcription factors from snapdragon (*Antirrhinum majus*) flavonoid biosynthesis branch were used to transform tomatoes. Under the control of a fruit-specific promoter Delila and Rosea1 genes were expressed, encoding

a bHLH and MYB-related transcription factors, respectively. 'Purple tomatoes' achieved high levels (2.83 mg/g fresh weight) of complex anthocyanin and flavonoid products (Butelli et al., 2008). Using the same approach *N. tabacum* plants were transformed (Fresquet-Corrales et al., 2017). The tomato anthocyanin content was further increased by 2-fold after crossing a tomato line transformed with *Arabidopsis thaliana* MYB12 with the previous Del/Ros1 purple tomato, naming the resultant as 'Indigo' (Del/Ros1 x AtMYB12) (Zhang et al., 2015). Other examples can be found in cereal grains, as in maize kernels (Liu et al., 2018) or rice (*Oryza sativa* L.) obtaining 'purple rice' by engineering regulatory and structural anthocyanin related genes (Das et al., 2020; Zhu et al., 2017).

Curcuminoids, as previously stated, are a subclass of phenolic compounds. These are extracted from the rhizomes of *Curcuma longa* L. (turmeric), a perennial plant native from India and surrounding Asian areas which belongs to the ginger family (*Zingiberaceae*) (Akter et al., 2019; Mandal, 2016). Traditionally, turmeric has been widely used as a culinary spice, colouring agent, in cosmetics, and as an herbal medicine (Prasad et al., 2014; Salehi et al., 2019; Zheng et al., 2018). The contribution of curcuminoids to the dry weight of the rhizome can be 2-4%, highly influenced by the cultivar and growth conditions. Curcumin (~75%) is the most abundant and active, while others, such as demethoxycurcumin (~ 20%) and bisdemethoxycurcumin (~ 5%) are less abundant (Chouhan et al., 2017; Stanić, 2017). Curcumin has received a lot of interest in recent years, since numerous studies suggest that it is able to modulate multiple signalling pathways, resulting in outstanding therapeutic effects due to its antioxidant, anticancer, anti-inflammatory, anti-apoptosis and antiviral properties (Bisht et al., 2010; Hu et al., 2021; Prasad et al., 2014; Salehi et al., 2019; Zheng et al., 2018). These protective effects have led to a great number of clinical trials being carried out on inflammatory, cardiovascular, skin, Alzheimer, respiratory, gastrointestinal or cancer disorders (Salehi et al., 2019). In spite of curcumin potential to treat and prevent different diseases, its application is restricted due to its low solubility in aqueous solutions and poor bioavailability (Chouhan et al., 2017; Ghosh et al., 2015; Hu et al., 2021; Salehiabar et al., 2018). Consequently, there is a growing interest in the heterologous production of the also called 'Indian saffron' to obtain this high-value

secondary metabolite in a cheaper and environmentally friendly manner (Couto et al., 2017; Kan et al., 2019; Katsuyama et al., 2009).

PLANT VIRUSES

The world is currently facing several challenges including environmental degradation, climate change, rapid human population growth and food insecurity. Simultaneously, there are unprecedented technological and scientific breakthroughs that offer great promise toward overcoming these dares. Plant health is vital to achieve global food security for a growing world population, expected to reach 10 billion by 2050. This requires effective management techniques in order to reach a 60% increase goal in food production without impairing natural ecosystems. In addition to abiotic stresses, crop plants are confronted with numerous biotic stresses resulting in 40% yield losses annually caused by nematodes, fungi, oomycetes, viruses, viroids or bacteria. Among plant diseases, plant viruses constitute a major cause, ranking only after fungi (Wang et al., 2020) with devastating crop losses estimated in more than $30 billion annually (Figure 7) (Jones and Naidu, 2019).

Plant virology is a discipline more than a century old. Nevertheless, historic literature indicates that humans have been aware of plant virus diseases long before, as with the famous Dutch ‘tulip mania’ in 1576. At the beginning, this field focused mainly on virus pathology as viruses caused serious diseases in cultivated crops for food and ornamentals with high economic impact (Lefeuvre et al., 2019; Sanfaçon, 2017). The precise year the first virus was found is obscure, but the German Adolf Mayer is often credited as the first researcher to describe in 1882 a tobacco disease that named tobacco mosaic disease and it is now known of virus aetiology. About the same time, in 1892 the Russian Dimitri Ivanovski reported the presence of a submicroscopic filterable infectious agent in tobacco plants. Then, the Dutch Martinus Beijerinck was the first scientist to use the term ‘contagium vivum fluidum’ or ‘virus’ for the mosaic disease agent in 1898. The discovery of the first non-cellular infectious agent, later determined to be tobacco mosaic virus (TMV), paved the way for the field of virology. Outstanding discoveries were made on viruses, the most abundant

biological entities on Earth (Balke and Zeltins, 2019; Lefeuvre et al., 2019; Roossinck et al., 2015).

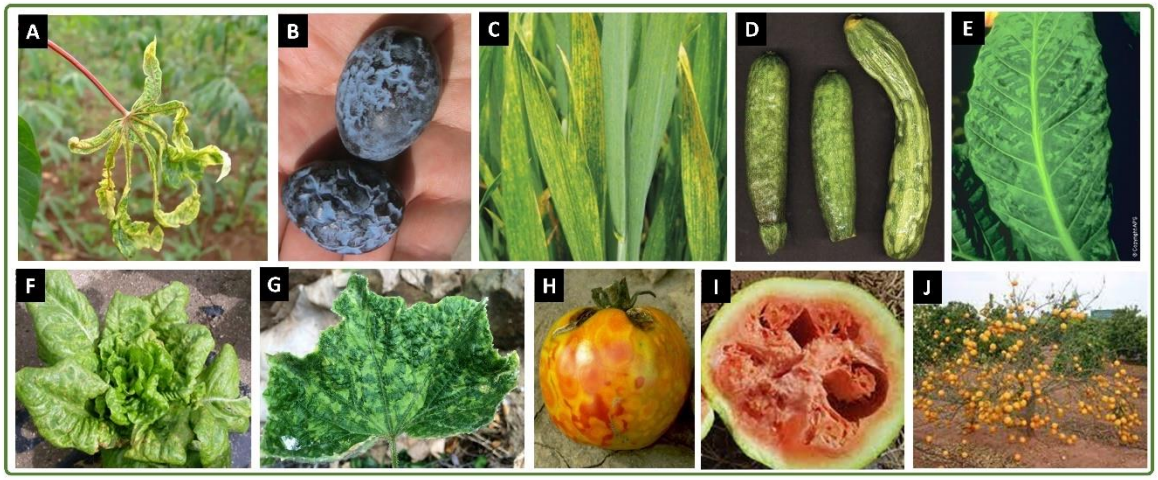

Figure 7. Symptomatology of some plan viruses on crops, reducing their yield and the product quality. **(A)** Cassava plant affected by African cassava mosaic virus (ACMV). **(B)** Severe symptoms of plum pox virus (PPV) on plum fruits. **(C)** Yellowing from wheat streak mosaic virus (WSMV). **(D)** Cucumber fruits affected by cucumber green mottle mosaic virus (CGMMV). **(E)** Mosaic pattern in tobacco leaves infected with tobacco mosaic virus (TMV). **(F)** Lettuce stunting caused by lettuce mosaic virus (LMV). **(G)** Zucchini leaves affected by zucchini yellow mosaic virus (ZYMV). **(H)** Tomato fruits infected with tomato spotted wilt virus (TSWV). **(I)** Watermelon fruit affected by ZYMV. **(J)** Orange tree affected by citrus tristeza virus (CTV).

Plant viruses are obligate intracellular parasites that rely on resources provided by the host cells for their life cycle (Balke and Zeltins, 2019), which means that for their replication they must recruit and use the host translation apparatus and energy resources (Mäkinen, 2020; Wang et al., 2020). According to the International Committee on Taxonomy of Viruses (ICTV), to date, there are a total amount of 9110 virus species recognized, being approximately 900 of them plant viruses (Balke and Zeltins, 2019; Walker et al., 2021). Recent viral metagenomic studies, which analyze viruses in environmental samples using next generation sequencing, have indicated that our knowledge underestimates the diversity of plant viruses (Edgar et al., 2022). Many of the newly discovered plant viruses have no obvious detrimental effects on wild hosts, some even are beneficial (Roossinck, 2012; Sanfaçon, 2017). These studies change the preestablished perception of how viruses interact with their hosts, suggesting that globally plant viruses are not just agents of destruction but have an essential impact on ecosystems (Lefeuvre et al., 2019).

Nearly half of the pathogens that cause emerging plant disease epidemics worldwide are viruses, and they are expanding along with their vectors in response to agricultural globalization and climate change-driven influences (Jones, 2021). Viruses frequently damage plants with effects that range from asymptomatic infections to total devastation (Jones & Naidu, 2019; Yang et al., 2021). Viral infections are a threat for crop production by impairing plant growth, decreasing yield and the quality of the products and, therefore, reducing marketability (Figure 7) (Jones and Naidu, 2019; Mäkinen, 2020). Plant viral disease outbreaks pose a threat to the sustainability of agricultural systems given a lack of direct curative measures (Lefeuvre et al., 2019). These outbreaks result in serious economic and social implications around the world, but especially in countries where agriculture is the primary source of income causing even famine (Jones, 2021; Jones and Naidu, 2019).

Plant viruses consist of a nucleic acid genome (DNA or RNA), encoding a minimal set of proteins critical for infection. The basis consists of polymerases for viral genome replication, movement proteins (MP) necessary for virus spread from cell to cell (Balke & Zeltins, 2019; Wang et al., 2020), and the coat proteins (CP) that protect the viral genome after replication. Plant viruses exhibit different strategies for gene expression, such as production of polyproteins, translation from subgenomic RNAs, ribosomal frameshift signals, internal ribosome entry sites and 'leaky stop' codons to achieve maximal coding capacity of the genome. Knowledge of these strategies is highly important for the construction of virus-based plant expression systems. Structurally, a significant part of plant virus particles is organized into flexible or rigid rod-shaped structures, while other viruses are isometric with icosahedral symmetry (Balke and Zeltins, 2019) (Figure 8A).

The infection cycle starts when viruses penetrate into host cells by means of mechanical wounds or with the help of vectors (e.g., aphids, nematodes or mites). Then, viral particles disassembly occurs when viral genomes are released inside the host cells after partial or total CP removal. After that, viral genome is replicated and translation of viral proteins take place through the host cell machinery (Wang et al., 2020). Viruses use various transmission pathways to infect plants (Figure 8B). Vertical transmission occurs between parents and their progeny by vegetative propagation from virus-infected material, seeds with infected embryos or parental pollen. On the

other hand, horizontal transmission refers to transmission to new plants by contact or vectors. Contact transmission occurs when infected plant organs rub a healthy plant. Alternatively, transmission can be also given when handling or pruning infected plants before healthy ones, animal grazing, parasitic plants, mechanical harm, wind, or contaminated soil or water (Jones and Naidu, 2019).

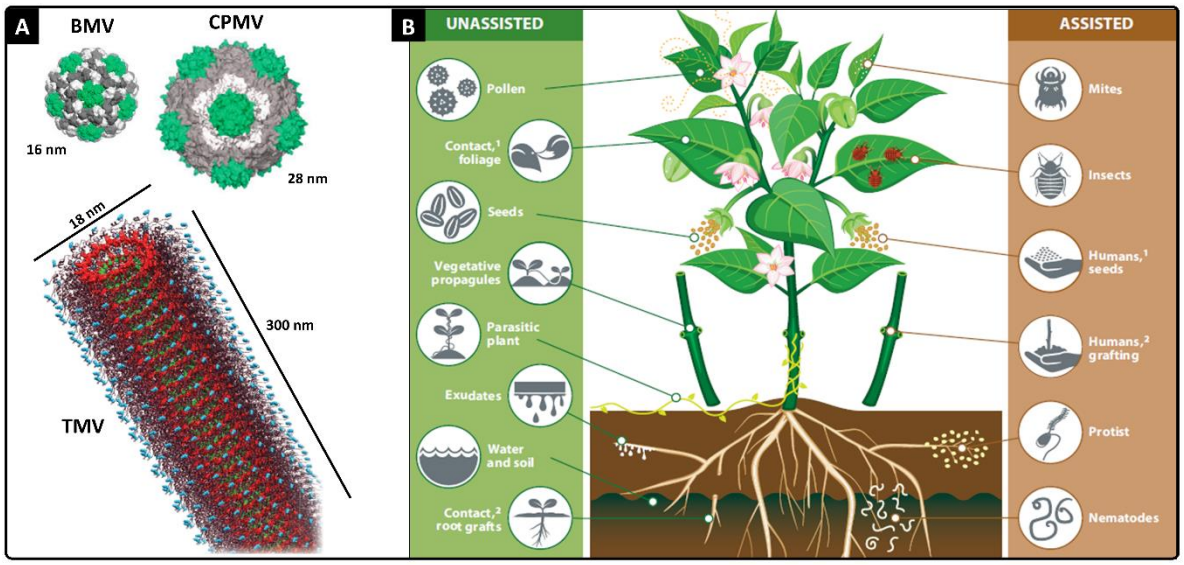

Figure 8. Shape diversity in plant virions. **(A)** Icosahedral plant viruses such as brome mosaic virus (BMV) or cowpea mosaic virus (CMPV) and a filamentous tobacco mosaic virus (TMV) (Shukla et al., 2020a; Zhang et al., 2018b). **(B)** The diversity of virus transmission pathways, both assisted and unassisted, by which plant viruses can spread from plant to plant, leading to local, regional or global virus spread (Jones & Naidu, 2019).

Vector-mediation is the most important mode of plant virus transmission. Vectors include arachnids, fungi, nematodes, some protists, but most importantly insects, especially the order *Hemiptera* transmitting more than 70% of known plant viruses. Aphids are particularly well suited to transmitting plant viruses because of their needle-like mouthparts that they use for sucking sap and the contents of plant cells (Lefeuvre et al., 2019). More in detail, insect-mediated transmission is categorized based on the virus localization in the vector, retention time, transmission and association with internal vector organs. Non-persistent transmission, also variously called semi-persistent or non-circulative, takes place when (stylet-borne, reversible and specific interactions of viral particles with molecular components of mouthparts happen (stylet-borne or foregut-born). In this transmission mode, the vector is infectious only for a few feeding probes.

On the other hand, persistent transmission occurs once the virus is acquired, and the vector typically remains viruliferous for lifetime. This latter can be either propagative or circulative depending on whether virus replicates inside insect vector or not, respectively (Gadhave et al., 2020; Lefeuvre et al., 2019). Many insect-transmitted plant viruses have likely also evolved complex mechanisms to manipulate their vectors and facilitate transmission. Plant viruses commonly have a host range that includes several species from one or more different plant families; however, they rarely are transmitted by more than a few very closely related insect species (Lefeuvre et al., 2019). An effort to rank the ten most relevant plant viruses, from both agronomic and scientific views, resulted in TMV, tomato spotted wilt virus (TSWV), tomato yellow leaf curl virus (TYLCV), cucumber mosaic virus (CMV), potato virus Y (PVY), cauliflower mosaic virus (CaMV), African cassava mosaic virus (ACMV), plum pox virus (PPV), potato virus X (PVX), citrus tristeza virus (CTV), barley yellow dwarf virus (BYDV), potato leafroll virus (PLRV) and tomato bushy stunt virus (TBSV) (Scholthof et al., 2011).

PLANT VIRUSES IN BIOTECHNOLOGY

Plant viruses have been intensively studied since its discovery at the end of the XIX century and despite their minimal genomes, they have the tremendous ability to hijack and to redirect the biosynthetic capacity of the host cell to synthetize high amount of viral proteins in a short period of time (Balke and Zeltins, 2019). This capacity arose the idea of repurposing plant viruses into transient expression vectors for the production of heterologous proteins and metabolites, for gene silencing to understand plant gene functions, and as scaffolds for nanoparticles (Figure 9) (Abrahamian et al., 2020; McGarry et al., 2017; Pasin et al., 2019; Sainsbury et al., 2010; Wang et al., 2020). Indeed, viral vectors are considered by the scientific community an alternative to stably transformed plants for industrial production of a wide range of compounds (Hefferon, 2017; Pasin et al., 2019).

The first plant viruses to be developed as expression vectors in the early 1980s were those with DNA genomes (e.g. *Geminiviridae* and *Caulimoviridae*), as they could be manipulated by early molecular biology techniques (Peyret and Lomonossoff,

2015). However, the majority of viruses found in plants have RNA genomes (Hull, 2002; Yang et al., 2021), although the geminiviruses have posed the most significant disease problems in recent years due to their emergence in crops (Roossinck, 2008). Therefore, when the technology for creating infectious complementary DNA (cDNA) copies from RNA genomes appeared, vectors based on RNA viruses became more popular (Sainsbury et al., 2010). Single stranded RNA (ssRNA) viruses have either positive or negative genomes (ssRNA+ or ssRNA-, respectively) packaged within their capsids. Of these, ssRNA+ have been more extensively studied and engineered because they do not require pre-existing proteins to initiate infection, unlike ssRNA- (Khakhar and Voytas, 2021).

Several vector design strategies have been developed in viruses, as the common gene replacement or complementation. Others include gene insertion in tandem with a viral protein and its separation with a self-cleaving 2A peptide, or the expression from a subgenomic promoter (Abrahamian et al., 2020). Another technical breakthrough for the development of viral vectors was the demonstration that virus infections could be launched by *A. tumefaciens*, in a technique known as 'agroinfection', later called 'agroinoculation'. Briefly, a suspension of transformed *A. tumefaciens* that harbour infectious clones of plant viruses is infiltrated into a plant leaf. Therefore, with only transient expression, viral nucleic acids are transferred into plant host cells (Mortimer et al., 2015; Pasin et al., 2019). Agroinoculation has become nowadays the most efficient and universal way of delivering DNA or RNA viruses to plants (Peyret and Lomonossoff, 2015).

Most viral vectors can be exploited for plant molecular farming purposes (Wang et al., 2020). Although a variety of plants have been used as expression hosts associated with agroinfiltration, there has been an increasing acceptance regarding the preferred use of *N. benthamiana*. This plant offers a rapid generation of biomass, and is also particularly susceptible to a wide range of viruses (Gleba et al., 2004; Margolin et al., 2020; Sanfaçon, 2017; Tsekoa et al., 2020). Using plant virus-derived vectors as an alternative to plant stable transformation includes some advantages. It is simpler, faster, costs are reduced, viral genomes are small and therefore easy to manipulate and the sequence inserted will be highly amplified during viral replication (Majer et al., 2017; Sainsbury et al., 2012). Besides, it allows to screen multiple construct variants

rapidly discarding the poor ones to further undergo long transformation programs (Abrahamian et al., 2020).

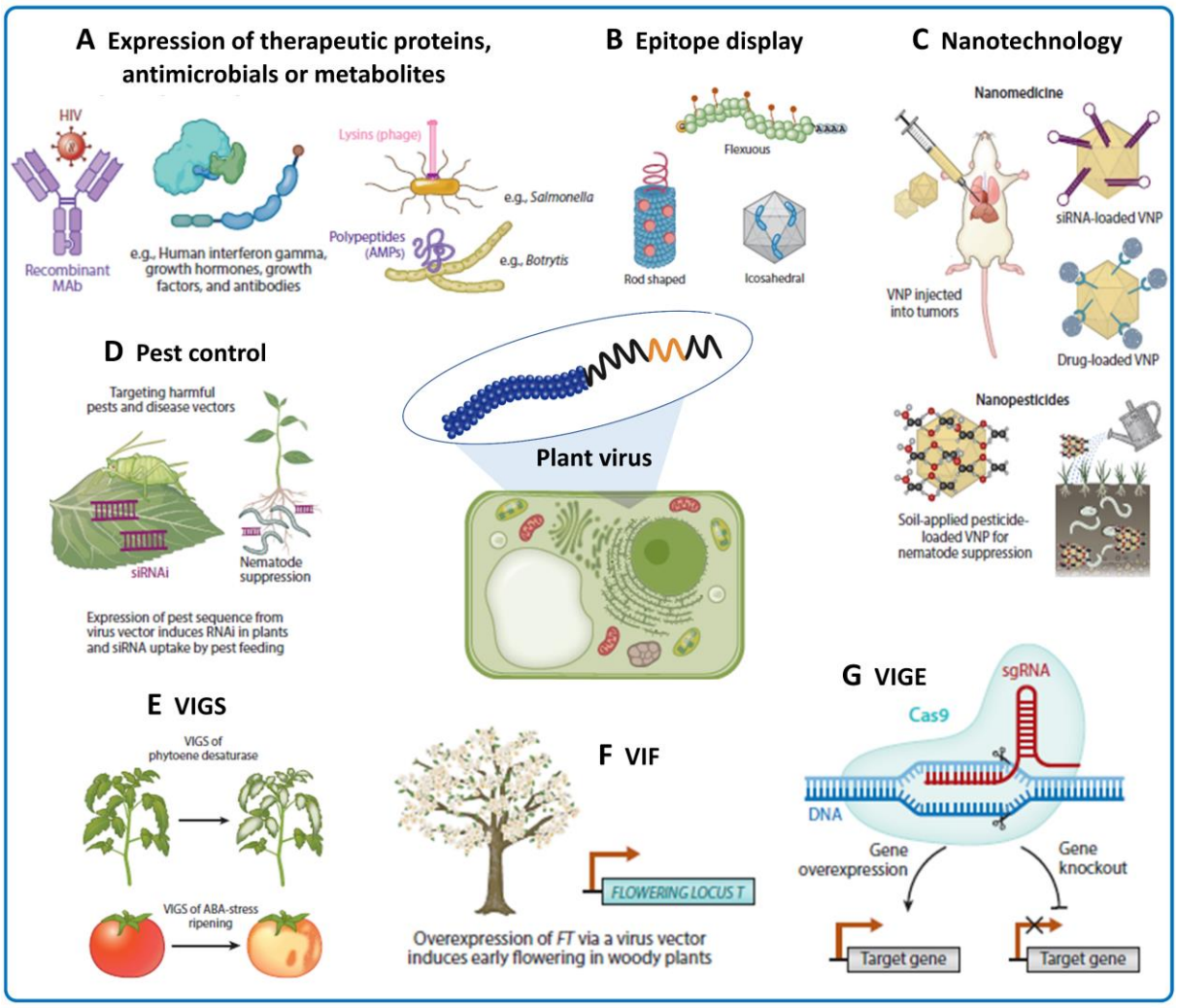

Figure 9. Diverse uses of virus vectors in biotechnology. **(A)** Expression of therapeutic proteins, antimicrobials to protect against animal or human pathogens as well as metabolites of interest. **(B)** Epitope display or vaccine production using virus-like particles (VLPs). **(C)** Viral nanoparticles (VNPs) used in nanomedicine and as nanopesticides: imaging, diagnostics, therapy, gene silencing, pesticide carriers. **(D)** Pest control by inducing RNA interference (RNAi) in pests and pathogens. **(E)** Virus-induced gene silencing (VIGS) for reverse genetics to determine gene function or to reduce expression of a selected gene. **(F)** Virus-induced flowering (VIF) helps in accelerating breeding programs by overexpression of FLOWERING LOCUS T (FT) in woody or recalcitrant plants. **(G)** Virus-induced gene editing (VIGE) expressing single-guide RNA (sgRNA) or/and Cas protein. Adapted from Abrahamian et al. (2020).

There are a great number of DNA and RNA viruses that have been transformed into expression vectors. One type of vectors are based on the 'full-virus' strategy, containing essentially a wild-type (wt) virus modified to carry and express a

heterologous sequence that encodes a gene of interest (Gleba et al., 2004). Typically, the gene of interest is under transcriptional control of a strong promoter derived from the wt or a related virus or as a fusion to one of the viral gene products (e.g. the CP) (Mortimer et al., 2015). These viral vectors typically retain the full capacity of replication, assembly of virions, cell-to-cell and systemic movement and resistance to host gene silencing. Therefore, as they can spread systemically, the entire plant turns into a biofactory until the plant clears the virus or collapses to the infection (Fischer & Buyel, 2020a; Khakhar & Voytas, 2021; Wang et al., 2020). However, this strategy have several limitations, namely limited cargo capacity (Gleba et al., 2007; Hefferon, 2017; Sainsbury et al., 2012; Wang et al., 2020); the gene of interest is susceptible to 'genetic drift' during virus replication, mutation deletion or complete loss over time affecting expression (Khakhar and Voytas, 2021). Bio-containment issues should be taken into consideration, since these viruses could potentially spread into the environment (Mortimer et al., 2015). This kind of vectors have several advantages, they spread systemically through the plant and viral replication amplifies the gene of interest. In addition, viral suppressors of gene silencing counter-act host response to clear expression of the gene of interest.

A new generation of virus expression vectors was developed to overcome some of previous limitations, based on 'deconstructed' or defective versions of viral genomes (Hefferon, 2017), which means that vital parts of the virus machinery required for, replication, cell-to-cell movement, systemic infection or spreading to new hosts are removed (Fischer and Buyel, 2020). In some cases, essential genes for replication are deleted from the viral genome and transferred to the genome of the host plant, which is genetically modified to provide those functions (Gleba et al., 2004). This serves a dual purpose: to provide more space for cloning the heterologous genes of interest and to create a biocontainment system in which only transgenic host plants can be infected by the viral vector (Bedoya et al., 2010; Majer et al., 2017; Molina-Hidalgo et al., 2021). Not all of the viral functions are absolutely required in an expression vector, but some are necessary for an efficient expression of the gene of interest (Gleba et al., 2004). Consequently, in other approaches, some genes can be deleted and the viral elements are kept to a minimum, forcing the deconstructed viral vectors to be expressed only in local leaves being delivered by agroinfiltration (Fischer and Buyel,

2020). Mutagenesis or deletion of genes essential for virus transmission has also been added (Abrahamian et al., 2020). Some of the initial disadvantages that were found in the initial molecular farming bubble, as insufficient expression and low yields, consistency and low recovery during processing (Fischer et al., 2012) have been overcome by the development of improved virus-based vectors (Fischer and Buyel, 2020). In general, viruses with isometric virions allow smaller inserts due to the need for genome packaging, although this can be overcome in some multipartite viruses by further division of the genome and complementation. Rod-shaped particles have less obvious packaging constraints, but larger inserts are frequently less stable than smaller ones; reducing the extent of duplications in the genome can increase stability of larger inserts (Abrahamian et al., 2020).

Many plant viruses have been used as backbones to develop virus-based expression systems, as tobamoviruses, potexviruses, geminiviruses, rhabdoviruses and comoviruses (Diego-Martin et al., 2020; Ma et al., 2020; Peyret & Lomonossoff, 2015; Sainsbury & Lomonossoff, 2014; Shanmugaraj et al., 2020). Here some of the most successful vectors are briefly summarized with special attention to their applications. Genus *Tobamovirus* (family *Virgaviridae*) consists of rigid rod-shaped virions that encapsidate ssRNA+ genomes, type member TMV. Despite its early discovery, TMV continues to be an important reference for the scientific community, serving as a virus model for research of viral structures, assembly mechanisms and viral life cycle, as well as biotechnological applications, including production of vaccines (Balke and Zeltins, 2019; Saxena et al., 2011). TMV has been widely used for gene expression and for peptide presentation. MagnICON is probably the most famous 'deconstructed' plant virus-based vector. This system consists of a hybrid genome with elements from TMV and turnip vein clearing virus (TVCV) (Figure 10A) split into three components, each of them in a different *A. tumefaciens clone* that is co-infiltrated into the same plant cell. By deleting the CP gene, it could spread only cell to cell within the leaf achieving yields of green fluorescent protein (GFP) as high as 5 mg/g of fresh weight tissue (Marillonnet et al., 2004). Later, the TRBO system was developed (Figure 10B), a single-module based on TMV. This vector relies on a CaMV 35S promoter and the CP gene was replaced with a multiple cloning site where the gene of interest is

inserted. Simpler than magnICON and comparable in terms of recombinant protein yield, replicons cannot move systemically (Lindbo, 2007).

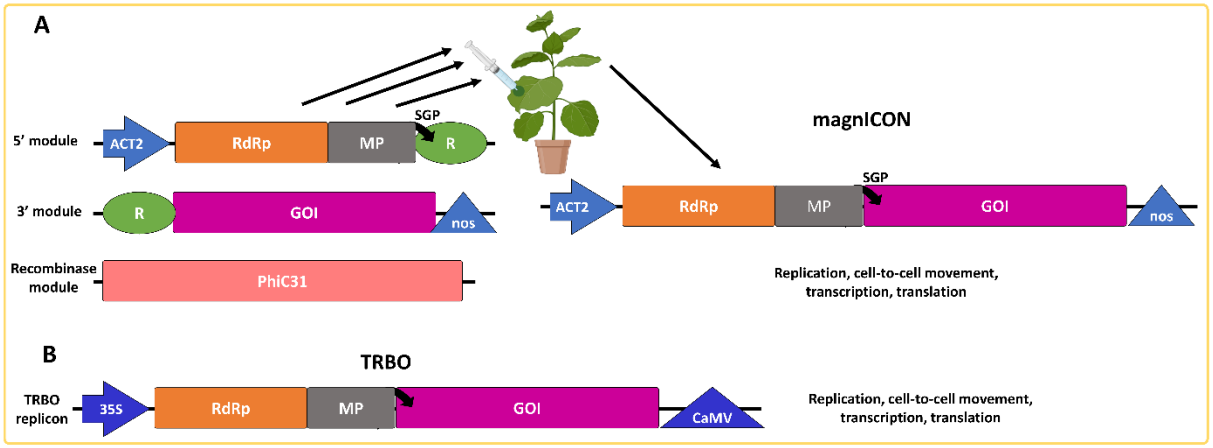

Figure 10. Deconstructed tobamovirus-based expression systems. **(A)** The magnICON system is based on three modules. The recombinase module allows the recombination of the 5' and 3' modules to form a complete replicon. *Arabidopsis* actin 2 promoter (ACT2), RNA-dependent RNA polymerase (RdRp), movement protein (MP), TMV subgenomic promoter (SGP) directing transcription of the gene of interest (GOI), recombination site (R), Nos terminator (nos), streptomyces phage 31 integrase (PhiC31). **(B)** The TRBO system consists only of a single module. 35S promoter (35S), cauliflower mosaic virus (CaMV) terminator. Adapted from Peyret and Lomonossoff (2015).

TMV vectors have been more recently used to produce the N protein of SARS-CoV-2 in *N. benthamiana* for serological diagnosis (Williams et al., 2021). In nanomedicine, the TMV central channel was loaded with phenanthriplatin, delivering efficiently the drug and excerting an antitumor activity against breast cancer in mice (Czapar et al., 2016). Similarly, TMV has been also loaded internally with streptokinase, a drug used to reduce the risk of bleeding (Pitek et al., 2018). Furthermore, TMV external surface can be also modified with targeting ligands administered as inactive forms, later converted into active forms to prevent off-target toxicity (Shukla et al., 2020a).

Potato virus X (PVX) is the type species of the genus *Potexvirus* in the family *Alphaflexiviridae*. PVX is a flexuous rod-shaped virus whose natural host range covers several plant families, especially those belonging to the *Solanaceae*. PVX flexuous filamentous virions (470–580 nm long) pack a ssRNA+ genome (circa 6,400 nt), containing five open reading frames (ORFs) between the 5′-methylguanosine cap and the 3′-poly(A) tail. The first ORF encodes a complex RNA-dependent RNA polymerase

(RdRp), followed by three overlapping genes, the triple gene block (TGB1, 2 and 3) encoding MPs involved in cell-to-cell movement, and lastly the CP gene at the 3' end (Fuentes et al., 2021; He et al., 2022). Studies on PVX structure, replication and spread have advanced its utilization for diverse biomedical and agricultural applications (Scholthof et al., 2011). PVX-based studies have demonstrated its potential as an expression system (Mardanova et al., 2017), and as a display scaffold for epitopes of interest. Its use as nanoparticle has been widely reported for tissue-specific imaging and drug delivery. In this sense, hepatitis C antigens (Uhde-Holzem et al., 2010), and human immunodeficiency virus (HIV) epitopes (Peyret and Lomonossoff, 2015) have been presented on its surface. Recent studies have suggested PVX ability to block tumour progression (Shukla et al., 2020b) by carrying monoclonal antibodies (Trastuzumab) to breast cancer cells (Esfandiari et al., 2016). PVX loaded with immunotherapeutics was also suggested to improve the negative effects in mouse models of melanoma, breast, ovarian and colon cancer (Lee et al., 2017). Furthermore, apoptosis triggered by a drug against cancer was more efficient when delivered by PVX compared to the soluble version (Le et al., 2019a, 2019b). More recently, PVX viral vectors have been used to express guide RNAs in virus-induced gene editing (VIGE) with CRISPR-Cas strategies (Uranga et al., 2021a, 2021b)

Comovirus is a genus whose members have a genome naturally bipartite, consisting of two separately encapsidated ssRNA+ molecules. Cowpea mosaic virus (CPMV) is the type member and the most used in biotechnology, a natural pathogen of cowpea (*Vigna unguiculata*), with icosahedral shape and a diameter of 30 nm (Sainsbury et al., 2010). RNA-1 encodes proteins involved in the replication of viral RNAs and polyprotein processing. The smaller RNA-2 encodes the MP and large and small CPs, essential for cell-to-cell movement and systemic spread. RNA-2 is totally dependent on RNA-1 for its replication. The development of CPMV-based expression systems has focused entirely on modifying the sequence of RNA-2, and when replication functions are required, unmodified RNA-1 is supplied by co-inoculation (Sainsbury et al., 2012). Later reports demonstrated that if most of the RNA-2 ORF is removed and replaced by GFP, this RNA2 deleted version is still replicated by RNA-1 if the sequences of 512 nucleotides from the 5' end and the entire 3' untranslated region (UTR) are maintained. Therefore, replication was not essential for expression.

Then, by removing two upstream initiation codons from the RNA-2 5' end upstream the main initiation site, an unexpected effect of enhanced protein expression was achieved by 10 to 15-fold compared with the deleted RNA-2 containing the wild-type 5' sequence. The resulting vector was named CPMV-hyper translatable or CPMV-HT. A series of user-friendly deconstructed vectors were subsequently developed from the RNA-2, the pEAQ series, allowing the easy insertion of sequences between the 5' and 3' sequences of a CPMV-HT cassette (Peyret and Lomonossoff, 2015) for the expression of foreign proteins without the need for viral replication. CPMV have been extensively studied for its use in nanomedicine as vaccine candidates for the display of heterologous immunogenic epitopes against animal and human pathogens, namely the bluetongue virus, HIV, Dengue or influenza virus (Hefferon, 2017). Other records related with cancer have proven its ability to act as immunotherapy agent if loaded with cytotoxic agents (Yildiz et al., 2013). Likewise, CPMV has been also used as bio-imaging vehicle able to bind to vimentin receptors, overexpressed on the surface of endothelial and cancer tissues (Berardi et al., 2018; Steinmetz et al., 2011). More recently, in relation to the current COVID-19 pandemic, the diagnosis of infected people it is crucial to reduce its spread (Capell et al., 2020). However, there is no universal positive RT-qPCR control. A diagnostic positive control reagent based on CPMV VLPs has been developed in *N. benthamiana* as production platform, allowing RT-qPCR standardization across different laboratories (Peyret et al., 2022).

GETTING TO KNOW A POTYVIRUS-BASED EXPRESSION VECTOR

Potyviridae is the largest family of RNA viruses infecting plant, including 12 genera with 235 species according to the ICTV, which cause significant losses in a wide range of crops across the globe (Walker et al., 2021; Wylie et al., 2017). Within *Potyviridae*, the largest and most extensively studied genus is *Potyvirus* (Revers and García, 2015), which encompasses more than 190 species. Potyviruses have ssRNA+ genomes and flexible and filamentous virions, 700-900 nm long and 11-15 nm wide. The majority of them are transmitted by aphids as *Myzus persicae*, *Aphis gossypii* or *A. craccivora* in a non-persistent and non-circulative manner (Gadhave et al., 2020). Some potyviruses are recognized as economically important viral pathogens. Some of the most

representative members of the genus includes the type member PVY, one of the most devastating pathogens infecting solanaceous crops; PPV as the most devastating viral disease of stone-fruit crops from the genus *Prunus*; tobacco etch virus (TEV) traditionally used as a model for RNA virus research (Bedoya & Daròs, 2010); turnip mosaic virus (TuMV); lettuce mosaic virus (LMV) or zucchini yellow mosaic virus (ZYMV) that infects all cultivated species in the family *Cucurbitaceae* (Figure 11) (Scholthof et al., 2011).

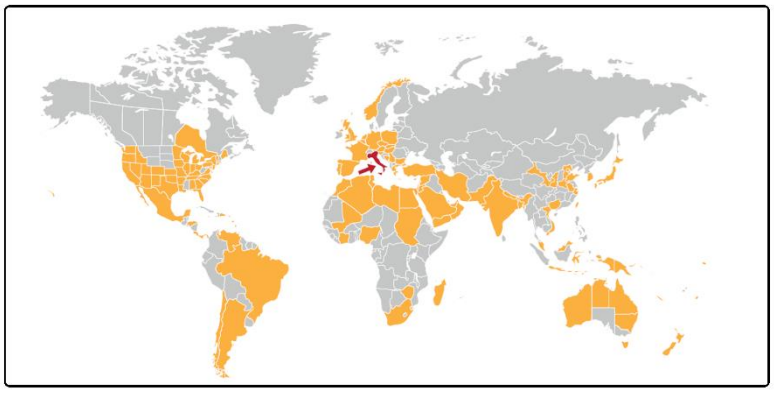

Figure 11. Rapid global spread of zucchini yellow mosaic virus (ZYMV), a potyvirus discovered in Italy in 1973 (red arrow). Dispersed mostly by international cucurbit seed trade, during the following decade it appeared in all continents within the following decade, with tropical and temperate climates (Jones, 2021).

When present in mixed infections with viruses from other groups, potyviruses often cause devastating synergistic interactions endangering food security (Jones and Naidu, 2019). Consequently, more research has focused on potyviruses than on other groups of plant viruses (Revers and García, 2015; Yang et al., 2021). Furthermore, plant biotechnologists have long been interested in potyviruses, firstly owing to their genome expression strategy, which allows the generation of heterologous proteins in an equimolar amount (Carrington et al., 1993). Secondly, the elongated architecture of the virion allows the accommodation of large amount of foreign material (Kelloniemi et al., 2008) and lastly, potyvirus genome also enables the insertion of foreign genes in multiple sites (Majer et al., 2015).

Potyvirus genome is a ~10 kb RNA molecule with a covalently attached viral protein genome-linked (VPg) to its 5' terminal end, essential in virus replication and translation, also involved in suppression of RNA silencing, and a poly(A) tail at its 3' terminal end (Figure 12). Plant virus genomes have a limited coding capacity in which

translation is a complex and tightly controlled process to manipulate plant developmental and defence processes (Sanfaçon, 2017; Yang et al., 2021). The potyviral RNA is an excellent example of this statement. Potyviruses are indeed fascinating since they mainly consist of a single ORF which encodes a large polyprotein (~350 kDa) eventually self-cleaved by three viral-encoded proteases (P1, HC-Pro and NIaPro) into a set of ten proteins. More in detail, the functional proteins include: P1, protein 1 protease, playing a significant role in virus replication; HC-Pro, helper component-protease, involved in suppression of gene silencing and in vector transmission; P3, protein 3, involved in virus replication, host range and symptom development; 6K1 and 6K2, six kilodalton peptides, where 6K2 is a small transmembrane protein probably anchoring the replication complex to the endoplasmic reticulum; CI, cytoplasmic inclusion, an helicase accumulating in inclusion bodies in the cytoplasm of infected plant cells; NIa, nuclear inclusion a, which is further cleaved into the VPg protein and the protease NIaPro; NIb, nuclear inclusion b, an RNA-dependent RNA polymerase and CP, coat protein with roles in virus movement, genome amplification and vector transmission. Recent studies have shown the presence of an additional short ORF ('pretty interesting potyvirus ORF', PIPO) embedded within the P3 cistron and expressed as a P3N-PIPO fusion product via transcriptional slippage with a different reading frame. Proteins P1 and HC-Pro are released by their intrinsic proteinase activities whereas NIaPro is responsible for the rest of the cleavages (Mäkinen, 2020; Those & Rnas, 2012; Yang et al., 2021).

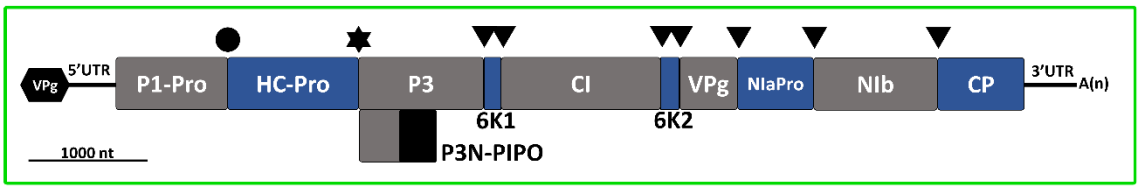

Figure 12. Schematic genome organization of a typical potyvirus. Lines represent 5' and 3' UTRs, A(n) represents poly(A) tail; boxes represent P1, HC-Pro, P3, P3N-PIPO, 6K1, CI, 6K2, VPg, NIaPro, NIb, and CP cistrons, as indicated. Cleavage sites of P1-Pro (circle), HC-Pro (star) and NIaPro (arrowhead) are marked. Scale bar corresponds to 1000 nt.

The phenomenon of viral exclusion occurs when the presence of a replicating RNA within a cell effectively prevents the replication of a second virus on the same cell. As a result, expression vectors based on monopartite genomes are restricted to the production of a single protein within a single cell unless a second, non-competing virus

is used to express a second protein (Sainsbury et al., 2012). This is a disadvantage in metabolic engineering since, frequently, coordinated expression of several enzymes in the same cell is needed to obtain a desired product. To overcome this constraint, a potyvirus-based vector system was developed for the production of recombinant proteins in equimolar amounts (Bedoya et al., 2010). This technology was based on the replacement of the NIb cistron by a cassette for the co-expression of multiple heterologous proteins. To ensure the release of the proteins of interest from the polyprotein after translation, they are flanked by sequence-specific cleavage recognition sites recognized by viral proteases (Carrington et al., 1993). The insertion positions for heterologous sequences have a crucial effect on protein accumulation (Arazi et al., 2001b; Beauchemin et al., 2005). Among the potyvirus genome there are two frequently used positions for the insertion of foreign sequences: between P1 and HC-Pro and between NIb and CP (Beauchemin et al., 2005; Dietrich and Maiss, 2003; Fernández-Fernández et al., 2001). Another insertion position can be used for this purpose as the amino terminus, enabling the delivery of the recombinant proteins to different subcellular localizations (Majer et al., 2015).

Potyviruses have been extensively exploited as biotechnological tools, especially for the expression of heterologous proteins in plants, including even a whole biosynthetic pathway (Bedoya et al., 2010, 2012; Cordero et al., 2017a, 2017b; Llorente et al., 2020; Majer et al., 2017). Numerous studies refer to viral vectors as tools to easily and quickly change and rewire the plant metabolism. In previous work, by inserting the transcription factors Rosea1 from *A. majus* in a PVY clone, its expression led to the accumulation of high amounts of anthocyanins; this pigmentation was also used to track the viral infection by the naked eye (Bedoya et al., 2012; Cordero et al., 2017b). Using a TEV-derived clone, it was also previously reported the expression of a whole heterologous metabolic pathway (crtE, crtB and crtI) from the soil bacteria *P. ananatis*, which led to the extraplastidial production of the health-promoting lycopene up to 10% of the carotenoid content in *N. tabacum* tissues. In the TEV-derived expression system developed, the ca. 1.5 kb viral cistron that codes for the NIb was replaced with a cassette that contains the heterologous sequences flanked by the native cleavage sites of NIaPro (Majer et al., 2017). Therefore, given the difficulties in rewiring metabolism using traditional transgene approaches, viral vector-based production provides a

plausible solution for engineering plant metabolic pathways with low cost and excellent performance (Wang et al., 2020).

Additionally, potyviruses have been used as expression vectors to produce nanoparticles for peptide displaying (Frías-Sánchez et al., 2021; Yuste-Calvo et al., 2019a) and more recently for VIGE (Uranga et al., 2021a, 2021b). Genome-editing technologies using CRISPR-Cas tools have revolutionized plant science and hold enormous promise to obtain improved and more nutritious, resistant, and productive crops. Most CRISPR-Cas strategies in plants rely on genetic transformation to supply the gene editing components, such as Cas nucleases or the single guide RNA (sgRNA), but other systems based on viral vectors have appeared as alternatives (Uranga et al., 2021a). To alleviate long breeding cycles and regulatory constraints, DNA-free delivery has arisen as an alternative. Recent report showed DNA-free gene editing in plants using a rhabdovirus vector that expressed both the Cas nuclease and the sgRNA (Ma et al., 2020) and a combination of PVX and TEV vectors (Uranga et al., 2021b).

VIRUSES AS NANOPARTICLES

Viral vectors have been recruited in basic and applied research as efficient tools for the expression of recombinant proteins (Venkataraman and Hefferon, 2021). In the last few years, there has been growing interest in the development and use of nanoparticles which are stable, biodegradable, biocompatible, non-toxic and easily produced at large scale with controllable chemical and physical properties (Jovčevska and Muyldermans, 2020). Viral nanoparticles (VNPs), including plant viruses and VLPs, naturally meet all of the above mentioned requirements, constituting unique scaffolds in nanotechnology (Figure 13) (Pasin et al., 2019; Steele et al., 2017; Yuste-Calvo et al., 2019a).

Furthermore, compared to synthetic nanomaterials, VNPs hold many more advantages, as structural homogeneity due to their regular and symmetrical geometries, size uniformity, well-characterized surface properties and highly stable capsids (Alemzadeh et al., 2018; Bruckman et al., 2013; Venkataraman and Hefferon, 2021; Wen and Steinmetz, 2016). Consequently, producing VNPs using plants avoiding transgenic approaches has great potential in different fields, as the time and cost can be markedly reduced (Shukla et al., 2020a). In particular, plant VNPs are of great

interest as plant virus show no clinical toxicity (Lee et al., 2017), do not infect mammals and therefore provide intrinsic safety, they have autonomous replication and assembly, and high expression yields can be achieved (Schillberg et al., 2003; Tschofen et al., 2016; Wang et al., 2020; Xu et al., 2012).

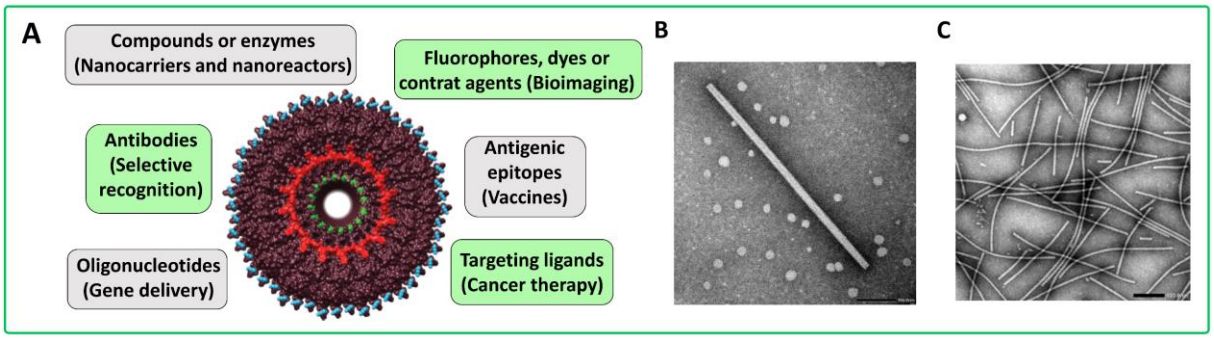

Figure 13. Biotechnological applications of VNPs. **(A)** Plant VNPs can be augmented with additional functionalities when they display imaging contrast agents, therapeutic moieties, and targeting ligands such as peptides or antibodies. Electron microscope micrographs of elongated viruses, such as PVX **(B)** or TEV **(C)**, which can be used as VNP scaffolds.

Plant viruses have been widely deployed as scaffolds since they contain a large number of CP subunits susceptible of being genetically or chemically modified (González-Gamboa et al., 2017; Shukla et al., 2020a). Viral CP genetic engineering will generate identical copies without batch-to-batch variations (Shukla et al., 2020a). Plant VNPs can be not only exploited by modifying their outer surface (Berardi et al., 2018; Bruckman et al., 2016, 2013; Thuenemann et al., 2021; Wicki et al., 2015), but also their inner cavity (Gleba et al., 2007), taking advantage of their nature as nucleic acid carriers used for targeted delivery (Venkataraman and Hefferon, 2021).

Plant VNPs applications expand from biomedicine (Sainsbury et al., 2010), agriculture to deal with pests (Cao et al., 2015), to the more new approaches in electronics (Shukla et al., 2020a). So far, many plant viruses have been widely engineered for biotechnological purposes, either rod-shaped or icosahedral viruses, mainly to produce therapeutic proteins or vaccine candidates in the case of TMV (Bruckman et al., 2016; Pitek et al., 2016), PVX (Esfandiari et al., 2016; Shukla et al., 2020b), CMV , pepino mosaic virus (Le et al., 2019b), TuMV (Frías-Sánchez et al., 2021; Yuste-Calvo et al., 2019a, 2019b), turnip yellow mosaic virus (TYMV) (Kim et al., 2018), cowpea chlorotic mottle virus (CCMV) (Cai et al., 2020, 2019) or CPMV (Berardi et al.,

2018; Ortega-Rivera et al., 2021; Peyret et al., 2022; Yildiz et al., 2013). In biomedicine, plant viruses have been widely developed as vaccine candidates, for gene therapy, for targeting particular cells and tissues with therapeutics, as well as for imaging carrying fluorescent labels or contrast agents (Shukla et al., 2020a). Although less numerous, there are already several reports about VNPs and their use in agriculture. Namely, plant VNPs can be loaded with small interfering RNAs (siRNAs) to silence target genes in insects (Abrahamian et al., 2020), as toxin vehicle for insects (Bonning et al., 2014) or as pesticide carriers against nematodes (Cao et al., 2015).

Initial focus was on icosahedral VNPs. However, icosahedral viruses display limitations for peptide display due to the geometry of the particles. In order to display more units per particle, elongated viruses can be used. Their capsids contain a larger number of CP units with helical symmetry (González-Gamboa et al., 2017). Many proof-of-concept works highlight the potential of filamentous plant virus nanotechnologies, particularly for targeting protein drug delivery for cancer therapy. These include some examples with TMV (Czapar et al., 2016; Shukla et al., 2020a), and PVX that was used for tissue-specific imaging and drug delivery (Le et al., 2019a, 2019b; Shukla et al., 2020b). VLPs derived from TuMV were also functionalized to display antigens as potential diagnostic and treatment tools in inflammatory processes or autoimmune diseases (Yuste-Calvo et al., 2019b).

NANOBODIES

Within the great variety of products with significant interest to be produced in plant molecular farming purposes, antibodies have stood out in the market for their diagnostic and therapeutic applications. Antibodies or immunoglobulins are soluble glycoproteins produced by B lymphocytes and play a key role in the vertebrate immune system. Their natural function is recognizing with high specificity foreign molecules or antigens to neutralize or eliminate them from the body. Antibodies have a conserved heterotetrameric architecture composed of two identical heavy chains (variable-V_H and constant heavy-C_H 1/2/3 domains) and two identical light chains (variable-V_L and constant light-C_L domain) connected with disulfide bonds (Figure 14A). Each B cell produces an antibody of a single antigen specificity, also known as a monoclonal

antibody. These have been employed for decades in clinical practice for the treatment of numerous cancer, infectious or autoimmune diseases (Lu et al., 2020) and even for delivering specifically a therapeutic drug to its target (Jovčevska and Muyldermans, 2020).

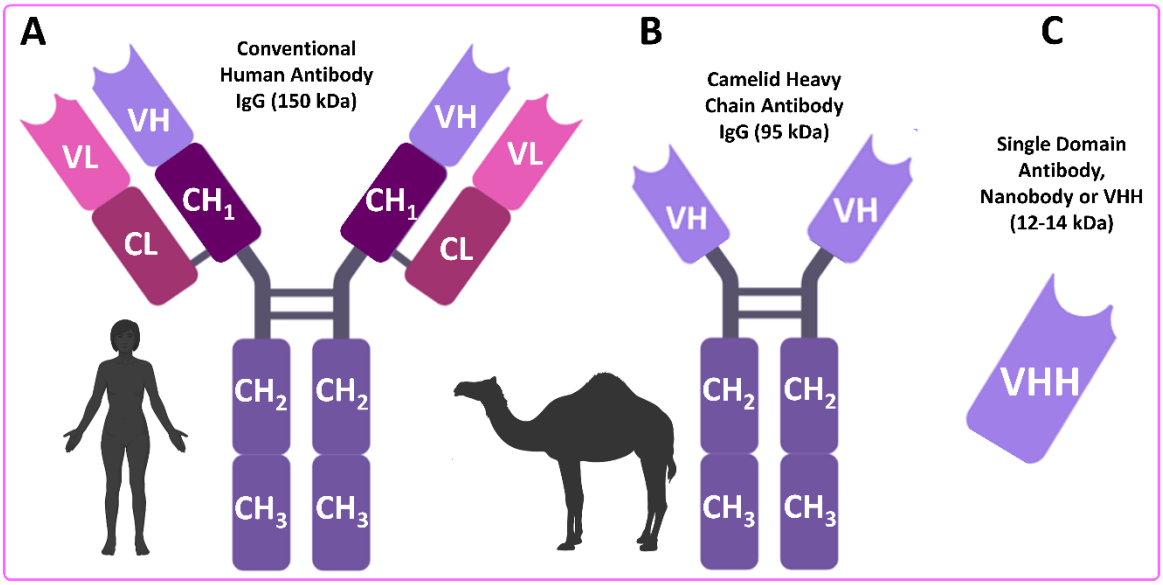

Figure 14. Comparison of human and camelid antibodies, and nanobodies. Variable (V), constant (C), heavy (H) and light (L) domains are indicated.

In addition to full-size monoclonal antibodies, smaller antibody fragments capable of antigen binding are also actively studied and employed in medicine and research (Yusibov et al., 2016). Nearly 30 years ago, the discovery that camelids (e.g., camels, dromedaries and llamas) naturally produce a unique type of antibody that is exclusively composed of heavy chains was a major breakthrough (Jovčevska and Muyldermans, 2020). These was later also observed in some shark species (Bailon Calderon et al., 2020). Besides conventional antibodies, these animals produce smaller heavy-chain-only antibodies (HCAbs) (~95 kDa), lacking light chains and also the C_H1 domain within the heavy chain (Figure 14B) (Edgue et al., 2017; Harmsen and De Haard, 2007) (Bailon Calderon et al., 2020).

HCAbs have a single variable antigen-binding domain (VHH), also known as nanobody (Figure 14C) (Wang et al., 2021). Nanobodies with 12–15 kDa, are the smallest known functional antigen-binding proteins (De Meyer et al., 2014; Harmsen and De Haard, 2007; Hemmer et al., 2018; Salema and Fernández, 2017; Wang et al.,

2016b; Yusibov et al., 2016). Due to this particular characteristic, nanobodies are extensively used in research, in medicine as diagnostics or therapeutics, agriculture or industry (De Meyer et al., 2014; Edgue et al., 2017). In biomedicine, nanobodies are attractive as diagnostics for non-invasive imaging to track the distribution of the disease (Rashidian and Ploegh, 2020; Sharifi et al., 2021), and also as therapeutics against different types of cancer, infectious diseases, autoimmune or neurological disorders (Bruckman et al., 2016; Muyldermans, 2021; Salema et al., 2016; Yusibov et al., 2016) or envenoming from snakes (Bailon Calderon et al., 2020). Furthermore, in the current COVID-19 pandemic, passive immunization is being studied with the development of neutralizing nanobodies, which target the receptor binding domain of the SARS-CoV-2 S protein (Koenig et al., 2021) (Sun et al., 2021).

Nanobodies show many advantageous features over conventional antibodies (Altunay et al., 2021), which makes them a preferable vehicle in nanotechnology. First, nanobodies are ten times smaller, with deeper penetration ability into tissues, maintaining a high antigen-binding affinity (Bailon Calderon et al., 2020) and high stability and solubility (Wang et al., 2021). Furthermore, nanobodies have the ability to withstand harsh conditions (e.g temperature, chaotropic agents and extremes pH), which probably result from their monomeric structure and efficient refolding capability after denaturation without compromising their antigen-binding capacity (Wang et al., 2021). The low molecular weight of nanobodies causes its rapid clearance through the kidneys and therefore a very short half-life. In order to increase its stability or half-life, nanobody conjugation to nanoparticles can be advantageous (Altunay et al., 2021; Jovčevska and Muyldermans, 2020). For such purposes, nanocarriers as liposomes, micelles and albumin nanoparticles have been introduced (Jovčevska and Muyldermans, 2020; Sharifi et al., 2021). Therefore, plant VNPs if engineered to display nanobodies can be tremendously useful for different targeted purposes (Bruckman et al., 2013; Thuenemann et al., 2021).regarding the easy, safe and scalable protein production in biofactory plants (Altunay et al., 2021; Edgue et al., 2017; Schillberg et al., 2003; Yusibov et al., 2016).

OBJECTIVES

The world is currently facing several challenges as climate change, habitat degradation or rapid human population growth and food insecurity. There is no doubt that plants are key in ecosystems and for our daily life. We are witnessing unprecedented technological and scientific breakthroughs that offer great promise toward overcoming these hurdles. In this sense, recent studies support that plants can also represent excellent biofactories from which products of interest can be obtained in a sustainable manner, including valuable proteins or metabolites of pharmaceutical or industrial interest. Plant production as heterologous expression systems arise with many advantages compared to traditional approaches. Among the techniques available in the plant molecular farming toolbox, viral vectors have gained remarkable interest. Plant viruses, besides causing tremendous losses in agriculture, due to their fascinating biological properties, can be converted into outstanding biotechnological tools. This Thesis has aimed to developing plant virus-based vectors to produce metabolites and nanoparticles of biotechnological interest in plants. More specifically, the objectives of this work have been:

1. To manipulate the carotenoid biosynthesis pathway in *Nicotiana benthamiana* using a potyvirus vector in order to obtain the appreciated saffron apocarotenoids.

2. To target the endogenous *N. benthamiana* phenylpropanoid biosynthesis pathway using viral vectors to produce curcuminoids.

3. To produce in zucchini (*Cucurbita pepo* L.) or *N. benthamiana* plants genetically encoded potyvirus-derived nanoparticles decorated with nanobodies.

CHAPTER 1

Efficient production of saffron crocins and picrocrocin in *Nicotiana benthamiana* using a virus-driven system

CHAPTER 1

Efficient production of saffron crocins and picrocrocin in *Nicotiana benthamiana* using a virus-driven system

Maricarmen Martí [a], Gianfranco Diretto [b], Verónica Aragonés [a], Sarah Frusciante [b], Oussama Ahrazem [c], Lourdes Gómez-Gómez [c], José-Antonio Daròs [a]

[a] Instituto de Biología Molecular y Celular de Plantas (Consejo Superior de Investigaciones Científicas-Universitat Politècnica de València), 46022, Valencia, Spain.

[b] Italian National Agency for New Technologies, Energy, and Sustainable Development, Casaccia Research Centre, 00123, Rome, Italy.

[c] Instituto Botánico, Departamento de Ciencia y Tecnología Agroforestal y Genética, Facultad de Farmacia, Universidad de Castilla-La Mancha, Campus Universitario S/ n, 02071, Albacete, Spain.

Adapted from the article published in 2020 at:
Metabolic Engineering 61 (2020) 238–250. DOI: 10.1016/j.ymben.2020.06.009

https://doi.org/10.1016/j.ymben.2020.06.009

Author contributions: all authors contributed to experiment design, performed experiments and analyzed the results. JAD, LGG, GD and MM wrote the manuscript with inputs from the rest of the authors. All authors reviewed and approved the published version of the manuscript.

ABSTRACT

Crocins and picrocrocin are glycosylated apocarotenoids responsible, respectively, for the color and the unique taste of the saffron spice, known as red gold due to its high price. Several studies have also shown the health-promoting properties of these compounds. However, their high costs hamper the wide use of these metabolites in the pharmaceutical sector. We have developed a virus-driven system to produce remarkable amounts of crocins and picrocrocin in adult *Nicotiana benthamiana* plants in only two weeks. The system consists of viral clones derived from tobacco etch potyvirus that express specific carotenoid cleavage dioxygenase (CCD) enzymes from *Crocus sativus* and *Buddleja davidii*. Metabolic analyses of infected tissues demonstrated that the sole virus-driven expression of *C. sativus* CsCCD2L or *B. davidii* BdCCD4.1 resulted in the production of crocins, picrocrocin and safranal. Using the recombinant virus that expressed CsCCD2L, accumulations of 0.2% of crocins and 0.8% of picrocrocin in leaf dry weight were reached in only two weeks. In an attempt to improve apocarotenoid content in *N. benthamiana*, co-expression of CsCCD2L with other carotenogenic enzymes, such as *Pantoea ananatis* phytoene synthase (PaCrtB) and saffron β-carotene hydroxylase 2 (BCH2), was performed using the same viral system. This combinatorial approach led to an additional crocin increase up to 0.35% in leaves in which CsCCD2L and PaCrtB were co-expressed. Considering that saffron apocarotenoids are costly harvested from flower stigma once a year, and that *Buddleja* spp. flowers accumulate lower amounts, this system may be an attractive alternative for the sustainable production of these appreciated metabolites.

Keywords: Apocarotenoids, crocins, picrocrocin, carotenoid cleavage dioxygenase, viral vector, tobacco etch virus, potyvirus.

1. INTRODUCTION

Plants possess an extremely rich secondary metabolism and, in addition to food, feed, fibers and fuel, also provide highly valuable metabolites for food, pharma and chemical industries. However, some of these metabolites are sometimes produced in

very limiting amounts. Plant metabolic engineering can address some of these natural limitations for nutritional improvement of foods or to create green factories that produce valuable compounds (Martin and Li, 2017; Yuan and Grotewold, 2015). Yet, the complex regulation of plant metabolic pathways and the particularly time-consuming approaches for stable genetic transformation of plant tissues highly limit quick progress in plant metabolic engineering. In this context, virus-derived vectors that fast and efficiently deliver biosynthetic enzymes and regulatory factors into adult plants may significantly contribute to solve some challenges (Sainsbury et al., 2012).

Carotenoids constitute an important group of natural products that humans cannot biosynthesize and must uptake from the diet. These compounds are synthesized by higher plants, algae, fungi and bacteria (Rodriguez-Concepcion et al., 2018). Yet, they play multiple roles in human physiology (Fiedor and Burda, 2014). Carotenoids are widely used as food colorants, nutraceuticals, animal feed, cosmetic additives and health supplements (Fraser and Bramley, 2004). In all living organisms, carotenoids act as substrates for the production of apocarotenoids (Ahrazem et al., 2016a). These are not only the simple breakdown products of carotenoids, as they act as hormones and are involved in signaling (Eroglu and Harrison, 2013; Jia et al., 2018; Walter et al., 2010). Apocarotenoids are present as volatiles, water soluble and insoluble compounds, and among those soluble, crocins are the most valuable pigments used in the food, and in less extent, in the pharmaceutical industries (Ahrazem et al., 2015). Crocins are glycosylated derivatives of the apocarotenoid crocetin. They are highly soluble in water and exhibit a strong coloring capacity. In addition, crocins are powerful free radical quenchers, a property associated to the broad range of health benefits they exhibit (Bukhari et al., 2018; Christodoulou et al., 2015; Georgiadou et al., 2012; Nam et al., 2010). The interest in the therapeutic properties of these compounds is increasing due to their analgesic and sedative properties (Amin and Hosseinzadeh, 2012), and neurological protection and anticancer activities (Finley and Gao, 2017; Skladnev and Johnstone, 2017). Further, clinical trials indicate that crocins have a positive effect in the treatment of depression and dementia (Lopresti and Drummond, 2014; Mazidi et al., 2016). Other apocarotenoids, such as safranal (2,6,6-trimethyl-1,3-cyclohexadiene-1-carboxaldehyde) and its precursor picrocrocin (β-D-glucopyranoside of hydroxyl-β-cyclocitral), have also been shown to

reduce the proliferation of different human carcinoma cells (Cheriyamundath et al., 2018; Jabini et al., 2017; Kyriakoudi et al., 2015) and to exert anti-inflammatory effects (Zhang et al., 2015).

Crocus sativus L. is the main natural source of crocins and picrocrocin, respectively responsible for the color and flavor of the highly appreciated spice, saffron (Tarantilis et al., 1995). Crocin pigments accumulate at huge levels in the flower stigma of these plants conferring this organ with a distinctive dark red coloration (Moraga et al., 2009). Yet, these metabolites reach huge prices in the market, due to the labor intensive activities associated to harvesting and processing the stigma collected from *C. sativus* flowers (Ahrazem et al., 2015). Besides *C. sativus*, gardenia (*Gardenia* spp.) fruits are also a commercial source of crocins, but at much lower scale. In addition, gardenia fruits do not accumulate picrocrocin (Moras et al., 2018; Pfister et al., 1996). Some other plants, such as *Buddleja* spp., also produce crocins, although they are not commercially exploited due to low accumulation (Liao et al., 1999). All these plants share the common feature of expressing carotenoid cleavage dioxygenase (CDD) activities, like the saffron CsCCD2L or the CCD4 subfamily recently identified in *Buddleja* spp. (Ahrazem et al., 2017).

In *C. sativus* and *Buddleja* spp., zeaxanthin is the precursor of crocetin (Fig. 1). Cleavage of the zeaxanthin molecule at the 7,8 and 7′,8′ double bonds render one molecule of crocetin dialdehyde and two molecules of 4-hydroxy-2,6,6-trimethyl-1-cyclohexene-1-carboxaldehyde (HTCC) (Ahrazem et al., 2017, 2016c; Frusciante et al., 2014). Crocetin dialdehyde is further transformed to crocetin by the action of aldehyde dehydrogenase (ALDH) enzymes (Demurtas et al., 2018; Gómez-Gómez et al., 2017, 2018). Next, crocetin serves as substrate of glucosyltransferase (UGT) activities that catalyze the production of crocins through transfer of glucose to both ends of the molecule (Côté et al., 2001; Demurtas et al., 2018; Moraga et al., 2004; Nagatoshi et al., 2012). The HTCC molecule is also recognized by UGTs, resulting in production of picrocrocin (Fig. 1) (Diretto et al., 2019a). In *C. sativus*, the plastidic CsCCD2L enzyme catalyzes the cleavage of zeaxanthin at 7,8;7′,8′ double bonds (Ahrazem et al., 2016c; Frusciante et al., 2014), which is closely related to the CCD1 subfamily (Ahrazem et al., 2016b, 2016a). In *Buddleja davidii*, the CCD enzymes that catalyze the same reaction belong to a novel group within the CCD4 subfamily of CCDs (Ahrazem et al., 2016a).

These *B. davidii* enzymes, BdCCD4.1 and BdCCD4.3, also localize in plastids and are expressed in the flower tissue (Ahrazem et al., 2017).

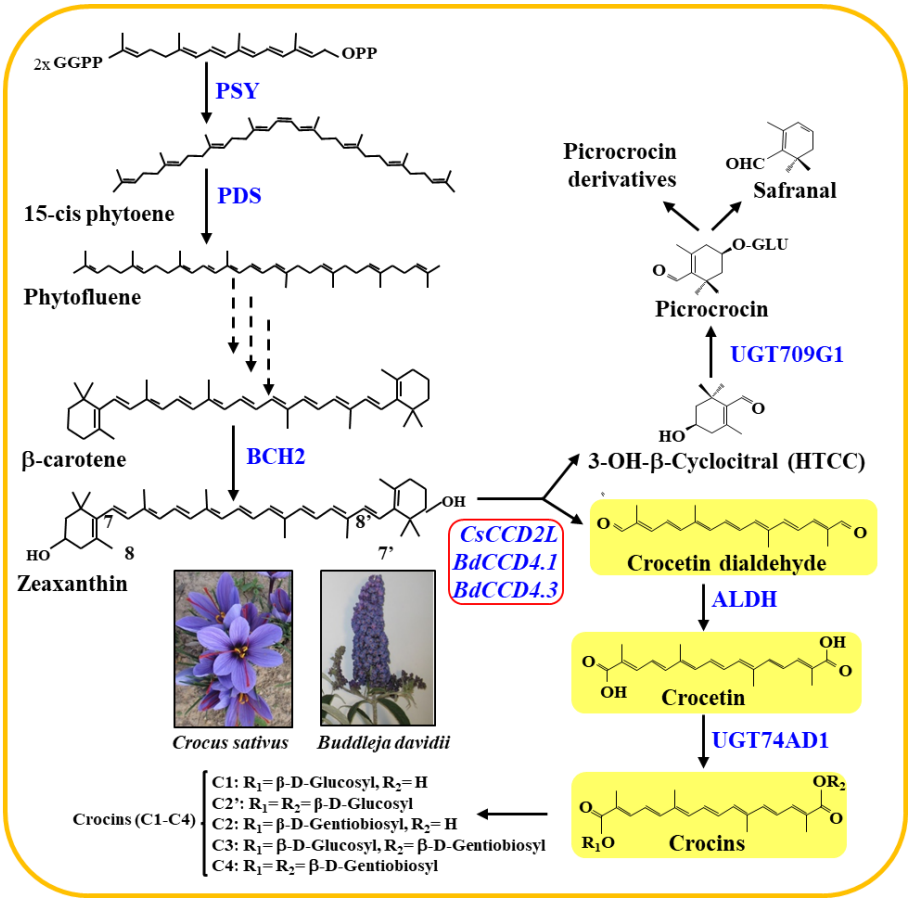

Fig. 1. Schematic overview of the crocins biosynthesis pathway in *C. sativus* and *B. davidii*. PSY, phytoene synthase; PDS, phytoene desaturase; BCH2, carotene hydroxylase 2; CsCCD2L, *C. sativus* carotenoid cleavage dioxygenase 2L; BdCCD4.1 and 4.3, *B. davidii* carotenoid cleavage dioxygenases 4.1 and 4.3; ALDH, aldehyde dehydrogenase; UGT74AD1, UDP-glucosyltransferase 74AD1. Five most common sugar combinations (R1 and R2) in crocins (C1 to C4) are also shown. Activities expressed in *N. benthamiana* are boxed in red.

Due to its high scientific and commercial interest, crocetin and crocins biosynthesis has arisen great attention, and attempts to metabolically engineer their pathway in microbial systems have been reported, although with limited success (Chai et al., 2017; Diretto, Ahrazem, et al., 2019; Tan et al., 2019; Wang et al., 2019). More in detail, the use of the saffron CsCCD2L enzyme resulted in a maximum accumulation of 1.22 mg/l, 15.70 mg/l, and 4.42 mg/l of crocetin in, respectively, *Saccharomyces cerevisiae* (Chai et al., 2017; Tan et al., 2019) and *Escherichia coli* (Wang et al., 2019). In a subsequent study aimed to confirm, *in planta*, the role of a novel UGT in picrocrocin biosynthesis (Diretto et al., 2019a), *Nicotiana benthamiana* leaves were transiently

transformed, *via Agrobacterium tumefaciens*, with CsCCD2L, alone or in combination with UGT709G1, which led to the production of 30.5 µg/g dry weight (DW) of crocins, with a glycosylation degree ranging from 1 to 4 (crocin 1-4) (unpublished data). Although promising, these results cannot be considered efficient and sustainable in the context of the development of an industrial system for the production of the saffron high-valued apocarotenoids.

Here we used a viral vector derived from *Tobacco etch virus* (TEV, genus *Potyvirus*; family *Potyviridae*) (Bedoya et al., 2010) to transiently express a series of CCD enzymes, alone or in combination with other carotenoid and non-carotenoid biosynthetic enzymes, in *N. benthamiana* plants. Interestingly, tissues infected with viruses that expressed CsCCD2L or BdCCD4.1 acquired yellow pigmentation visible to the naked eye. Metabolite analyses of these tissues demonstrated the accumulation of crocins and picrocrocin, reaching levels attractive enough for their commercial production, up to 0.35% and 0.8% of DW, respectively, in leaves in which CsCCD2L and *Pantoea ananatis* phytoene synthase (PaCrtB) were simultaneously expressed.

2. MATERIALS AND METHODS

2.1. Plasmid construction

Plasmids were constructed by standard molecular biology techniques, including PCR amplifications of cDNAs with the high-fidelity Phusion DNA polymerase (Thermo Scientific) and Gibson DNA assembly (Gibson et al., 2009), using the NEBuilder HiFi DNA Assembly Master Mix (New England Biolabs). To generate a transformed *N. benthamiana* line that stably expresses TEV nuclear inclusion *b* (NIb), we built the plasmid p235KNIbd. This plasmid is a derivative of pCLEAN-G181 (Thole et al., 2007) and between the left and right borders of *A. tumefaciens* transfer DNA (T-DNA) contains two in tandem cassettes in which the neomycin phosphotransferase (NPTII; kanamycin resistance) and the TEV NIb are expressed under the control of *Cauliflower mosaic virus* (CaMV) 35S promoter and terminator. The exact nucleotide sequence of the p235KNIbd T-DNA is in Supplementary Fig. S1. Plasmids pGTEVΔNIb-CsCCD2L, -BdCCD4.1, -BdCCD4.3, -CsCCD2L/PaCrtB, -CsCCD2L/CsBCH2 and -

CsCCD2L/CsLPT1 were built on the basis of pGTEVa (Bedoya et al., 2012) that contains a wild-type TEV cDNA (GenBank accession number DQ986288 with the two silent and neutral mutations G273A and A1119G) flanked by the CaMV 35S promoter and terminator in a binary vector that also derives from pCLEAN-G181. These plasmids were built, as explained above, by PCR amplification of CsCCD2L (Ahrazem et al., 2016c), BdCCD4.1 and BdCCD4.3 (Ahrazem et al., 2017), PaCrtB (Majer et al., 2017), β-carotene hydroxylase 2 (CsBCH2) (Castillo et al., 2005) and CsLPT1 (Gómez-Gómez et al., 2010) cDNAs and assembly into a pGTEVa version in which the NIb cistron was deleted (pGTEVaΔNIb) (Majer et al., 2015). The exact sequences of the TEV recombinant clones (TEVΔNIb-CsCCD2L, -BdCCD4.1, -BdCCD4.3, -CsCCD2L/PaCrtB, -CsCCD2L/CsBCH2 and -CsCCD2L/CsLPT1) contained in the resulting plasmids are in Supplementary Fig. S2. The plasmid expressing the recombinant TEVΔNIb-aGFP clone (Supplementary Fig. S2) was previously described (Majer et al., 2015).

2.2. Plant transformation

The LBA4404 strain of *A. tumefaciens* was sequentially transformed with the helper plasmid pSoup (Hellens et al., 2000) and p235KNIbd. Clones containing both plasmids were selected in plates containing 50 μg/ml rifampicin, 50 μg/ml kanamycin and 7.5 μg/ml tetracycline. A liquid culture grown from a selected colony was used to transform *N. benthamiana* (Clemente, 2006). Briefly, *N. benthamiana* leaf explants were incubated with the *A. tumefaciens* culture at an optical density (600 nm) of 0.5 for 30 min and then incubated on solid media. Four days later, explants were transferred to plates with organogenesis media containing 100 μg/ml of kanamycin. Explants were repeatedly transferred to fresh organogenesis plates every three weeks until shoots emerged. These shoots were first transferred to rooting media and, when roots appeared, cultivated in a greenhouse with regular soil until seeds were harvested. Transformation with the *NIb* cDNA was confirmed by PCR. Batches of seedlings from four independent transformed lines were screened for efficient complementation of TEV clones lacking NIb by mechanical inoculation of TEVΔNIb-Ros1 (Bedoya et al., 2010).

2.3. Plant inoculation

A. tumefaciens C58C1 competent cells, previously transformed with the helper plasmid pCLEAN-S48 (Thole et al., 2007), were electroporated with different plasmids that contained the TEV recombinant clones and selected in plates with 50 µg/ml rifampicin, 50 µg/ml kanamycin and 7.5 µg/ml tetracycline. Liquid cultures of selected colonies were brought to an optical density of 0.5 (600 nm) in agroinoculation solution (10 mM MES-NaOH, pH 5.6, 10 mM $MgCl_2$ and 150 µM acetosyringone) and incubated for 2 h at 28ºC. Using a needleless syringe, these cultures were used to infiltrate one leaf of five-week-old plants of the selected *N. benthamiana* transformed line that stably expresses TEV NIb. After inoculation, plants were kept in a growth chamber at 25ºC under a 12 h day-night photoperiod with an average photon flux density of 240 $\mu mol \cdot m^{-2} \cdot s^{-1}$. Leaves were collected at different days post-inoculation (dpi) as indicated; in the case of the time-course experiments, leaf samples were collected at 8 time-points (0, 4, 8, 11, 13, 15, 18 and 20 dpi).

2.4. Analysis of virus progeny

Viral progeny was analyzed by reverse transcription (RT)-PCR using RevertAid reverse transcriptase (Thermo Scientific) and Phusion DNA polymerase followed by electrophoretic separation of the amplification products in 1% agarose gels that were stained with ethidium bromide. RNA from *N. benthamiana* plants was purified from upper non-inoculated leaves at 15 dpi using silica-gel columns (Zymo Research). For virus infection diagnosis, a cDNA corresponding to the TEV coat protein (CP) cistron (804 bp) was amplified. Aliquots of the RNA preparations were subjected to RT using primer PI (5'-CTCGCACTACATAGGAGAATTAGAC-3'), followed by PCR amplification with primers PII (5'-AGTGGCACTGTGGGTGCTGGTGTTG-3') and PIII (5'-CTGGCGGACCCCTAATAG-3'). To analyze the potential deletion of the inserted *CDD* cDNAs, RNA aliquots were reverse transcribed using primer PIV (5'-GCTGTTTGTCACTCAATGACACATTAT-3') and amplified by PCR with primers PV (5'-AAAATAACAAATCTCAACACAACATATAC-3') and PVI (5'-CCGCGGTCTCCCCATTATGCACAAGTTGAGTGGTAGC-3').

2.5. Metabolite extraction and analysis

Polar and apolar metabolites were extracted from 50 mg of lyophilized leaf tissue. For polar metabolites analyses (crocins and picrocrocin), the tissues were extracted in cold 50% methanol. The soluble fraction was analyzed by high performance liquid chromatography-diode array detector-high resolution mass spectrometry (HPLC-DAD-HRMS) and HPLC-DAD (Ahrazem et al., 2018; Moraga et al., 2009). The liposoluble fractions (crocetin, HTCC, 3-OH-β-cyclocitral, carotenoids and chlorophylls) were extracted with 0.5:1 ml cold extraction solvents (50:50 methanol and $CHCl_3$), and analyzed by HPLC-DAD-HRMS and HPLC-DAD as previously described (Ahrazem et al., 2018; Castillo et al., 2005; D'Esposito et al., 2017; Fasano et al., 2016). Metabolites were identified as previously described (Demurtas et al., 2019), on the basis of absorption spectra and retention times relative to standard compounds when available (trans- and cis-crocin 3 and trans-crocin 4). Metabolite identity was confirmed by accurate m/z masses and experimental m/z fragmentation. The cis configuration was recognition by the exhibition of a broader absorption peak in the range of 260-300 nm.

Pigments were quantified by integrating peak areas that were converted to concentrations in comparison with authentic standards. or were normalized to the ion peak area of the internal standard (formononetin; fold internal standard). Chlorophyll a and b were determined by measuring absorbance at 645 nm and 663 nm as previously described (Richardson et al., 2002). Mass spectrometry carotenoid, chlorophyll derivative and apocarotenoid identification and quantification was carried out as previously described (Ahrazem et al., 2018; Diretto et al., 2019a; Rambla et al., 2016). Mass spectrometry analysis of other isoprenoids (tocochromanols and quinones) were performed as reported before (Sulli et al., 2017). Picrocrocin derivatives, as previously reported (D'Archivio et al., 2016; Moras et al., 2018), were tentatively identified according to their m/z accurate masses as included in the PubChem database for monoisotopic masses or by using the Mass Spectrometry Adduct Calculator from the Metabolomics Fiehn Lab for adduct ions; and were further validated by isotopic pattern ratio and the comparison between theoretical and experimental m/z fragmentation, by using the MassFrontier 7.0 software (Thermo Fisher Scientific).

2.6. Subcellular localization of crocins

N. benthamiana plants were mock-inoculated or infected with TEVΔNIb-CsCCD2L or TEVΔNIb. Eleven dpi, symptomatic leaves from these plants were infiltrated with *A. tumefaciens* harboring a construct to express the γ tonoplast intrinsic protein (γTIP), fused to mCherry (γTIP-mCherry) (Demurtas et al., 2019). Two days after this infiltration, 13 days after viral inoculation, to determine the subcellular localization of crocins in *N. benthamiana* tissues, laser scanning confocal microscopy (LSCM) was performed using a Zeiss 7080 Axio Observer equipped with a C-Apochromat 40X/1.20 W corrective water immersion objective lens. For the multicolor detection of crocins and chlorophylls, as well as the red fluorescence from mCherry, imaging was performed using the sequential channel acquisition mode. A 458-nm laser was used for excitation of crocins and chlorophylls autofluorescence, which was detected between 465 to 620 nm and 690 to 740 nm, respectively. mCherry was excited with a 561-nm laser and detected between 590 to 640 nm. Images were processed using the FIJI software (http://fiji.sc/Fiji).

2.7. Statistics and bioinformatics

Statistical validation of the data (ANOVA+ Tukey's t-test) and heatmap visualization were performed as previously described (Cappelli et al., 2018; Grosso et al., 2018).

3. RESULTS

3.1. TEV recombinant clones that express CCD enzymes in N. benthamiana

The goal of this work was to develop a heterologous system to efficiently produce highly appreciated and scarce apocarotenoids in plant tissues. For this purpose, we planned to use an expression vector derived from TEV, more specifically TEVΔNIb (Bedoya et al., 2010), recently employed to rewire the lycopene biosynthetic pathway from the plastid to the cytosol of plant cells (Majer et al., 2017). Since CCD is

the first enzyme in the apocarotenoid biosynthetic pathway (Fig. 1), we started exploring the virus-based expression of a series of CCD enzymes from well-known crocins producing plants: namely *C. sativus* CsCCD2L (Ahrazem et al., 2016c), and *B. davidii* BdCCD4.1 and BdCCD4.3 (Ahrazem et al., 2017).

In TEVΔNIb, the approximately 1.6 kb corresponding to the NIb cistron, coding for the viral RNA-dependent RNA polymerase, is deleted to increase the space to insert foreign genetic information. Then, the viral recombinant clones only infect plants in which NIb is supplied in *trans* (Bedoya et al., 2010). We chose *N. benthamiana* as the biofactory plant for apocarotenoid production because of the amenable genetic transformation, the high amounts of biomass achievable and the fast growth. For this aim, as the first step in our work, we transformed *N. benthamiana* leaf tissue using *A. tumefaciens* and regenerated adult plants that constitutively expressed TEV NIb under the control of CaMV 35S promoter and terminator. To screen for transformed lines that efficiently complemented TEVΔNIb deletion mutants, we inoculated the plants with TEVΔNIb-Ros1, a viral clone in which the NIb cistron was replaced by a cDNA encoding for the MYB-type transcription factor Rosea1 from *Antirrhinum majus* L., whose expression induces accumulation of colored anthocyanins in infected tissues and facilitates visual tracking of infection (Bedoya et al., 2010; Bedoya et al., 2012). On the basis of anthocyanin accumulation, we selected a *N. benthamiana* transformed line that efficiently complemented the replication and systemic movement of TEVΔNIb-Ros1 (Supplementary Fig. S3). Then, by self-pollination and TEVΔNIb-Ros1 inoculation of the progeny, we selected a transformed homozygous line that was used in all subsequent experiments.

Next, on the context of a TEV lacking NIb, we constructed three recombinant clones (Fig. 2A) to express *C. sativus CsCCD2L* (TEVΔNIb-CsCCD2L), *B. davidii BdCCD4.1* and *BdCCD4.3* (TEVΔNIb-BdCCD4.1 and TEVΔNIb-BdCCD4.3). These CCDs are plastidic enzymes that are encoded in the nucleus and contain native amino-terminal transit peptides. To target these enzymes to plastids, we inserted their cDNAs in a position corresponding to the amino terminus of the viral polyprotein in the virus genome (Majer et al., 2015). CCD cDNAs also contained a sequence corresponding to an artificial NIa protease (NIaPro) cleavage site at the 3' end to mediate the release of the heterologous protein from the viral polyprotein. Based on previous observations,

we used the -8/+3 site that splits NIb and CP in TEV. The exact sequences of these clones are in Supplementary Fig. S2.

Finally, transformed *N. benthamiana* plants that express NIb were agroinoculated with the three TEV recombinant clones. As a control in this experiment, some plants were agroinoculated with TEVΔNIb-aGFP (Fig. 2A and Supplementary Fig. S2), which is a recombinant clone that expresses GFP from the amino-terminal position in the viral polyprotein. Interestingly, 7 dpi, even before symptoms were observed, we noticed a distinctive yellow pigmentation in systemic tissues of the plants agroinoculated with TEVΔNIb-CsCCD2L. Symptoms of infection were soon observed (approximately 8 dpi) in plants agroinoculated with TEVΔNIb-aGFP, -CsCCD2L and -BdCCD4.1. Distinctive yellow pigmentation was also observed in symptomatic tissues of plants agroinoculated with TEVΔNIb-BdCCD4.1, although with some delay comparing to TEVΔNIb-CsCCD2L. Yellow pigmentation of symptomatic tissues in plants inoculated with TEVΔNIb-CsCCD2L was more intense than that in tissues of plants inoculated with TEVΔNIb-BdCCD4.1. Plants inoculated with TEVΔNIb-BdCCD4.3 showed mild symptoms of infection at approximately 13 dpi and yellow pigmentation was never observed. Fig. 2B shows pictures of representative leaves of all these plants at 13 dpi. RT-PCR analysis confirmed TEV infection in all inoculated plants (Fig. 2C).

Observation of symptomatic tissues with a fluorescence stereomicroscope confirmed expression of GFP only in plants inoculated with the TEVΔNIb-aGFP control (Supplementary Fig. S4). Analysis of viral progeny at 15 dpi by RT-PCR indicated that, while the inserts of TEVΔNIb-aGFP, -CsCCD2L are perfectly stable in the recombinant virus, those of TEVΔNIb-BdCCD4.1 and TEVΔNIb-BdCCD4.3 are partially and completely lost, respectively, at this time post-inoculation (Fig. 2D). Based on distinctive yellow color, these results suggested that the virus-driven expression of CsCCD2L or BdCCD4.1 in *N. benthamiana* tissues may induce apocarotenoid accumulation.

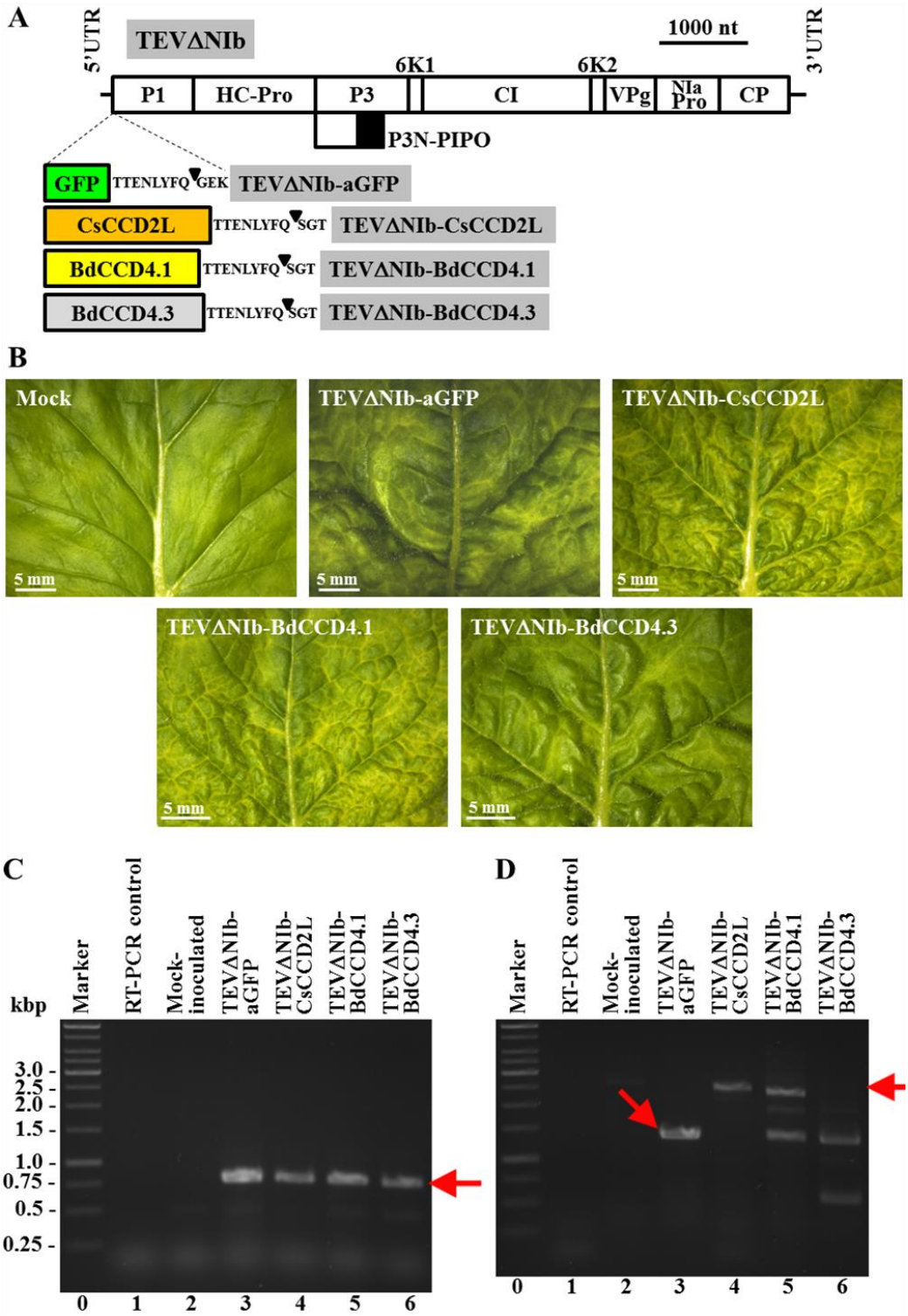

Fig. 2. Inoculation of *N. benthamiana* plants that stably express NIb with TEVΔNIb recombinant clones that express different CCDs. **(A)** Schematic representation of TEVΔNIb genome indicating the position where the GFP (green box) and the different CCDs (CsCCD2L, orange box; BdCCD4.1, yellow box; and BdCCD4.3, gray box) were inserted. The sequence of the artificial NIaPro cleavage site to mediate the release of the recombinant proteins from the viral polyprotein is also indicated. The black triangle indicates the exact cleavage site. Lines represent TEV 5' and 3' UTR and boxes represent P1, HC-Pro, P3, P3N-PIPO, 6K1, CI, 6K2, VPg, NIaPro and CP cistrons, as indicated. Scale bar corresponds to 1000 nt. **(B)** Pictures of representative leaves from plants mock-inoculated and agroinoculated with TEVΔNIb-aGFP,

TEVΔNIb-CsCCD2L, TEVΔNIb-BdCCD4.1 and TEVΔNIb-BdCCD4.3, as indicated, taken at 13 dpi. Scale bars correspond to 5 mm. **(C)** Virus diagnosis and **(D)** analysis of the progeny of recombinant TEV in *N. benthamiana* plants mock-inoculated and agroinoculated with TEVΔNIb-aGFP, TEVΔNIb-CsCCD2L, -BdCCD4.1 and -BdCCD4.3. RNA was extracted at 15 dpi and subjected to RT-PCR amplification. PCR products were separated in a 1% agarose gel that was stained with ethidium bromide. Representative samples of triplicate analyses are shown. (C and D) Lanes 0, DNA marker ladder with sizes (in bp) on the left; lanes 1, RT-PCR controls with no RNA added; lanes 2, mock-inoculated plants; lanes 3 to 6, plants inoculated with TEVΔNIb-aGFP (lanes 3), TEVΔNIb-CsCCD2L (lanes 4), TEVΔNIb -BdCCD4.1 (lanes 4) and TEVΔNIb -BdCCD4.3 (lanes 5). The arrows point to the bands corresponding to (C) the TEV CP, and (D) the full-length viral progenies cDNAs.

3.2. Analysis of apocarotenoids in infected tissues

Symptomatic leaf tissues from plants infected with TEVΔNIb-aGFP, TEVΔNIb-CsCCD2L and TEVΔNIb-BdCCD4.1 were subjected to extraction and analysis by HPLC-DAD-HRMS to determine their apocarotenoid and carotenoid profiles. Tissues from mock-inoculated controls were also included in the analysis. The tissues from the plants infected with TEVΔNIb-BdCCD4.3 were discarded due to the absence of pigmentation and rapid deletion of BdCCD4.3 cDNA in the viral progeny. Analysis of the polar fraction of tissues infected with TEVΔNIb-CsCCD2L and TEVΔNIb-BdCCD4.1 showed a series of peaks with maximum absorbance from 433 to 439 nm. These peaks were not observed in extracts from tissues from mock-inoculated plants or plants infected with the TEVΔNIb-aGFP control (Fig. 3). Mass spectrometry chromatograms evidenced the presence, for all the fore mentioned peaks, of the crocetin aglycon (m/z 329.1747 (M+H)), thus supporting the presence of crocins (Supplementary Fig. S5).

Further analyses of the sugar moieties conjugated with crocetin lead to the identification of crocins with different degrees of glycosylation from one glucose molecule to five in the infected tissues in which CCDs were expressed (Fig. 4A and Supplementary Table S1). However, predominant crocins were those conjugated with three and four glucose molecules. Interestingly, CCD-infected *N. benthamiana* leaves, displayed a different pattern of crocin accumulation compared to that typical from saffron stigma (Fig. 3A), with trans-crocin 4, followed by trans-crocin 3 and 2, being the most abundant crocin species. Minor changes were also observed between TEVΔNIb-CsCCD2L and TEVΔNIb-BdCCD4.1 samples (Supplementary Table S2): in the former, trans-crocin 3 was the most abundant (30.84%), followed by cis-crocin 4 (17.04%) and

trans-crocin 2 (16.84%); whereas similar amounts in cis-crocin 5, cis-crocin 4 and trans-crocin 3 were found in the latter (20.92, 20.62 and 18.31%, respectively). Picrocrocin, safranal and several derivatives were also identified in the polar fraction of tissues infected with TEVΔNIb-CsCCD2L and TEVΔNIb-BdCCD4.1 (Fig. 4B and Supplementary Table S1). All these polar apocarotenoids were absent in the control tissues non-infected and infected with TEVΔNIb-aGFP (Fig. 4B). Overall, and in agreement with the most intense visual phenotype, TEVΔNIb-CsCCD2L-infected tissues displayed a higher accumulation in all the linear and cyclic apocarotenoids than TEVΔNIb-BdCCD4.1-infected tissues (Fig. 4, Table 1 and Supplementary Table S1).

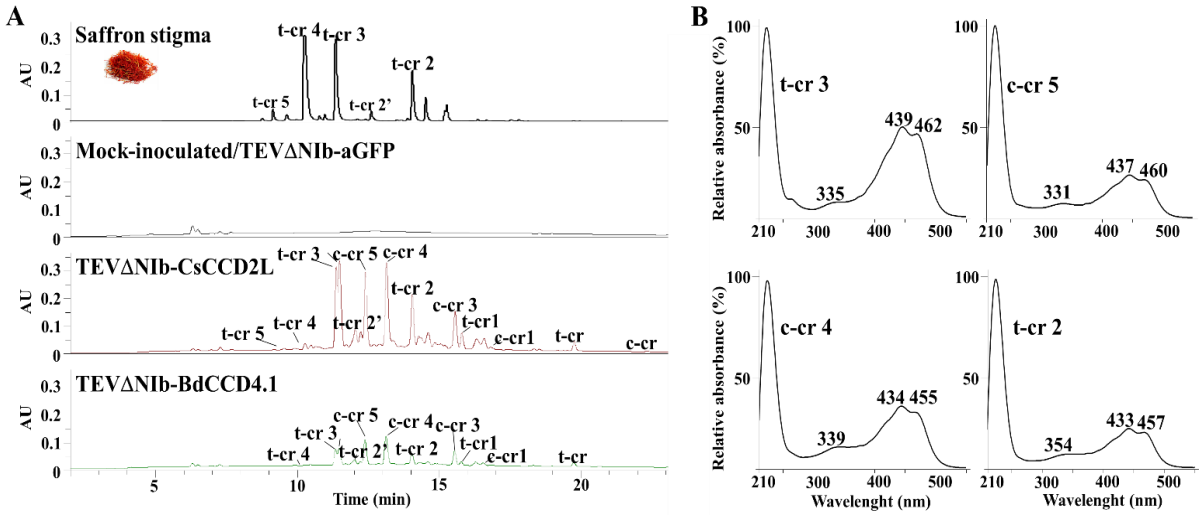

Fig. 3. Heterologous production of crocins in *N. benthamiana* tissues infected with recombinant viruses expressing CCD enzymes. **(A)** Chromatographic profile run on an HPLC-PDA-HRMS and detected at 440 nm of the polar fraction of tissues infected with TEVΔNIb-aGFP, TEVΔNIb-CsCCD2L and TEVΔNIb-BdCCD4.1. The profile of saffron stigma is also included as a control. Peaks abbreviations correspond to: c-cr, *cis*-crocetin; t-cr, *trans*-crocetin; c-cr1, *cis*-crocin 1; t-cr1, *trans*-crocin 1; t-cr2, *trans*-crocin 2; t-cr2', *trans*-crocin 2'; c-cr3, *cis*-crocin 3, t-cr3, *trans*-crocin 3; c-cr4, *cis*-crocin 4; t-cr4, *trans*-crocin 4; c-cr5, *cis*-crocin 5; t-cr5, *trans*-crocetin 5. **(B)** Absorbance spectra of the major crocins detected in the polar extracts of *N. benthamiana* tissues infected with TEVΔNIb-CsCCD2L and TEVΔNIb-BdCCD4.1. Analyses were performed at 13 dpi.

In the polar and apolar fractions of TEVΔNIb-CsCCD2L and TEVΔNIb-BdCCD4.1-infected leaves, we also detected the presence of crocetin dialdehyde and HTCC, which are the products of the enzymatic cleavage step, and crocetin and safranal, which are produced by the activity of ALDH enzymes and the spontaneous deglycosilation of picrocrocin, respectively (Fig. 4 and Supplementary Table S1). None

of these metabolites were found in the TEVΔNIb-aGFP-infected and mock-inoculated control tissues.

Table 1. Ratios of **(A)** crocins- and **(B)** picrocrocin-related apocarotenoid levels in tissues infected with TEVΔNIb-CsCCD2L and TEVΔNIb-BdCCD4.1.

A	CsCCD2L /BdCCD4.1
crocetin dialdehyde	3.206
cis-crocetin	1.139
trans-crocetin	1.113
cis-crocin 1	3.318
trans-crocin 1	1.755
trans-crocin 2	3.605
trans-crocin 2'	2.420
cis-crocin 3	2.137
trans-crocin 3	4.915
trans-crocin 4	5.580
cis-crocin 5	2.448
trans-crocin 5	-

B	CsCCD2L /BdCCD4.1
HTCC	1.573
picrocrocin isomer 1	4.237
picrocrocin isomer 2	1.405
picrocrocin-derivivative 4	8.577
picrocrocin-derivivative 7	6.474
safranal	3.805

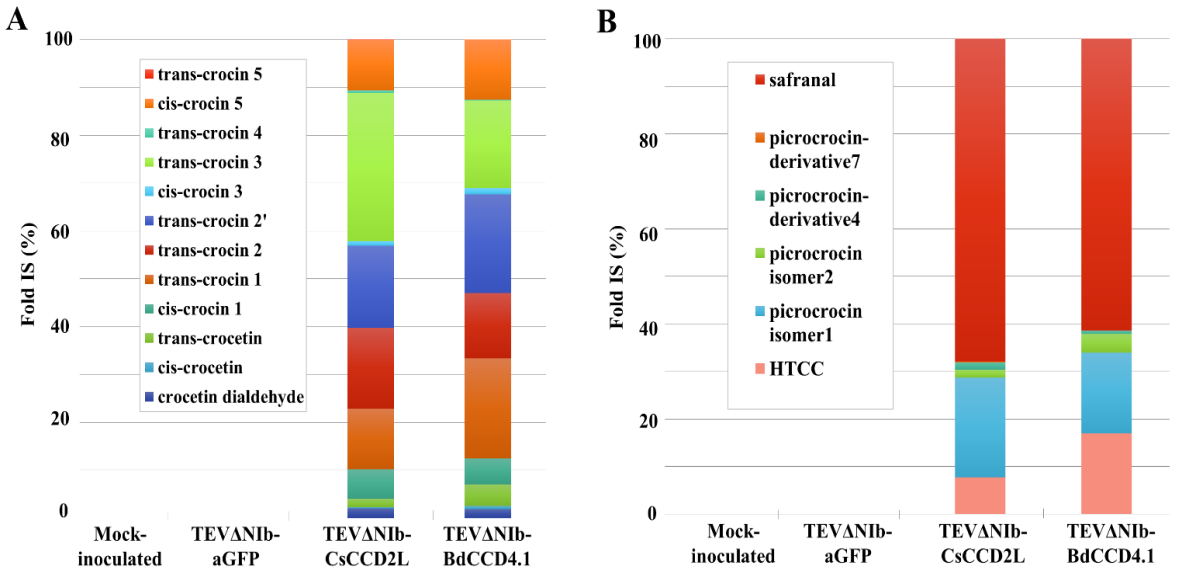

Fig. 4. Apocarotenoid content and composition of *N. benthamiana* tissues from mock-inoculated plants and plants infected with TEVΔNIb-aGFP, TEVΔNIb-CsCCD2L and TEVΔNIb-BdCCD4.1. **(A)** Crocetin dialdehyde, crocetin and crocins accumulation. **(B)** Levels of safranal, picrocrocin and its derivatives, and HTCC. Data are averages ± sd of three biological replicates and expressed as % of fold internal standard (IS) levels. sd values are in Supplementary Table S1. Analyses were performed at 13 dpi.

Subsequently, the levels of different carotenoids and chlorophylls were also investigated in the apolar fractions (Fig. 5 and Supplementary Table S3). As expected,

virus infection negatively affected the isoprenoid pools, with most of carotenoids and chlorophylls reduced in all infected tissues compared to those from mock-inoculated plants. However, the comparison between tissues infected with TEVΔNIb-aGFP and both CCD viruses highlighted a series of alterations at metabolite level.

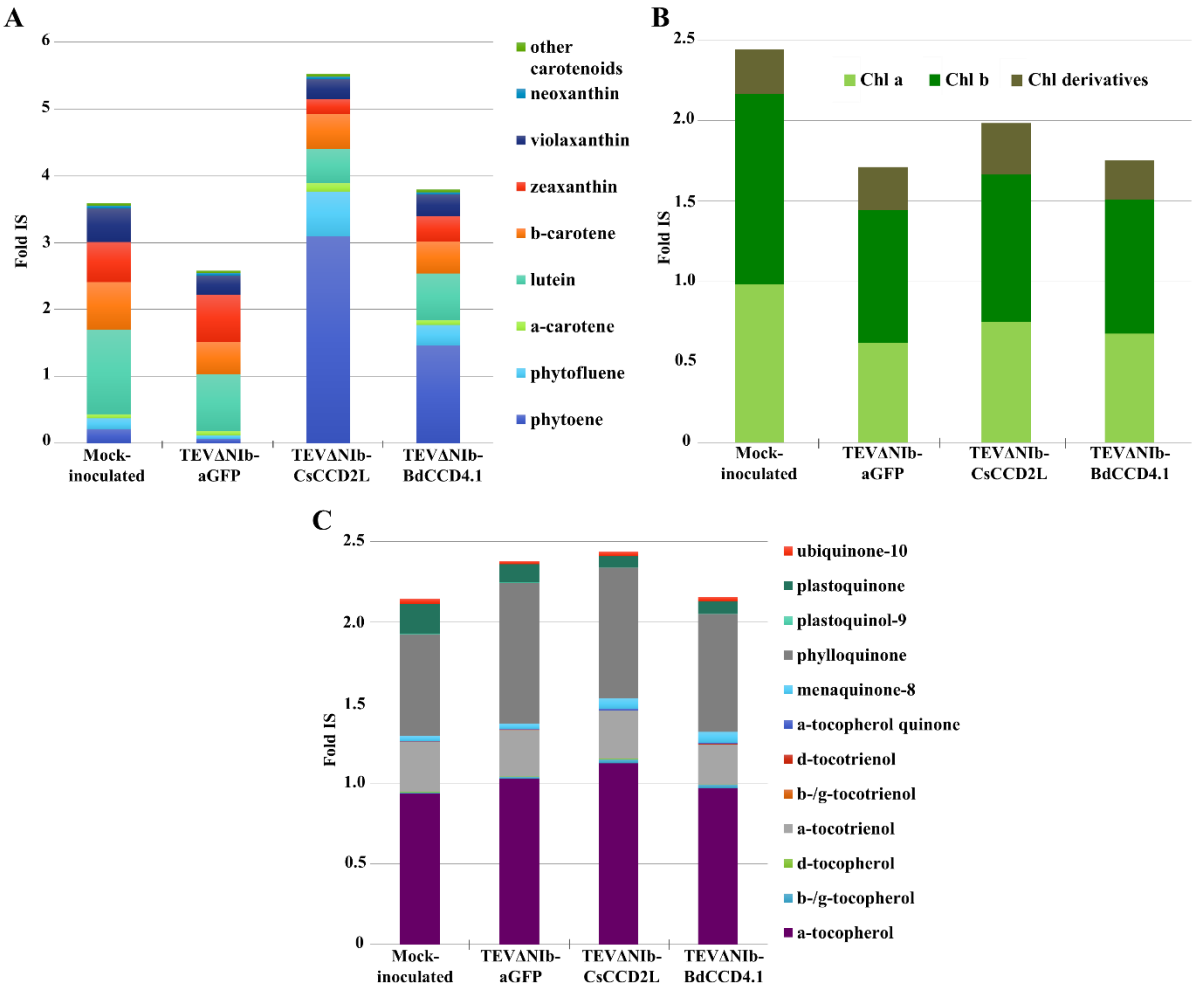

Fig. 5. Relative quantities of **(A)** carotenoids **(B)** chlorophylls and **(C)** quinones and tocochromanols detected by HPLC-DAD-HRMS in tissues of mock-inoculated and infected (TEVΔNIb-aGFP, TEVΔNIb-CsCCD2L and TEVΔNIb-BdCCD4.1) *N. benthamiana* plants. Data are averages ± sd of three biological replicates and expressed as fold internal standard (IS). sd values are in Supplementary Table S3. Analyses were performed at 13 dpi.

The most striking differences were in the contents of phytoene and phytofluene, as well as zeaxanthin and lutein. While the formers increased in the TEVΔNIb-CsCCD2L and TEVΔNIb-BdCCD4.1-infected tissues, the levels of zeaxanthin and lutein were strongly reduced (Fig. 5A and Table S3A). On the contrary, no significant alterations in chlorophyll levels were observed in tissues infected with the two CCD viruses when compared to the TEVΔNIb-aGFP-infected control (Fig. 5B and Supplementary Table

S3B). Other typical leaf isoprenoids, such as tocochromanols and quinones, displayed only few changes in CCD versus control tissues: for instance, β-/γ-tocopherol, α-tocopherol quinone and menaquinone-8 increased, whereas plastoquinone was reduced in CsCCD2L and BdCCD4.1-infected tissues compared to mock-inoculated and GFP-infected leaves (Fig. 5C and Supplementary Table S3C).

Finally, in order to decipher the source of the differential apocarotenoid accumulation in CCD-expressing *N. benthamiana* leaves, we performed a comparative *in vitro* assay (Ahrazem et al., 2017; Frusciante et al., 2014), of recombinant CsCCD2L and BdCCD4.1 expressed in *E. coli*. CsCCD2L displayed a higher efficiency of zeaxanthin cleavage and crocetin dialdehyde production compared to BdCCD4.1 (Supplementary Table S5), further supporting the results obtained in *N. benthamiana* with the virus-based system.

3.3. Subcellular accumulation of apocarotenoids in tissues infected with CCD-expressing viruses

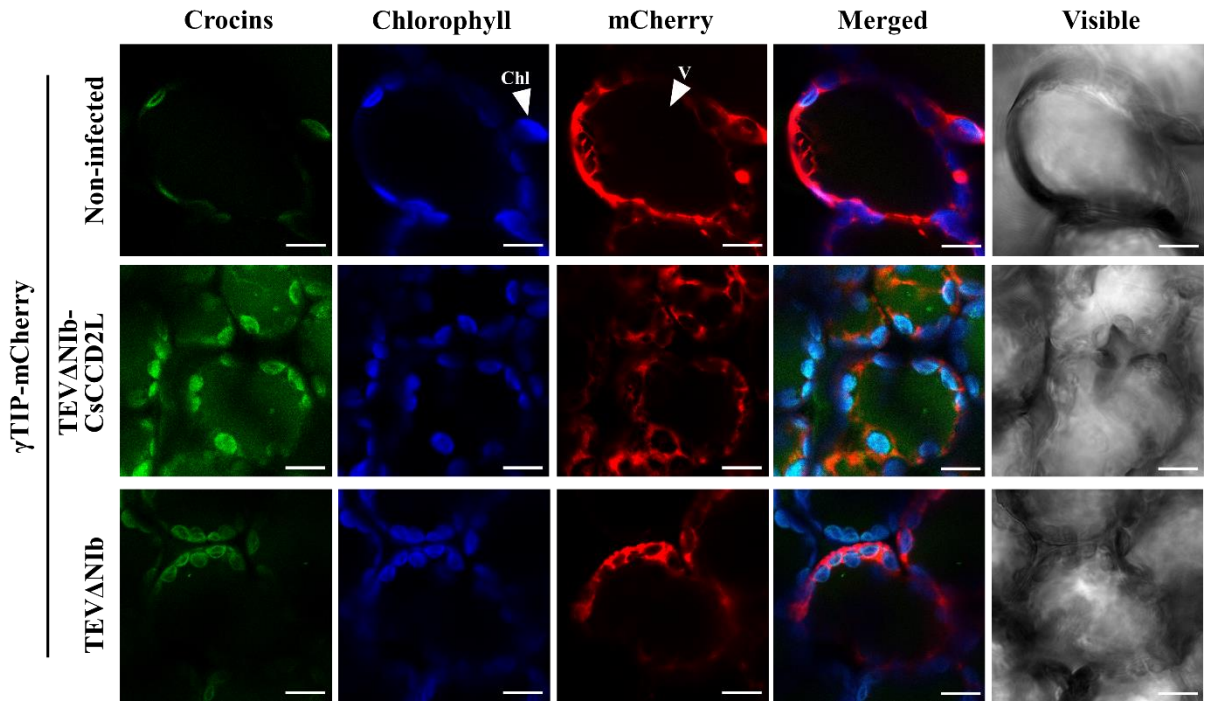

Fig. 6. LSCM images of crocins (green), chlorophyll autofluorescence (blue) and mCherry (red) in leaves of *N. benthamiana* plants non-infected or infected with TEVΔNIb-CsCCD2L and TEVΔNIb, as indicated, at 13 dpi. Leaves were infiltrated to express the tonoplast marker γTIP fused to mCherry 2 days before analysis. Merged images of fluorescent signals and images under bright field are also shown. White arrows point to a representative chloroplast (Chl) and vacuole (V). Scale bars indicate 10 μm.

On the basis of the differential autofluorescence of chlorophylls and carotenoids, we analyzed the subcellular localization of crocins that accumulate in symptomatic tissues of plants infected with TEVΔNIb-CsCCD2L. LSCM images showed an intense fluorescence signal from crocins in the vacuoles of tissues infected with TEVΔNIb-CsCCD2L, while tissues mock-inoculated or infected with TEVΔNIb only showed chlorophyll fluorescence (Fig. 6). Vacuolar accumulation of crocins was deduced from the localization of the tonoplast marker γTIP-mCherry (Demurtas et al., 2019).

3.4. Time course accumulation of crocins and picrocrocin in inoculated plants

Next, we researched the point with the maximum apocarotenoid accumulation in inoculated plants. For this aim, we carried out a time-course analysis focusing only on the virus recombinant clone TEVΔNIb-CsCCD2L that induces the highest apocarotenoid accumulation in *N. benthamiana* tissues. After plant agroinoculation, upper systemic tissues were collected at 0, 4, 8, 11, 13, 15, 18 and 20 dpi from three independent replicate plants per time point. Pigments were extracted and analyzed by HPLC-DAD. In these tissues, accumulation of total crocins increased from approximately 8 to 13 dpi, reaching a plateau up to the end of the analysis (20 dpi) (Fig. 7A). Picrocrocin levels showed identical behavior (Fig. 7B), as well the direct products of CCD activity, HTTC and crocetin (Fig. 7E). Accumulation of lutein, β-carotene and chlorophylls was also evaluated in all these samples. In contrast to apocarotenoids, accumulation of lutein and β-carotene (Fig. 7C) as well as chlorophylls a and b (Fig. 7D) dropped as infection progressed.

These results indicate that the virus-driven system to produce apocarotenoids in *N. benthamiana* developed here reaches the highest yield in only 13 days after inoculating the plants and this yield is maintained during at least one week with no apparent loss. This experiment also revealed the remarkable accumulation of 2.18±0.23 mg of crocins and 8.24±2.93 mg of picrocrocin per gram of *N. benthamiana* dry weight leaf tissue with the sole virus-driven expression of *C. sativus* CsCCD2L.

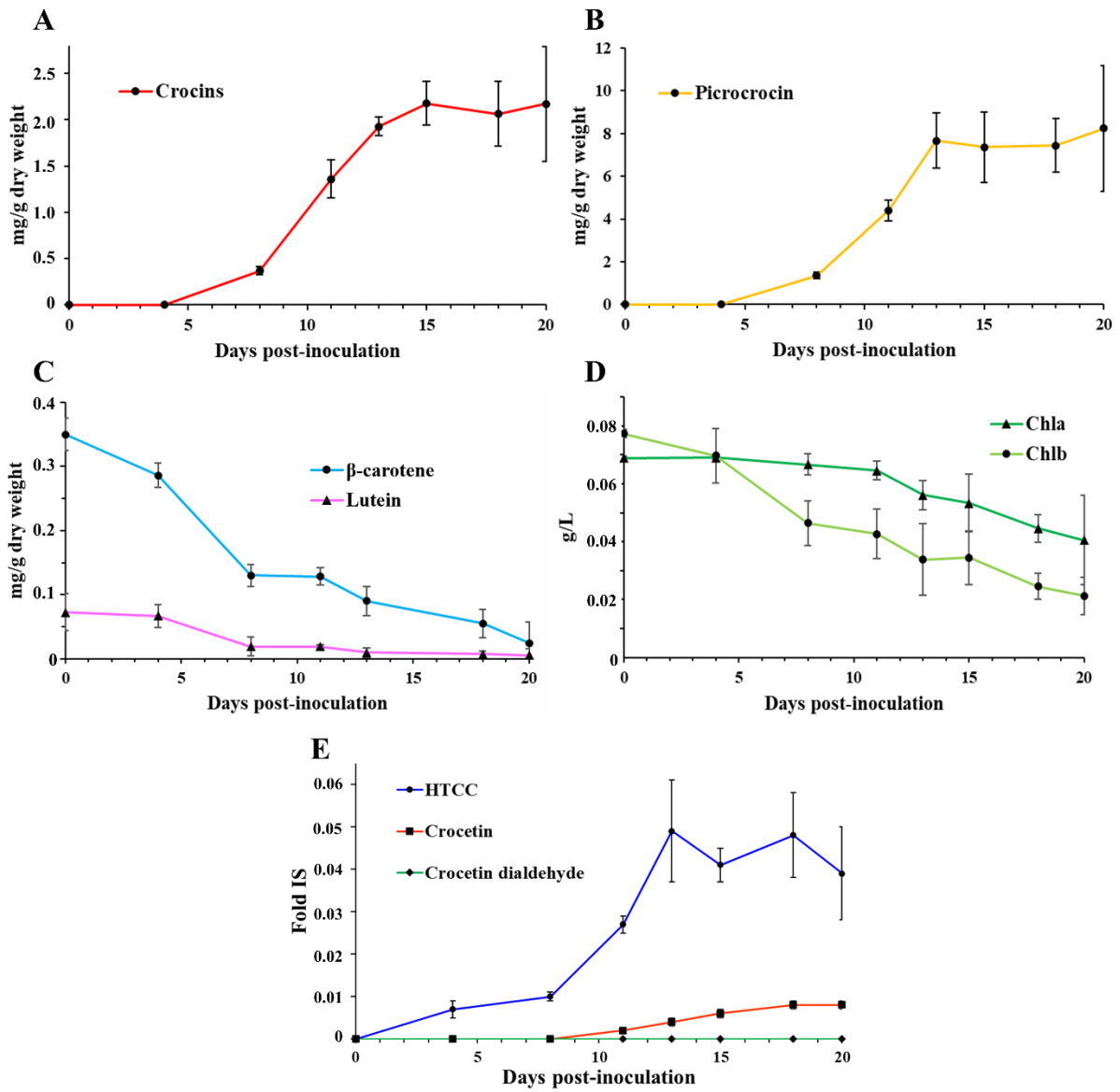

Fig. 7. Time-course accumulation of **(A)** crocins, **(B)** picrocrocin, **(C)** β-carotene and lutein, **(D)** chlorophyll a and b, and **(E)** HTCC, crocetin and crocetin dialdehyde, as indicated, in systemic tissues of *N. benthamiana* plants agroinoculated with TEVΔNIb-CsCCD2L. Fold level between the signal intensities of the indicated metabolites and the internal standard α-tocopherol acetate (Fold IS). Data are average ± sd of at least three biological replicates.

3.5. Virus-based combined expression of CsCCD2L and other carotenogenic and non-carotenogenic enzymes

In order to further improve apocarotenoid accumulation in inoculated *N. benthamiana* plants, we combined expression of CsCCD2L with two carotenoid enzymes (Fig. 8A), acting early and late in the biosynthetic pathway, namely *P. ananatis* PaCrtB, and saffron CsBCH2; or with a non-carotenoid transporter, the saffron lipid

transfer protein 1 (CsLTP1), involved in the transport of secondary metabolites (Wang et al., 2016).

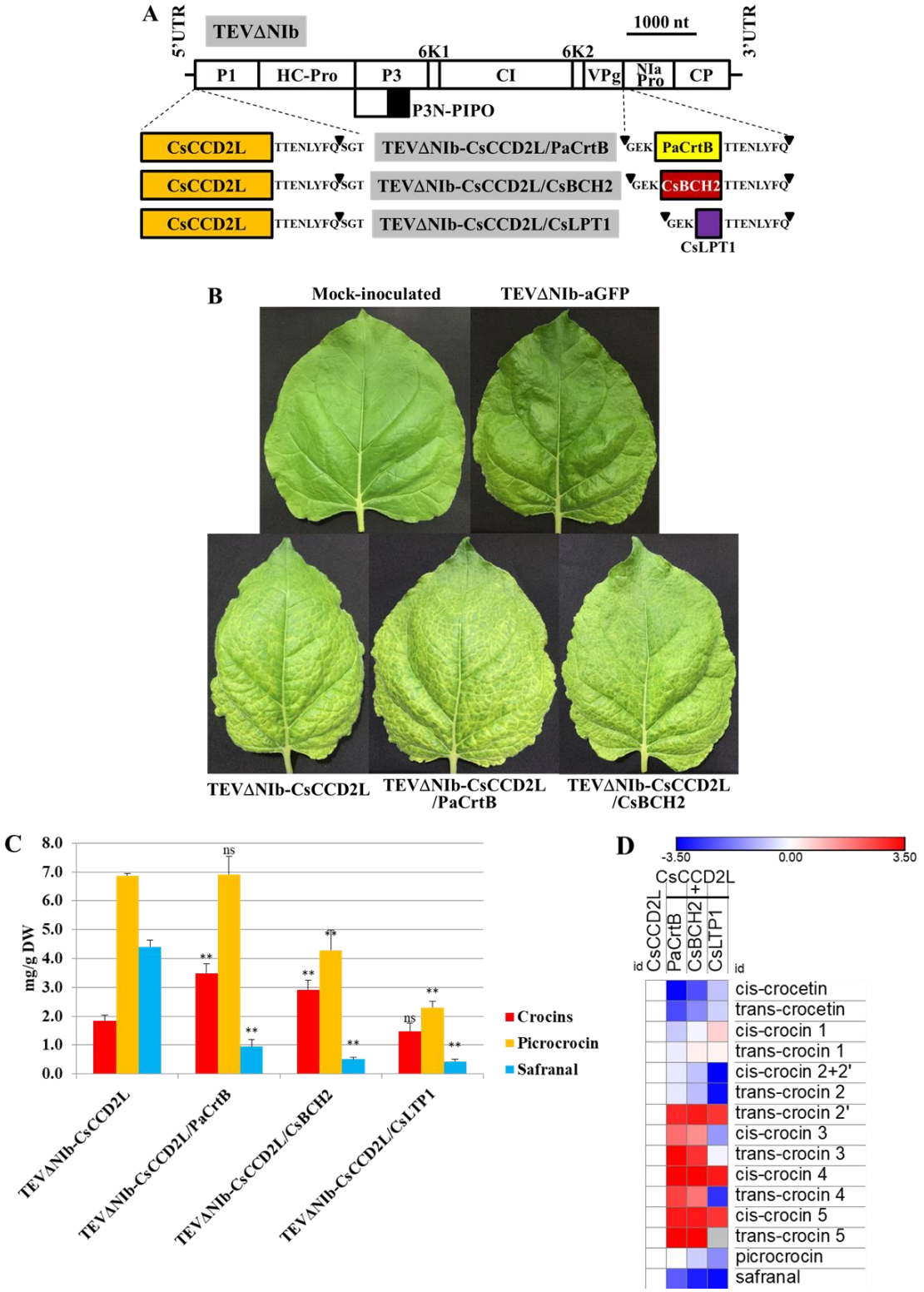

Fig. 8. Apocarotenoid accumulation in *N. benthamiana* tissues inoculated with viral vectors carrying CsCCD2L, alone or in combination with PaCrtB, CsBCH2 and CsLTP1. **(A)** Schematic representation of TEVΔNIb-CsCCD2L/PaCrtB, - CsCCD2L/CsBCH2 and -CsCCD2L/CsLPT1. The cDNAs corresponding to CsCCD2L, PaCrtB, CsBCH2 and CsLPT1 are indicated by

orange, yellow, red and purple boxes respective. Other details are the same as in Fig. 2A. **(B)** Representative leaves from plants mock-inoculated and agroinoculated with TEVΔNIb-aGFP, TEVΔNIb-CsCCD2L, TEVΔNIb-CsCCD2L/PaCrtB and TEVΔNIb-CsCCD2L/CsBCH2, at 13 dpi. **(C)** Total crocins, picrocrocin and safranal contents, expressed as mg/g of DW. Asterisks indicate significant differences according a t-test (pValue: *<0.05; **<0.01; ns, not significant) carried out in the comparisons CsCCD2L vs CsCCD2L+PaCrtB, CsCCD2L+CsBCH2 or CsCCD2L+CsLTP1. **(D)** Relative accumulation of single crocins, picrocrocin and safranal, normalized on the CsCCD2L-alone sample and visualized as heatmap of log_2 values. Data are average ± sd of three biological replicates. Analyses were performed at 13 dpi.

Interestingly, virus-based co-expression of CsCCD2L and PaCrtB induced a stronger yellow phenotype (Fig. 8B), and a higher content in crocins (3.493±0.325 mg/g DW; Fig. 8C and Table S4). Improved crocins levels were also observed when CsCCD2L was co-expressed with CsBCH2, although at a lesser extent in this case (2.198±0.338 mg/g DW). On the contrary, co-expression of LPT1 did not result in an increment of total apocarotenoid content (Fig. 8C and Table S4). Interestingly, when compared to tissues in which CsCCD2L alone was expressed, a preferential over-accumulation for higher glycosylated crocins was observed, while lower glycosylated species were down-represented (Fig. 8D).

4. DISCUSSION

The carotenoid biosynthetic pathway in higher plants has been manipulated by genetic engineering, both at the nuclear and transplastomic levels, to increase the general amounts of carotenoids or to produce specific carotenoids of interest, such as ketocarotenoids (Apel and Bock, 2009; Diretto et al., 2019b, 2007; Farré et al., 2014; Giorio et al., 2007; Hasunuma et al., 2008; Nogueira et al., 2019; Zhu et al., 2018). However, these projects also showed that the stable genetic transformation of nuclear or plastid genomes from higher plants is a work-intensive and time-consuming process, which frequently drives to unpredicted results, due to the complex regulation of metabolic pathways. Although no exempted of important limitations, chief among them is the amount of exogenous genetic information plant virus-derived expression systems can carry, they represent an attractive alternative for some plant metabolic engineering goals. Here, we used a virus-driven system that allows the production of noteworthy amounts of appreciated apocarotenoids, such as crocins and picrocrocin, in adult *N.*

benthamiana plants in as little as 13 days (Fig. 7). For this, we manipulated the genome of a 10-kb potyvirus, a quick straight-forward process that can be easily scaled-up for the high-throughput analysis of many enzymes and regulatory factors and engineered versions thereof.

In this virus-driven system, the expression of an appropriate CCD in *N. benthamiana* is sufficient to trigger the apocarotenoid pathway in this plant. Recently, it was observed the same situation in a transient expression system (Diretto et al., 2019a). These observations indicate that the zeaxanthin cleavage is the limiting step of apocarotenoid biosynthesis in this species, while aldehyde dehydrogenation and glycosylation steps can be efficiently complemented by endogenous orthologue enzymes. A similar situation was previously observed with other secondary metabolites. Indeed, a large portion of hydroxyl- and carboxyl-containing terpenoid compounds heterologously produced in plants are glycosylated by endogenous UGTs. For example, in transgenic maize expressing a geraniol synthase gene from *Lippia dulcis*, geranoyl-6-*O*-malonyl-β-D-glucopyranoside was the most abundant geraniol-derived compound (Yang et al., 2011). In another study, *N. benthamiana* plants transiently expressing the *Artemesia annua* genes of the artemisin biosynthetic pathway accumulated glycosylated versions of intermediate metabolites (Ting et al., 2013). Likewise, in tomato plants expressing the chrysanthemyl diphosphate synthase gene from *Tanacetum cinerariifolium*, the 62% of trans-chrysanthemic acid was converted into malonyl glycosides (Xu et al., 2018).

Zeaxanthin, the crocins precursor, is not a major carotenoid in plant leaves grown under regular light conditions, although its level increases during high light stress (Demmig-Adams et al., 2012). However, the efficient virus-driven production of all the intermediate and final products of the apocarotenoid biosynthetic pathway in *N. benthamiana* (Fig. 4) suggests that CCD is able to intercept the leaf metabolic flux in order to diverge it towards the production of apocarotenoids. Similarly, the observed reduction in lutein (Fig. 5A) may result from the CCD activity on the β-ring of this molecule, which confirms, at least for the *C. sativus* enzyme, the previous *in vitro* data showing that lutein can act as substrate of this cleavage activity (Frusciante et al., 2014). Although *N. benthamiana* leaves infected with CsCCD2L and BdCCD4.1 recombinant viruses are able to accumulate crocins, it has to be mentioned that, at the

qualitative level, their profiles are distinct with respect to the saffron stigma: while in the formers the major crocin species are the trans-crocin 3, together with cis-crocin 4, trans-crocin 2, cis-crocin 3 and cis-crocin 5, saffron stigmas are characterized by the presence, in decreasing order of accumulation, of trans-crocin 4, trans-crocin 3 and trans-crocin 2. These results suggest not only the implication of promiscuous glucosyltransferase enzymes differing form those in saffron, but also the different conditions in which crocins are produced in saffron and *N. benthamiana*, which implies respectively the absence or presence of light during this process, which can effectively influence the cis- or trans- configuration of crocetin (Rubio-Moraga et al., 2010). Co-expression of the homologous saffron UGTs may contribute to a closer crocin profile in *N. benthamiana*. A higher bioactivity of the trans- forms has been previously demonstrated, at least for crocetin (Zhang et al., 2017), thus making the crocins pool accumulated in the CsCCD2L and BdCCD4.1 leaves a good source of bioactive molecules. The *C. sativus* and *B. davidii* enzymes also generated a different crocins pattern: this finding can be explained by a distinct specificity and kinetics, which might influence the subsequent glucosylation step. Another remarkable observation is the dramatic increase of phytoene and phytofluene levels in *N. benthamiana* tissues as a consequence of the virus-driven expression of CCDs (Fig. 5A). These are upstream intermediates in the carotenoid biosynthetic pathway. Previous reports indicated that the overexpression of downstream enzymes or the increased storage of end-metabolites in the carotenoid pathway can drain the metabolic flux towards the synthesis and accumulation of the end-products (Diretto et al., 2007; Lopez et al., 2008). In our virus-driven system, expression of CsCCD2L and BdCCD4.1 seem to induce the same effect, promoting the activities of the phytoene synthase (PSY) and phytoene desaturase (PDS), which results in a higher accumulation of their metabolic intermediate products phytoene and phytofluene. In this context, the observed amounts of phytoene and phytofluene might be a consequence of PSY and PDS catalyzing the rate-limiting steps of the pathway in *N. benthamiana*, as previously described in other species (Maass et al., 2009; Xu et al., 2006). Levels of additional plastidic metabolites in the groups of tocochromanols and quinones only showed minor fluctuations, which indicates that perturbations in carotenoid and apocarotenoid biosynthesis do not necessarily affect other related pathways that share common

precursors, such as geranylgeranyl diphosphate (GGPP) (Fig. 5C). Our results also indicate that the decrease in the chlorophyll levels do not depend on CCD expression, but on viral infection, since it was also observed in the control tissues infected with TEVΔNIb-aGFP (Fig. 5B). This finding agrees with the effect of plant virus infection on photosynthetic machinery (Li et al., 2016).

In our virus-driven experiments, CsCCD2L was more efficient in the production of crocetin dialdehyde and crocins than BdCCD4.1. This suggests that the *C. sativus* CCD used here (CsCCD2L) is definitively a highly active enzyme, completely compatible with the virus vector and the host plant. Indeed, *C. sativus* stigma is the main commercial source for these apocarotenoids (Castillo et al., 2005; Rubio Moraga et al., 2013). Apocarotenoids are also present, although at lower levels, in the flowers of *Buddleja* spp., where they are restricted to the calix.

Virus-driven expression of CsCCD2L in adult *N. benthamiana* plants allowed the accumulation of the notable amounts of 2.18±0.23 mg of crocins and 8.24±2.93 mg of picrocrocin per gram (dry weight) of infected tissues in only 13 dpi (Fig. 7). These amounts are much higher than those obtained with a classic *A. tumefaciens*-mediated transient expression of the CsCCD2L enzyme in *N. benthamiana* leaves, alone or in combination with UGT709G1 (30.5 µg/g DW of crocins (unpublished data) and 4.13 µg/g DW of picrocrocin (Diretto et al., 2019a)), and highlight the opportunity to exploit the viral system for the production of valuable secondary metabolites. A huge range of values has been reported for crocins and picrocrocin in saffron in different studies. Crocins reported values in saffron samples from Spain ranged from 0.85 to 32.40 mg/g dry weight (Alonso et al., 2001). Other reports showed 24.87 mg/g from China (Tong et al., 2015), 26.60 mg/g from Greece (Koulakiotis et al., 2015), 29.00 mg/g from Morocco (Gonda et al., 2012), 32.60 mg/g from Iran, 49.80 mg/g from Italy (Masi et al., 2016) or 89.00 mg/g from Nepal (Li et al., 2018). In *Gardenia* fruits, crocins levels range from 2.60 to 8.37 mg/g (Ouyang et al., 2011; Wu et al., 2014). The picrocrocin content ranges from 7.90 to 129.40 mg/g in Spanish saffron. In Greek saffron, 6.70 mg/g were reported (Koulakiotis et al., 2015), and 10.70-2.16 mg/g in Indian, 21.80-6.15 mg/g in Iranian and 42.20-280.00 mg/g in Moroccan saffron (Lage and Cantrell, 2009). The different values obtained in those samples are also a consequence of the different procedures followed to obtain the saffron spice. Most methods involve a dehydration

step by heating, which causes the conversion of picrocrocin to safranal. Although lower than those from natural sources, the crocins and picrocrocin contents of *N. benthamiana* tissues achieved with our virus-driven system may still be attractive for commercial purposes because, in contrast to *C. sativus* stigma or *Gardenia* spp. fruits, *N. benthamiana* infected tissues can be quickly and easily obtained in practically unlimited amounts. Moreover, the virus-driven production of crocins and picrocrocin in *N. benthamiana* may still be optimized by increasing, for instance, the zeaxanthin precursor. PSY over-expression in plants was shown to increase the flux of the whole biosynthetic carotenoid pathway (Nisar et al., 2015), as well as the zeaxanthin pool (Lagarde et al., 2000; Römer et al., 2002). In addition, the virus-based cytosolic expression of a bacterial PSY (*P. ananatis* crtB) also induced general carotenoid accumulation, and particularly increased phytoene levels in tobacco infected tissues (Majer et al., 2017). On the other side, BCH overexpression resulted in increased zeaxanthin and β-β-xanthophyll contents, both in microbes and plants (Arango et al., 2014; Du et al., 2010; Lagarde et al., 2000). In this context, we selected PaCrtB and CsBCH2, together with CsLTP1, involved in carotenoid transport, as additional targets to improve apocarotenoid contents in *N. benthamiana* leaves, which allowed a further increase of 1.9 and 1.6 fold in CsCCD2L/PaCrtB and CsCCD2L/CsBCH2, respectively, compared to the sole expression of CsCCD2L (Fig. 8). Other targets to improve apocarotenoid accumulation could include the knocking out of enzymatic steps opposing zeaxanthin accumulation, as zeaxanthin epoxydase (ZEP), which uses zeaxanthin as substrate to yield violaxanthin, or lycopene ε-cyclase (LCY-ε) that converts lycopene in δ-carotene, thus diverging the metabolic flux towards the synthesis of ε-δ- (lutein), rather than β-β-xanthophylls (as zeaxanthin), which will be object of future attempts.

In summary, here we describe a new technology that allows production of remarkable amounts of highly appreciated crocins and picrocrocin in adult *N. benthamiana* plants in as little as 13 dpi. This achievement is the consequence of *N. benthamiana*, a species that accumulate negligible amounts of apocarotenoids, only requiring the expression of an appropriate CCD to trigger the apocarotenoid biosynthetic pathway, and can be further improved through the combination with the overexpression of early or late carotenoid structural genes.

ACKNOWLEDGEMENTS

We thank K. Schreiber and C. Mares (IBMCP, CSIC-UPV, Valencia, Spain) for technical assistance during plant transformation. We thank M. Gascón and M.D. Gómez-Jiménez (IBMCP, CSIC-UPV, Valencia, Spain) for helpful assistance with LSCM analyses. We thank D. Dubbala (IBMCP, CSIC-UPV, Valencia, Spain) for English revision. This work was supported by grants BIO2016-77000-R and BIO2017-83184-R from the Spanish Ministerio de Ciencia, Innovación y Universidades (co-financed European Union FEDER funds). M.M. was the recipient of a predoctoral fellowship from the Spanish Ministerio de Educación, Cultura y Deporte (FPU16/05294). G.D. and L.G.G. are participants of the European COST action CA15136 (EUROCAROTEN). L.G.G. is a participant of the CARNET network (BIO2015-71703-REDT and BIO2017-90877-RED).

CONFLICT OF INTEREST

The authors declare no conflict of interest.

REFERENCES

Ahrazem, O., Argandoña, J., Fiore, A., Aguado, C., Luján, R., Rubio-Moraga, Á., Marro, M., Araujo-Andrade, C., Loza-Alvarez, P., Diretto, G., Gómez-Gómez, L., 2018. Transcriptome analysis in tissue sectors with contrasting crocins accumulation provides novel insights into apocarotenoid biosynthesis and regulation during chromoplast biogenesis. Sci. Rep. 8, 2843. https://doi.org/10.1038/s41598-018-21225-z

Ahrazem, O., Diretto, G., Argandoña, J., Rubio-Moraga, A., Julve, J.M., Orzáez, D., Granell, A., Gómez-Gómez, L., 2017. Evolutionarily distinct carotenoid cleavage dioxygenases are responsible for crocetin production in Buddleja davidii. J. Exp. Bot. 68, 4663–4677. https://doi.org/10.1093/jxb/erx277

Ahrazem, O., Gómez-Gómez, L., Rodrigo, M.J., Avalos, J., Limón, M.C., 2016a. Carotenoid cleavage oxygenases from microbes and photosynthetic organisms: Features and functions. Int. J. Mol. Sci. 17 (11), 1781. https://doi.org/10.3390/ijms17111781

Ahrazem, O., Rubio-Moraga, A., Argandoña-Picazo, J., Castillo, R., Gómez-Gómez, L., 2016b. Intron retention and rhythmic diel pattern regulation of carotenoid cleavage dioxygenase 2 during crocetin biosynthesis in saffron. Plant Mol. Biol. 91, 355–374. https://doi.org/10.1007/s11103-016-0473-8

Ahrazem, O., Rubio-Moraga, A., Berman, J., Capell, T., Christou, P., Zhu, C., Gómez-Gómez, L., 2016c. The carotenoid cleavage dioxygenase CCD2 catalysing the synthesis of crocetin in spring crocuses and saffron is a plastidial enzyme. New Phytol. 209, 650–663. https://doi.org/10.1111/nph.13609

Ahrazem, O., Rubio-Moraga, A., Nebauer, S.G., Molina, R.V., Gómez-Gómez, L., 2015. Saffron: Its Phytochemistry, Developmental Processes, and Biotechnological Prospects. J. Agric. Food Chem. 63, 8751–8764. https://doi.org/10.1021/acs.jafc.5b03194

Alonso, G.L., Salinas, M.R., Garijo, J., Sánchez-Fernández, M.A., 2001. Composition of crocins and picrocrocin from Spanish saffron (Crocus sativus L.). J. Food Qual. 24, 219–233. https://doi.org/10.1111/j.1745-4557.2001.tb00604.x

Amin, B., Hosseinzadeh, H., 2012. Evaluation of aqueous and ethanolic extracts of saffron, Crocus sativus L., and its constituents, safranal and crocin in allodynia and hyperalgesia induced by chronic constriction injury model of neuropathic pain in rats. Fitoterapia 83, 888–895. https://doi.org/10.1016/j.fitote.2012.03.022

Apel, W., Bock, R., 2009. Enhancement of carotenoid biosynthesis in transplastomic tomatoes by induced lycopene-to-provitamin A conversion. Plant Physiol. 151, 59–66. https://doi.org/10.1104/pp.109.140533

Arango, J., Jourdan, M., Geoffriau, E., Beyer, P., Welsch, R., 2014. Carotene hydroxylase activity determines the levels of both α-carotene and total carotenoids in orange carrots. Plant Cell 26, 2223–2233. https://doi.org/10.1105/tpc.113.122127

Bedoya, L., Martínez, F., Rubio, L., Daròs, J.A., 2010. Simultaneous equimolar expression of multiple proteins in plants from a disarmed potyvirus vector. J. Biotechnol. 150, 268–275. https://doi.org/10.1016/j.jbiotec.2010.08.006

Bedoya, L.C., Martínez, F., Orzáez, D., Daròs, J.A., 2012. Visual tracking of plant virus infection and movement using a reporter MYB transcription factor that activates anthocyanin biosynthesis. Plant Physiol. 158, 1130–1138. https://doi.org/10.1104/pp.111.192922

Bukhari, S.I., Manzoor, M., Dhar, M.K., 2018. A comprehensive review of the pharmacological potential of Crocus sativus and its bioactive apocarotenoids. Biomed. Pharmacother. 98, 733–745. https://doi.org/10.1016/j.biopha.2017.12.090

Cappelli, G., Giovannini, D., Basso, A.L., Demurtas, O.C., Diretto, G., Santi, C., Girelli, G., Bacchetta, L., Mariani, F., 2018. A Corylus avellana L. extract enhances human macrophage bactericidal response against Staphylococcus aureus by increasing the expression of anti-inflammatory and iron metabolism genes. J. Funct. Foods 45, 499–511. https://doi.org/10.1016/j.jff.2018.04.007

Castillo, R., Fernández, J.A., Gómez-Gómez, L., 2005. Implications of carotenoid biosynthetic genes in apocarotenoid formation during the stigma development of Crocus sativus and its closer relatives. Plant Physiol. 139, 674–689. https://doi.org/10.1104/pp.105.067827

Chai, F., Wang, Y., Mei, X., Yao, M., Chen, Y., Liu, H., Xiao, W., Yuan, Y., 2017. Heterologous biosynthesis and manipulation of crocetin in Saccharomyces cerevisiae. Microb. Cell Fact. 16, 54. https://doi.org/10.1186/s12934-017-0665-1

Cheriyamundath, S., Choudhary, S., Lopus, M., 2018. Safranal Inhibits HeLa Cell Viability by Perturbing the Reassembly Potential of Microtubules. Phytother. Res. 32, 170–173. https://doi.org/10.1002/ptr.5938

Christodoulou, E., Kadoglou, N.P., Kostomitsopoulos, N., Valsami, G., 2015. Saffron: A natural product with potential pharmaceutical applications. J. Pharm. Pharmacol. 67, 1634–1649. https://doi.org/10.1111/jphp.12456

Clemente, T., 2006. Nicotiana (Nicotiana tobaccum, Nicotiana benthamiana). Methods Mol. Biol. 343, 143–154. https://doi.org/10.1385/1-59745-130-4:143

Côté, F., Cormier, F., Dufresne, C., Willemot, C., 2001. A highly specific glucosyltransferase is involved in the synthesis of crocetin glucosylesters in Crocus sativus cultured cells. J. Plant Physiol. 158, 553–560. https://doi.org/10.1078/0176-1617-00305

D'Archivio, A.A., Giannitto, A., Maggi, M.A., Ruggieri, F., 2016. Geographical classification of Italian saffron (Crocus sativus L.) based on chemical constituents determined by high-performance liquid-chromatography and by using linear discriminant analysis. Food Chem. 212, 110–116. https://doi.org/10.1016/j.foodchem.2016.05.149

D'Esposito, D., Ferriello, F., Molin, A.D., Diretto, G., Sacco, A., Minio, A., Barone, A., Di Monaco, R., Cavella, S., Tardella, L., Giuliano, G., Delledonne, M., Frusciante, L., Ercolano, M.R., 2017. Unraveling the complexity of transcriptomic, metabolomic and quality environmental response of tomato fruit. BMC Plant Biol. 17, 66. https://doi.org/10.1186/s12870-017-1008-4

Demmig-Adams, B., Cohu, C.M., Muller, O., Adams, W.W., 2012. Modulation of photosynthetic energy conversion efficiency in nature: From seconds to seasons, in: Photosynthesis Research. 113 (1-3), pp. 75–88. https://doi.org/10.1007/s11120-012-9761-6

Demurtas, O.C., de Brito Francisco, R., Diretto, G., Ferrante, P., Frusciante, S., Pietrella, M., Aprea, G., Borghi, L., Feeney, M., Frigerio, L., Coricello, A., Costa, G., Alcaro, S., Martinoia, E., Giuliano, G., 2019. ABCC Transporters Mediate the Vacuolar Accumulation of Crocins in Saffron Stigmas. Plant Cell 31, 2789–2804. https://doi.org/10.1105/tpc.19.00193

Demurtas, O.C., Frusciante, S., Ferrante, P., Diretto, G., Azad, N.H., Pietrella, M., Aprea, G., Taddei, A.R., Romano, E., Mi, J., Al-Babili, S., Frigerio, L., Giuliano, G., 2018. Candidate Enzymes for Saffron Crocin Biosynthesis Are Localized in Multiple Cellular Compartments. Plant Physiol. 177, 990–1006. https://doi.org/10.1104/pp.17.01815

Diretto, G., Ahrazem, O., Rubio-Moraga, Á., Fiore, A., Sevi, F., Argandoña, J., Gómez-Gómez, L., 2019a. UGT709G1: a novel uridine diphosphate glycosyltransferase involved in the biosynthesis of picrocrocin, the precursor of safranal in saffron (Crocus sativus). New Phytol. 224, 725–740. https://doi.org/10.1111/nph.16079

Diretto, G., Al-Babili, S., Tavazza, R., Papacchioli, V., Beyer, P., Giuliano, G., 2007. Metabolic engineering of potato carotenoid content through tuber-specific overexpression of a bacterial mini-pathway. PLoS One 2, e350. https://doi.org/10.1371/journal.pone.0000350

Diretto, G., Frusciante, S., Fabbri, C., Schauer, N., Busta, L., Wang, Z., Matas, A.J., Fiore, A., Rose, J.K.C., Fernie, A.R., Jetter, R., Mattei, B., Giovannoni, J., Giuliano, G., 2019b. Manipulation of β-carotene levels in tomato fruits results in increased ABA content and extended shelf-life. Plant Biotechnol. J. 18, pp. 1185-1199. pbi.13283. https://doi.org/10.1111/pbi.13283

Du, H., Wang, N., Cui, F., Li, X., Xiao, J., Xiong, L., 2010. Characterization of the β-carotene hydroxylase gene DSM2 conferring drought and oxidative stress resistance by increasing xanthophylls and abscisic acid synthesis in rice. Plant Physiol. 154, 1304–1318. https://doi.org/10.1104/pp.110.163741

Eroglu, A., Harrison, E.H., 2013. Carotenoid metabolism in mammals, including man: Formation, occurrence, and function of apocarotenoids. J. Lipid Res. 54 (7), pp.1719-1730. https://doi.org/10.1194/jlr.R039537

Farré, G., Blancquaert, D., Capell, T., Van Der Straeten, D., Christou, P., Zhu, C., 2014. Engineering complex metabolic pathways in plants. Annu. Rev. Plant Biol. 65, 187–223. https://doi.org/10.1146/annurev-arplant-050213-035825

Fasano, C., Diretto, G., Aversano, R., D'Agostino, N., Di Matteo, A., Frusciante, L., Giuliano, G., Carputo, D., 2016. Transcriptome and metabolome of synthetic Solanum autotetraploids reveal key genomic stress events following polyploidization. New Phytol. 210, 1382–94. https://doi.org/10.1111/nph.13878

Fiedor, J., Burda, K., 2014. Potential role of carotenoids as antioxidants in human health and disease. Nutrients 6, 466–488. https://doi.org/10.3390/nu6020466

Finley, J.W., Gao, S., 2017. A Perspective on Crocus sativus L. (Saffron) Constituent Crocin: A Potent Water-Soluble Antioxidant and Potential Therapy for Alzheimer's Disease. J. Agric. Food Chem. 65, 1005–1020. https://doi.org/10.1021/acs.jafc.6b04398

Fraser, P.D., Bramley, P.M., 2004. The biosynthesis and nutritional uses of carotenoids. Prog. Lipid Res. 43, 228–265. https://doi.org/10.1016/j.plipres.2003.10.002

Frusciante, S., Diretto, G., Bruno, M., Ferrante, P., Pietrella, M., Prado-Cabrero, A., Rubio-Moraga, A., Beyer, P., Gomez-Gomez, L., Al-Babili, S., Giuliano, G., 2014. Novel carotenoid cleavage dioxygenase catalyzes the first dedicated step in saffron crocin biosynthesis. Proc. Natl. Acad. Sci.

U. S. A. 111, 12246–12251. https://doi.org/10.1073/pnas.1404629111

Georgiadou, G., Tarantilis, P.A., Pitsikas, N., 2012. Effects of the active constituents of Crocus Sativus L., crocins, in an animal model of obsessive-compulsive disorder. Neurosci. Lett. 528, 27–30. https://doi.org/10.1016/j.neulet.2012.08.081

Gibson, D.G., Young, L., Chuang, R.Y., Venter, J.C., Hutchison 3rd, C.A., Smith, H.O., 2009. Enzymatic assembly of DNA molecules up to several hundred kilobases. Nat. Methods 6, 343–345. https://doi.org/10.1038/nmeth.1318

Giorio, G., Stigliani, A.L., D'Ambrosio, C., 2007. Agronomic performance and transcriptional analysis of carotenoid biosynthesis in fruits of transgenic HighCaro and control tomato lines under field conditions. Transgenic Res. 16, 15–28. https://doi.org/10.1007/s11248-006-9025-3

Gómez-Gómez, L., Feo-Brito, F., Rubio-Moraga, A., Galindo, P.A., Prieto, A., Ahrazem, O., 2010. Involvement of lipid transfer proteins in saffron hypersensitivity: Molecular cloning of the potential allergens. J. Investig. Allergol. Clin. Immunol. 20, 407–412.

Gómez-Gómez, L., Pacios, L.F., Diaz-Perales, A., Garrido-Arandia, M., Argandoña, J., Rubio-Moraga, Á., Ahrazem, O., 2018. Expression and interaction analysis among saffron ALDHs and crocetin dialdehyde. Int. J. Mol. Sci. 19 (5), 1409. https://doi.org/10.3390/ijms19051409

Gómez-Gómez, L., Parra-Vega, V., Rivas-Sendra, A., Seguí-Simarro, J.M., Molina, R.V., Pallotti, C., Rubio-Moraga, Á., Diretto, G., Prieto, A., Ahrazem, O., 2017. Unraveling massive crocins transport and accumulation through proteome and microscopy tools during the development of saffron stigma. Int. J. Mol. Sci. 18 (1), 76. https://doi.org/10.3390/ijms18010076

Gonda, S., Parizsa, P., Surányi, G., Gyémánt, G., Vasas, G., 2012. Quantification of main bioactive metabolites from saffron (Crocus sativus) stigmas by a micellar electrokinetic chromatographic (MEKC) method. J. Pharm. Biomed. Anal. 66, 68–74. https://doi.org/10.1016/j.jpba.2012.03.002

Grosso, V., Farina, A., Giorgi, D., Nardi, L., Diretto, G., Lucretti, S., 2018. A high-throughput flow cytometry system for early screening of in vitro made polyploids in Dendrobium hybrids. Plant Cell. Tissue Organ Cult. 132, 57–70. https://doi.org/10.1007/s11240-017-1310-8

Hasunuma, T., Miyazawa, S., Yoshimura, S., Shinzaki, Y., Tomizawa, K., Shindo, K., Choi, S.K., Misawa, N., Miyake, C., 2008. Biosynthesis of astaxanthin in tobacco leaves by transplastomic engineering. Plant J. 55, 857–868. https://doi.org/10.1111/j.1365-313X.2008.03559.x

Hellens, R.P., Edwards, E.A., Leyland, N.R., Bean, S., Mullineaux, P.M., 2000. pGreen: a versatile and flexible binary Ti vector for Agrobacterium -mediated plant transformation. Plant Mol.Biol. 42, 819–832.

Jabini, R., Ehtesham-Gharaee, M., Dalirsani, Z., Mosaffa, F., Delavarian, Z., Behravan, J., 2017. Evaluation of the Cytotoxic Activity of Crocin and Safranal, Constituents of Saffron, in Oral Squamous Cell Carcinoma (KB Cell Line). Nutr. Cancer 69, 911–919. https://doi.org/10.1080/01635581.2017.1339816

Jia, K.P., Baz, L., Al-Babili, S., 2018. From carotenoids to strigolactones. J. Exp. Bot. 69 (9), pp 2189-2204. https://doi.org/10.1093/jxb/erx476

Koulakiotis, N.S., Gikas, E., Iatrou, G., Lamari, F.N., Tsarbopoulos, A., 2015. Quantitation of crocins and picrocrocin in saffron by hplc: Application to quality control and phytochemical differentiation from other crocus taxa. Planta Med. 81, 606–612. https://doi.org/10.1055/s-0035-1545873

Kyriakoudi, A., O'Callaghan, Y.C., Galvin, K., Tsimidou, M.Z., O'Brien, N.M., 2015. Cellular Transport and Bioactivity of a Major Saffron Apocarotenoid, Picrocrocin (4-(beta-D-Glucopyranosyloxy)-2,6,6-trimethyl-1-cyclohexene-1-carboxaldehyde). J. Agric. Food Chem. 63, 8662–8668. https://doi.org/10.1021/acs.jafc.5b03363

Lagarde, D., Beuf, L., Vermaas, W., 2000. Increased production of zeaxanthin and other pigments by application of genetic engineering techniques to Synechocystis sp. strain PCC 6803. Appl. Environ. Microbiol. 66, 64–72. https://doi.org/10.1128/AEM.66.1.64-72.2000

Lage, M., Cantrell, C.L., 2009. Quantification of saffron (Crocus sativus L.) metabolites crocins, picrocrocin and safranal for quality determination of the spice grown under different environmental

Moroccan conditions. Sci. Hortic. (Amsterdam). 121, 366–373. https://doi.org/10.1016/j.scienta.2009.02.017

Li, S., Shao, Q., Lu, Z., Duan, C., Yi, H., Su, L., 2018. Rapid determination of crocins in saffron by near-infrared spectroscopy combined with chemometric techniques. Spectrochim. Acta - Part A Mol. Biomol. Spectrosc. 190 (5), pp 283-289. https://doi.org/10.1016/j.saa.2017.09.030

Li, Y., Cui, H., Cui, X., Wang, A., 2016. The altered photosynthetic machinery during compatible virus infection. Curr. Opin. Virol. 17, 19–24. https://doi.org/10.1016/j.coviro.2015.11.002

Liao, Y.H., Houghton, P.J., Hoult, J.R.S., 1999. Novel and known constituents from Buddleja species and their activity against leukocyte eicosanoid generation. J. Nat. Prod. 62, 1241–1245. https://doi.org/10.1021/np990092+

Lopez, A.B., Van Eck, J., Conlin, B.J., Paolillo, D.J., O'Neill, J., Li, L., 2008. Effect of the cauliflower or transgene on carotenoid accumulation and chromoplast formation in transgenic potato tubers. J. Exp. Bot. 59, 213–223. https://doi.org/10.1093/jxb/erm299

Lopresti, A.L., Drummond, P.D., 2014. Saffron (Crocus sativus) for depression: A systematic review of clinical studies and examination of underlying antidepressant mechanisms of action. Hum. Psychopharmacol 29 (6), pp. 517-527. https://doi.org/10.1002/hup.2434

Maass, D., Arango, J., Wüst, F., Beyer, P., Welsch, R., 2009. Carotenoid crystal formation in arabidopsis and carrot roots caused by increased phytoene synthase protein levels. PLoS One 4 (3), e6373. https://doi.org/10.1371/journal.pone.0006373

Majer, E., Llorente, B., Rodríguez-Concepción, M., Daròs, J.A., 2017. Rewiring carotenoid biosynthesis in plants using a viral vector. Sci. Rep. 7. https://doi.org/10.1038/srep41645

Majer, E., Navarro, J.A., Daròs, J.A., 2015. A potyvirus vector efficiently targets recombinant proteins to chloroplasts, mitochondria and nuclei in plant cells when expressed at the amino terminus of the polyprotein. Biotechnol. J. 10, 1792–1802. https://doi.org/10.1002/biot.201500042

Martin, C., Li, J., 2017. Medicine is not health care, food is health care: plant metabolic engineering, diet and human health. New Phytol. 216, 699–719. https://doi.org/10.1111/nph.14730

Masi, E., Taiti, C., Heimler, D., Vignolini, P., Romani, A., Mancuso, S., 2016. PTR-TOF-MS and HPLC analysis in the characterization of saffron (Crocus sativus L.) from Italy and Iran. Food Chem. 192, 75–81. https://doi.org/10.1016/j.foodchem.2015.06.090

Mazidi, M., Shemshian, M., Mousavi, S.H., Norouzy, A., Kermani, T., Moghiman, T., Sadeghi, A., Mokhber, N., Ghayour-Mobarhan, M., Ferns, G.A.A., 2016. A double-blind, randomized and placebo-controlled trial of Saffron (Crocus sativus L.) in the treatment of anxiety and depression. J. Complement. Integr. Med. 13, 195–199. https://doi.org/10.1515/jcim-2015-0043

Moraga, A.R., Nohales, P.F., Pérez, J.A., Gómez-Gómez, L., 2004. Glucosylation of the saffron apocarotenoid crocetin by a glucosyltransferase isolated from Crocus sativus stigmas. Planta 219, 955–966. https://doi.org/10.1007/s00425-004-1299-1

Moraga, Á.R., Rambla, J.L., Ahrazem, O., Granell, A., Gómez-Gómez, L., 2009. Metabolite and target transcript analyses during Crocus sativus stigma development. Phytochemistry 70, 1009–1016. https://doi.org/10.1016/j.phytochem.2009.04.022

Moras, B., Loffredo, L., Rey, S., 2018. Quality assessment of saffron (Crocus sativus L.) extracts via UHPLC-DAD-MS analysis and detection of adulteration using gardenia fruit extract (Gardenia jasminoides Ellis). Food Chem. 257, 325–332. https://doi.org/10.1016/j.foodchem.2018.03.025

Nagatoshi, M., Terasaka, K., Owaki, M., Sota, M., Inukai, T., Nagatsu, A., Mizukami, H., 2012. UGT75L6 and UGT94E5 mediate sequential glucosylation of crocetin to crocin in Gardenia jasminoides. FEBS Lett. 586, 1055–1061. https://doi.org/10.1016/j.febslet.2012.03.003

Nam, K.N., Park, Y.M., Jung, H.J., Lee, J.Y., Min, B.D., Park, S.U., Jung, W.S., Cho, K.H., Park, J.H., Kang, I., Hong, J.W., Lee, E.H., 2010. Anti-inflammatory effects of crocin and crocetin in rat brain microglial cells. Eur. J. Pharmacol. 648, 110–116. https://doi.org/10.1016/j.ejphar.2010.09.003

Nisar, N., Li, L., Lu, S., Khin, N.C., Pogson, B.J., 2015. Carotenoid metabolism in plants. Mol. Plant 8, 68–82. https://doi.org/10.1016/j.molp.2014.12.007

Nogueira, M., Enfissi, E.M.A., Welsch, R., Beyer, P., Zurbriggen, M.D., Fraser, P.D., 2019. Construction of a fusion enzyme for astaxanthin formation and its characterisation in microbial and plant hosts: A new tool for engineering ketocarotenoids. Metab. Eng. 52, 243–252. https://doi.org/10.1016/j.ymben.2018.12.006

Ouyang, E., Zhang, C., Li, X., 2011. Simultaneous determination of geniposide, chlorogenic acid, crocin1, and rutin in crude and processed fructus gardeniae extracts by high performance liquid chromatography. Pharmacogn. Mag. 7, 267–270. https://doi.org/10.4103/0973-1296.90391

Pfister, S., Meyer, P., Steck, A., Pfander, H., 1996. Isolation and Structure Elucidation of Carotenoid-Glycosyl Esters in Gardenia Fruits (Gardenia jasminoides Ellis) and Saffron (Crocus sativus Linne). J. Agric. Food Chem. 44, 2612–2615. https://doi.org/10.1021/jf950713e

Rambla, J.L., Trapero-Mozos, A., Diretto, G., Moraga, A.R., Granell, A., Gómez, L.G., Ahrazem, O., 2016. Gene-metabolite networks of volatile metabolism in Airen and Tempranillo grape cultivars revealed a distinct mechanism of aroma bouquet production. Front. Plant Sci. 7. https://doi.org/10.3389/fpls.2016.01619

Richardson, A.D., Duigan, S.P., Berlyn, G.P., 2002. An evaluation of noninvasive methods to estimate foliar chlorophyll content. New Phytol. 153, 185–194. https://doi.org/10.1046/j.0028-646X.2001.00289.x

Rodriguez-Concepcion, M., Avalos, J., Bonet, M.L., Boronat, A., Gomez-Gomez, L., Hornero-Mendez, D., Limon, M.C., Meléndez-Martínez, A.J., Olmedilla-Alonso, B., Palou, A., Ribot, J., Rodrigo, M.J., Zacarias, L., Zhu, C., 2018. A global perspective on carotenoids: Metabolism, biotechnology, and benefits for nutrition and health. Prog. Lipid Res. 70, 62–93. https://doi.org/10.1016/j.plipres.2018.04.004

Römer, S., Lübeck, J., Kauder, F., Steiger, S., Adomat, C., Sandmann, G., 2002. Genetic engineering of a zeaxanthin-rich potato by antisense inactivation and co-suppression of carotenoid epoxidation. Metab. Eng. 4, 263–272. https://doi.org/10.1006/mben.2002.0234

Rubio-Moraga, A., Trapero, A., Ahrazem, O., Gómez-Gómez, L., 2010. Crocins transport in Crocus sativus: The long road from a senescent stigma to a newborn corm. Phytochemistry 71, 1506–1513. https://doi.org/10.1016/j.phytochem.2010.05.026

Rubio Moraga, A., Ahrazem, O., Rambla, J.L., Granell, A., Gómez Gómez, L., 2013. Crocins with High Levels of Sugar Conjugation Contribute to the Yellow Colours of Early-Spring Flowering Crocus Tepals. PLoS One 8. https://doi.org/10.1371/journal.pone.0071946

Sainsbury, F., Saxena, P., Geisler, K., Osbourn, A., Lomonossoff, G.P., 2012. Using a virus-derived system to manipulate plant natural product biosynthetic pathways. Methods Enzym. 517, 185–202. https://doi.org/10.1016/B978-0-12-404634-4.00009-7

Skladnev, N. V., Johnstone, D.M., 2017. Neuroprotective properties of dietary saffron: More than just a chemical scavenger? Neural Regen. Res. https://doi.org/10.4103/1673-5374.198976

Sulli, M., Mandolino, G., Sturaro, M., Onofri, C., Diretto, G., Parisi, B., Giuliano, G., 2017. Molecular and biochemical characterization of a potato collection with contrasting tuber carotenoid content. PLoS One 12 (9): e0184143. https://doi.org/10.1371/journal.pone.0184143

Tan, H., Chen, X., Liang, N., Chen, R., Chen, J., Hu, C., Li, Qi, Li, Qing, Pei, W., Xiao, W., Yuan, Y., Chen, W., Zhang, L., 2019. Transcriptome analysis reveals novel enzymes for apo-carotenoid biosynthesis in saffron and allows construction of a pathway for crocetin synthesis in yeast. J. Exp. Bot. 70, 4819–4834. https://doi.org/10.1093/jxb/erz211

Tarantilis, P.A., Tsoupras, G., Polissiou, M., 1995. Determination of saffron (Crocus sativus L.) components in crude plant extract using high-performance liquid chromatography-UV-visible photodiode-array detection-mass spectrometry. J. Chromatogr. A 699, 107–118. https://doi.org/10.1016/0021-9673(95)00044-N

Thole, V., Worland, B., Snape, J.W., Vain, P., 2007. The pCLEAN dual binary vector system for Agrobacterium-mediated plant transformation. Plant Physiol. 145, 1211–1219.

Ting, H.M., Wang, B., Rydén, A.M., Woittiez, L., Van Herpen, T., Verstappen, F.W.A., Ruyter-Spira, C.,

Beekwilder, J., Bouwmeester, H.J., Van der Krol, A., 2013. The metabolite chemotype of Nicotiana benthamiana transiently expressing artemisinin biosynthetic pathway genes is a function of CYP71AV1 type and relative gene dosage. New Phytol. 199, 352–366. https://doi.org/10.1111/nph.12274

Walter, M.H., Floss, D.S., Strack, D., 2010. Apocarotenoids: Hormones, mycorrhizal metabolites and aroma volatiles. Planta 232, pp. 1-17. https://doi.org/10.1007/s00425-010-1156-3

Wang, B., Kashkooli, A.B., Sallets, A., Ting, H.M., de Ruijter, N.C.A., Olofsson, L., Brodelius, P., Pottier, M., Boutry, M., Bouwmeester, H., van der Krol, A.R., 2016. Transient production of artemisinin in Nicotiana benthamiana is boosted by a specific lipid transfer protein from A. annua. Metab. Eng. 38, 159–169. https://doi.org/10.1016/j.ymben.2016.07.004

Wang, W., He, P., Zhao, D., Ye, L., Dai, L., Zhang, X., Sun, Y., Zheng, J., Bi, C., 2019. Construction of Escherichia coli cell factories for crocin biosynthesis. Microb. Cell Fact. 18, 120. https://doi.org/10.1186/s12934-019-1166-1

Wu, X., Zhou, Y., Yin, F., Mao, C., Li, L., Cai, B., Lu, T., 2014. Quality control and producing areas differentiation of Gardeniae Fructus for eight bioactive constituents by HPLC-DAD-ESI/MS. Phytomedicine 21, 551–559. https://doi.org/10.1016/j.phymed.2013.10.002

Xu, C.J., Fraser, P.D., Wang, W.J., Bramley, P.M., 2006. Differences in the carotenoid content of ordinary citrus and lycopene-accumulating mutants. J. Agric. Food Chem. 54, 5474–5481. https://doi.org/10.1021/jf060702t

Xu, H., Lybrand, D., Bennewitz, S., Tissier, A., Last, R.L., Pichersky, E., 2018. Production of trans-chrysanthemic acid, the monoterpene acid moiety of natural pyrethrin insecticides, in tomato fruit. Metab. Eng. 47, 271–278. https://doi.org/10.1016/j.ymben.2018.04.004

Yang, T., Stoopen, G., Yalpani, N., Vervoort, J., de Vos, R., Voster, A., Verstappen, F.W.A., Bouwmeester, H.J., Jongsma, M.A., 2011. Metabolic engineering of geranic acid in maize to achieve fungal resistance is compromised by novel glycosylation patterns. Metab. Eng. 13, 414–425. https://doi.org/10.1016/j.ymben.2011.01.011

Yuan, L., Grotewold, E., 2015. Metabolic engineering to enhance the value of plants as green factories. Metab. Eng. 27, 83–91. https://doi.org/10.1016/j.ymben.2014.11.005

Zhang, C., Ma, J., Fan, L., Zou, Y., Dang, X., Wang, K., Song, J., 2015. Neuroprotective effects of safranal in a rat model of traumatic injury to the spinal cord by anti-apoptotic, anti-inflammatory and edema-attenuating. Tissue Cell 47, 291–300. https://doi.org/10.1016/j.tice.2015.03.007

Zhang, Y., Fei, F., Zhen, L., Zhu, X., Wang, J., Li, S., Geng, J., Sun, R., Yu, X., Chen, T., Feng, S., Wang, P., Yang, N., Zhu, Y., Huang, J., Zhao, Y., Aa, J., Wang, G., 2017. Sensitive analysis and simultaneous assessment of pharmacokinetic properties of crocin and crocetin after oral administration in rats. J. Chromatogr. B. Analyt. Technol. Biomed. Life Sci. 1044–1045, 1–7. https://doi.org/10.1016/j.jchromb.2016.12.003

Zhu, Q., Zeng, D., Yu, S., Cui, C., Li, J., Li, H., Chen, J., Zhang, R., Zhao, X., Chen, L., Liu, Y.G., 2018. From Golden Rice to aSTARice: Bioengineering Astaxanthin Biosynthesis in Rice Endosperm. Mol. Plant 11, 1440–1448. https://doi.org/10.1016/j.molp.2018.09.007

SUPPLEMENTARY DATA

Fig. S1. Nucleotide sequence of the cDNA transferred to the *Nicotiana benthamiana* transformed line using *Agrobacterium tume*faciens to prepare the virus-drive expression system.

TGGCAGGATATATTGTGGTGTAAACGTTCCTGCGGCGGTCGAGATGGATCTTGGCAGGATATATTGTGGTGTAAA
CGTTCCTGCGGCCGCAAGGGCTATTGAGACTTTTCAACAAAGGGTAATATCGGGAAACCTCCTCGGATTCCATTG
CCCAGCTATCTGTCACTTCATCAAAAGGACAGTAGAAAAGGAAGGTGGCACCTACAAATGCCATCATTGCGATAA
AGGAAAGGCTATCGTTCAAGATGCCTCTGCCGACAGTGGTCCCAAAGATGGACCCCCACCCACGAGGAGCATCGT
GGAAAAAGAAGACGTTCCAACCACGTCTTCAAAGCAAGTGGATTGATGTGATATCTCCACTGACGTAAGGGATGA
CGCACAATCCCACTATCCTTCGCAAGACCTTCCTCTATATAAGGAAGTTCATTTCATTTGGAGAGGACACGCTGA
AATCACCAGTCTCTCTCTACAAATCTATCTCTCTCGAGCTTTCGCAGATCTGTCGATCGACCATGGGGATTGAAC
AAGATGGATTGCACGCAGGTTCTCCGGCCGCTTGGGTGGAGAGGCTATTCGGCTATGACTGGGCACAACAGACAA
TCGGCTGCTCTGATGCCGCCGTGTTCCGGCTGTCAGCGCAGGGGCGCCCGGTTCTTTTTGTCAAGACCGACCTGT
CCGGTGCCCTGAATGAACTCCAGGACGAGGCAGCGCGGCTATCGTGGCTGGCCACGACGGGCGTTCCTTGCGCAG
CTGTGCTCGACGTTGTCACTGAAGCGGGAAGGGACTGGCTGCTATTGGGCGAAGTGCCGGGGCAGGATCTCCTGT
CATCTCACCTTGCTCCTGCCGAGAAAGTATCCATCATGGCTGATGCAATGCGGCGGCTGCATACGCTTGATCCGG
CTACCTGCCCATTCGACCACCAAGCGAAACATCGCATCGAGCGAGCACGTACTCGGATGGAAGCCGGTCTTGTCG
ATCAGGATGATCTGGACGAAGAGCATCAGGGGCTCGCGCCAGCCGAACTGTTCGCCAGGCTCAAGGCGCGCATGC
CCGACGGCGAGGATCTCGTCGTGACACATGGCGATGCCTGCTTGCCGAATATCATGGTGGAAAATGGCCGCTTTT
CTGGATTCATCGACTGTGGCCGGCTGGGTGTGGCGGACCGCTATCAGGACATAGCGTTGGCTACCCGTGATATTG
CTGAAGAGCTTGGCGGCGAATGGGCTGACCGCTTCCTCGTGCTTTACGGTATCGCCGCTCCCGATTCGCAGCGCA
TCGCCTTCTATCGCCTTCTTGACGAGTTCTTCTGAGCGGGACTCTGGGGTTCGGATCGATCCTCTAGCTAGAGTC
GATCGACAAGCTCGAGTTTCTCCATAATAATGTGTGAGTAGTTCCCAGATAAGGGAATTAGGGTTCCTATAGGGT
TTCGCTCATGTGTTGAGCATATAAGAAACCCTTAGTATGTATTTGTATTTGTAAAATACTTCTATCAATAAAATT
TCTAATTCCTAAAACCAAAATCCAGTACTAAAATCCAGATCCCCCGAATTAATTCGGCGTTAATTCAGTACATTA
GCGGCCGCGATTCCATTGCCCAGCTATCTGTCACTTTATTGTGAAGATAGTGGAAAAGGAAGGTGGCTCCTACAA
ATGCCATCATTGCGATAAAGGAAAGGCCATCGTTGAAGATGCCTCTGCCGACAGTGGTCCCAAAGATGGACCCCC
ACCCACGAGGAGCATCGTGGAAAAAGAAGACGTTCCAACCACGTCTTCAAAGCAAGTGGATTGATGTGATAGATT
CCATTGCCCAGCTATCTGTCACTTTATTGTGAAGATAGTGGAAAAGGAAGGTGGCTCCTACAAATGCCATCATTG
CGATAAAGGAAAGGCCATCGTTGAAGATGCCTCTGCCGACAGTGGTCCCAAAGATGGACCCCCACCCACGAGGAG
CATCGTGGAAAAAGAAGACGTTCCAACCACGTCTTCAAAGCAAGTGGATTGATGTGATATCTCCACTGACGTAAG
GGATGACGCACAATCCCACTATCCTTCGCAAGACCCTTCCTCTATATAAGGAAGTTCATTTCATTTGGAGAGGTA
TTAAAATCTTAATAGGTTTTGATAAAAGCGAACGTGGGGAAACCCGAACCAAACCTTCTTCTAAACTCTCTCTCA
TCTCTCTTAAAGCAAACTTCTCTCTTGTCTTTCTTGCGTGAGCGATCTTCAACGTTGTCAGATCGTGCTTCGGCA
CCAGTACAACGTTTTCTTTCACTGAAGCGAAATCAAAGATCTCTTTGTGGACACGTAGTGCGGCGCCATTAAATA
ACGTGTACTTGTCCTATTCTTGTCGGTGTGGTCTTGGGAAAAGAAAGCTTGCTGGAGGCTGCTGTTCAGCCCCAT
ACATTACTTGTTACGATTCTGCTGACTTTCGGCGGGTGCAATATCTCTACTTCTGCTTGACGAGGTATTGTTGCC
TGTACTTCTTTCTTCTTCTTCTTGCTGATTGGTTCTATAAGAAATCTAGTATTTTCTTTGAAACAGAGTTTTCCC
GTGGTTTTCGAACTTGGAGAAAGATTGTTAAGCTTCTGTATATTCTGCCCAAATTTGAAATGGGGGAGAAGAGGA
AATGGGTCGTGGAAGCACTGTCAGGGAACTTGAGGCCAGTGGCTGAGTGTCCCAGTCAGTTAGTCACAAAGCATG
TGGTTAAAGGAAAGTGTCCCCTCTTTGAGCTCTACTTGCAGTTGAATCCAGAAAAGGAAGCATATTTTAAACCGA
TGATGGGAGCATATAAGCCAAGTCGACTTAATAGAGAGGCGTTCCTCAAGGACATTCTAAAATATGCTAGTGAAA
TTGAGATTGGGAATGTGGATTGTGACTTGCTGGAGCTTGCAATAAGCATGCTCATCACAAAGCTCAAGGCGTTAG
GATTCCCAACTGTGAACTACATCACTGACCCAGAGGAAATTTTTAGTGCATTGAATATGAAAGCAGCTATGGGAG
CACTATACAAAGGCAAGAAGAAAGAAGCTCTCAGCGAGCTCACACTAGATGAGCAGGAGGCAATGCTCAAAGCAA
GTTGCCTGCGACTGTATACGGGAAAGCTGGGAATTTGGAATGGCTCATTGAAAGCAGAGTTGCGTCCAATTGAGA
AGGTTGAAAACAACAAAACGCGAACTTTCACAGCAGCACCAATAGACACTCTTCTTGCTGGTAAAGTTTGCGTGG
ATGATTTCAACAATCAATTTTATGATCTCAACATAAAGGCACCATGGACAGTTGGTATGACTAAGTTTTATCAGG
GGTGGAATGAATTGATGGAGGCTTTACCAAGTGGGTGGGTGTATTGTGACGCTGATGGTTCGCAATTCGACAGTT
CCTTGACTCCATTCCTCATTAATGCTGTATTGAAAGTGCGACTTGCCTTCATGGAGGAATGGGATATTGGTGAGC
AAATGCTGCGAAATTTGTACACTGAGATAGTGTATACACCAATCCTCACACCGGATGGTACTATCATTAAGAAGC
ATAAAGGCAACAATAGCGGGCAACCTTCAACAGTGGTGGACAACACACTCATGGTCATTATTGCAATGTTATACA
CATGTGAGAAGTGTGGAATCAACAAGGAAGAGATTGTGTATTACGTCAATGGCGATGACCTATTGATTGCCATTC
ACCCAGATAAAGCTGAGAGGTTGAGTGGATTCAAAGAATCTTTCGGAGAGTTGGGCCTGAAATATGAATTTGACT
GCACCACCAGGGACAAGACACAGTTGTGGTTCATGTCACACAGGGCTTTGGAGAGGGATGGCATGTATATACCAA

AGCTAGAAGAAGAAAGGATTGTTTCTATTTTGGAATGGGACAGATCCAAAGAGCCGTCACATAGGCTTGAAGCCA
TCTGTGCATCAATGATCGAAGCATGGGGTTATGACAAGCTGGTTGAAGAAATCCGCAATTTCTATGCATGGGTTT
TGGAACAAGCGCCGTATTCACAGCTTGCAGAAGAAGGAAAGGCGCCATATCTGGCTGAGACTGCGCTTAAGTTTT
TGTACACATCTCAGCACGGAACAAACTCTGAGATAGAAGAGTATTTAAAAGTGTTGTATGATTACGATATTCCAA
CGACTGAGAATCTTTATTTTCAGTAACTCTGGTTTCATTAAATTTTCTTTAGTTTGAATTTACTGTTATTCGGTG
TGCATTTCTATGTTTGGTGAGCGGTTTTCTGTGCTCAGAGTGTGTTTATTTTATGTAATTTAATTTCTTTGTGAG
CTCCTGTTTAGCAGGTCGTCCCTTCAGCAAGGACACAAAAAGATTTTAATTTTATTCGCTGAAATCACCAGTCTC
TCTCTACAAATCTATCTCTCTCTATTTTCTCCATAAATAATGTGTGAGTAGTTTCCCGATAAGGGAAATTAGGGT
TCTTATAGGGTTTCGCTCATGTGTTGAGCATATAAGAAACCCTTAGTATGTATTTGTATTTGTAAAATACTTCTA
TCAATAAAATTTCTAATTCCTAAAACCAAAATCCAGGGGCCCTCGACGTTCCTTGACAGGATATATTGGCGGGTA
AACTAAGTCGCTGTATGTGTTTGTTTG

The cDNAs of the **Neomycin phosphotransferase II (NPTII)** and ***Tobacco etch virus* (TEV) NIb** are in blue and black, respectively. Initiation Met and stop codons are underlined. Note that an ATG has been added to the 5' end of NIb cDNA that naturally lacks this codon because it is produced by proteolytic processing. *A. tumefaciens* T-DNA **right border (RB)** with **overdrive** (underlined) is in blue on yellow background and **double left border (LB)** is in blue on red background. ***Cauliflower mosaic virus* (CaMV) 35S promoter** and **terminator** are in red and fuchsia, respectively. Note that NIb is expressed from a **partially duplicated** version of CaMV 35S promoter. NIb open reading frame (ORF) is flanked by a **modified version of the 5' and 3' untranslated regions (UTRs) of *Cowpea mosaic virus* (CPMV) RNA-2**.

Fig. S2. Nucleotide sequences of TEVΔNIb (sequence variant DQ986288 that include the two silent mutations G273A and A1119G, in red, and lacks the whole NIb cistron) and the derived recombinant viruses TEVΔNIb-aGFP, -CsCCD2L, -BdCCD4.1, -BdCCD4.3, -CsCCD2L/PaCrtB, -CsCCD2L/CsBCH2 and -CsCCD2L/CsLPT1. The boundaries of viral cistrons are indicated on blue background. Initiation Met and stop codons are underlined.

>TEVΔNIb (8004 bp)
AAAATAACAAATCTCAACACAACATATACAAAACAAACGAATCTCAAGCAATCAAGCATTCTACTTCTATTGCAG
CAATTTAAATCATTTCTTTTAAAGCAAAAGCAATTTTCTGAAAATTTTCACCATTTACGAACGATAGCCATGGCA
CTCATCTTTGGCACAGTCAACGCTAACATCCTGAAGGAAGTGTTCGGTGGAGCTCGTATGGCTTGCGTTACCAGC
GCACATATGGCTGGAGCGAATGGAAGCATTTTGAAGAAGGCAGAAGAAACCTCTCGTGCAATCATGCACAAACCA
GTGATCTTCGGAGAAGACTACATTACCGAGGCAGACTTGCCTTACACACCACTCCATTTAGAGGTCGATGCTGAA
ATGGAGCGGATGTATTATCTTGGTCGTCGCGCGCTCACCCATGGCAAGAGACGCAAAGTTTCTGTGAATAACAAG
AGGAACAGGAGAAGGAAAGTGGCCAAAACGTACGTGGGGCGTGATTCCATTGTTGAGAAGATTGTAGTGCCCCAC
ACCGAGAGAAAGGTTGATACCACAGCAGCAGTGGAAGACATTTGCAATGAAGCTACCACTCAACTTGTGCATAAT
AGTATGCCAAAGCGTAAGAAGCAGAAAAACTTCTTGCCCGCCACTTCACTAAGTAACGTGTATGCCCAAACTTGG
AGCATAGTGCGCAAACGCCATATGCAGGTGGAGATCATTAGCAAGAAGAGCGTCCGAGCGAGGGTCAAGAGATTT
GAGGGCTCGGTGCAATTGTTCGCAAGTGTGCGTCACATGTATGGCGAGAGGAAAAGGGTGGACTTACGTATTGAC
AACTGGCAGCAAGAGACACTTCTAGACCTTGCTAAAAGATTTAAGAATGAGAGAGTGGATCAATCGAAGCTCACT
TTTGGTTCAAGTGGCCTAGTTTTGAGGCAAGGCTCGTACGGACCTGCGCATTGGTATCGACATGGTATGTTCATT
GTACGCGGTCGGTCGGATGGGATGTTGGTGGATGCTCGTGCGAAGGTAACGTTCGCTGTTTGTCACTCAATGACA
CATTATAGCGACAAATCAATCTCTGAGGCATTCTTCATACCATACTCTAAGAAATTCTTGGAGTTGAGGCCAGAT
GGAATCTCCCATGAGTGTACAAGAGGAGTATCAGTTGAGCGGTGCGGTGAGGTGGCTGCAATCCTGACACAAGCA
CTTTCACCGTGTGGTAAGATCACATGCAAACGTTGCATGGTTGAAACACCTGACATTGTTGAGGGTGAGTCGGGA
GACAGTGTCACCAACCAAGGTAAGCTCCTAGCAATGCTGAAAGAACAGTATCCAGATTTCCCAATGGCCGAGAAA
CTACTCACAAGGTTTTTGCAACAGAAATCACTAGTAAATACAAATTTGACAGCCTGCGTGAGCGTCAAACAACTC
ATTGGTGACCGCAAACAAGCTCCATTCACACACGTACTGGCTGTCAGCGAAATTCTGTTTAAAGGCAATAAACTA
ACAGGGGCCGATCTCGAAGAGGCAAGCACACATATGCTTGAAATAGCAAGGTTCTTGAACAATCGCACTGAAAAT
ATGCGCATTGGCCACCTTGGTTCTTTCAGAAATAAAATCTCATCGAAGGCCCATGTGAATAACGCACTCATGTGT
GATAATCAACTTGATCAGAATGGGAATTTTATTTGGGGACTAAGGGGTGCACACGCAAAGAGGTTTCTTAAAGGA
TTTTTCACTGAGATTGACCCAAATGAAGGATACGATAAGTATGTTATCAGGAAACATATCAGGGGTAGCAGAAAG
CTAGCAATTGGCAATTTGATAATGTCAACTGACTTCCAGACGCTCAGGCAACAAATTCAAGGCGAAACTATTGAG
CGTAAAGAAATTGGGAATCACTGCATTTCAATGCGGAATGGTAATTACGTGTACCCATGTTGTTGTGTTACTCTT
GAAGATGGTAAGGCTCAATATTCGGATCTAAAGCATCCAACGAAGAGACATCTGGTCATTGGCAACTCTGGCGAT
TCAAAGTACCTAGACCTTCCAGTTCTCAATGAAGAGAAAATGTATATAGCTAATGAAGGTTATTGCTACATGAAC

ATTTTCTTTGCTCTACTAGTGAATGTCAAGGAAGAGGATGCAAAGGACTTCACCAAGTTTATAAGGGACACAATT
GTTCCAAAGCTTGGAGCGTGGCCAACAATGCAAGATGTTGCAACTGCATGCTACTTACTTTCCATTCTTTACCCA
GATGTCCTGAGTGCTGAATTACCCAGAATTTTGGTTGATCATGACAACAAAACAATGCATGTTTTGGATTCGTAT
GGGTCTAGAACGACAGGATACCACATGTTGAAAATGAACACAACATCCCAGCTAATTGAATTCGTTCATTCAGGT
TTGGAATCCGAAATGAAAACTTACAATGTTGGAGGATGAACCGAGATATGGTCACACAAGGTGCAATTGAGATG
TTGATCAAGTCCATATACAAACCACATCTCATGAAGCAGTTACTTGAGGAGGAGCCATACATAATTGTCCTGGCA
ATAGTCTCCCCTTCAATTTTAATTGCCATGTACAACTCTGGAACTTTTGAGCAGGCGTTACAAATGTGGTTGCCA
AATACAATGAGGTTAGCTAACCTCGCTGCCATCTTGTCAGCCTTGGCGCAAAAGTTAACTTTGGCAGACTTGTTC
GTCCAGCAGCGTAATTTGATTAATGAGTATGCGCAGGTAATTTTGGACAATCTGATTGACGGTGTCAGGGTTAAC
CATTCGCTATCCCTAGCAATGGAAATTGTTACTATTAAGCTGGCCACCCAAGAGATGGACATGGCGTTGAGGGAA
GGTGGCTATGCTGTGACCTCTGAAAAGGTGCATGAAATGTTGGAAAAAAACTATGTAAAGGCTTTGAAGGATGCA
TGGGACGAATTAACTTGGTTGGAAAAATTCTCCGCAATCAGGCATTCAAGAAAGCTCTTGAAATTTGGGCGAAAG
CCTTTAATCATGAAAAACACCGTAGATTGCGGCGGACATATAGACTTGTCTGTGAAATCGCTTTTCAAGTTCCAC
TTGGAACTCCTGAAGGGAACCATCTCAAGAGCCGTAAATGGTGGTGCAAGAAAGGTAAGAGTAGCGAAGAATGCC
ATGACAAAAGGGGTTTTTCTCAAAATCTACAGCATGCTTCCTGACGTCTACAAGTTTATCACAGTCTCGAGTGTC
CTTTCCTTGTTGTTGACATTCTTATTTCAAATTGACTGCATGATAAGGGCACACCGAGAGGCGAAGGTTGCTGCA
CAGTTGCAGAAAGAGAGCGAGTGGGACAATATCATCAATAGAACTTTCCAGTATTCTAAGCTTGAAAATCCTATT
GGCTATCGCTCTACAGCGGAGGAAAGACTCCAATCAGAACACCCCGAGGCTTTCGAGTACTACAAGTTTTGCATT
GGAAAGGAAGACCTCGTTGAACAGGCAAAACAACCGGAGATAGCATACTTTGAAAAGATTATAGCTTTCATCACA
CTTGTATTAATGGCTTTTGACGCTGAGCGGAGTGATGGAGTGTTCAAGATACTCAATAAGTTCAAAGGAATACTG
AGCTCAACGGAGAGGGAGATCATCTACACGCAGAGTTTGGATGATTACGTTACAACCTTTGATGACAATATGACA
ATCAACCTCGAGTTGAATATGGATGAACTCCACAAGACGAGCCTTCCTGGAGTCACTTTTAAGCAATGGTGGAAC
AACCAAATCAGCCGAGGCAACGTGAAGCCACATTATAGAACTGAGGGGCACTTCATGGAGTTTACCAGAGATACT
GCGGCATCGGTTGCCAGCGAGATATCACACTCACCCGCAAGAGATTTTCTTGTGAGAGGTGCTGTTGGATCTGGA
AAATCCACAGGACTTCCATACCATTTATCAAAGAGAGGGAGAGTGTTAATGCTTGAGCCTACCAGACCACTCACA
GATAACGTGCACAAGCAACTGAGAAGTGAACCATTTAACTGCTTCCCAACTTTGAGGATGAGAGGGAAGTCAACT
TTTGGGTCATCACCGATTACAGTCATGACTAGTGGATTCGCTTTACACCATTTTGCACGAAACATAGCTGAGGTA
AAAACATACGATTTTGTCATAATTGATGAATGTCATGTGAATGATGCTTCTGCTATAGCGTTTAGGAATCTACTG
TTTGAACATGAATTTGAAGGAAAAGTCCTCAAAGTGTCAGCCACACCACCAGGTAGAGAAGTTGAATTCACAACT
CAGTTTCCCGTGAAACTCAAGATAGAAGAGGCTCTTAGCTTTCAGGAATTTGTAAGTTTACAAGGGACAGGTGCC
AACGCCGATGTGATTAGTTGTGGCGACAACATACTAGTATATGTTGCTAGCTACAATGATGTTGATAGTCTTGGC
AAGCTCCTTGTGCAAAAGGGATACAAAGTGTCGAAGATTGATGGAAGAACAATGAAGAGTGGAGGAACTGAAATA
ATCACTGAAGGTACTTCAGTGAAAAAGCATTTCATAGTCGCAACTAATATTATTGAGAATGGTGTAACCATTGAC
ATTGATGTAGTTGTGGATTTTGGGACTAAGGTTGTACCAGTTTTGGATGTGGACAATAGAGCGGTGCAGTACAAC
AAAACTGTGGTGAGTTATGGGGAGCGCATCCAAAGACTCGGTAGAGTTGGGCGACACAAGGAAGGAGTAGCACTT
CGAATTGGCCAAACAAATAAAACACTGGTTGAAATTCCAGAAATGGTTGCCACTGAAGCTGCCTTTCTATGCTTC
ATGTACAATTTGCCAGTGACAACACAGAGTGTTTCAACCACACTGCTGGAAAATGCCACATTATTACAAGCTAGA
ACTATGGCACAGTTTGAGCTATCATATTTTTACACAATTAATTTTGTGCGATTTGATGGTAGTATGCATCCAGTC
ATACATGACAAGCTGAAGCGCTTTAAGCTACACACTTGTGAGACATTCCTCAATAAGTTGGCGATCCCAAATAAA
GGCTTATCCTCTTGGCTTACGAGTGGAGAGTATAAGCGACTTGGTTACATAGCAGAGGATGCTGGCATAAGAATC
CCATTCGTGTGCAAAGAAATTCCAGACTCCTTGCATGAGGAAATTTGGCACATTGTAGTCGCCCATAAAGGTGAC
TCGGGTATTGGGAGGCTCACTAGCGTACAGGCAGCAAAGGTTGTTTATACTCTGCAAACGGATGTGCACTCAATT
GCGAGGACTCTAGCATGCATCAATAGACTCATAGCACATGAACAAATGAAGCAGAGTCATTTTGAAGCCGCAACT
GGGAGAGCATTTTCCTTCACAAATTACTCAATACAAAGCATATTTGACACGCTGAAAGCAAATTATGCTACAAAG
CATACGAAAGAAAATATTGCAGTGCTTCAGCAGGCAAAAGATCAATTGCTAGAGTTTTCGAACCTAGCAAAGGAT
CAAGATGTCACGGGTATCATCCAAGACTTCAATCACCTGGAAACTATCTATCTCCAATCAGATAGCGAAGTGGCT
AAGCATCTGAAGCTTAAAAGTCACTGGAATAAAAGCCAAATCACTAGGGACATCATAATAGCTTTGTCTGTGTTA
ATTGGTGGTGGATGGATGCTTGCAACGTACTTCAAGGACAAGTTCAATGAACCAGTCTATTTCCAAGGGAAGAAG
AATCAGAAGCACAAGCTTAAGATGAGAGAGGCGCGTGGGGCTAGAGGGCAATATGAGGTTGCAGCGGAGCCAGAG
GCGCTAGAACATTACTTTGGAAGCGCATATAATAACAAAGGAAAGCGCAAGGGCACCACGAGAGGAATGGGTGCA
AAGTCTCGGAAATTCATAAACATGTATGGGTTTGATCCAACTGATTTTTCATACATTAGGTTTGTGGATCCATTG
ACAGGTCACACTATTGATGAGTCCACAAACGCACCTATTGATTTAGTGCAGCATGAGTTTGGAAAGGTTAGAACA
CGCATGTTAATTGACGATGAGATAGAGCCTCAAAGTCTTAGCACCCACACCACAATCCATGCTTATTTGGTGAAT
AGTGGCACGAAGAAAGTTCTTAAGGTTGATTTAACACCACACTCGTCGCTACGTGCGAGTGAGAAATCAACAGCA
ATAATGGGATTTCCTGAAAGGGAGAATGAATTGCGTCAAACCGGCATGGCAGTGCCAGTGGCTTATGATCAATTG
CCACCAAAGAGTGAGGACTTGACGTTTGAAGGAGAAAGCTTGTTTAAGGGACCACGTGATTACAACCCGATATCG
AGCACCATTTGTCACTTGACGAATGAATCTGATGGGCACACAACATCGTTGTATGGTATTGGATTTGGTCCCTTC
ATCATTACAAACAAGCACTTGTTTAGAAGAAATAATGGAACACTGTTGGTCCAATCACTACATGGTGTATTCAAG
GTCAAGAACACCACGACTTTGCAACAACACCTCATTGATGGGAGGGACATGATAATTATTCGCATGCCTAAGGAT
TTCCCACCATTTCCTCAAAAGCTGAAATTTAGAGAGCCACAAAGGGAAGAGCGCATATGTCTTGTGACAACCAAC
TTCCAAACTAAGAGCATGTCTAGCATGGTGTCAGACACTAGTTGCACATTCCCTTCATCTGATGGCATATTCTGG

AAGCATTGGATTCAAACCAAGGATGGGCAGTGTGGCAGTCCATTAGTATCAACTAGAGATGGGTTCATTGTTGGT
ATACACTCAGCATCGAATTTCACCAACACAAACAATTATTTCACAAGCGTGCCGAAAAACTTCATGGAATTGTTG
ACAAATCAGGAGGCGCAGCAGTGGGTTAGTGGTTGGCGATTAAATGCTGACTCAGTATTGTGGGGGGGCCATAAA
GTTTTCATGAGCAAACCTGAAGAGCCTTTTCAGCCAGTTAAGGAAGCGACTCAACTCATGAGTGAATTGGTGTAC
TCGCAAAGTGGCACTGTGGGTGCTGGTGTTGACGCTGGTAAGAAGAAAGATCAAAAGGATGATAAAGTCGCTGAG
CAGGCTTCAAAGGATAGGGATGTTAATGCTGGAACTTCAGGAACATTCTCAGTTCCACGAATAAATGCTATGGCC
ACAAAACTTCAATATCCAAGGATGAGGGGAGAGGTGGTTGTAAACTTGAATCACCTTTTAGGATACAAGCCACAG
CAAATTGATTTGTCAAATGCTCGAGCCACACATGAGCAGTTTGCCGCGTGGCATCAGGCAGTGATGACAGCCTAT
GGAGTGAATGAAGAGCAAATGAAAATATTGCTAAATGGATTTATGGTGTGGTGCATAGAAAATGGGACTTCCCCA
AATTTGAACGGAACTTGGGTTATGATGGATGGTGAGGAGCAAGTTTCATACCCGCTGAAACCAATGGTTGAAAAC
GCGCAGCCAACACTGAGGCAAATTATGACACACTTCAGTGACCTGGCTGAAGCGTATATTGAGATGAGGAATAGG
GAGCGACCATACATGCCTAGGTATGGTCTACAGAGAAACATTACAGACATGAGTTTGTCACGCTATGCGTTCGAC
TTCTATGAGCTAACTTCAAAAACACCTGTTAGAGCGAGGGAGGCGCATATGCAAATGAAAGCTGCTGCAGTACGA
AACAGTGGAACTAGGTTATTTGGTCTTGATGGCAACGTGGGTACTGCAGAGGAAGACACTGAACGGCACACAGCG
CACGATGTGAACCGTAACATGCACACACTATTAGGGGTCCGCCAGTGATAGTTTCTGCGTGTCTTTGCTTTCCGC
TTTTAAGCTTATTGTAATATATATGAATAGCTATTCACAGTGGGACTTGGTCTTGTGTTGAATGGTATCTTATAT
GTTTTAATATGTCTTATTAGTCTCATTACTTAGGCGAACGACAAAGTGAGGTCACCTCGGTCTAATTCTCCTATG
TAGTGCGAGAAAAAAAAAAAAAAAAAAAAAAAAAAAAAAAAAAAAAAAAAA

>TEVΔNIb-aGFP (insert between possitions 144 and 145 of TEVΔNIb; artificial NIaPro cleavage site is on gray background)
ATGGTGAGCAAGGGCGAGGAGCTGTTCACCGGGGTGGTGCCCATCCTGGTCGAGCTGGACGGCGACGTAAACGGC
CACAAGTTCAGCGTGTCCGGCGAGGGCGAGGGCGATGCCACCTACGGCAAGCTGACCCTGAAGTTCATCTGCACC
ACCGGCAAGCTGCCCGTGCCCTGGCCCACCCTCGTGACCACCCTGACCTACGGCGTGCAGTGCTTCAGCCGCTAC
CCCGACCACATGAAGCAGCACGACTTCTTCAAGTCCGCCATGCCCGAAGGCTACGTCCAGGAGCGCACCATCTTC
TTCAAGGACGACGGCAACTACAAGACCCGCGCCGAGGTGAAGTTCGAGGGCGACACCCTGGTGAACCGCATCGAG
CTGAAGGGCATCGACTTCAAGGAGGACGGCAACATCCTGGGGCACAAGCTGGAGTACAACTACAACAGCCACAAC
GTCTATATCATGGCCGACAAGCAGAAGAACGGCATCAAGGTGAACTTCAAGATCCGCCACAACATCGAGGACGGC
AGCGTGCAGCTCGCCGACCACTACCAGCAGAACACCCCCATCGGCGACGGCCCCGTGCTGCTGCCCGACAACCAC
TACCTGAGCACCCAGTCCGCCCTGAGCAAAGACCCCAACGAGAAGCGCGATCACATGGTCCTGCTGGAGTTCGTG
ACCGCCGCCGGGATCACTCTCGGCATGGACGAGCTGTACAAGACGACTGAGAATCTTTATTTTCAGGGGGAGAAG

>TEVΔNIb-CsCCD2L (insert between possitions 144 and 145 of TEVΔNIb; artificial NIaPro cleavage site is on gray background)
ATGGAATCTCCTGCTACTAAATTACCTGCACCTCTGCTGATGTTATCTTCTTCTCCATTCCTTCTCCCTTCTCCT
AATAAGAGCTCCTCCATCTTCCTTCCACGTAAATTAGGGCCGCTACCTCCAAAATATTATTATTACAATTGCTGC
CATCCTAAGAGTAGATCAATCTCAGTAGTATCAATGGCAAATAAGGAGGAGGCAGAGACCAGTAAGAAGAAGCCC
AAACCATTAAAAGTACTAATTACCAAAGTGGATCCGAAGCCGAGGAAGGGCATGGCATCCGTCGCAGTGGACTTA
CTCGAGAAGGCCTTTGTATACCTATTGTCCGGAAATTCTGCAGCTGATCGTAGTAGTAGTAGTGGTCGTCGTCGT
CGTAAAGAGCATTACTACCTCTCCGGCAATTATGCGCCCGTCGGACACGAAACCCCGCCCTCCGACCACCTCCCC
ATTCATGGATCCCTTCCTGAATGCTTGAATGGAGTGTTTCTGAGAGTTGGTCCTAACCCCAAGTTTGCTCCCGTA
GCCGGATACAATTGGGTCGATGGAGATGGAATGATTCATGGATTGCGTATTAAAGATGGAAAAGCAACTTATCTA
TCTCGATATATTAAAACGTCACGGTTTAAACAAGAAGAATATTTTGGAAGAGCAAAATTTATGAAGATTGGAGAT
CTAAGGGGATTGCTTGGGTTCTTTACGATCTTAATACTAGTACTTCGAACAACATTGAAAGTAATAGACATTTCA
TATGGAAGAGGGACGGGTAATACAGCTCTTGTGTATCATAATGGCTTACTATTGGCTCTATCAGAAGAAGATAAA
CCTTATGTTGTTAAAGTTTTAGAAGATGGAGACTTGCAAACTCTTGGGATATTGGATTATGACAAGAAATTGTCA
CATCCATTCACCGCTCATCCAAAGATCGATCCGTTAACTGATGAGATGTTTACCTTTGGATATTCCATCTCGCCT
CCGTATCTTACTTATCGAGTCATTTCCAAGGATGGAGTGATGCAAGATCCAGTGCAAATCTCAATTACATCCCCT
ACCATAATGCATGATTTTGCTATTACTGAAAATTATGCCATCTTCATGGACCTGCCCTTGTATTTCCAACCAGAG
GAAATGGTAAAGGGGAAATTTGTCTCTTCATTTCACCCTACAAAAAGAGCTCGTATCGGTGTGCTTCCACGATAT
GCAAAAGACGAGCATCCAATTCGATGGTTCGATCTTCCAAGTTGCTTCATGACTCATAATGCAAATGCTTGGGAA
GAGAATGATGAAGTTGTGCTATTCACATGTCGCCTTGAGAGTCCTGATCTTGACATGCTTAGTGGACCTGCGGAA
GAAGAGATTGGGAATTCAAAAAGTGAGCTTTACGAAATGAGGTTCAATTTGAAAACTGGAATTACTTCACAAAAG
CAACTATCTGTACCTAGTGTTGATTTTCCTCGGATCAACCAAAGTTATACTGGCAGGAAACAGCAATATGTTTAT
TGTACTCTTGGCAACACCAAGATTAAGGGCATTGTGAAGTTTGATCTGCAAATTGAACCAGAAGCCGGAAAGACA
ATGCTTGAAGTTGGAGGAAATGTACAAGGCATCTTTGAGTTGGGACCTAGAAGATATGGTTCAGAGGCAATATTT
GTGCCATGCCAACCTGGCATCAAATCTGATGAGGATGACGGTTACTTGATATTCTTTGTACACGACGAAAACAAT
GGGAAATCTGAGGTCAATGTCATCGATGCAAAGACAATGTCTGCAGAACCTGTGGCTGTTGTGGAACTTCCAAGC
AGGGTTCCATATGGATTCCATGCCTTGTTTCTGAATGAGGAAGAACTTCAGAAGCACCAAGCAGAGACAACAACC
GAAAATTTATATTTCCAGTCTGGAACA

>TEVΔNIb-BdCCD4.1 (insert between possitions 144 and 145 of TEVΔNIb; artificial NIaPro cleavage site is on gray background)

ATGAACTCCCTTTATTCTTCCTCTTTCCTTTCCAAATTTCCAATGAATGTTTCATCACTTGGAATAATTGACAAG
AACCCTCAAACAAAGATTAATCCCATTTATTCCGTACCAACGTTCCATGCCCGTCTAACCGAAAAACCCTTTCGC
GGAAAGCCTTTATATGAGAGGAGAAGAAATGATGAATCTTTGTATGCAAAAATGTTGAAATCATTAGATGATTTC
ATATGCAAGTTCATGAGTGAAGTACCCCTGGACCCCTCCAACGATCCAAAACACATACTGGTGGGCAACTTTGCA
CCGGTGGACGAGCTTCCTCCGACTCCATGTGAGGTGGTGGAAGGCTCCCTTCCGATATGTGTGGAGGGTGCATAC
ATCCGCAACGGTCCCAACCCTCCGATCACCCCTCACGGTCCGTACCATCTCTTTGATGGAGATGGAATGCTTCAC
TCCATCACAATCTCAAAAGGCAAAGCCACCTTTTGTAGTCGTTATGTTAAGACTTATAAATATTTGGTGGAACAA
AACATAGGCTATCCGGTCTTCCCAAGTCCTTTCTCCTCCTTTAATAATGGCCTCTCGGCTTCTATAGCGCGTTTA
GTCGTATTAACGGTAGCACGAGTGCTGGTTACTAGGTGTTTGGATCCTAGACCTAATGGGTTTGGAACGGGGAAT
ACTAGTTTAGGTTTATTTGGCGGGAAACTCTTTGCGCTATGTGAGTCTGATCTTCCTTATGCTATAAAAGTGACA
TCGGATGGGGATATAATAACTCTTGATCGCCATGATTTTTACACCGGTGATCCGTTACTCAGAATGACTGCACAC
CCAAAGATTGATTTAGAGACTGGACAAGTCTTCGCTTTCAGATGTGACATAACATCTCCATTCTTGACATTTTTC
CGAATCGATTCATCTGGAAGAAAAGGCCCCGATTTTCCAATCTTCTCCTTGCACGGACCGTCACTCATTCATGAT
TTTGCTCTTACCAAACATTATGTCATATTCCAGGATACACAGGTTGAACTTAATCCAATGGAGATAACTAGAGGA
AGATCACCAATTGTAGTTGACCATACCAAAGTGCCCCGGCTAGGCATTTTACCACGCAACGCCATGAATGAAACT
GAACTGTCGTGGATTGATGTACCAGGATTAAACATGTCACACTTTATTAATGCTTGGGAAGAAGATGGCGGAAAC
AAAATAGTAATTGTTGCTTTTAATGTATTATCAGGGTTGGATTCCCTATATTTGTTCAATTCCTCAATGGAAAAA
ATTACAATTGACCTCAAGGCAAAGAAGATTGAAAGACATCCATTGTCCACTAAAAATCTCGAGTTAGGAGTTATT
AATCCTGCTTACGCCGGAAAGAAAAACAAGTATGTATATGCGGCAATTATAAGTCAAACACCAAAGGCAGCAGGG
GTGATTAAGCTTGACATATCACAGCTCCCTAATGCTGATAGTAGTAATTGCATGGTGGCTAGCCGACTTTATGGT
TCGAGCTGTTATGGTGGTGAACCTTACTTTGTCGCAAGGGAGCCTGATAATCCAGAGGCTGAAGAGGATGATGGT
TATCTAGTCACATACATGCATGATGAGAATAGCGAGGAATCGTGGTTCTTGGTTATGAACGCCAAATCCCCAACT
CTTGACATTGTTGCTAGTGTTAGATTACCTGGTAGAGTGCCTTATGGCTTCCACGGACTTTTTGTCAGGGAAGGT
GACCTCAACAAGCTGGACAACCGAAAATTTATATTTCCAGTCTGGAACA

>TEVΔNIb-BdCCD4.3 (insert between possitions 144 and 145 of TEVΔNIb; artificial NIaPro cleavage site is on gray background)

ATGGACACCCTTTCTTCCTTTTTCCTTCAAAAATATGTTCCAAGTCATTCACTCACACCATCCCCGCCATTACTC
CTTAAATTCAATATTTCATCTCTTAAAATTGATAAAAAATGCGATAGATTAAATCATCAAAAATCTATGATCACA
ACATCAATTTTGCATCAAAAAAAGCTTAAAACGTTAAACACTCCGAAAAACCCTTCAACCTCAGAAATTACAAAA
ATAAAAAAACAATCTTTTCTTACTATTTTCTTCAACTCATTAGATAATTTCATATGCAATTTCATAGACCCCCCA
CTCCGCCCCTCCATCGACCCTAACCACGTCCTCTCCGGCAACTTCGCCCCCGTCGGCGAGCTCCCCCCCACCGCG
TGCGACGTCGTCGAGGGCTCCCTTCCGCCGTCGTTAAACGGCGCGTACATTCGCAACGGCCCAAACCCTCAGTTC
ATCCCCCGTGGGCCCTACCACCTATTCGACGGCGATGGCATGCTCCACGCCGTCACCATCTCCGGCGGCAAAGCC
ACATTCTGCAGCCGCTTCGTCAAGACTTATAAGTACACGCTGGAGCGAGAGATCGGCTCGCCGGTTATTCTGAAC
GTGTTCTCCGCCTTCAACGGCTTGCTGGCTTCGCTGGCGCGCTGCGCCGTATCATCAGGCCGCGTCCTCACCGGA
CAATACGACCCCCGCCGCGGCGCCGGCCGCGCCAACACAAGCTTAGCGTTGATTAGCGGAAAGTTATTCGCTCAC
GAAGAATGTGACCTTCCCTACGGAATAAAATTAACATGTGATGGCGATATAATCACTTTAGGCCGCCATGAATTT
CTCGGTGAGCAGTTTACGGCGATGACGGCGCACCCGAAAATCGACATGGAAACCGGCGAGACCTTTGCTTTCAGA
TACAGTTTCCTGCCGCCGTTCTTAACATATTTCAGGATCAACGGGGATGGAATTATGCAACACGAAGTGCCGATT
TTCTCCTTGAAGCAATCGTCATTCATCCACGACTTCGCAATATCCAAAAACTACGTCGTTTTCCCAGATACGCAG
ATTGTGATAAAACCTAGAGATATGTTGAGAGGGAGGGTGCCATTAAGAGTTGATCTTGAAAAAGTGCCGAGGCTT
GGGATTATGCCGAGATACGCGGTGGATGAGAGGGAAATGTGGTGGGTTGATGTGTCGGGGTTTAATATAATACAC
GCGGTGAATGCGTGGGAGGAGGAAGACGACGGCGGCGACACCATTGTGATGGTGGCGCCGAATGCTTTGGGGGTG
GAGCATGTGTTGGAGCGTATGGATTTGGTTCACTCATCCTTGGAAAGAATTCAAATAAATTTGAAGGAGAAGAGT
GTGACGAGACGCCCGGTGTCCACAGCAAATCTCGAGTTTGCGGTCATCAATCCGGCTTACGTTGGGAAGAAGAAC
AGGTATGTGTATGCAGCAGTAGGAGATCCAATGCCAAAGATAGTAGGTGTTGTGAAGGTGGACTTATCACTTTCC
ACGGCCAACTCCGGCGACTGCACGGTGGCTAGACGCCTATACGGGCCCGGCTGCTACGGCGGTGAACCATTTTTT
GTGGCAAGGGAGCCGGATAATCCGGCGGCGGAGGAGGATGATGGCTATCTAATAACTTATATGCATAATGAAAAT
ACTGAAGAATCAAAGTTTTTAGTAATGGATGCAAAATCCCCTACTCTTCAAATTCTTGCTGCTGTTAAGCTACCC
CAACGAGTTCCCTATGGCTTCCATGGAATCTTTGTGCCGGAATCTCACTTGCGTAAACTAACAACCGAAAATTTA
TATTTCCAGTCTGGAACA

>TEVΔNIb-CsCCD2L/PaCrtB
(insert between possitions 144 and 145 of TEVΔNIb; artificial NIaPro cleavage site is on gray background)

ATGGAATCTCCTGCTACTAAATTACCTGCACCTCTGCTGATGTTATCTTCTTCTCCATTCCTTCTCCCTTCTCCT
AATAAGAGCTCCTCCATCTTCCTTCCACGTAAATTAGGGCCGCTACCTCCAAAATATTATTATTACAATTGCTGC

CATCCTAAGAGTAGATCAATCTCAGTAGTATCAATGGCAAATAAGGAGGAGGCAGAGACCAGTAAGAAGAAGCCC
AAACCATTAAAAGTACTAATTACCAAAGTGGATCCGAAGCCGAGGAAGGGCATGGCATCCGTCGCAGTGGACTTA
CTCGAGAAGGCCTTTGTATACCTATTGTCCGGAAATTCTGCAGCTGATCGTAGTAGTAGTAGTGGTCGTCGTCGT
CGTAAAGAGCATTACTACCTCTCCGGCAATTATGCGCCCGTCGGACACGAAACCCCGCCCTCCGACCACCTCCCC
ATTCATGGATCCCTTCCTGAATGCTTGAATGGAGTGTTTCTGAGAGTTGGTCCTAACCCCAAGTTTGCTCCCGTA
GCCGGATACAATTGGGTCGATGGAGATGGAATGATTCATGGATTGCGTATTAAAGATGGAAAAGCAACTTATCTA
TCTCGATATATTAAAACGTCACGGTTTAAACAAGAAGAATATTTTGGAAGAGCAAAATTTATGAAGATTGGAGAT
CTAAGGGGATTGCTTGGGTTCTTTACGATCTTAATACTAGTACTTCGAACAACATTGAAAGTAATAGACATTTCA
TATGGAAGAGGGACGGGTAATACAGCTCTTGTGTATCATAATGGCTTACTATTGGCTCTATCAGAAGAAGATAAA
CCTTATGTTGTTAAAGTTTTAGAAGATGGAGACTTGCAAACTCTTGGGATATTGGATTATGACAAGAAATTGTCA
CATCCATTCACCGCTCATCCAAAGATCGATCCGTTAACTGATGAGATGTTTACCTTTGGATATTCCATCTCGCCT
CCGTATCTTACTTATCGAGTCATTTCCAAGGATGGAGTGATGCAAGATCCAGTGCAAATCTCAATTACATCCCCT
ACCATAATGCATGATTTTGCTATTACTGAAAATTATGCCATCTTCATGGACCTGCCCTTGTATTTCCAACCAGAG
GAAATGGTAAAGGGGAAATTTGTCTCTTCATTTCACCCTACAAAAAGAGCTCGTATCGGTGTGCTTCCACGATAT
GCAAAAGACGAGCATCCAATTCGATGGTTCGATCTTCCAAGTTGCTTCATGACTCATAATGCAAATGCTTGGGAA
GAGAATGATGAAGTTGTGCTATTCACATGTCGCCTTGAGAGTCCTGATCTTGACATGCTTAGTGGACCTGCGGAA
GAAGAGATTGGGAATTCAAAAAGTGAGCTTTACGAAATGAGGTTCAATTTGAAAACTGGAATTACTTCACAAAAG
CAACTATCTGTACCTAGTGTTGATTTTCCTCGGATCAACCAAAGTTATACTGGCAGGAAACAGCAATATGTTTAT
TGTACTCTTGGCAACACCAAGATTAAGGGCATTGTGAAGTTTGATCTGCAAATTGAACCAGAAGCCGGAAAGACA
ATGCTTGAAGTTGGAGGAAATGTACAAGGCATCTTTGAGTTGGGACCTAGAAGATATGGTTCAGAGGCAATATTT
GTGCCATGCCAACCTGGCATCAAATCTGATGAGGATGACGGTTACTTGATATTCTTTGTACACGACGAAAACAAT
GGGAAATCTGAGGTCAATGTCATCGATGCAAAGACAATGTCTGCAGAACCTGTGGCTGTTGTGGAACTTCCAAGC
AGGGTTCCATATGGATTCCATGCCTTGTTTCTGAATGAGGAAGAACTTCAGAAGCACCAAGCAGAGACAACAACC
GAAAATTTATATTTCCAGTCTGGAACA

(insert between possitions 6981 and 6982 of TEVΔNIb; sequences to complete native NIaPro cleavage sites are on yellow background)

GGGGAGAAGATGAATAATCCGTCGTTACTCAATCATGCGGTCGAAACGATGGCAGTTGGCTCGAAAAGTTTTGCG
ACAGCCTCAAAGTTATTTGATGCAAAAACCCGGCGCAGCGTACTGATGCTCTACGCCTGGTGCCGCCATTGTGAC
GATGTTATTGACGATCAGACGCTGGGCTTTCAGGCCCGGCAGCCTGCCTTACAAACGCCCGAACAACGTCTGATG
CAACTTGAGATGAAAACGCGCCAGGCCTATGCAGGATCGCAGATGCACGAACCGGCGTTTGCGGCTTTTCAGGAA
GTGGCTATGGCTCATGATATCGCCCCGGCTTACGCGTTTGATCATCTGGAAGGCTTCGCCATGGATGTACGCGAA
GCGCAATACAGCCAACTGGATGATACGCTGCGCTATTGCTATCACGTTGCAGGCGTTGTCGGCTTGATGATGGCG
CAAATCATGGGCGTGCGGGATAACGCCACGCTGGACCGCGCCTGTGACCTTGGGCTGGCATTTCAGTTGACCAAT
ATTGCTCGCGATATTGTGGACGATGCGCATGCGGGCCGCTGTTATCTGCCGGCAAGCTGGCTGGAGCATGAAGGT
CTGAACAAAGAGAATTATGCGGCACCTGAAAACCGTCAGGCGCTGAGCCGTATCGCCCGTCGTTTGGTGCAGGAA
GCAGAACCTTACTATTTGTCTGCCACAGCCGGCCTGGCAGGGTTGCCCCTGCGTTCCGCCTGGGCAATCGCTACG
GCGAAGCAGGTTTACCGGAAAATAGGTGTCAAAGTTGAACAGGCCGGTCAGCAAGCCTGGGATCAGCGGCAGTCA
ACGACCACGCCCGAAAAATTAACGCTGCTGCTGGCCGCCTCTGGTCAGGCCCTTACTTCCCGGATGCGGGCTCAT
CCTCCCCGCCCTGCGCATCTCTGGCAGCGCCCGCTCACGACTGAGAATCTTTATTTTCAG

>TEVΔNIb-CsCCD2L/CsBCH2

(insert between possitions 144 and 145 of TEVΔNIb; artificial NIaPro cleavage site is on gray background)

ATGGAATCTCCTGCTACTAAATTACCTGCACCTCTGCTGATGTTATCTTCTTCTCCATTCCTTCTCCCTTCTCCT
AATAAGAGCTCCTCCATCTTCCTTCCACGTAAATTAGGGCCGCTACCTCCAAAATATTATTATTACAATTGCTGC
CATCCTAAGAGTAGATCAATCTCAGTAGTATCAATGGCAAATAAGGAGGAGGCAGAGACCAGTAAGAAGAAGCCC
AAACCATTAAAAGTACTAATTACCAAAGTGGATCCGAAGCCGAGGAAGGGCATGGCATCCGTCGCAGTGGACTTA
CTCGAGAAGGCCTTTGTATACCTATTGTCCGGAAATTCTGCAGCTGATCGTAGTAGTAGTAGTGGTCGTCGTCGT
CGTAAAGAGCATTACTACCTCTCCGGCAATTATGCGCCCGTCGGACACGAAACCCCGCCCTCCGACCACCTCCCC
ATTCATGGATCCCTTCCTGAATGCTTGAATGGAGTGTTTCTGAGAGTTGGTCCTAACCCCAAGTTTGCTCCCGTA
GCCGGATACAATTGGGTCGATGGAGATGGAATGATTCATGGATTGCGTATTAAAGATGGAAAAGCAACTTATCTA
TCTCGATATATTAAAACGTCACGGTTTAAACAAGAAGAATATTTTGGAAGAGCAAAATTTATGAAGATTGGAGAT
CTAAGGGGATTGCTTGGGTTCTTTACGATCTTAATACTAGTACTTCGAACAACATTGAAAGTAATAGACATTTCA
TATGGAAGAGGGACGGGTAATACAGCTCTTGTGTATCATAATGGCTTACTATTGGCTCTATCAGAAGAAGATAAA
CCTTATGTTGTTAAAGTTTTAGAAGATGGAGACTTGCAAACTCTTGGGATATTGGATTATGACAAGAAATTGTCA
CATCCATTCACCGCTCATCCAAAGATCGATCCGTTAACTGATGAGATGTTTACCTTTGGATATTCCATCTCGCCT
CCGTATCTTACTTATCGAGTCATTTCCAAGGATGGAGTGATGCAAGATCCAGTGCAAATCTCAATTACATCCCCT
ACCATAATGCATGATTTTGCTATTACTGAAAATTATGCCATCTTCATGGACCTGCCCTTGTATTTCCAACCAGAG
GAAATGGTAAAGGGGAAATTTGTCTCTTCATTTCACCCTACAAAAAGAGCTCGTATCGGTGTGCTTCCACGATAT
GCAAAAGACGAGCATCCAATTCGATGGTTCGATCTTCCAAGTTGCTTCATGACTCATAATGCAAATGCTTGGGAA

GAGAATGATGAAGTTGTGCTATTCACATGTCGCCTTGAGAGTCCTGATCTTGACATGCTTAGTGGACCTGCGGAA
GAAGAGATTGGGAATTCAAAAAGTGAGCTTTACGAAATGAGGTTCAATTTGAAAACTGGAATTACTTCACAAAAG
CAACTATCTGTACCTAGTGTTGATTTTCCTCGGATCAACCAAAGTTATACTGGCAGGAAACAGCAATATGTTTAT
TGTACTCTTGGCAACACCAAGATTAAGGGCATTGTGAAGTTTGATCTGCAAATTGAACCAGAAGCCGGAAAGACA
ATGCTTGAAGTTGGAGGAAATGTACAAGGCATCTTTGAGTTGGGACCTAGAAGATATGGTTCAGAGGCAATATTT
GTGCCATGCCAACCTGGCATCAAATCTGATGAGGATGACGGTTACTTGATATTCTTTGTACACGACGAAAACAAT
GGGAAATCTGAGGTCAATGTCATCGATGCAAAGACAATGTCTGCAGAACCTGTGGCTGTTGTGGAACTTCCAAGC
AGGGTTCCATATGGATTCCATGCCTTGTTTCTGAATGAGGAAGAACTTCAGAAGCACCAAGCAGAGACAACAACC
GAAAATTTATATTTCCAGTCTGGAACA

(insert between possitions 6981 and 6982 of TEVΔNIb; sequences to complete native NIaPro cleavage sites are on yellow background)

GGGGAGAAGATGTCGGCCAGAATCTCCCCCTCCGCCACCACCCTCGCCGCCTCCTTCCGCCGCCCTCCG
TCTGGCGCACGCATCCTCCTCCTCCCTTCGCTCCCTGTCCGCCGCCCCGTCGAACTCCGGCCGCCGTTGCTTCAT
CGTCGGCGTCGGACGGCGACAGTGTTTTTCGTTCTCGCCGAAGAAAAAACAACTCCTTTTCTTGACGACGTGGAG
GAAGAGAAGAGTATTGCGCCGTCAAATCGGGCGGCTGAGAGGTCGGCGCGGAAGCGGTCGGAGCGGACCACGTAC
CTCATAGCCGCGGTTATGTCGAGCTTGGGCATCACATCCATGGCCGCCGCAGCCGTCTACTACCGCTTCGCTTGG
CAAATGGAGGGAGGGGATGTGCCAGTGACGGAGATGGCGGGAACGTTCGCTCTCTCGGTCGGGGCGGCGGTGGGG
ATGGAGTTCTGGGCCAGGTGGGCCCACCGGGCCCTCTGGCACGCGTCGCTCTGGCACATGCACGAGTCCCACCAC
CGGCCGAGGGAGGGCGCTTTCGAACTCAACGACGTCTTCGCCATAATCAACGCGGTCCCCGCCATAGCCCTGCTC
AACTTCGGCTTCTTCCACAGAGGTCTTCTCCCCGGCCTCTGTTTCGGCGCCGGGCTGGGGATCACGCTGTTTGGT
ATTGCGTACATGTTCGTCCACGACGGGCTAGTCCACCGGCGGTTCCCTGTGGGGCCCATAGCCGACGTGCCCTAC
TTCCAGCGCGTCGCCGCTGCTCACCAGATCCACCACTCGGAGAAGTTCGAAGGGGTGCCCTATGGACTGTTCATG
GGGCCCAAGGTCGGTGCGGTTTCTTTTTGTTGTTTTCCTCTCTTAACGACTGAGAATCTTTATTTTCAG

>TEVΔNIb-CsCCD2L/CsLPT1

(insert between possitions 144 and 145 of TEVΔNIb; artificial NIaPro cleavage site is on gray background)

ATGGAATCTCCTGCTACTAAATTACCTGCACCTCTGCTGATGTTATCTTCTTCTCCATTCCTTCTCCCTTCTCCT
AATAAGAGCTCCTCCATCTTCCTTCCACGTAAATTAGGGCCGCTACCTCCAAAATATTATTATTACAATTGCTGC
CATCCTAAGAGTAGATCAATCTCAGTAGTATCAATGGCAAATAAGGAGGAGGCAGAGACCAGTAAGAAGAAGCCC
AAACCATTAAAAGTACTAATTACCAAAGTGGATCCGAAGCCGAGGAAGGGCATGGCATCCGTCGCAGTGGACTTA
CTCGAGAAGGCCTTTGTATACCTATTGTCCGGAAATTCTGCAGCTGATCGTAGTAGTAGTAGTGGTCGTCGTCGT
CGTAAAGAGCATTACTACCTCTCCGGCAATTATGCGCCCGTCGGACACGAAACCCCGCCCTCCGACCACCTCCCC
ATTCATGGATCCCTTCCTGAATGCTTGAATGGAGTGTTTCTGAGAGTTGGTCCTAACCCCAAGTTTGCTCCCGTA
GCCGGATACAATTGGGTCGATGGAGATGGAATGATTCATGGATTGCGTATTAAAGATGGAAAAGCAACTTATCTA
TCTCGATATATTAAAACGTCACGGTTTAAACAAGAAGAATATTTTGGAAGAGCAAAATTTATGAAGATTGGAGAT
CTAAGGGGATTGCTTGGGTTCTTTACGATCTTAATACTAGTACTTCGAACAACATTGAAAGTAATAGACATTTCA
TATGGAAGAGGGACGGGTAATACAGCTCTTGTGTATCATAATGGCTTACTATTGGCTCTATCAGAAGAAGATAAA
CCTTATGTTGTTAAAGTTTTAGAAGATGGAGACTTGCAAACTCTTGGGATATTGGATTATGACAAGAAATTGTCA
CATCCATTCACCGCTCATCCAAAGATCGATCCGTTAACTGATGAGATGTTTACCTTTGGATATTCCATCTCGCCT
CCGTATCTTACTTATCGAGTCATTTCCAAGGATGGAGTGATGCAAGATCCAGTGCAAATCTCAATTACATCCCCT
ACCATAATGCATGATTTTGCTATTACTGAAAATTATGCCATCTTCATGGACCTGCCCTTGTATTTCCAACCAGAG
GAAATGGTAAAGGGGAAATTTGTCTCTTCATTTCACCCTACAAAAAGAGCTCGTATCGGTGTGCTTCCACGATAT
GCAAAAGACGAGCATCCAATTCGATGGTTCGATCTTCCAAGTTGCTTCATGACTCATAATGCAAATGCTTGGGAA
GAGAATGATGAAGTTGTGCTATTCACATGTCGCCTTGAGAGTCCTGATCTTGACATGCTTAGTGGACCTGCGGAA
GAAGAGATTGGGAATTCAAAAAGTGAGCTTTACGAAATGAGGTTCAATTTGAAAACTGGAATTACTTCACAAAAG
CAACTATCTGTACCTAGTGTTGATTTTCCTCGGATCAACCAAAGTTATACTGGCAGGAAACAGCAATATGTTTAT
TGTACTCTTGGCAACACCAAGATTAAGGGCATTGTGAAGTTTGATCTGCAAATTGAACCAGAAGCCGGAAAGACA
ATGCTTGAAGTTGGAGGAAATGTACAAGGCATCTTTGAGTTGGGACCTAGAAGATATGGTTCAGAGGCAATATTT
GTGCCATGCCAACCTGGCATCAAATCTGATGAGGATGACGGTTACTTGATATTCTTTGTACACGACGAAAACAAT
GGGAAATCTGAGGTCAATGTCATCGATGCAAAGACAATGTCTGCAGAACCTGTGGCTGTTGTGGAACTTCCAAGC
AGGGTTCCATATGGATTCCATGCCTTGTTTCTGAATGAGGAAGAACTTCAGAAGCACCAAGCAGAGACAACAACC
GAAAATTTATATTTCCAGTCTGGAACA

(insert between possitions 6981 and 6982 of TEVΔNIb; sequences to complete native NIaPro cleavage sites are on yellow background)

GGGGAGAAGATGGCTCGCCAAGTTGCTCTGTGCTCTGTCCTGGTGATCGCTGCCTTCCTCTTCATCTCCTCCCCT
CGTGCCGAGAGCGCAGTCACCTGCAGCACTGTGGCCTCTGCGGTATCACCGTGCATCGGTTATGTTCGCGGCCAG
GGCGCACTGACTGGCGCGTGCTGCAGCGGCGTGAAGGGCCTTGCTGCAGCGGCAACCACCCCCCCTGACCGTCGG
ACTGCATGCAGCTGCCTCAAGTCAATGGCTGGCAAAATCAGCGGCCTGAACCCTAGTCTCGCAAAAGGCCTCCCC

GGCAAGTGCGGTGCCAGCGTCCCCTATGTCATCAGCACATCCACTGACTGCACTAAGGTGGCAACGACTGAGAAT
CTTTATTTTCAG

Fig. S3. Complementation of a TEV mutant that lacks NIb in the transformed *N. benthamiana* line that stably expresses TEV NIb. **(A)** Wild-type and **(B)** NIb-expressing *N. benthamiana* plants were mechanically inoculated with TEVΔNIb-Ros1, a recombinant virus in which the NIb cistron is replaced by the Rosea1 visual marker that induces anthocyanin accumulation. Pictures were taken 11 days post-inoculation (dpi).

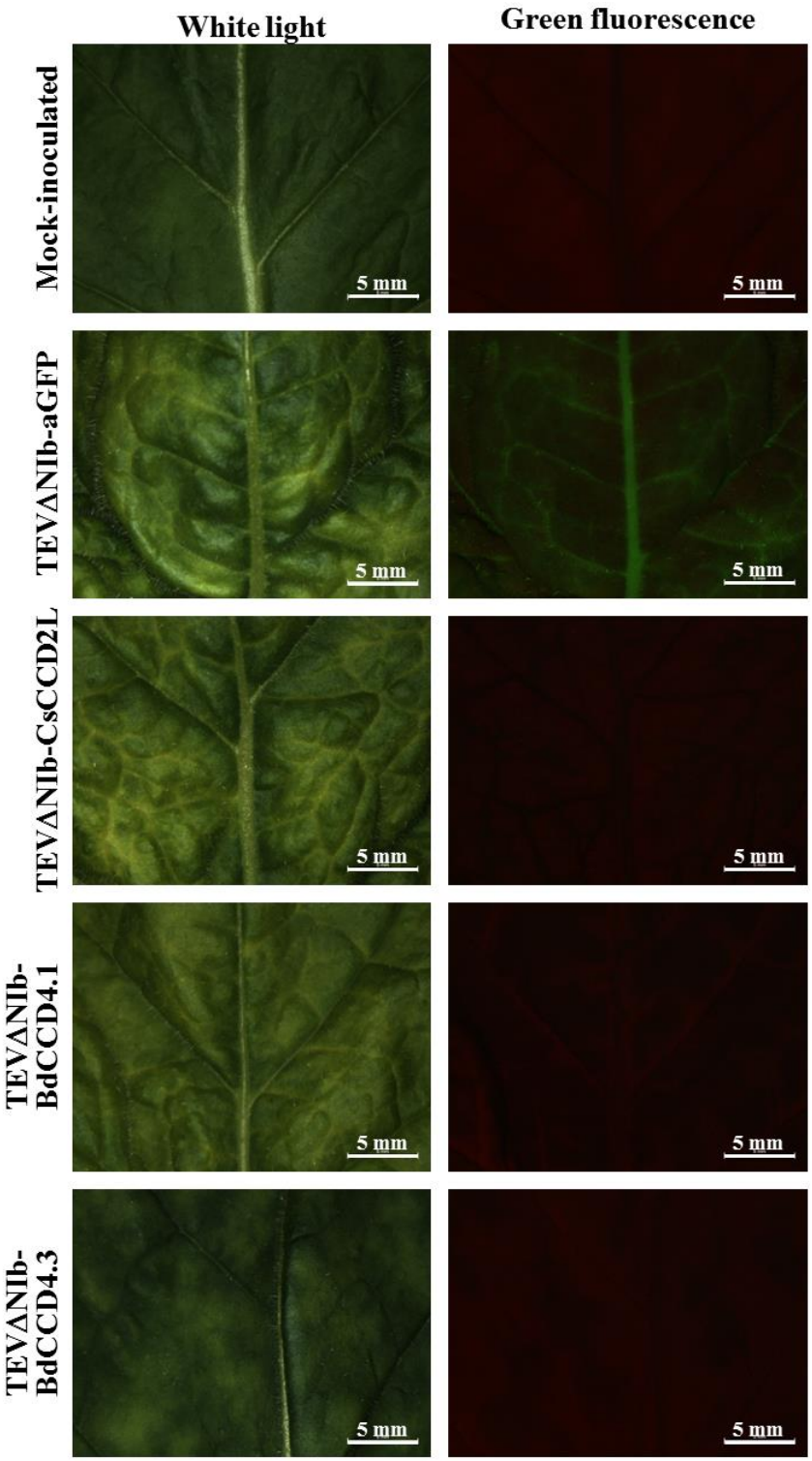

Fig. S4. Fluorescence stereomicroscope analysis of tissues from plants mock-inoculated and agroinoculated with TEVΔNIb-aGFP, TEVΔNIb-CsCCD2L, -BdCCD4.1 and -BdCCD4.3. Pictures at 15 dpi were taken with a Leica MZ 16 F stereomicroscope under white light and under UV illumination with the GFP2 (Leica) fluorescence filter. Scale bars correspond to 5 mm.

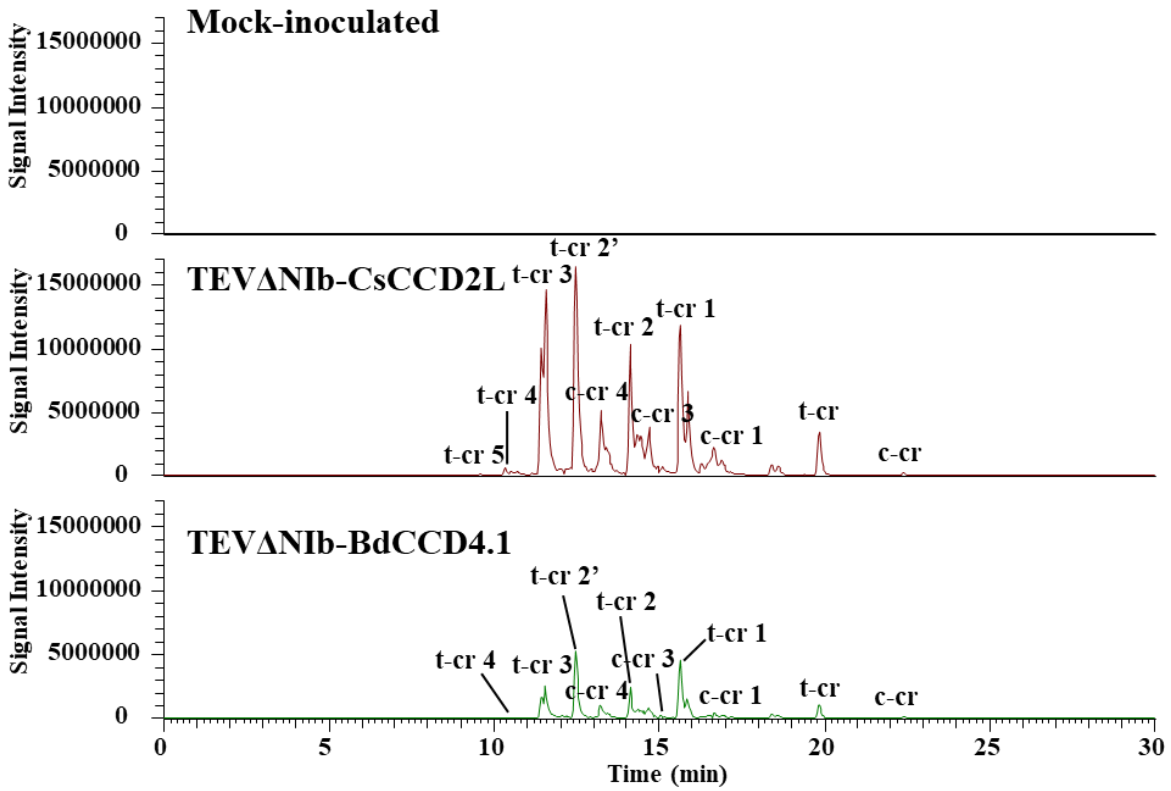

Fig. S5. Crocetin ion extraction (m/z 329.1747 (M+H+)) in control and CsCCD2L and BdCCD4.1 polar fraction chromatograms. Metabolites were extracted from infected leaves and run on an HPLC-PDA-HRMS system. The apocarotenoids have an accurate mass and a chromatographic mobility identical to those of the authentic standards, when available.

SUPPLEMENTARY TABLES

Table S1. LC-HRMS of crocins- **(A)** and picrocrocin-related **(B)** apocarotenoid levels in infected leaves. Data are avg ± sd of, at least, three biological replicates; nd (not detected). Values are reported as fold level between the signal intensities of the apocarotenoid metabolite on the signal intensity of the internal standard (formononetin).

A		TEVΔNIb-		
	Mock	aGFP	CsCCD2L	BdCCD4.1
crocetin dialdehyde	nd	nd	0,14±0,01	0,043±0,004
cis-crocetin	nd	nd	0,01±0	0,003±0,001
trans-crocetin	nd	nd	0,06±0,01	0,03±0,01
cis-crocin 1	nd	nd	0,01±0	0,01±0,001
trans-crocin 1	nd	nd	0,12±0,03	0,11±0,02
trans-crocin 2	nd	nd	1,15±0,11	0,32±0,02
trans-crocin 2'	nd	nd	0,42±0,04	0,13±0,01
cis-crocin 3	nd	nd	0,71±0,03	0,29±0,08
trans-crocin 3	nd	nd	2,09±0,28	0,43±0,09
cis-crocin 4	nd	nd	1,16±0,03	0,48±0,14
trans-crocin 4	nd	nd	0,04±0,01	0,007±0,001
cis-crocin 5	nd	nd	0,85±0,03	0,49±0,12
trans-crocin 5	nd	nd	0,02±0,01	nd
trans-crocin 6	nd	nd	0,007±0,002	nd
trans-crocin 7	nd	nd	0,013±0,003	nd
trans-crocin 8	nd	nd	0,009±0,002	nd

B		TEVΔNIb-		
	Mock	aGFP	CsCCD2L	BdCCD4.1
HTCC	nd	nd	0,007±0	0,004±0,001
picrocrocin isomer 1	nd	nd	0,019±0,004	0,004±0,001
picrocrocin isomer 2	nd	nd	0,001±0	0,001±0
picrocrocin isomer unknown	nd	nd	0,018±0,004	0,003±0,001
picrocrocin-gentibiose-isomer 1	nd	nd	0±0	0±0
picrocrocin-gentibiose-isomer 2	nd	nd	0±0	0±0
picrocrocin-gentibiose-isomer 3	nd	nd	0±0	0±0
Picrocrocin-derivivative 4	nd	nd	0,001±0,0001	0±0
Picrocrocin-derivivative 7	nd	nd	0,001±0,0001	0±0
Picrocrocin-derivivative 9	nd	nd	0±0	0±0

Table S2. Relative abundance, as % on the total, of apocarotenoid levels in CsCCD2L and BdCCD4.1 leaves. **(A)** crocins-related metabolites and **(B)** picrocrocin-related metabolites.

A	TEVΔNIb-	
	CsCCD2L	BdCCD4.1
crocetin dialdehyde	2,00	1,83
cis-crocetin	0,08	0,14
trans-crocetin	0,94	1,29
cis-crocin 1	0,15	0,37
trans-crocin 1	1,72	4,52
trans-crocin 2	16,84	13,68
trans-crocin 2'	6,19	5,46
cis-crocin 3	10,48	12,54
trans-crocin 3	30,74	18,31
cis-crocin 4	17,04	20,62
trans-crocin 4	0,57	0,30
cis-crocin 5	12,54	20,92
trans-crocin 5	0,27	-
trans-crocin 6	0,11	-
trans-crocin 7	0,19	-
trans-crocin 8	0,14	-

B	TEVΔNIb-	
	CsCCD2L	BdCCD4.1
HTCC	14,61	32,31
picrocrocin isomer 1	39,49	32,44
picrocrocin isomer 2	3,05	7,56
picrocrocin isomer unknown	36,44	25,01
picrocrocin-gentibiose-isomer 1	0,11	0,06
picrocrocin-gentibiose-isomer 2	0,11	0,05
picrocrocin-gentibiose-isomer 3	0,07	0,08
Picrocrocin-derivivative 4	3,01	1,22
Picrocrocin-derivivative 7	3,01	1,22
Picrocrocin-derivivative 9	0,10	0,05

Table S3. LC-HRMS of carotenoid- **(A)**, chlorophyll-related **(B)**, and tocochromanols and quinones **(C)** levels in infected leaves. Data are avg ± sd of at least three biological replicates; nd (not detected). Values are reported as fold level between the signal intensities of the apocarotenoid metabolite on the signal intensity of the internal standard (a-tocopherol acetate). Asterisks indicate significant differences according a t-test (pValue: *<0.05; **<0.01) carried out in the comparisons Not infected vs GFP, CCD2L vs GFP and CCD4.1 vs GFP.

A		TEVΔNIb-		
	Mock	aGFP	CsCCD2L	BdCCD4.1
phytoene	0,21±0,02	0,06±0,02**	3,1±0,29**	1,46±0,25**
phytofluene	0,16±0,02	0,06±0,01**	0,66±0,16**	0,31±0,05**
a-carotene	0,06±0	0,06±0,01	0,13±0,04	0,08±0,01
lutein	1,27±0,15	0,85±0,03*	0,41±0,08*	0,6±0,05*
b-carotene	0,71±0,1	0,49±0,03**	0,52±0,1	0,48±0,05
zeaxanthin	0,6±0,1	0,71±0,2	0,22±0,03**	0,38±0,02**
violaxanthin	0,5±0,06	0,28±0,02**	0,3±0,05	0,32±0,03
neoxanthin	0,044±0,005	0,04±0,003	0,04±0,01	0,039±0,002
other carotenoids	0,04±0,01	0,04±0,004	0,05±0,01	0,04±0,02

B		TEVΔNIb-		
	Mock	aGFP	CsCCD2L	BdCCD4.1
chlorophyll a	0,98±0,11	0,62±0,08*	0,75±0,17	0,68±0,07
chlorophyll b	1,18±0,18	0,82±0,02	0,91±0,18	0,83±0,06
chlorophyll derivatives	0,28±0,02	0,27±0,02	0,32±0,11	0,24±0,05

C		TEVΔNIb-		
	Mock	aGFP	CsCCD2L	BdCCD4.1
a-tocopherol	0,94±0,13	1,03±0,14	1,12±0,22	0,97±0,12
b-/g-tocopherol	0,01±0	0,01±0,002	0,02±0**	0,02±0,01*
d-tocopherol	0±0	0,0033±0,001	0,01±0	0±0
a-tocotrienol	0,31±0,02	0,29±0,02	0,3±0,06	0,25±0,03
b-/g-tocotrienol	0±0	0,001±0,0003	nd	0,001±0,0002
d-tocotrienol	0±0	0,002±0,0004**	0±0	0,001±0,0001*
a-tocopherol quinone	0±0	0,0037±0,001	0,01±0**	0,01±0,002*
menaquinone-8	0,03±0	0,03±0,01	0,07±0,01**	0,07±0,01**
phylloquinone	0,63±0,16	0,87±0,13	0,81±0,19	0,73±0,18
plastoquinol-9	0±0	0,0021±0,0005	0±0	0,00226±0,0005
plastoquinone	0,19±0,03	0,11±0,02*	0,07±0,01**	0,08±0,01**
ubiquinone-10	0,03±0	0,02±0,003*	0,03±0,01	0,0261±0,004

Table S4. LC-HRMS of crocins- **(A)** and picrocrocin and safranal **(B)** apocarotenoid levels in infected leaves. Data are avg ± sd of at least three biological replicates; nd (not detected). Values are reported as absolute amounts (in mg/g DW) by using authentical standards and external calibration curves. Asterisks indicate significant differences according a t-test (pValue: *<0.05; **<0.01) carried out in the comparisons CsCCD2L vs CsCCD2L+PaCrtB, CsCCD2L+CsBCH2 or CsCCD2L+CsLTP1.

A	**TEVΔNIb-**				
mg/g DW	**aGFP**	**CsCCD2L**	**PaCrtB**	**CsBCH2**	**CsLTP1**
cis-crocetin	nd	0,03±0,01	0,003±0,001**	0,01±0**	0,02±0*
trans-crocetin	nd	0,2±0,04	0,036±0,004**	0,07±0,01**	0,13±0,03
cis-crocin 1	nd	0,06±0,01	0,04±0,01**	0,05±0,01	0,09±0
trans-crocin 1	nd	0,33±0,04	0,27±0,02	0,38±0,04	0,36±0,11
cis-crocin 2+2'	nd	0,21±0,01	0,17±0,02*	0,12±0,02**	0,02±0**
trans-crocin 2	nd	0,74±0,03	0,59±0,04**	0,4±0,05**	0,07±0,01**
trans-crocin 2'	nd	0,06±0,01	0,45±0,05**	0,51±0,06**	0,39±0,08*
cis-crocin 3	nd	0,05±0	0,19±0,02**	0,14±0,01**	0,02±0**
trans-crocin 3	nd	0,1±0,04	1,15±0,07**	0,74±0,08**	0,09±0
cis-crocin 4	nd	0,01±0	0,21±0,02**	0,15±0,02**	0,05±0,01*
trans-crocin 4	nd	0,01±0	0,09±0,01**	0,05±0,01*	0±0*
cis-crocin 5	nd	0,03±0,01	0,29±0,05**	0,29±0,03**	0,22±0,03*
trans-crocin 5	nd	nd	0,008±0,002**	0,004±0**	nd
Total crocins	nd	1,83±0,2	3,49±0,33**	2,92±0,33**	1,47±0,29

B	**TEVΔNIb-**				
mg/g DW	**aGFP**	**CsCCD2L**	**PaCrtB**	**CsBCH2**	**CsLTP1**
picrocrocin	nd	6,87±0,07	6,91±0,62	4,29±0,71	2,3±0,21**
safranal	nd	4,41±0,24	0,94±0,24	0,51±0,06	0,43±0,08**

Table S5. Percentage conversion of CsCCD2L and BdCCD4.1 enzymes on zeaxanthin substrate in *in vitro* assays performed for 6 h at 20°C and 16 h at 28°C. Data are the average of three independent assays. Asterisks indicate significant differences according a t-test (pValue: *<0.05; **<0.01) carried out in the comparisons BdCCD4.1 vs. CsCCD2L.

	% Conversion	
	6 h	**16 h**
CsCCD2L	3.83 ± 0.87	7.43 ± 1.01
BdCCD4.1	1.8 0 ± 0.4*	4.03 ± 0.60**

CHAPTER 2

Virus-based heterologous production of turmeric curcumin in *Nicotiana benthamiana*

CHAPTER 2

Virus-based heterologous production of turmeric curcumin in *Nicotiana benthamiana*

Maricarmen Martí[a], Gianfranco Diretto[b], Sarah Frusciante[b], Alessia Fiore[b], José-Antonio Daròs[a]

[a]Instituto de Biología Molecular y Celular de Plantas (Consejo Superior de Investigaciones Científicas-Universitat Politècnica de València), 46022 Valencia, Spain

[b]Italian National Agency for New Technologies, Energy, and Sustainable Development, Casaccia Research Centre, 00123, Rome, Italy.

This chapter will be soon submitted for publication.

Author contributions: All authors participated in work conception and design of the experiments. MM, GD, SF performed the experiments. All authors analyzed the results. MM and JAD wrote the manuscript with inputs from the rest of the authors.

ABSTRACT

Turmeric (*Curcuma longa* L.) rhizome has been traditionally used as a food additive. It contains curcuminoids, especially curcumin, polyphenols widely appreciated for its beneficial effects to treat different diseases. However, curcumin therapeutic application has been restricted due to the low yield, poor bioavailability and costly extraction processes. We have successfully produced curcumin and other curcurminoids in *Nicotiana benthamiana* plants by using a multigene engineering strategy where two key enzymes from the curcuminoid biosynthetic pathway, *C. longa* diketide-CoA synthase 1 (DCS1) and curcumin synthase 3 (CURS3), were co-expressed using vectors derived from tobacco etch virus (TEV, genus *Potyvirus*) alone or in combination with potato virus X (PVX, genus *Potexvirus*). Metabolic analysis of plant tissue showed that the double infection with TEVΔN-DCS1 and PVX-CURS3 led to the production of curcumin, dihydrocurcumin, dihydro-demethoxycurcumin, demethoxycurcumin, dihydro-bisdemethoxycurcumin and bisdemethoxycurcumin. Curcumin quantification indicated that sequential inoculation of both viral vectors was more efficient than co-inoculation (6.5 ± 0.6 versus 1.9 ± 0.3 µg/g dry weight, DW, respectively). DCS1 and CURS3 expression using a single viral vector (TEVΔN-DCS1-CURS3) led to a 2-fold increase in curcumin accumulation (11.7 ± 1.5 µg/g DW). A time-course analysis of curcuminoid production using the TEVΔN-DCS1-CURS3 vector resulted in 22 ± 4 µg/g DW at 11 days post-inoculation. In sum, the virus-based expression of two *C. longa* curcuminoid biosynthetic enzymes allows the heterologous production of the highly appreciated curcumin in adult *N. benthamiana* plants in less than two weeks.

Keywords**:** curcuminoids; curcumin; turmeric; viral vector; diketide-CoA synthase 1; curcumin synthase 3; tobacco etch virus; potato virus X

1. INTRODUCTION

Plants produce a plethora of specialized metabolites that are vital for their survival, i.e. their reproduction, climate resilience, to establish symbiotic relationships and to fend off predators, pests and pathogens (Arya et al., 2020). These natural compounds are

widely used by humans in the food, pharma, cosmetic or chemical industries. In fact, plant secondary metabolites play a leading role in drug discovery due to their specialized and complex skeletal structures and functional groups that render an enormous array of bioactive properties (Arya et al., 2020; Chouhan et al., 2017). Many phytochemicals are highly demanded and economically valued (Ashrafizadeh et al., 2020). However, extraction of plant-derived natural products from native sources not unfrequently encounters difficulties to meet commercial demand. To a limited production in natural conditions, danger of overexploitation of native plant species must be added. Chemical synthesis, when possible, also suffers of drawbacks such as expensive precursors, use of toxic catalysts and extreme reaction conditions. Metabolic engineering of plants and microbes arises as an alternative approach to produce bioactive natural compounds ensuring sustainability while satisfying the commercial demands (Arya et al., 2020; Chouhan et al., 2017).

Molecular farming uses plants as biological factories (biofactories) to produce compounds of interest, such as proteins and metabolites (Fischer and Buyel, 2020). Approaches in molecular farming are typically based on plant stable genetic transformation, a time-consuming and resource-intensive process. Transient expression in plant tissues, by contrast, has emerged as an alternative manufacturing system, as it is very rapid, generating the product of interest in a matter of days (Fischer and Buyel, 2020; Mohammadinejad et al., 2019; Shanmugaraj et al., 2020). The use of viral vectors for the transient expression of heterologous genes in plants exhibits two additional advantages; viral genomes are small and easy to manipulate, and genes of interest are exponentially amplified during viral replication (Clark and Maselko, 2020; Sainsbury et al., 2012; Shanmugaraj et al., 2020).

Turmeric (*Curcuma longa* L.) is a herbaceous plant that belongs to the ginger family (*Zingiberaceae*) and is native to the Indian subcontinent (Mandal, 2016). Turmeric rhizome has been used as a food additive, especially in Asian cuisine –it gives curry its characteristic yellowish color–, and in cosmetics (Esatbeyoglu et al., 2012). Besides, turmeric has been widely used for thousands of years for medicinal purposes to treat different diseases (Prasad et al., 2014). Curcuminoids are polyphenols found in the rhizome from many *Curcuma* species, with *C. longa* the one that accumulates the highest amounts (Akter et al., 2019; Chouhan et al., 2017; Prasad et al., 2014).

Curcuminoid biosynthesis in *C. longa* is a multistep process, in which p-coumaroyl-CoA is produced from the amino acid phenylalanine. Condensation of p-coumaroyl-CoA with malonyl-CoA results in the formation of a diketide intermediate, which through the catalytic activity of several curcumin synthase (CURS) enzymes end up with production of curcumin and other curcuminoids (Katsuyama et al., 2009) (Fig. 1). Key enzymes in this process are *C. longa* diketide-CoA synthase 1 (DCS1) and CURS3 (unpublished data).

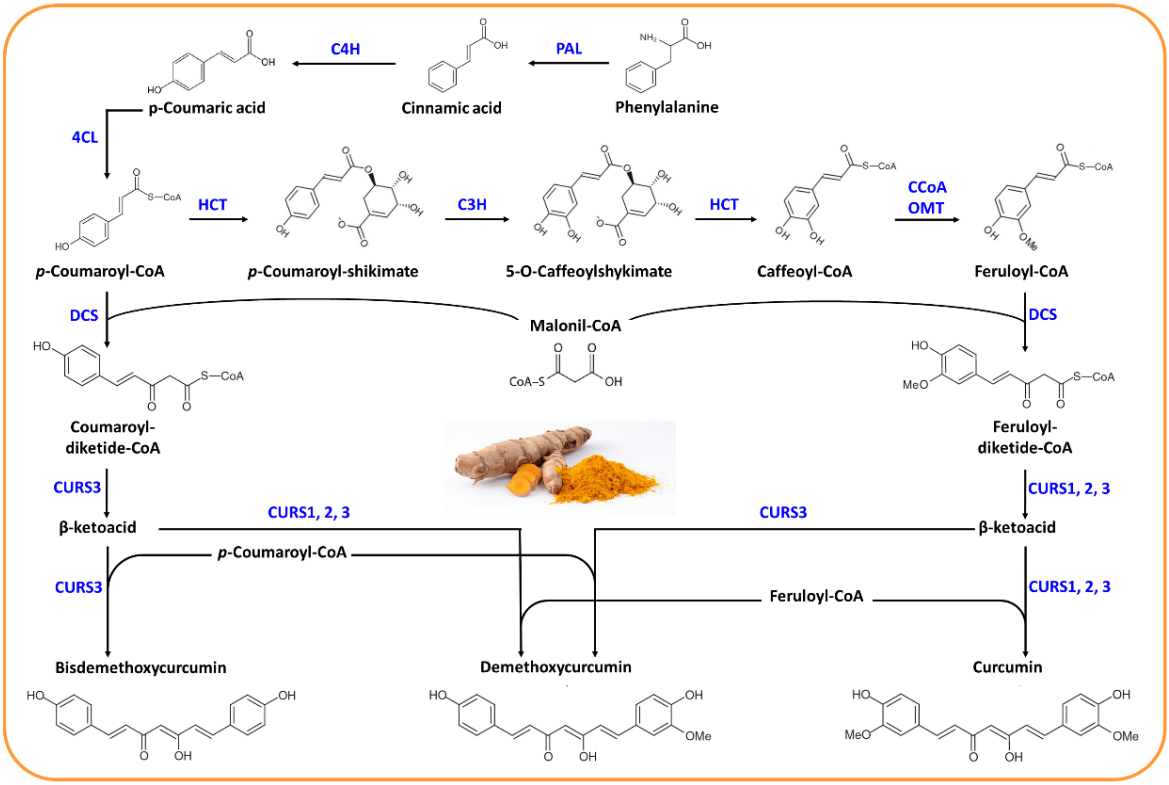

Figure 1. Curcuminoid biosynthetic pathway in turmeric (*C. longa*). Phenylalanine ammonia-lyase (PAL), cinnamic acid 4-hydroxylase (C4H), 4-coumarate-CoA ligase (4CL), hydroxycinnamoyl transferase (HCT), p-coumarate-3- hydroxylase (C3H), caffeoyl CoA O-methyltransferase (CCoAOMT), diketide-CoA synthase (DCS), and curcumin synthase 1, 2 and 3 (CURS1, 2 and 3).

Heterologous curcumin production has been intensively studied due to the metabolite's wide range of biological properties, such as its ability to modulate multiple signaling molecules, such as transcription factors, enzymes, and secondary messengers, thereby controlling the expression of many genes associated with disease (Ashrafizadeh et al., 2020; Ghosh et al., 2015; Mandal, 2016). More in detail, curcumin is considered a health-promoting metabolite due to antioxidant, anti-inflammatory, and

antimicrobial activities. It is also considered anti-diabetic, cardioprotective, hepatoprotective, capable of lowering dyslipidemia, regulator of blood pressure, protective against ischemic/reperfusion injury, anti-Alzheimer, anti-Parkinson or antitumor, and beneficial in liver and urinary tract diseases (Ashrafizadeh et al., 2020; Chouhan et al., 2017; Couto et al., 2017; Gómez-Estaca et al., 2017; Katsuyama et al., 2009; Stanić, 2017). However, the underlying mechanisms of all these health promoting activities remain unclear (Ghosh et al., 2015).

Despite the remarkable potential to prevent and treat a wide spectrum of diseases, therapeutic application of curcumin has been restricted due to low aqueous solubility and low chemical stability, as well as poor bioavailability due to rapid elimination from the body (Chouhan et al., 2017; Couto et al., 2017; Ghosh et al., 2015; Stanić, 2017). Different strategies have been developed to overcome these limitations, such as the conjugation with chitosan or cyclodextrins, or encapsulation within lipid particles (Ghosh et al., 2015; Mandal, 2016; Stanić, 2017). Besides, curcumin is typically obtained with a low yield using costly, energy-intensive and environmentally unfriendly extraction processes. Chemical synthesis is not an alternative due to molecular complexity. Therefore, metabolic engineering and molecular farming remain as an attractive alternative for commercial curcumin production (Couto et al., 2017; Rodrigues et al., 2015).

In this study, we set up a system for the heterologous production of curcumin in *Nicotiana benthamiana* plants by using a multigene engineering strategy where two biosynthetic enzymes, namely *C. longa* DCS1 and CURS3, were co-expressed using viral vectors to create an artificial curcuminoid biosynthetic pathway. For this purpose, we used a vector derived from tobacco etch virus (TEV, genus *Potyvirus*; family *Potyviridae*), alone or in combination with a second compatible vector derived from potato virus X (PVX, genus *Potexvirus*; family *Alphaflexiviridae*). As a result, a curcumin accumulation of up to 22 ± 4 µg per g of *N. benthamiana* leaf dry weigh (DW) was obtained after only 11 days post-inoculation (dpi).

2. MATERIALS AND METHODS

2.1. Plasmid construction

Plasmids pGTEVΔN-DCS1, pGTEVΔN-DCS1-CURS3, pPVX-mCherry, pPVX-CURS3 and pPVX-CCoAOMT-1 were built using standard molecular biology techniques, including polymerase chain reaction (PCR) with the high-fidelity Phusion DNA polymerase (Thermo Scientific), restriction enzyme digestion, ligation with T4 DNA ligase (Thermo Scientific), and Gibson DNA assembly (Gibson et al., 2009) using the NEBuilder HiFi DNA assembly master mix (New England Biolabs). *C. longa* DCS1 and CURS3 cDNAs, along with *N. tabacum* CCoAOMT-1 cDNA, were amplified by PCR from plasmids pDGB3α1-DCS1, pDGB3α2-CURS3 and pDGB3α2-OMT, respectively (Diretto et al., unpublished results). Plasmid pGTEVa (Bedoya et al., 2012) contains the infectious cDNA of a wild-type TEV (GenBank accession number DQ986288) including two silent and neutral mutations (G273A and A1119G) for cloning purposes, flanked by cauliflower mosaic virus (CaMV) 35S promoter and terminator in a binary vector that derives from pCLEAN-G181 (Thole et al., 2007). DCS1 and a combination of DCS1 and CURS3 cDNAs were inserted in pGTEVa replacing most of the cDNA corresponding to the viral cistron that encodes the RNA-dependent RNA polymerase nuclear inclusion b (NIb) (Fig. 2A). The exact sequences of the resulting plasmids pGTEVΔN-DCS1 and pGTEVΔN-DCS1-CURS3 are in Supplementary Fig. S1.

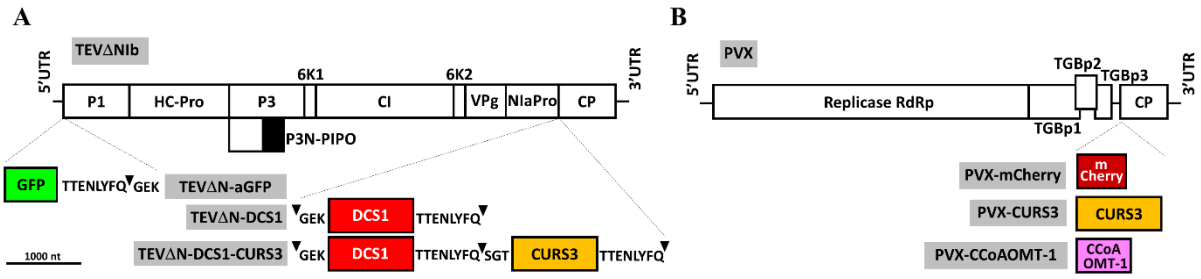

Figure 2. Schematic representation of (**A**) TEVΔNIb and (**B**) PVX, and derived recombinant viruses thereof, as indicated in grey rectangles. Lines represent 5' and 3' untranslated regions (UTR), and white boxes denote viral genes, as indicated. Heterologous GFP and mCherry coding regions are represented by green and dark red boxes. *C. longa* DCS1, CURS3 and *N. tabacum* CCoAOMT-1 coding regions are represented by light red, orange and purple boxes, respectively. (**A**) The amino acid sequences of the artificial NIaPro cleavage sites that mediate the release of the heterologous proteins from the TEV polyprotein are indicated. Arrowheads indicate cleavage sites. Scale bar corresponds to 1000 nt.

PVX recombinant plasmids were constructed on the basis of the plasmid pPVX, which contains a full-length PVX cDNA (GenBank accession number MT799816), flanked by the CaMV 35S promoter and *Agrobacterium tumefaciens Nopaline synthase* (*NoS*) terminator. Heterologous cDNAs of all the PVX recombinant clones are transcribed from the native PVX coat protein (CP) promoter, and a deleted version of PVX CP, lacking its 29 initial codons, is expressed from a heterologous promoter that derived from bamboo mosaic virus (BaMV) (Dickmeis et al., 2014) (Fig. 2B).The exact sequences of pPVX-mCherry, pPVX-CURS3, and pPVX-CCoAOMT-1 are in Supplementary Fig. S2. Plasmids pGTEVΔNIb-aGFP and pGTEVΔNIb-mCherry for TEV-based expression of the green fluorescent protein (GFP) and the red fluorescent protein mCherry were previously described (Majer et al., 2015, Bedoya et al., 2010) (Supplementary Fig. S1).

2.2. Plant inoculation

A. tumefaciens C58C1, which carried helper plasmid pCLEAN-S48 (Thole et al., 2007), was electroporated with plasmids that contained the different viral clones. Transformed cells were selected in lysogenic broth (LB) agar plates with 50 µg/ml rifampicin, 50 µg/ml kanamycin and 7.5 µg/ml tetracycline. Single colonies were further grown in LB liquid medium containing 50 µg/mL kanamycin at 28°C for 24 h. At an optical density at 600 nm (OD_{600}) between 1 and 2, cells were pelleted and resuspended to an OD_{600} of 0.5 in agroinoculation buffer (10 mM MES-NaOH, pH 5.6, 10 mM $MgCl_2$ and 150 µM acetosyringone) and induced for 2 h at 28ºC. Using a needleless syringe, cultures were used to infiltrate two leaves of four-week-old transgenic *N. benthamiana* plants that stably express TEV NIb (Martí et al., 2020). In the different experiments, PVX-derived clones were inoculated at the same time as TEV clones (co-inoculation, C) or 3 days later (sequential inoculation, S), as indicated. After inoculation, plants were kept in a growth chamber at 25ºC under a 12 h day-night photoperiod with an average photon flux density of 240 $\mu mol \cdot m^{-2} \cdot s^{-1}$. Leaves were collected at different dpi and kept at -80ºC until used.

2.3. Analysis of virus progeny

Leaf samples from upper non-inoculated leaves of *N. benthamiana* plants were harvested at 11 dpi and total RNA was purified using silica-gel columns (Zymo Research). Viral progeny was analyzed by reverse transcription (RT)-PCR using RevertAid reverse transcriptase (Thermo Scientific) and Phusion high-fidelity DNA polymerase followed by electrophoretic separation of the amplification products in 1% agarose gels, which were stained with ethidium bromide. For virus infection diagnosis, a cDNA corresponding to the TEV CP cistron (804 bp) was amplified. Aliquots of the RNA preparations were subjected to RT using primer PI (5'-CTCGCACTACATAGGAGAATTAGAC-3'), followed by PCR amplification with primers PII (5'-AGTGGCACTGTGGGTGCTGGTGTTG-3') and PIII (5'-CTGGCGGACCCCTAATAG-3'). To analyze the presence of the inserted cDNAs in the viral progeny, RNA aliquots from mock-inoculated and TEVΔN-aGFP infected plants were reverse transcribed using primer PIV (5'-GCTGTTTGTCACTCAATGACACATTAT-3') and amplified by PCR with primers PV (5'-AAAATAACAAATCTCAACACAACATATAC-3') and PVI (5'-CCGCGGTCTCCCCATTATGCACAAGTTGAGTGGTAGC-3'), while RNA from TEVΔN-DCS1-CURS3 infected plants was reverse transcribed using primer PVII (5'-TACCTAGGCATGTATGGTCGCTCCC-3') and amplified by PCR with primers PVIII (5'-CCTGAAGAGCCTTTTCAGCCAG-3') and PIX (5'-TTGATCTTTCTTCTTACCAGCG-3').

2.4. Metabolic analysis

Polar and nonpolar extracts from mock-inoculated and infected plants were analyzed by high performance liquid chromatography (HPLC) with a system equipped with a photodiode array (PDA) detector (Dionex) coupled to a Q-Exactive high resolution mass spectrometer (HRMS) (Thermo Fisher Scientific) operating in positive/negative heated electrospray ionization (HESI). HPLC-HRMS analysis of *N. benthamiana* metabolites were performed as previously described (Demurtas et al., 2019, 2018; Grosso et al., 2018) with some minor modifications. For HPLC separation of polar and

semipolar metabolites (curcuminoids and phenylpropanoid precursors), freeze-dried and homogenized plant tissue powder were extracted with cold 75% (v/v) methanol, 0.1% (v/v) formic acid, spiked with 5 µg/ml formononetin. For liquid chromatography, samples were injected on a C18 Luna reverse-phase column (100 × 2.1 mm, 2.5 µm; Phenomenex) where the mobile phases were composed of water with 0.1% (v/v) formic acid (A) and acetonitrile with 0.1% (v/v) formic acid (B), at a total flow rate of 250 µl/min. The separation of polar and semipolar metabolites was performed using a gradient of 95%A/5% B for 0.5 min, followed by a 24-min linear gradient to 25%A/75% B, 1 min isocratic, before going back to the initial conditions in 7 min.

The liposoluble fractions (chlorophylls, carotenoids, and other isoprenoids such as quinones and tocochromanols) were extracted with 0.5 ml cold (1:1) methanol:chloroform (v/v) spiked with 50 µg/ml formononetin. HPLC separation of nonpolar metabolites was performed as described previously (Demurtas et al., 2018), injecting samples on a C30 reverse-phase column (100 × 3.0 mm; YMC Europe). Briefly, the mobile phases consisted of methanol (A), water:methanol (20:80, v/v) containing 0.2% ammonium acetate (B), and tert-butyl methyl ether (C) at a total flow rate of 800 µl/min. The separation was developed using a gradient of 95%A/5%B for 1.3 min, followed by 80%A/5%B/15% C for 2 min, followed by a subsequent 9.2-min linear gradient to 30%A/5%B/65%C. Mass spectrometry ionization of polar, semipolar and nonpolar metabolites was performed as previously described (Demurtas et al., 2018).

Identification of metabolites was achieved by comparing chromatographic (retention times) and spectral (absorption spectra) properties with authentic standards, if available; using literature data; or on databases, as stated previously (López et al., 2021). The ion peak areas of the metabolites were standardized to the ion peak areas of the internal standard (formononetin or α-tocopherol acetate for polar/semipolar and nonpolar metabolites, respectively), allowing for relative quantification expressed as fold internal standard (IS). For absolute quantification, peak integration areas were converted to concentrations in comparison with authentic standards (curcumin).

2.5. Confocal microscopy

Upper non-inoculated leaves from plants infected with TEVΔNIb-aGFP, PVX-mCherry and doubly infected with TEVΔNIb-aGFP and PVX-mCherry were analyzed at 10 dpi by laser scanning confocal microscopy (LSCM) using a Zeiss LSM 780 Axio Observer equipped with a C-Apochromat 40X/1.20 W corrective water immersion objective lens. For the multicolor detection of GFP and chlorophylls, as well as the red fluorescence from mCherry, imaging was performed using the sequential channel acquisition mode. A 458-nm laser was used for excitation of GFP and chlorophyll autofluorescence; they were detected between 490 to 535 nm and 685 to 760 nm, respectively. mCherry was excited using a 561-nm laser, detecting the red signal between 590 to 640 nm. Post-acquisition image processing was performed using FIJI (http://fiji.sc/Fiji).

Subcellular curcumin localization was also investigated by LSCM owing to its green fluorescence (Gómez-Estaca et al., 2017). Upper non-inoculated leaves from mock-inoculated plants or infected with TEVΔNIb-mCherry or TEVΔN-DCS1-CURS3 were analyzed at 11 dpi. For the detection of curcumin, a 458-nm laser was used for excitation, and fluorescence was recorded between 490 to 555 nm. Tissues infected with TEVΔN-DCS1-CURS3 were further subjected to an emission fingerprinting (spectral imaging coupled with subsequent image processing using linear unmixing) (Zimmermann et al., 2014) to separate mixed fluorescent signals from chlorophylls and curcumin using the Zeiss Zen Black software.

2.6. Statistics and bioinformatics

Statistical analyses (ANOVA+ Tukey's t-test) were performed by using the IBM SPSS Statistics software. Heatmap visualization was carried out with the online tool from Morpheus (https://software.broadinstitute.org/morpheus/) as previously described (Cappelli et al., 2018; Grosso et al., 2018).

3. RESULTS

3.1. TEV and PVX cellular coinfection

After identifying *C. longa* DCS1 and CURS3 as the key enzymes for the heterologous production of curcuminoids in *N. benthamiana* (Diretto et al., unpublished results), the goal of this work was to set up a virus-based system for the rapid and efficient production of these appreciated metabolites in adult plants of this species. For this purpose, we first planned to co-express both biosynthetic enzymes in the same cells using two different viral vectors that belong to distinct families and that we expected to efficiently co-infect plants. More specifically, we intended to express DCS1 and CURS3 using vectors derived from TEV and PVX, respectively. In the case of the TEV vector, we used a TEVΔN version in which most of viral NIb cistron (~1.6 kb) is deleted. The viral RNA-dependent RNA polymerase NIb is in turn expressed from a transgene in the *N. benthamiana* plants (Martí et al., 2020). This modality serves two purposes: cargo capacity in the viral vector is increased and the resulting vector only replicates in NIb plants as a biosecurity measure.

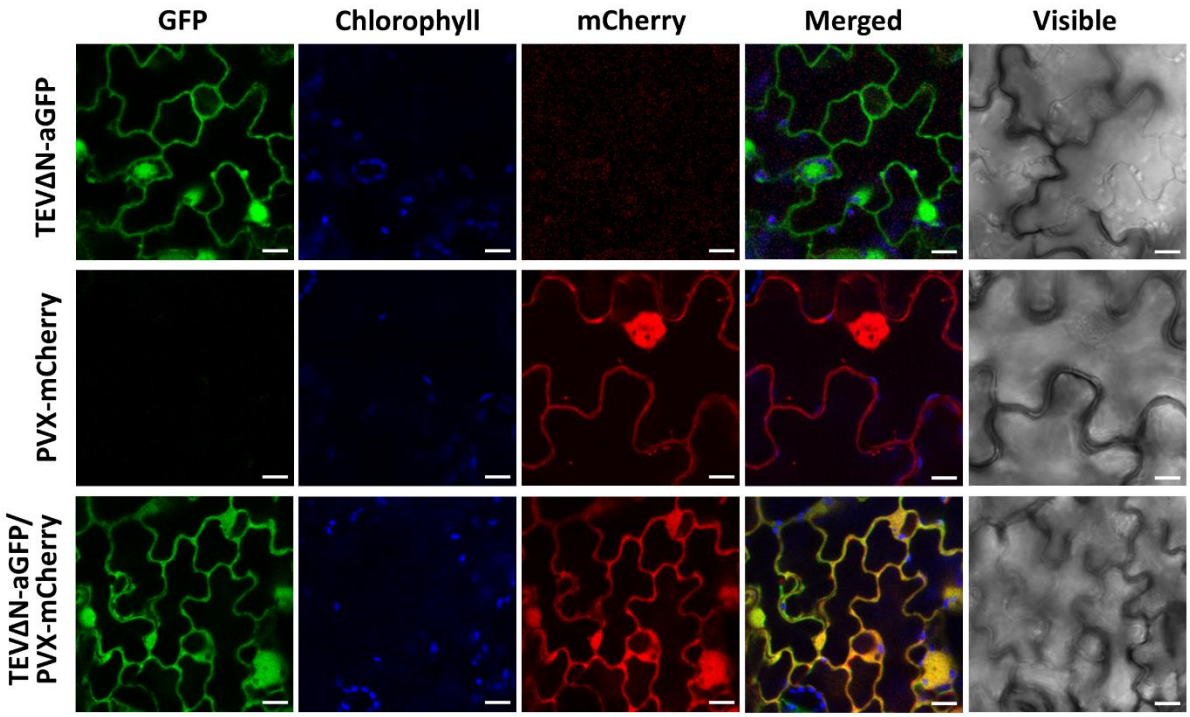

Figure 3. LSCM images of symptomatic tissues from *N. benthamiana* plants infected with TEVΔN-aGFP, PVX-mCherry or co-infected with both viruses, as indicated, at 10 dpi. The green and red fluorescence of GFP and mCherry, respectively, is shown. Chlorophyll

autofluorescence is shown in blue. Merged images of fluorescent signals from GFP, chlorophyll and mCherry, and images under bright field are also shown. Scale bars indicate 10 μm.

To confirm that these two viral vectors are able to efficiently co-infect the same cells to simultaneously deploy both biosynthetic enzymes, we used recombinant clones that express fluorescent proteins. Symptomatic upper leaves from plants infected with TEVΔN-aGFP or PVX-mCherry and co-infected with both viruses were analyzed by LSCM at 10 dpi. Tissues from plants co-inoculated with TEVΔN-aGFP and PVX-mCherry, in contrast to those from the single-infected controls, showed co-localized green and red fluorescence from GFP and mCherry, respectively (Fig. 3). This result supports the potential use of TEVΔN and PVX vectors to simultaneously express different biosynthetic enzymes that must act coordinately in the same cells.

3.2. Production of curcuminoids in infected plants

Next, we co-inoculated NIb-expressing *N. benthamiana* plants with recombinant viruses TEVΔN-DCS1 and PVX-CURS3 to co-express *C. longa* DCS1 and CURS3 (Fig. 2). Plants were either co-inoculated with the two recombinant clones at the same time or PVX-CURS3 was inoculated 3 days after TEVΔN-DCS1. As controls, some plants were inoculated with TEVΔN-aGFP, TEVΔN-DCS1 and PVX-CURS3 separately. All inoculated plants showed symptoms of infection around 8 dpi, and a mild yellow pigmentation was observed exclusively in systemic tissues of plants inoculated with both TEVΔN-DCS1 and PVX-CURS3. Plants subjected to sequential inoculation with these two viruses showed a more intense pigmentation compared to those co-inoculated. Based on the distinctive yellow color with respect to controls, these results suggested that the virus-driven expression of DCS1 and CURS3 with two different viral vectors in *N. benthamiana* induces curcuminoid accumulation. Symptomatic tissues were harvested at 13 dpi and subjected to metabolic analysis by HPLC-DAD-HRMS to determine curcuminoid profiles (Fig. 4).

Analysis of the polar fraction from tissues co-infected with TEVΔN-DCS1 and PVX-CURS3 showed a substantial accumulation of curcumin and dihydrocurcumin, and minor accumulation of other curcuminoids, such as dihydro-demethoxycurcumin, demethoxycurcumin, dihydro-bisdemethoxycurcumin and bisdemethoxycurcumin

(Fig. 4A). None of these compounds were detected in tissues from plants infected either with TEVΔN-aGFP (Fig. 4A) or from plants singly infected by TEVΔN-DCS1 or PVX-CURS3. In our HPLC-DAD-HRMS analysis, ion peak areas of the different curcuminoids were normalized to the ion peak area of the IS formomonetin. In tissues co-infected with TEVΔN-DCS1 and PVX-CURS3, relative curcumin accumulation was significantly higher, 1.5-fold in those subjected to sequential inoculation than those subjected to co-inoculation (0.46 ± 0.06 versus 0.31 ± 0.06, expressed as fold IS) (Fig. 4A). The same tendency was observed in the accumulation of demethoxycurcumin, where significant differences were also observed up to 2-fold increase. Most abundant curcuminoid in co-infected tissues was dihydrocurcumin with 0.51 ± 0.07 and 0.6 ± 0.1 fold IS for sequential inoculation and co-inoculation, respectively. However, this difference, as those in other curcuminoids, was not statistically significant among both treatments (Fig. 4A). Bearing in mind that curcumin is the most demanded curcuminoid that accumulates in turmeric rhizome, an absolute quantification of this compound was performed using a proper standard. This analysis confirmed higher curcumin accumulation in plants subjected to sequential inoculation versus those simultaneously co-inoculated (6.5 ± 0.6 and 1.9 ± 0.3 µg/g DW, respectively) at 13 dpi (Fig. 4B).

Next, we explored the effect of co-expressing both DCS1 and CURS3 from the same viral vector. More specifically, we inoculated plants with TEVΔN-DCS1-CURS3 (Fig. 2A). In this viral recombinant clone, DCS1 and CURS3 are released from the viral polyprotein using a combination of native and artificial nuclear inclusion *a* (NIa) protease (NIaPro) cleavage sites (Supplementary Fig. S1). Interestingly, the single virus strategy induced a higher curcuminoid accumulation at 13 dpi than the two-virus-vector strategy (compare panels A and C in Fig. 4). Using a single vector, the two most abundant curcuminoids, curcumin and dihydro-bisdemethoxycurcumin, displayed a 2-fold improved accumulation (Fig. 4C). The less abundant dihydro-demethoxycurcumin, demethoxycurcumin and dihydro-bisdemethoxycurcumin improved accumulation 7, 1.7 and 18-fold, respectively, compared to the two-virus strategy (Fig. 4C). In an attempt to further improve curcuminoid accumulation, some plants were co-infected with PVX-CCoAOMT-1 (Fig. 2B), a PVX clone designed to express *N. tabacum* CCoAOMT-1 to increase the pool of curcuminoid precursors. Contrary to expected, no boost effect was observed (Fig. 4C). Curcumin accumulation in tissues infected with

TEVΔN-DCS1-CURS3 was ca. 12 µg/g DW (Fig. 4D), approximately doubling the amount reached by using the two-viral-vector strategy with sequential inoculation (compare panels B and D in Fig. 4). In both approaches, dihydrocurcumin was the most abundant curcuminoid, followed by curcumin (Fig. 4A and C).

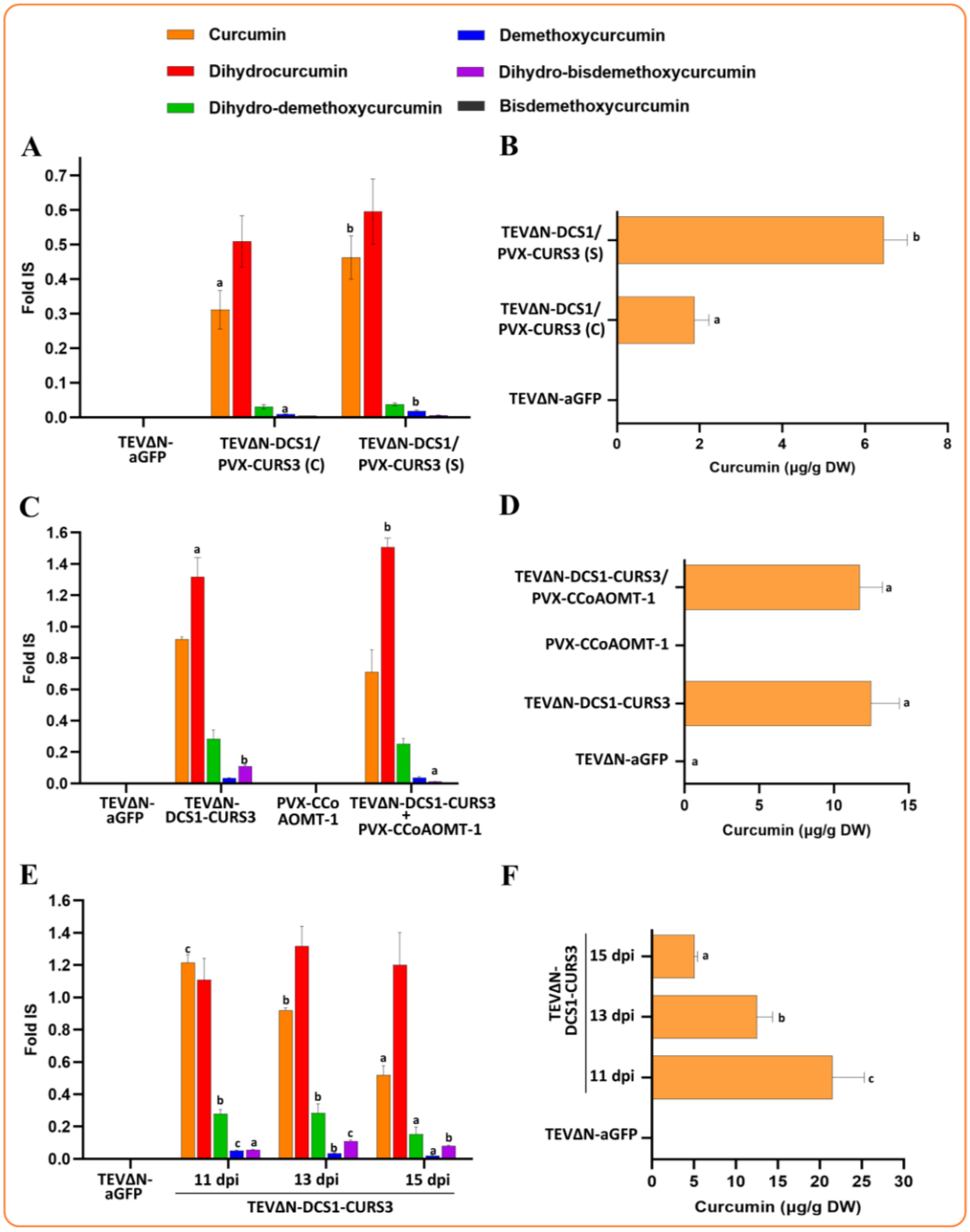

Figure 4. Curcuminoid accumulation in tissues from plants infected with a series of TEVΔN and PVX-derived recombinant viruses, as indicated. **(A**, **C**, **E**) Relative amount of curcumin, dihydrocurcumin, dihydro-demethoxycurcumin, demethoxycurcumin, dihydro-bisdemethoxycurcumin and bisdemethoxycurcumin in tissues of infected *N. benthamiana* plants, as indicated. Some plants were subjected to co-inoculation (C) or sequential (S) inoculation with two viral vectors. Histograms represent average ± standard deviation (SD) of

three biological replicates and expressed as fold internal standard (IS). (**B**, **D**, **F**) Curcumin absolute accumulation in symptomatic tissues of inoculated plants. Histograms represent average ± SD of three biological replicates and expressed as µg/g dry weight (DW). Analyses were performed at 13 dpi, or as indicated.

3.3. Time-course accumulation of curcuminoids in inoculated plants

Next, we searched the time-point with the maximum curcuminoid accumulation in infected plants. To this aim, we carried out a time-course analysis focusing on the viral recombinant clone TEVΔN-DCS1-CURS3. Samples were collected at 11, 13 and 15 dpi; plants were severely affected by viral infection at later times. Three independent replicate plants were analyzed per time point. Highest curcumin accumulation was observed at the earliest time of 11 dpi, reaching up to 1.21 ± 0.05 fold IS (Fig. 4E). Curcumin accumulation decreased significantly at later times. Quantitative analysis of curcumin accumulation at 11 dpi showed 22 ± 4 µg/g DW (Fig. 4F).

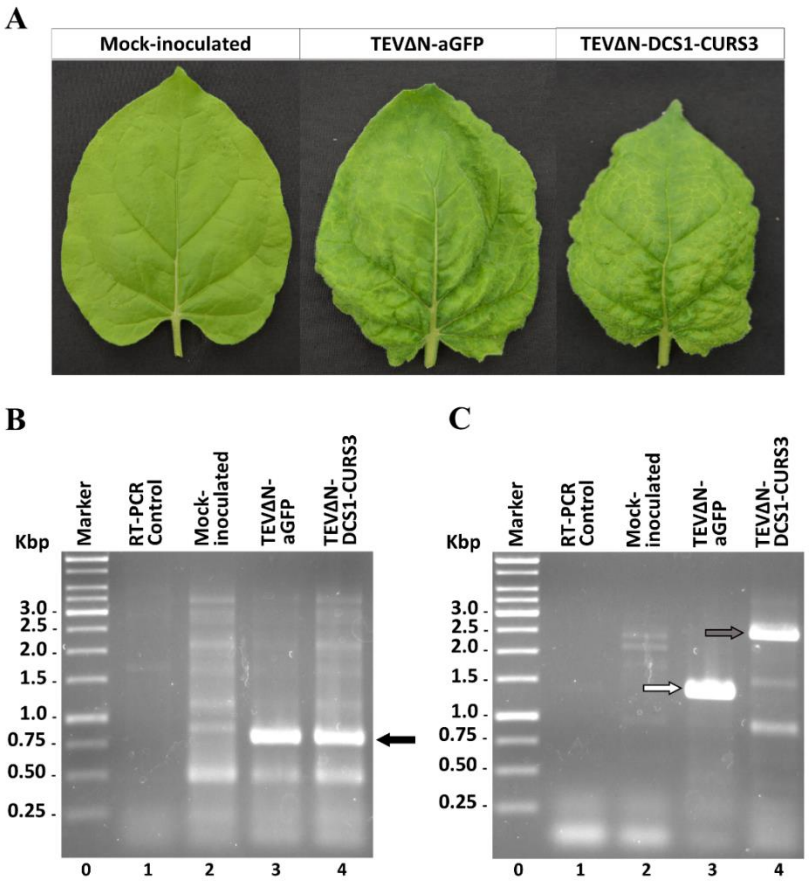

Figure 5. (**A**) Pictures (11 dpi) of representative leaves from plants mock-inoculated and infected with TEVΔN-aGFP and TEVΔN-DCS1-CURS3, as indicated. (**B**) Virus diagnosis and (**C**) analysis of the heterologous cDNAs in the progeny of recombinant TEVΔN vectors. RNA preparations from *N. benthamiana* plants mock-inoculated and agroinoculated with TEVΔN-

aGFP or TEVΔ-DCS1-CURS3 (11 dpi) were subjected to RT-PCR. Reaction products were separated by electrophoresis in a 1% agarose gel that was stained with ethidium bromide. Representative samples of triplicate analyses are shown. (**B** and **C**) Lanes 0, DNA marker ladder with sizes (in bp) on the left; lanes 1, RT-PCR controls with no RNA added; lanes 2, mock-inoculated plants; lanes 3 and 4, plants inoculated with TEVΔN-aGFP (lanes 3) and TEVΔN-DCS1-CURS3 (lanes 4). The arrows point to the bands corresponding to (**B**) the TEV CP cistron (black arrow), and (**C**) the heterologous cDNAs inserted in the viral progenies (GFP, white arrow; DCS1-CURS3, grey arrow).

Fig. 5A shows pictures of representative leaves of plants mock-inoculated and infected with TEVΔN-aGFP or TEVΔN-DCS1-CURS3 at 11 dpi. Yellow pigmentation was apparent in TEVΔN-DCS1-CURS3-infected plants at 11 dpi in agreement with peak curcumin accumulation. RT-PCR analysis of symptomatic tissue from inoculated plants at 11 dpi confirmed both TEVΔN infection and the presence of the inserted DSC1 an CURS3 cDNAs in viral progeny (Fig. 5B and C). However, comparison with control plants infected with TEVΔN-aGFP also indicate that the inserted cDNA is partially lost in TEVΔN-DCS1-CURS3 progeny at this time post-inoculation (Fig. 5C, compare lanes 3 and 4).

3.4. Vacuolar accumulation of curcumin in tissues infected with DCS1 and CURS3

The subcellular localization of curcumin accumulated in symptomatic tissues of plants infected with TEVΔN-DCS1-CURS3 was analyzed based on the differential fluorescence emission between chlorophylls and curcumin. LSCM images showed a green fluorescence signal likely originating from curcumin in the vacuoles of tissues infected with TEVΔN-DCS1-CURS3 (Fig. 6A). Tissues from mock-inoculated plants or plants infected with TEVΔNIb-mCherry did not exhibit green fluorescence in the vacuoles under the same conditions, showing only the chlorophyll autofluorescence in the chloroplasts or red signal from mCherry in the cytoplasm, respectively. In order to separate the overlapping fluorescent emission signals from curcumin and chlorophylls, tissues from plants infected with TEVΔN-DCS1-CURS3 were subjected to an emission fingerprinting, which confirmed that the green fluorescent emission originating from the vacuoles has different spectral properties to those from chlorophylls originating from the chloroplasts (Fig. 6B).

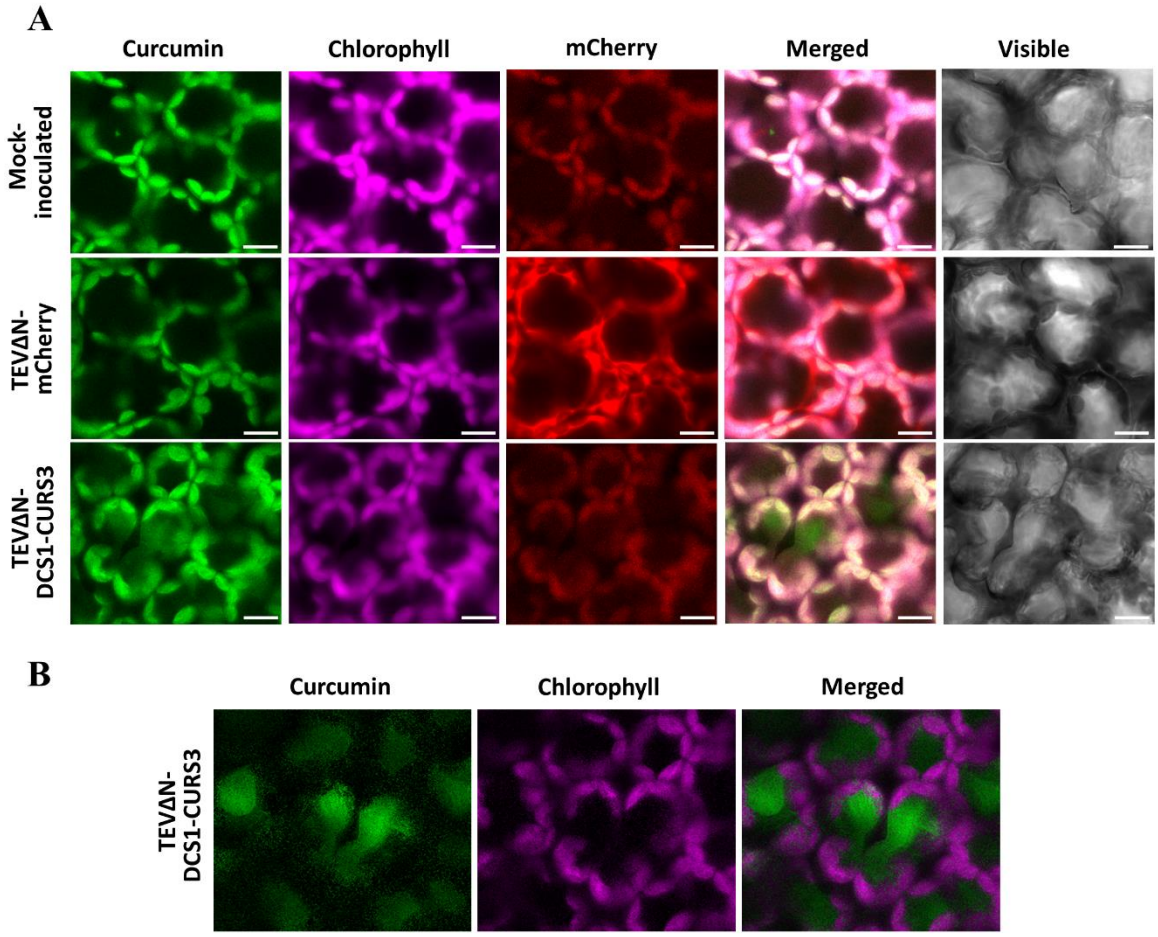

Figure 6. LSCM images of tissues from *N. benthamiana* plants mock-inoculated and infected with TEVΔN-mCherry or TEVΔN-DCS1-CURS3, as indicated, at 11 dpi. (**A**) Pictures show the fluorescent emissions from curcumin (green), chlorophylls (purple) and mCherry. Merged images of fluorescent signals and images under bright field are also shown. Scale bars indicate 10 μm. (**B**) Emission fingerprinting of tissues from plants infected with TEVΔN-DCS1-CURS3 using linear unmixing to separate overlapping mixed fluorescent emission signals.

3.5. Analysis of phenylpropanoid precursors, chlorophylls, carotenoids, quinones and tocochromanols

In plants, curcuminoids originate from the same branch of the phenylpropanoid pathway that leads to the synthesis of flavonols, anthocyanins and lignin (Fig. 7). To understand how the virus-driven curcuminoid accumulation impacts related metabolites, some phenylpropanoid precursors, chlorophylls, carotenoids, quinones and tocochromanols were analyzed by HPLC-DAD-HRMS. Relative accumulation of single metabolites in tissues infected with TEVΔN-DCS1-CURS3 were compared to control tissues infected with TEVΔN-aGFP. Curcuminoid production was accompanied

of a significant down-accumulation of *p*-coumaroyl-CoA and upstream precursors (Fig. 7, blue circles). Metabolites in others branches of the pathway were found significantly over-accumulated (Fig. 7, red circles). Subsequently, the levels of chlorophylls, carotenoid, quinones and tocochromanols were also quantified in the nonpolar fractions, but no substantial changes were observed between tissues infected with TEVΔN-DCS1-CURS3 and control tissues infected with TEVΔN-aGFP (Fig. 8, neutral colors predominate).

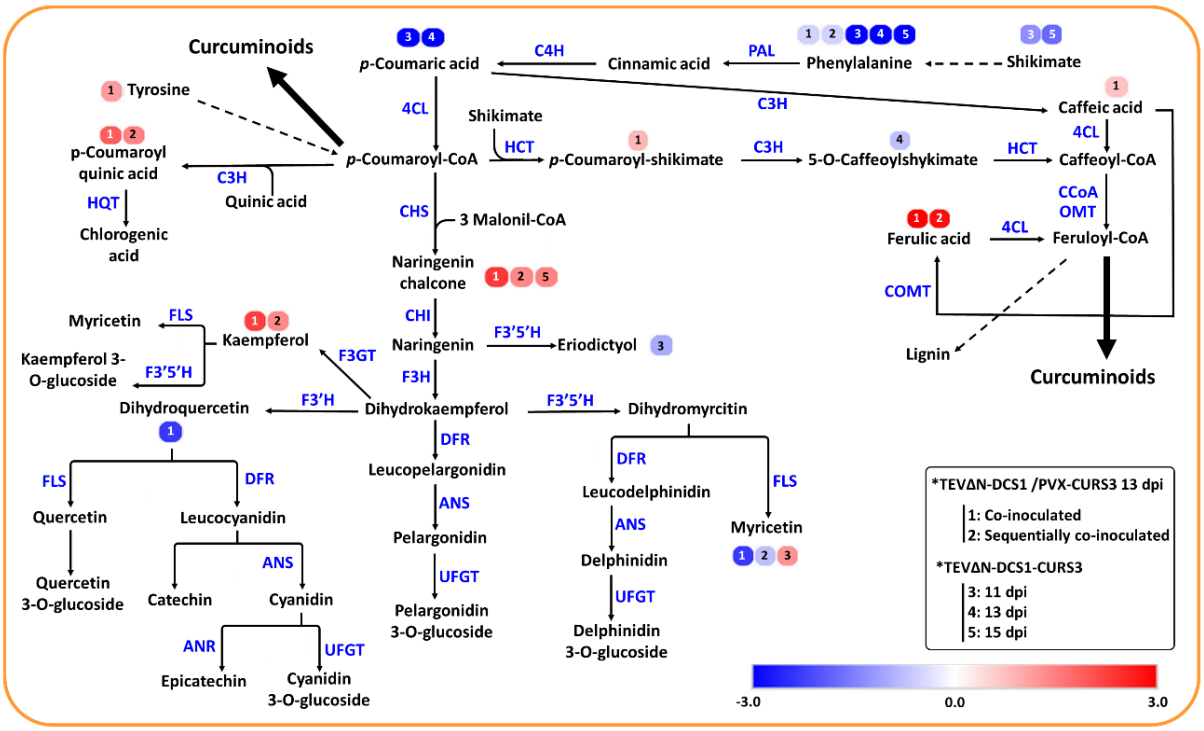

Figure 7. Schematic representation of the phenylpropanoid metabolic pathway that leads to the synthesis of curcuminoids, flavonols, anthocyanins and lignin in plants. Heatmap visualization of relative metabolite accumulation in symptomatic tissues from plants co-infected (13 dpi) with TEVΔN-DCS1 and PVX-CURS3 (1, co-inouclation; 2, sequential inoculation) or infected with TEVΔN-DCS1-CURS3 at 11, 13 and 15 dpi (3, 4 and 5, repectively) with respect to tissues from plants infected with TEVΔN-aGFP. Blue and red circles represent the values of log2-transformed relative accumulation with respect to the control (TEVΔN-aGFP) according to the color scale shown. Metabolites were analyzed by HPLC-DAD-HRMS. Data are average of three biological replicates. Phenylalanine ammonia-lyase (PAL), cinnamic acid 4-hydroxylase (C4H), 4-coumaroyl-CoA ligase (4CL), hydroxycinnamoyl transferase (HCT), p-coumarate-3- hydroxylase (C3H), caffeoyl coenzyme A (CoA) O-methyltransferase (CCoAOMT), caffeic acid O-methyltransferase (COMT), chalcone synthase (CHS), chalcone isomerase (CHI), flavonoid 3′,5′-hydroxylase (F3′5′H), flavanone 3-hydroxylase (F3H), flavonoid-3-O glycosyltransferase (F3GT), flavonoid 3′-hydroxylase (F3′H), flavonol synthase (FLS), dihydroflavonol 4-reductase (DFR), anthocyanidin synthase (ANS), UDP-glucose:flavonoid 3-O-glucosyl transferase (UFGT), anthocyanidin reductase (ANR), and hydroxycinnamoyl-CoA quinate transferase (HQT); other abbreviations as in the legend to Fig. 1.

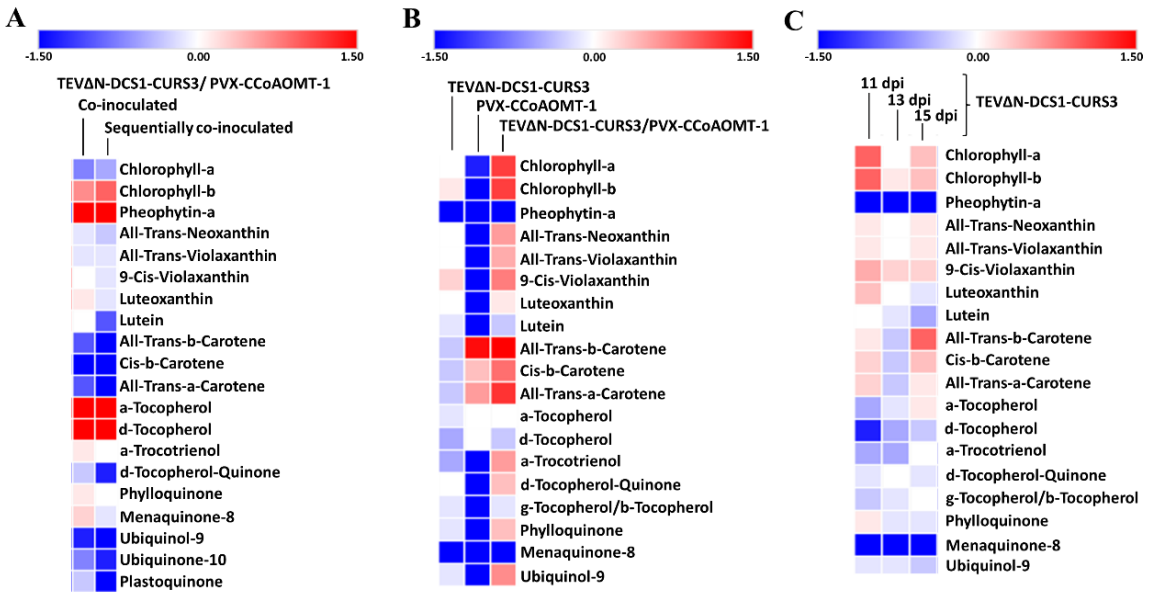

Figure 8. Relative accumulation of chlorophylls, carotenoids, quinones and tocochromanols in symptomatic tissues from N. benthamiana plants infected with normalized on the TEVΔNIb-aGFP samples and visualized as heatmap. (A) Tissues from plants infected with TEVΔNIb-DCS1, PVX-CCoAOMT-1, TEVΔN-DCS1/PVX-CURS3 co-inoculated or sequentially co-inoculated. (B) Tissues from plants infected with TEVΔNIb-DCS1-CURS3, PVX-CCoAOMT-1 and TEVΔN-DCS1-CURS3/PVX-CCoAOMT-1, at 13 dpi. (C) Tissues from plants infected with TEVΔNIb-DCS1-CURS3. Analyses were performed at 11, 13 or 15 dpi, as indicated. Metabolites were detected by HPLC-DAD-HRMS in tissues of infected *N. benthamiana* plants. Blue and red squares represent the values of log2-transformed relative accumulation with respect to the control samples according to the color scale shown. Metabolites were detected by HPLC-DAD-HRMS in tissues of infected *N. benthamiana* plants. Data are average ± SD of three biological replicates.

4. DISCUSSION

Plants provide several phytochemicals, such as polyphenols, carotenoids, sterols or polyunsaturated fatty acids that due to their commercial potential are in demand (Ashrafizadeh et al., 2020). More specifically, polyphenols, namely anthocyanins, flavonols, resveratrol, epicatechins (Martin and Li, 2017), and more recently curcuminoids (Singh et al., 2021; Wu et al., 2020), are raising interest due to their health promoting properties. However, polyphenol accumulation in plants is frequently low and strongly differ among species and tissues; it is also subjected to seasonal and geographical variations. Production of these compounds in biofactory systems is considered an alternative to extraction from natural sources. Microbes, such as *Escherichia coli* and *Saccharomyces cerevisiae*, but also in *Corynebacterium*

glutamicum and *Lactococcus lactis*, have been explored as a sustainable chassis for the production of multiple polyphenolic compounds or their direct precursors (Dudnik et al., 2018; Gomes et al., 2022; Milke et al., 2019). Plants have also been suggested as potential biofactories for the production of polyphenolic compounds. Metabolite production in plants entails some advantages in terms of cost and scalability. In addition, mammalian pathogens do not infect plants, which also add advantages in terms of security. Certain plants, such as *N. benthamiana*, can be grown in high density and still produce large amounts of biomass in a matter of weeks (Peyret and Lomonossoff, 2015; Sainsbury and Lomonossoff, 2014).

Plants display a wide metabolic capacity. For this reason, the insertion of a single or a few heterologous genes are frequently sufficient to trigger the biosynthesis of many compounds of interest (Arya et al., 2020). In some approaches, this heterologous gene or few genes can be efficiently expressed using viral vectors. Expression of *Antirrhinum majus* transcription factor Rosea1 using a viral vector allows high accumulation of anthocyanins in tobacco tissues (Bedoya et al., 2010; Cordero et al., 2017). Similarly, the expression of *Pantoea ananatis* phytoene synthase (crtB) leads to carotenoid accumulation (Llorente et al., 2020; Majer et al., 2017). Large accumulation in *N. benthamiana* leaves of some apocarotenoids, namely crocins and picrocrocin, naturally present in saffron stigma was recently achieved in *N. benthamiana* using a TEV vector by co-expressing a *Crocus sativus* carotenoid cleavage dioxygenase (CCD2L) and crtB (Martí et al., 2020). Here, we show that the heterologous production of curcumin and other curcuminoids in *N. benthamiana* is also possible by transient expression of *C. longa* DCS1 and CURS3 using viral vectors (Fig. 4).

Heterologous curcuminoid production was first achieved in *E. coli* by creating an artificial biosynthetic pathway. Some genes were expressed for this, notably rice (*Oryza sativa*) curcuminoid synthase, to reach around 100 mg of curcuminoids per liter of culture (Katsuyama et al., 2008). A similar approach in *E. coli* was later used to produce 6.95 mg/l of bisdemethoxycurcumin (Kim et al., 2017). Other organisms have also been used as platforms for curcuminoid production, such as the filamentous fungus *Aspergillus oryzae*, in which 64 µg of curcumin were obtained per agar medium plate. By strengthening the supply of the precursor malonyl-CoA, there was a

significant increase in the yield up to 404 ± 9 µg/plate (Kan et al., 2019). In any case, the highest amounts of curcumin production achieved in a heterologous system have been reported in *E. coli*. By optimizing the strain, culture media, time of expression induction and inductor concentration, 817.7 mM (301 mg/l) of curcumin were accomplished (Couto et al., 2017). Ferulic acid was later used as curcuminoid source by expressing caffeic acid O-methyltransferase, which uses caffeic acid as substrate, to improve curcuminoid accumulation to 1529 µM (563 mg/l) (Rodrigues et al., 2020). Ferulic acid has also been used as a source for curcumin production in *S. cerevisiae*, although in this case accumulation was lower (2.7 mg/l) (Rainha et al., 2022).

In this work, to produce curcuminoids in *N. benthamiana* plants our initial attempt was to use a two-virus-vector strategy (TEVΔN-DCS1 and PVX-CURS3). However, using single virus (TEVΔN-DCS1-CURS3) that co-expressed both biosynthetic enzymes, higher curcuminoid accumulation was obtained (Fig. 4B and D). This result suggests that, despite the recombinant virus being larger, the coordinated expression of both enzymes from the same vector compensates the expected inestability due to vector size. TEVΔN-DCS1-CURS3 induced accumulation of a series of curcuminoids, particularly dihydrocurcumin and curcumin (Fig. 4). More in detail, curcumin accumulation in *N. benthamiana* tissues was doubled (12 ± 0.6 versus 6.5 ± 0.6 µg/g DW) when the single virus was used (Fig. 4B and D). This accumulation was further improved to 22 ± 4 µg/g DW after optimizing harvest time to 11 dpi (Fig. 4F). Improving the precursor supply was previously shown to have a major effect on polyphenol accumulation. This was here explored by expressing *N. tabacum* CCoAOMT-1 using a second viral vector, although the expected boost was not achieved (Fig. 4D).

The curcumin accumulation of 22 ± 4 µg/g DW in *N. benthamiana* leaves reported here is lower than those reported in some heterologous microbial systems or in natural sources. Curcuminoid content of turmeric rhizomes depends on the varieties (Lan et al., 2018). Reported accumulations are highly variable and ranged from 1 µg/g to 300 mg/g in different studies. Values of 1-2 µg/g (Esatbeyoglu et al., 2012), 11 mg/g (Degot et al., 2021), 125 mg/g (Dutta, 2015), or 304.9 ± 0.1 mg/g (Burapan et al., 2020) have been reported. Despite the low accumulation when compared to natural sources, heterologous curcuminoid production in plants still represents an attractive goal due

to drawbacks in natural sources (Yixuan et al., 2021). However, further optimization, through overexpression of early or late phenylpropanoid biosynthetic enzymes or silencing genes from other competing branches of the pathway, is required. This may be achieved using more sophisticated viral vectors, plant stable transformation or a combination of both strategies.

ACKNOWLEDGEMENTS

We thank M. Gascón (IBMCP, CSIC-UPV, Valencia, Spain) for helpful assistance with LSCM analyses. This work was supported by grant PID2020-114691RB-I00 from the Spanish Ministerio de Ciencia e Innovación through the Agencia Estatal de Investigación (co-financed European Regional Development Fund). M.M. was the recipient of a predoctoral contract from the Spanish Ministerio de Educación, Cultura y Deporte (FPU16/05294). G.D. is participant of the European COST action CA15136 (EUROCAROTEN).

CONFLICT OF INTEREST

The authors declare no conflict of interest.

REFERENCES

Akter, J., Hossain, M.A., Takara, K., Islam, M.Z., Hou, D.X., 2019. Antioxidant activity of different species and varieties of turmeric (Curcuma spp): Isolation of active compounds. Comp. Biochem. Physiol. Part - C Toxicol. Pharmacol. 215, 9–17. https://doi.org/10.1016/j.cbpc.2018.09.002

Arya, S.S., Rookes, J.E., Cahill, D.M., Lenka, S.K., 2020. Next-generation metabolic engineering approaches towards development of plant cell suspension cultures as specialized metabolite producing biofactories. Biotechnol. Adv. 45, 107635. https://doi.org/10.1016/j.biotechadv.2020.107635

Ashrafizadeh, M., Rafiei, H., Mohammadinejad, R., Afshar, E.G., Farkhondeh, T., Samarghandian, S., 2020. Potential therapeutic effects of curcumin mediated by JAK/STAT signaling pathway: A review. Phyther. Res. 34, 1745–1760. https://doi.org/10.1002/ptr.6642

Bedoya, L., Martínez, F., Rubio, L., Daròs, J.A., 2010. Simultaneous equimolar expression of multiple proteins in plants from a disarmed potyvirus vector. J. Biotechnol. 150, 268–275. https://doi.org/10.1016/j.jbiotec.2010.08.006

Bedoya, L.C., Martínez, F., Orzáez, D., Daròs, J.A., 2012. Visual tracking of plant virus infection and movement using a reporter MYB transcription factor that activates anthocyanin biosynthesis. Plant Physiol. 158, 1130–1138. https://doi.org/10.1104/pp.111.192922

Burapan, S., Kim, M., Paisooksantivatana, Y., Eser, B.E., Han, J., 2020. Thai Curcuma species: Antioxidant and bioactive compounds. Foods 9, 1–11. https://doi.org/10.3390/foods9091219

Cappelli, G., Giovannini, D., Basso, A.L., Demurtas, O.C., Diretto, G., Santi, C., Girelli, G., Bacchetta, L., Mariani, F., 2018. A Corylus avellana L. extract enhances human macrophage bactericidal response against Staphylococcus aureus by increasing the expression of anti-inflammatory and iron metabolism genes. J. Funct. Foods 45, 499–511. https://doi.org/10.1016/j.jff.2018.04.007

Chouhan, S., Sharma, K., Zha, J., Guleria, S., Koffas, M.A.G., 2017. Recent advances in the recombinant biosynthesis of polyphenols. Front. Microbiol. 8. https://doi.org/10.3389/fmicb.2017.02259

Clark, M., Maselko, M., 2020. Transgene Biocontainment Strategies for Molecular Farming. Front. Plant Sci. 11, 1–11. https://doi.org/10.3389/fpls.2020.00210

Cordero, T., Mohamed, M.A., López-Moya, J.J., Daròs, J.A., 2017. A recombinant Potato virus Y infectious clone tagged with the Rosea1 visual marker (PVY-Ros1) facilitates the analysis of viral infectivity and allows the production of large amounts of anthocyanins in plants. Front. Microbiol. 8, 1–11. https://doi.org/10.3389/fmicb.2017.00611

Couto, M.R., Rodrigues, J.L., Rodrigues, L.R., 2017. Optimization of fermentation conditions for the production of curcumin by engineered Escherichia coli. J. R. Soc. Interface 14, 1–8. https://doi.org/10.1098/rsif.2017.0470

Degot, P., Huber, V., Touraud, D., Kunz, W., 2021. Curcumin extracts from Curcuma Longa – Improvement of concentration, purity, and stability in food-approved and water-soluble surfactant-free microemulsions. Food Chem. 339, 128140. https://doi.org/10.1016/j.foodchem.2020.128140

Demurtas, O.C., de Brito Francisco, R., Diretto, G., Ferrante, P., Frusciante, S., Pietrella, M., Aprea, G., Borghi, L., Feeney, M., Frigerio, L., Coricello, A., Costa, G., Alcaro, S., Martinoia, E., Giuliano, G., 2019. ABCC Transporters Mediate the Vacuolar Accumulation of Crocins in Saffron Stigmas. Plant Cell 31, 2789–2804. https://doi.org/10.1105/tpc.19.00193

Demurtas, O.C., Frusciante, S., Ferrante, P., Diretto, G., Azad, N.H., Pietrella, M., Aprea, G., Taddei, A.R., Romano, E., Mi, J., Al-Babili, S., Frigerio, L., Giuliano, G., 2018. Candidate enzymes for saffron crocin biosynthesis are localized in multiple cellular compartments. Plant Physiol. 177, 990–1006. https://doi.org/10.1104/pp.17.01815

Dickmeis, C., Fischer, R., Commandeur, U., 2014. Potato virus X-based expression vectors are stabilized for long-term production of proteins and larger inserts. Biotechnol. JournalJournal 9, 1369–1379. https://doi.org/10.1002/biot.201400347

Dudnik, A., Gaspar, P., Neves, A.R., Forster, J., 2018. Engineering of Microbial Cell Factories for the Production of Plant Polyphenols with Health-Beneficial Properties, Current Pharmaceutical Design. https://doi.org/10.2174/1381612824666180515152049

Esatbeyoglu, T., Huebbe, P., Ernst, I.M.A., Chin, D., Wagner, A.E., Rimbach, G., 2012. Curcumin-from molecule to biological function. Angew. Chemie - Int. Ed. 51, 5308–5332. https://doi.org/10.1002/anie.201107724

Fischer, R., Buyel, J.F., 2020. Molecular farming – The slope of enlightenment. Biotechnol. Adv. 40, 107519. https://doi.org/10.1016/j.biotechadv.2020.107519

Ghosh, S., Banerjee, S., Sil, P.C., 2015. The beneficial role of curcumin on inflammation, diabetes and neurodegenerative disease: A recent update. Food Chem. Toxicol. 83, 111–124. https://doi.org/10.1016/j.fct.2015.05.022

Gibson, D.G., Young, L., Chuang, R.-Y., Venter, J.C., Hutchison III, C.A., Smith, H.O., 2009. Enzymatic assembly of DNA molecules up to several hundred kilobases. Nat. Methods 6, 343–345. https://doi.org/10.1038/nmeth.1318

Gomes, D., Rainha, J., Rodrigues, L.R., Rodrigues, J.L., 2022. Synthetic Biology of Yeasts, in: Farshad Darvishi Harzevili (Ed.), Synthetic Biology of Yeasts. Springer, pp. 119–156. https://doi.org/10.1007/978-3-030-89680-5

Gómez-Estaca, J., Balaguer, M.P., López-Carballo, G., Gavara, R., Hernández-Muñoz, P., 2017. Improving antioxidant and antimicrobial properties of curcumin by means of encapsulation in

gelatin through electrohydrodynamic atomization. Food Hydrocoll. 70, 313–320. https://doi.org/10.1016/j.foodhyd.2017.04.019

Grosso, V., Farina, A., Giorgi, D., Nardi, L., Diretto, G., Lucretti, S., 2018. A high-throughput flow cytometry system for early screening of in vitro made polyploids in Dendrobium hybrids. Plant Cell. Tissue Organ Cult. 132, 57–70. https://doi.org/10.1007/s11240-017-1310-8

Kan, E., Katsuyama, Y., Maruyama, J.I., Tamano, K., Koyama, Y., Ohnishi, Y., 2019. Production of the plant polyketide curcumin in Aspergillus oryzae: Strengthening malonyl-CoA supply for yield improvement. Biosci. Biotechnol. Biochem. 83, 1372–1381. https://doi.org/10.1080/09168451.2019.1606699

Katsuyama, Y., Kita, T., Funa, N., Horinouchi, S., 2009. Curcuminoid biosynthesis by two type III polyketide synthases in the herb Curcuma longa. J. Biol. Chem. 284, 11160–11170. https://doi.org/10.1074/jbc.M900070200

Katsuyama, Y., Matsuzawa, M., Funa, N., Horinouchi, S., 2008. Production of curcuminoids by Escherichia coli carrying an artificial biosynthesis pathway. Microbiology 154, 2620–2628. https://doi.org/10.1099/mic.0.2008/018721-0

Kim, E.J., Cha, M.N., Kim, B.G., Ahn, J.H., 2017. Production of curcuminoids in engineered escherichia coli. J. Microbiol. Biotechnol. 27, 975–982. https://doi.org/10.4014/jmb.1701.01030

Lan, T.T.P., Huy, N.D., Luong, N.N., Nghi, N. Van, Tan, T.H., Quan, L.V., Loc, N.H., 2018. Identification and Characterization of Genes in the Curcuminoid Pathway of Curcuma zedoaria Roscoe. Curr. Pharm. Biotechnol. 19, 839–846. https://doi.org/10.2174/1389201019666181008112244

Llorente, B., Torres-Montilla, S., Morelli, L., Florez-Sarasa, I., Matus, J.T., Ezquerro, M., D'Andrea, L., Houhou, F., Majer, E., Picó, B., Cebolla, J., Troncoso, A., Fernie, A.R., Daròs, J.A., Rodriguez-Concepcion, M., 2020. Synthetic conversion of leaf chloroplasts into carotenoid-rich plastids reveals mechanistic basis of natural chromoplast development. Proc. Natl. Acad. Sci. U. S. A. 117, 21796–21803. https://doi.org/10.1073/pnas.2004405117

López, A.J., Frusciante, S., Niza, E., Ahrazem, O., Rubio-Moraga, Á., Diretto, G., Gómez-Gómez, L., 2021. A new glycosyltransferase enzyme from family 91, ugt91p3, is responsible for the final glucosylation step of crocins in saffron (Crocus sativus l.). Int. J. Mol. Sci. 22, 1–17. https://doi.org/10.3390/ijms22168815

Lyu, X., Lee, J., Chen, W.N., 2019. Potential Natural Food Preservatives and Their Sustainable Production in Yeast: Terpenoids and Polyphenols. J. Agric. Food Chem. 67, 4397–4417. https://doi.org/10.1021/acs.jafc.8b07141

Majer, E., Llorente, B., Rodríguez-Concepción, M., Daròs, J.A., 2017. Rewiring carotenoid biosynthesis in plants using a viral vector. Sci. Rep. 7, 1–10. https://doi.org/10.1038/srep41645

Majer, E., Navarro, J.A., Daròs, J.A., 2015. A potyvirus vector efficiently targets recombinant proteins to chloroplasts, mitochondria and nuclei in plant cells when expressed at the amino terminus of the polyprotein. Biotechnol. J. 10, 1792–1802. https://doi.org/10.1002/biot.201500042

Mandal, S., 2016. Curcumin, a Promising Anti-Cancer Therapeutic: It'S Bioactivity and Development of Drug Delivery Vehicles. Int. J. Drug Res. Tech. Int. J. Drug Res. Technol. 6, 43–57. https://doi.org/10.1016/j.jconrel.2015.04.025

Martí, M., Diretto, G., Aragonés, V., Frusciante, S., Ahrazem, O., Gómez-Gómez, L., Daròs, J.A., 2020. Efficient production of saffron crocins and picrocrocin in Nicotiana benthamiana using a virus-driven system. Metab. Eng. 61, 238–250. https://doi.org/10.1016/j.ymben.2020.06.009

Martin, C., Li, J., 2017. Medicine is not health care, food is health care: plant metabolic engineering, diet and human health. New Phytol. 216, 699–719. https://doi.org/10.1111/nph.14730

Milke, L., Ferreira, P., Kallscheuer, N., Braga, A., Vogt, M., Kappelmann, J., Oliveira, J., Silva, A.R., Rocha, I., Bott, M., Noack, S., Faria, N., Marienhagen, J., 2019. Modulation of the central carbon metabolism of Corynebacterium glutamicum improves malonyl-CoA availability and increases plant polyphenol synthesis. Biotechnol. Bioeng. 116, 1380–1391. https://doi.org/10.1002/bit.26939

Mohammadinejad, R., Shavandi, A., Raie, D.S., Sangeetha, J., Soleimani, M., Shokrian Hajibehzad, S.,

Thangadurai, D., Hospet, R., Popoola, J.O., Arzani, A., Gómez-Lim, M.A., Iravani, S., Varma, R.S., 2019. Plant molecular farming: Production of metallic nanoparticles and therapeutic proteins using green factories. Green Chem. 21, 1845–1865. https://doi.org/10.1039/c9gc00335e

Peyret, H., Lomonossoff, G.P., 2015. When plant virology met Agrobacterium: The rise of the deconstructed clones. Plant Biotechnol. J. 13, 1121–1135. https://doi.org/10.1111/pbi.12412

Prasad, S., Gupta, S.C., Tyagi, A.K., Aggarwal, B.B., 2014. Curcumin, a component of golden spice: From bedside to bench and back. Biotechnol. Adv. 32, 1053–1064. https://doi.org/10.1016/j.biotechadv.2014.04.004

Rainha, J., Gomes, D., Rodrigues, L.R., Rodrigues, J.L., 2020. Synthetic biology approaches to engineer saccharomyces cerevisiae towards the industrial production of valuable polyphenolic compounds. Life 10. https://doi.org/10.3390/life10050056

Rainha, J., Rodrigues, J.L., Faria, C., Rodrigues, L.R., 2022. Curcumin biosynthesis from ferulic acid by engineered Saccharomyces cerevisiae. Biotechnol. J. 17, 1–8. https://doi.org/10.1002/biot.202100400

Rodrigues, J.L., Gomes, D., Rodrigues, L.R., 2020. A Combinatorial Approach to Optimize the Production of Curcuminoids From Tyrosine in Escherichia coli. Front. Bioeng. Biotechnol. 8, 1–15. https://doi.org/10.3389/fbioe.2020.00059

Rodrigues, J.L., Prather, K.L.J., Kluskens, L.D., Rodrigues, L.R., 2015. Heterologous Production of Curcuminoids. Microbiol. Mol. Biol. Rev. 79, 39–60. https://doi.org/10.1128/mmbr.00031-14

Sainsbury, F., Lomonossoff, G.P., 2014. Transient expressions of synthetic biology in plants. Curr. Opin. Plant Biol. 19, 1–7. https://doi.org/10.1016/j.pbi.2014.02.003

Sainsbury, F., Saxena, P., Geisler, K., Osbourn, A., Lomonossoff, G.P., 2012. Using a virus-derived system to manipulate plant natural product biosynthetic pathways, 1st ed, Methods in Enzymology. Elsevier Inc. https://doi.org/10.1016/B978-0-12-404634-4.00009-7

Shanmugaraj, B., Bulaon, C.J.I., Phoolcharoen, W., 2020. Plant molecular farming: A viable platform for recombinant biopharmaceutical production. Plants 9, 1–19. https://doi.org/10.3390/plants9070842

Singh, S., Pandey, P., Akhtar, M.Q., Negi, A.S., Banerjee, S., 2021. A new synthetic biology approach for the production of curcumin and its glucoside in Atropa belladonna hairy roots. J. Biotechnol. 328, 23–33. https://doi.org/10.1016/j.jbiotec.2020.12.022

Stanić, Z., 2017. Curcumin, a Compound from Natural Sources, a True Scientific Challenge – A Review. Plant Foods Hum. Nutr. 72, 1–12. https://doi.org/10.1007/s11130-016-0590-1

Thole, V, Worland, B., Snape, J.W., Vain, P., 2007. The pCLEAN dual binary vector system for Agrobacterium-mediated plant transformation. Plant Physiol. 145, 1211–1219.

Thole, Vera, Worland, B., Snape, J.W., Vain, P., 2007. The pCLEAN dual binary vector system for Agrobacterium-mediated plant transformation. Plant Physiol. 145, 1211–1219. https://doi.org/10.1104/pp.107.108563

Wu, J., Chen, W., Zhang, Y., Zhang, X., Jin, J.M., Tang, S.Y., 2020. Metabolic Engineering for Improved Curcumin Biosynthesis in Escherichia coli. J. Agric. Food Chem. 68, 10772–10779. https://doi.org/10.1021/acs.jafc.0c04276

Yixuan, L., Qaria, M.A., Sivasamy, S., Jianzhong, S., Daochen, Z., 2021. Curcumin production and bioavailability: A comprehensive review of curcumin extraction, synthesis, biotransformation and delivery systems. Ind. Crops Prod. 172, 114050. https://doi.org/10.1016/j.indcrop.2021.114050

Zimmermann, T., Marrison, J., Hogg, K., O'Toole, P., 2014. Clearing Up the Signal: Spectral Imaging and Linear Unmixing in Fluorescence Microscopy. Confocal Microscopy Methods in Molecular Biology Vol 1075. Humana Press, New York.

SUPPLEMENTARY DATA

Figure S1. Nucleotide sequences of TEVΔNIb (sequence variant DQ986288 that include the two silent mutations G273A and A1119G, in red, and lacks the whole NIb cistron) and the derived recombinant viruses TEVΔN-aGFP, -DCS1 and -DCS1-CURS3. The boundaries of viral cistrons are indicated on blue background. Initiation Met and stop codons are underlined. cDNAs corresponding to **green fluorescent protein** (GFP), red fluorescent protein **mCherry**, *Curcuma longa* **diketide-CoA synthase 1** (DCS1) and **curcumin synthase 3** (CURS3) are coloured on green, dark red, light red and blue, respectively.

>TEVΔNIb
AAAATAACAAATCTCAACACAACATATACAAAACAAACGAATCTCAAGCAATCAAGCATTCTACTTCTATTGCAG
CAATTTAAATCATTTCTTTTAAAGCAAAAGCAATTTTCTGAAAATTTTCACCATTTACGAACGATAGCCATGGCA
CTCATCTTTGGCACAGTCAACGCTAACATCCTGAAGGAAGTGTTCGGTGGAGCTCGTATGGCTTGCGTTACCAGC
GCACATATGGCTGGAGCGAATGGAAGCATTTTGAAGAAGGCAGAAGAACCTCTCGTGCAATCATGCACAAACCA
GTGATCTTCGGAGAAGACTACATTACCGAGGCAGACTTGCCTTACACACCACTCCATTTAGAGGTCGATGCTGAA
ATGGAGCGGATGTATTATCTTGGTCGTCGCGCGCTCACCCATGGCAAGAGACGCAAAGTTTCTGTGAATAACAAG
AGGAACAGGAGAAGGAAAGTGGCCAAAACGTACGTGGGGCGTGATTCCATTGTTGAGAAGATTGTAGTGCCCCAC
ACCGAGAGAAAGGTTGATACCACAGCAGCAGTGGAAGACATTTGCAATGAAGCTACCACTCAACTTGTGCATAAT
AGTATGCCAAAGCGTAAGAAGCAGAAAAACTTCTTGCCCGCCACTTCACTAAGTAACGTGTATGCCCAAACTTGG
AGCATAGTGCGCAAACGCCATATGCAGGTGGAGATCATTAGCAAGAAGAGCGTCCGAGCGAGGGTCAAGAGATTT
GAGGGCTCGGTGCAATTGTTCGCAAGTGTGCGTCACATGTATGGCGAGAGGAAAAGGGTGGACTTACGTATTGAC
AACTGGCAGCAAGAGACACTTCTAGACCTTGCTAAAAGATTTAAGAATGAGAGAGTGGATCAATCGAAGCTCACT
TTTGGTTCAAGTGGCCTAGTTTTGAGGCAAGGCTCGTACGGACCTGCGCATTGGTATCGACATGGTATGTTCATT
GTACGCGGTCGGTCGGATGGGATGTTGGTGGATGCTCGTGCGAAGGTAACGTTCGCTGTTTGTCACTCAATGACA
CATTATAGCGACAAATCAATCTCTGAGGCATTCTTCATACCATACTCTAAGAAATTCTTGGAGTTGAGGCCAGAT
GGAATCTCCCATGAGTGTACAAGAGGAGTATCAGTTGAGCGGTGCGGTGAGGTGGCTGCAATCCTGACACAAGCA
CTTTCACCGTGTGGTAAGATCACATGCAAACGTTGCATGGTTGAAACACCTGACATTGTTGAGGGTGAGTCGGGA
GACAGTGTCACCAACCAAGGTAAGCTCCTAGCAATGCTGAAAGAACAGTATCCAGATTTCCCAATGGCCGAGAAA
CTACTCACAAGGTTTTTGCAACAGAAATCACTAGTAAATACAAATTTGACAGCCTGCGTGAGCGTCAAACAACTC
ATTGGTGACCGCAAACAAGCTCCATTCACACACGTACTGGCTGTCAGCGAAATTCTGTTTAAAGGCAATAAACTA
ACAGGGGCCGATCTCGAAGAGGCAAGCACACATATGCTTGAAATAGCAAGGTTCTTGAACAATCGCACTGAAAAT
ATGCGCATTGGCCACCTTGGTTCTTTCAGAAATAAAATCTCATCGAAGGCCCATGTGAATAACGCACTCATGTGT
GATAATCAACTTGATCAGAATGGGAATTTTATTTGGGGACTAAGGGGTGCACACGCAAAGAGGTTTCTTAAAGGA
TTTTTCACTGAGATTGACCCAAATGAAGGATACGATAAGTATGTTATCAGGAAACATATCAGGGGTAGCAGAAAG
CTAGCAATTGGCAATTTGATAATGTCAACTGACTTCCAGACGCTCAGGCAACAAATTCAAGGCGAAACTATTGAG
CGTAAAGAAATTGGGAATCACTGCATTTCAATGCGGAATGGTAATTACGTGTACCCATGTTGTTGTGTTACTCTT
GAAGATGGTAAGGCTCAATATTCGGATCTAAAGCATCCAACGAAGAGACATCTGGTCATTGGCAACTCTGGCGAT
TCAAAGTACCTAGACCTTCCAGTTCTCAATGAAGAGAAAATGTATATAGCTAATGAAGGTTATTGCTACATGAAC
ATTTTCTTTGCTCTACTAGTGAATGTCAAGGAAGAGGATGCAAAGGACTTCACCAAGTTTATAAGGGACACAATT
GTTCCAAAGCTTGGAGCGTGGCCAACAATGCAAGATGTTGCAACTGCATGCTACTTACTTTCCATTCTTTACCCA
GATGTCCTGAGTGCTGAATTACCCAGAATTTTGGTTGATCATGACAACAAAACAATGCATGTTTTGGATTCGTAT
GGGTCTAGAACGACAGGATACCACATGTTGAAAATGAACACAACATCCCAGCTAATTGAATTCGTTCATTCAGGT
TTGGAATCCGAAATGAAAACTTACAATGTTGGAGGGATGAACCGAGATATGGTCACACAAGGTGCAATTGAGATG
TTGATCAAGTCCATATACAAACCACATCTCATGAAGCAGTTACTTGAGGAGGAGCCATACATAATTGTCCTGGCA
ATAGTCTCCCCTTCAATTTTAATTGCCATGTACAACTCTGGAACTTTTGAGCAGGCGTTACAAATGTGGTTGCCA
AATACAATGAGGTTAGCTAACCTCGCTGCCATCTTGTCAGCCTTGGCGCAAAAGTTAACTTTGGCAGACTTGTTC
GTCCAGCAGCGTAATTTGATTAATGAGTATGCGCAGGTAATTTTGGACAATCTGATTGACGGTGTCAGGGTTAAC
CATTCGCTATCCCTAGCAATGGAAATTGTTACTATTAAGCTGGCCACCCAAGAGATGGACATGGCGTTGAGGGAA
GGTGGCTATGCTGTGACCTCTGAAAAGGTGCATGAAATGTTGGAAAAAAACTATGTAAAGGCTTTGAAGGATGCA
TGGGACGAATTAACTTGGTTGGAAAAATTCTCCGCAATCAGGCATTCAAGAAAGCTCTTGAAATTTGGGCGAAAG
CCTTTAATCATGAAAAACACCGTAGATTGCGGCGGACATATAGACTTGTCTGTGAAATCGCTTTTCAAGTTCCAC
TTGGAACTCCTGAAGGGAACCATCTCAAGAGCCGTAAATGGTGGTGCAAGAAAGGTAAGAGTAGCGAAGAATGCC
ATGACAAAAGGGGTTTTTCTCAAAATCTACAGCATGCTTCCTGACGTCTACAAGTTTATCACAGTCTCGAGTGTC
CTTTCCTTGTTGTTGACATTCTTATTTCAAATTGACTGCATGATAAGGGCACACCGAGAGGCGAAGGTTGCTGCA
CAGTTGCAGAAAGAGAGCGAGTGGGACAATATCATCAATAGAACTTTCCAGTATTCTAAGCTTGAAAATCCTATT
GGCTATCGCTCTACAGCGGAGGAAAGACTCCAATCAGAACACCCCGAGGCTTTCGAGTACTACAAGTTTTGCATT
GGAAAGGAAGACCTCGTTGAACAGGCAAAACAACCGGAGATAGCATACTTTGAAAAGATTATAGCTTTCATCACA

CTTGTATTAATGGCTTTTGACGCTGAGCGGAGTGATGGAGTGTTCAAGATACTCAATAAGTTCAAAGGAATACTG
AGCTCAACGGAGAGGGAGATCATCTACACGCAGAGTTTGGATGATTACGTTACAACCTTTGATGACAATATGACA
ATCAACCTCGAGTTGAATATGGATGAACTCCACAAGACGAGCCTTCCTGGAGTCACTTTTAAGCAATGGTGGAAC
AACCAAATCAGCCGAGGCAACGTGAAGCCACATTATAGAACTGAGGGGCACTTCATGGAGTTTACCAGAGATACT
GCGGCATCGGTTGCCAGCGAGATATCACACTCACCCGCAAGAGATTTTCTTGTGAGAGGTGCTGTTGGATCTGGA
AAATCCACAGGACTTCCATACCATTTATCAAAGAGAGGGAGAGTGTTAATGCTTGAGCCTACCAGACCACTCACA
GATAACGTGCACAAGCAACTGAGAAGTGAACCATTTAACTGCTTCCCAACTTTGAGGATGAGAGGGAAGTCAACT
TTTGGGTCATCACCGATTACAGTCATGACTAGTGGATTCGCTTTACACCATTTTGCACGAAACATAGCTGAGGTA
AAAACATACGATTTTGTCATAATTGATGAATGTCATGTGAATGATGCTTCTGCTATAGCGTTTAGGAATCTACTG
TTTGAACATGAATTTGAAGGAAAAGTCCTCAAAGTGTCAGCCACACCACCAGGTAGAGAAGTTGAATTCACAACT
CAGTTTCCCGTGAAACTCAAGATAGAAGAGGCTCTTAGCTTTCAGGAATTTGTAAGTTTACAAGGGACAGGTGCC
AACGCCGATGTGATTAGTTGTGGCGACAACATACTAGTATATGTTGCTAGCTACAATGATGTTGATAGTCTTGGC
AAGCTCCTTGTGCAAAAGGGATACAAAGTGTCGAAGATTGATGGAAGAACAATGAAGAGTGGAGGAACTGAAATA
ATCACTGAAGGTACTTCAGTGAAAAAGCATTTCATAGTCGCAACTAATATTATTGAGAATGGTGTAACCATTGAC
ATTGATGTAGTTGTGGATTTTGGGACTAAGGTTGTACCAGTTTTGGATGTGGACAATAGAGCGGTGCAGTACAAC
AAAACTGTGGTGAGTTATGGGGAGCGCATCCAAAGACTCGGTAGAGTTGGGCGACACAAGGAAGGAGTAGCACTT
CGAATTGGCCAAACAAATAAAACACTGGTTGAAATTCCAGAAATGGTTGCCACTGAAGCTGCCTTTCTATGCTTC
ATGTACAATTTGCCAGTGACAACACAGAGTGTTTCAACCACACTGCTGGAAAATGCCACATTATTACAAGCTAGA
ACTATGGCACAGTTTGAGCTATCATATTTTTACACAATTAATTTTGTGCGATTTGATGGTAGTATGCATCCAGTC
ATACATGACAAGCTGAAGCGCTTTAAGCTACACACTTGTGAGACATTCCTCAATAAGTTGGCGATCCCAAATAAA
GGCTTATCCTCTTGGCTTACGAGTGGAGAGTATAAGCGACTTGGTTACATAGCAGAGGATGCTGGCATAAGAATC
CCATTCGTGTGCAAAGAAATTCCAGACTCCTTGCATGAGGAAATTTGGCACATTGTAGTCGCCCATAAAGGTGAC
TCGGGTATTGGGAGGCTCACTAGCGTACAGGCAGCAAAGGTTGTTTATACTCTGCAAACGGATGTGCACTCAATT
GCGAGGACTCTAGCATGCATCAATAGACTCATAGCACATGAACAAATGAAGCAGAGTCATTTTGAAGCCGCAACT
GGGAGAGCATTTTCCTTCACAAATTACTCAATACAAAGCATATTTGACACGCTGAAAGCAAATTATGCTACAAAG
CATACGAAAGAAAATATTGCAGTGCTTCAGCAGGCAAAAGATCAATTGCTAGAGTTTTCGAACCTAGCAAAGGAT
CAAGATGTCACGGGTATCATCCAAGACTTCAATCACCTGGAAACTATCTATCTCCAATCAGATAGCGAAGTGGCT
AAGCATCTGAAGCTTAAAAGTCACTGGAATAAAAGCCAAATCACTAGGGACATCATAATAGCTTTGTCTGTGTTA
ATTGGTGGTGGATGGATGCTTGCAACGTACTTCAAGGACAAGTTCAATGAACCAGTCTATTTCCAAGGGAAGAAG
AATCAGAAGCACAAGCTTAAGATGAGAGAGGCGCGTGGGGCTAGAGGGCAATATGAGGTTGCAGCGGAGCCAGAG
GCGCTAGAACATTACTTTGGAAGCGCATATAATAACAAAGGAAAGCGCAAGGGCACCACGAGAGGAATGGGTGCA
AAGTCTCGGAAATTCATAAACATGTATGGGTTTGATCCAACTGATTTTTCATACATTAGGTTTGTGGATCCATTG
ACAGGTCACACTATTGATGAGTCCACAAACGCACCTATTGATTTAGTGCAGCATGAGTTTGGAAAGGTTAGAACA
CGCATGTTAATTGACGATGAGATAGAGCCTCAAAGTCTTAGCACCCACACCACAATCCATGCTTATTTGGTGAAT
AGTGGCACGAAGAAAGTTCTTAAGGTTGATTTAACACCACACTCGTCGCTACGTGCGAGTGAGAAATCAACAGCA
ATAATGGGATTTCCTGAAAGGGAGAATGAATTGCGTCAAACCGGCATGGCAGTGCCAGTGGCTTATGATCAATTG
CCACCAAAGAGTGAGGACTTGACGTTTGAAGGAGAAAGCTTGTTTAAGGGACCACGTGATTACAACCCGATATCG
AGCACCATTTGTCACTTGACGAATGAATCTGATGGGCACACAACATCGTTGTATGGTATTGGATTTGGTCCCTTC
ATCATTACAAACAAGCACTTGTTTAGAAGAAATAATGGAACACTGTTGGTCCAATCACTACATGGTGTATTCAAG
GTCAAGAACACCACGACTTTGCAACAACACCTCATTGATGGGAGGGACATGATAATTATTCGCATGCCTAAGGAT
TTCCCACCATTTCCTCAAAAGCTGAAATTTAGAGAGCCACAAAGGGAAGAGCGCATATGTCTTGTGACAACCAAC
TTCCAAACTAAGAGCATGTCTAGCATGGTGTCAGACACTAGTTGCACATTCCCTTCATCTGATGGCATATTCTGG
AAGCATTGGATTCAAACCAAGGATGGGCAGTGTGGCAGTCCATTAGTATCAACTAGAGATGGGTTCATTGTTGGT
ATACACTCAGCATCGAATTTCACCAACACAAACAATTATTTCACAAGCGTGCCGAAAAACTTCATGGAATTGTTG
ACAAATCAGGAGGCGCAGCAGTGGGTTAGTGGTTGGCGATTAAATGCTGACTCAGTATTGTGGGGGGGCCATAAA
GTTTTCATGAGCAAACCTGAAGAGCCTTTTCAGCCAGTTAAGGAAGCGACTCAACTCATGAGTGAATTGGTGTAC
TCGCAAAGTGGCACTGTGGGTGCTGGTGTTGACGCTGGTAAGAAGAAAGATCAAAAGGATGATAAAGTCGCTGAG
CAGGCTTCAAAGGATAGGGATGTTAATGCTGGAACTTCAGGAACATTCTCAGTTCCACGAATAAATGCTATGGCC
ACAAAACTTCAATATCCAAGGATGAGGGGAGAGGTGGTTGTAAACTTGAATCACCTTTTAGGATACAAGCCACAG
CAAATTGATTTGTCAAATGCTCGAGCCACACATGAGCAGTTTGCCGCGTGGCATCAGGCAGTGATGACAGCCTAT
GGAGTGAATGAAGAGCAAATGAAAATATTGCTAAATGGATTTATGGTGTGGTGCATAGAAAATGGGACTTCCCCA
AATTTGAACGGAACTTGGGTTATGATGGATGGTGAGGAGCAAGTTTCATACCCGCTGAAACCAATGGTTGAAAAC
GCGCAGCCAACACTGAGGCAAATTATGACACACTTCAGTGACCTGGCTGAAGCGTATATTGAGATGAGGAATAGG
GAGCGACCATACATGCCTAGGTATGGTCTACAGAGAAACATTACAGACATGAGTTTGTCACGCTATGCGTTCGAC
TTCTATGAGCTAACTTCAAAAACACCTGTTAGAGCGAGGGAGGCGCATATGCAAATGAAAGCTGCTGCAGTACGA
AACAGTGGAACTAGGTTATTTGGTCTTGATGGCAACGTGGGTACTGCAGAGGAAGACACTGAACGGCACACAGCG
CACGATGTGAACCGTAACATGCACACACTATTAGGGGTCCGCCAGTGATAGTTTCTGCGTGTCTTTGCTTTCCGC
TTTTAAGCTTATTGTAATATATATGAATAGCTATTCACAGTGGGACTTGGTCTTGTGTTGAATGGTATCTTATAT
GTTTTAATATGTCTTATTAGTCTCATTACTTAGGCGAACGACAAAGTGAGGTCACCTCGGTCTAATTCTCCTATG
TAGTGCGAGAAAAAAAAAAAAAAAAAAAAAAAAAAAAAAAAAAAAAAAAA

>TEVΔN-aGFP (insert between possitions 144 and 145 of TEVΔNIb; artificial NIaPro cleavage site is on gray background)

ATGGTGAGCAAGGGCGAGGAGCTGTTCACCGGGGTGGTGCCCATCCTGGTCGAGCTGGACGGCGACGTAAACGGC
CACAAGTTCAGCGTGTCCGGCGAGGGCGAGGGCGATGCCACCTACGGCAAGCTGACCCTGAAGTTCATCTGCACC
ACCGGCAAGCTGCCCGTGCCCTGGCCCACCCTCGTGACCACCCTGACCTACGGCGTGCAGTGCTTCAGCCGCTAC
CCCGACCACATGAAGCAGCACGACTTCTTCAAGTCCGCCATGCCCGAAGGCTACGTCCAGGAGCGCACCATCTTC
TTCAAGGACGACGGCAACTACAAGACCCGCGCCGAGGTGAAGTTCGAGGGCGACACCCTGGTGAACCGCATCGAG
CTGAAGGGCATCGACTTCAAGGAGGACGGCAACATCCTGGGGCACAAGCTGGAGTACAACTACAACAGCCACAAC
GTCTATATCATGGCCGACAAGCAGAAGAACGGCATCAAGGTGAACTTCAAGATCCGCCACAACATCGAGGACGGC
AGCGTGCAGCTCGCCGACCACTACCAGCAGAACACCCCCATCGGCGACGGCCCCGTGCTGCTGCCCGACAACCAC
TACCTGAGCACCCAGTCCGCCCTGAGCAAAGACCCCAACGAGAAGCGCGATCACATGGTCCTGCTGGAGTTCGTG
ACCGCCGCCGGGATCACTCTCGGCATGGACGAGCTGTACAAGACGACTGAGAATCTTTATTTTCAGGGGGAGAAG

>TEVΔNIb-mCherry (dark red; insert between possitions 144 and 145 of TEVΔNIb; artificial NIaPro cleavage site is on gray background)

ATGGTTAGCAAAGGCGAGGAGGATAACATGGCCATCATCAAGGAGTTCATGCGCTTCAAGGTGCACATGGAGGGC
TCCGTGAACGGCCACGAGTTCGAGATCGAGGGCGAGGGCGAGGGCCGCCCCTACGAGGGCACCCAGACCGCCAAG
CTGAAGGTGACCAAGGGTGGCCCCCTGCCCTTCGCCTGGGACATCCTGTCCCCTCAGTTCATGTACGGCTCCAAG
GCCTACGTGAAGCACCCCGCCGACATCCCCGACTACTTGAAGCTGTCCTTCCCCGAGGGCTTCAAGTGGGAGCGC
GTGATGAACTTCGAGGACGGCGGCGTGGTGACCGTGACCCAGGACTCCTCCCTGCAGGACGGCGAGTTCATCTAC
AAGGTGAAGCTGCGCGGCACCAACTTCCCCTCCGACGGCCCCGTAATGCAGAAGAAGACCATGGGCTGGGAGGCC
TCCTCCGAGCGGATGTACCCCGAGGACGGCGCCCTGAAGGGCGAGATCAAGCAGAGGCTGAAGCTGAAGGACGGC
GGCCACTACGACGCTGAGGTCAAGACCACCTACAAGGCCAAGAAGCCCGTGCAGCTGCCCGGCGCCTACAACGTC
AACATCAAGTTGGACATCACCTCCCACAACGAGGACTACACCATCGTGGAACAGTACGAACGCGCCGAGGGCCGC
CACTCCACCGGCGGCATGGATGAGCTGTATAAGACGACTGAGAATCTTTATTTTCAGGGGGAGAAG

>TEVΔNIb-DCS1 (insert between possitions 6981 and 6982 of TEVΔNIb; DCS1 cDNA in light red flanked by sequences to complete native NIaPro/NIb and NIb/CP cleavage sites

GGGGAGAAGATGGAAGCGAACGGCTACCGGATAACTCACAGCGCCGATGGGCCGGCGACGATCTTGGCCATCGGC
ACCTCCAACCCCACCAACGTCGTCGACCAGAACGCTTATCCCGACTTCTATTTCCGGGTCACCAACTCCGAGCAT
CTGCAGGAACTCAAAGCCAAGTTTAGGCGCATCTGTGAGAAAGCGGCGATCAGGAAGAGGCACTTGTACTTGACC
GAGGAGATTTTGCGGGAGAATCCTAGCTTGCTGGCTCCCATGGCGCCGTCGTTCGACGCGCGGCAGGCGATCGTG
GTGGAGGCGGTGCCGAAGCTGGCGAAGGAGGCGGCGGAGAAGGCGATCAAGGAGTGGGGCCGCCCCAAATCGGAC
ATCACGCACCTCGTCTTCTGCTCCGCGAGCGGAATCGACATGCCCGGCTCCGACCTGCAGCTTCTCAAGCTGCTC
GGGCTCCCGCCGAGCGTCAATCGCGTCATGCTCTACAACGTCGGGTGCCACGCCGGTGGCACCGCCCTCCGCGTC
GCCAAGGACCTCGCGGAGAACAACCGCGGCGCGCGGGTGCTCGCCGTCTGCTCCGAGGTCACCGTGCTCTCCTAC
CGCGGCCCCCACCCCGCCCACATCGAGAGCCTCTTCGTGCAAGCTCTGTTTGGCGACGGCGCCGCCGCGCTCGTG
GTCGGGTCCGACCCCGTCGATGGCGTCGAGCGCCCCATCTTCGAAATCGCCTCGGCATCCCAAGTGATGCTTCCG
GAGAGCGCAGAGGCGGTGGGCGGCCACCTCCGCGAAATTGGGCTGACCTTCCACCTCAAGAGCCAGCTTCCGTCG
ATCATCGCGAGCAACATCGAGCAGAGCCTGACGACTGCGTGCTCGCCGCTGGGGCTGTCGGACTGGAACCAGCTG
TTCTGGGCGGTTCACCCCGGCGGCCGAGCGATCCTGGACCAGGTGGAGGCGCGGCTCGGACTGGAGAAGGACCGG
CTCGCCGCGACGCGGCACGTACTCAGCGAGTACGGCAACATGCAGAGCGCCACGGTGCTGTTCATCCTGGACGAG
ATGCGGAACCGCTCGGCTGCGGAGGGCCACGCCACCACCGGCGAGGGGCTCGACTGGGGCGTGCTGTTGGGCTTC
GGCCCGGGACTCTCCATCGAGACAGTCGTCCTCCATAGTTGCAGACTGAACACGACTGAGAATCTTTATTTTCAG

>TEVΔNIb-DCS1-CURS3 (insert between possitions 6981 and 6982 of TEVΔNIb; DCS1 and CURS3 cDNA in light red and blue, repectively; enzyme cDNAs are separated by an artificial NIaPro cleavage site on gray background; DCS1-CURS3 cDNAS are flanked by sequences to complete native NIaPro/NIb and NIb/CP cleavage sites

GGGGAGAAGATGGAAGCGAACGGCTACCGGATAACTCACAGCGCCGATGGGCCGGCGACGATCTTGGCCATCGGC
ACCTCCAACCCCACCAACGTCGTCGACCAGAACGCTTATCCCGACTTCTATTTCCGGGTCACCAACTCCGAGCAT
CTGCAGGAACTCAAAGCCAAGTTTAGGCGCATCTGTGAGAAAGCGGCGATCAGGAAGAGGCACTTGTACTTGACC
GAGGAGATTTTGCGGGAGAATCCTAGCTTGCTGGCTCCCATGGCGCCGTCGTTCGACGCGCGGCAGGCGATCGTG
GTGGAGGCGGTGCCGAAGCTGGCGAAGGAGGCGGCGGAGAAGGCGATCAAGGAGTGGGGCCGCCCCAAATCGGAC
ATCACGCACCTCGTCTTCTGCTCCGCGAGCGGAATCGACATGCCCGGCTCCGACCTGCAGCTTCTCAAGCTGCTC
GGGCTCCCGCCGAGCGTCAATCGCGTCATGCTCTACAACGTCGGGTGCCACGCCGGTGGCACCGCCCTCCGCGTC
GCCAAGGACCTCGCGGAGAACAACCGCGGCGCGCGGGTGCTCGCCGTCTGCTCCGAGGTCACCGTGCTCTCCTAC
CGCGGCCCCCACCCCGCCCACATCGAGAGCCTCTTCGTGCAAGCTCTGTTTGGCGACGGCGCCGCCGCGCTCGTG
GTCGGGTCCGACCCCGTCGATGGCGTCGAGCGCCCCATCTTCGAAATCGCCTCGGCATCCCAAGTGATGCTTCCG

GAGAGCGCAGAGGCGGTGGGCGGCCACCTCCGCGAAATTGGGCTGACCTTCCACCTCAAGAGCCAGCTTCCGTCG
ATCATCGCGAGCAACATCGAGCAGAGCCTGACGACTGCGTGCTCGCCGCTGGGGCTGTCGGACTGGAACCAGCTG
TTCTGGGCGGTTCACCCCGGCGGCCGAGCGATCCTGGACCAGGTGGAGGCGCGGCTCGGACTGGAGAAGGACCGG
CTCGCCGCGACGCGGCACGTACTCAGCGAGTACGGCAACATGCAGAGCGCCACGGTGCTGTTCATCCTGGACGAG
ATGCGGAACCGCTCGGCTGCGGAGGGCCACGCCACCACCGGCGAGGGGCTCGACTGGGGCGTGCTGTTGGGCTTC
GGCCCGGGACTCTCCATCGAGACAGTCGTCCTCCATAGTTGCAGACTGAACACTACAGAGAACCTCTACTTTCAA
TCAGGTACAATGGGCAGCCTGCAGGCAATGCGCAGGGCACAGCGGGCTCAAGGCCCGGCCACCATCATGGCTGTC
GGCACCTCCAACCCGCCTAACCTCTACGAGCAGACCTCCTACCCCGACTTCTATTTCCGCGTCACCAACTCCGAC
CACAAGCACGAGCTCAAGAACAAATTCCGTGTTATCTGTGAGAAGACGAAGGTGAAAAGACGGTACTTGCACTTG
ACGGAGGAGATCCTGAAGCAGAGGCCCAAGCTCTGCTCCTACATGGAGCCCTCCTTCGACGATCGGCAGGACATC
GTGGTGGAGGAGATACCAAAGCTGGCGAAGGAGGCGGCGGAGAAGGCGATCAAGGAGTGGGGCCGCCCCAAGTCG
GAGATCACCCACTTGGTGTTCTGCTCCATCAGCGGTATCGACATGCCCGGCGCCGATTACCGCCTCGCCACCCTC
CTCGGCCTCCCCCTGTCCGTCAACCGCCTCATGCTCTACAGCCAGGCCTGCCACATGGGCGCGCAGATGCTGCGC
ATAGCCAAGGACCTCGCGGAGAACAACCGGGGCGCGCGCGTCCTGGCCGTATCCTGCGAAATCACTGTGCTCAGC
TTCCGCGGTCCGGACGCGGGCGACTTCGAGGCCCTCGCGTGTCAGGCCGGCTTCGGCGACGGTGCCGCTGCCGTC
GTCGTCGGGGCCGACCCCCTCCCGGGCGTCGAGAGGCCCATCTACGAGATCGCGGCGGCGATGCAGGAAACGGTG
CCGGAGAGCGAGAGGGCGGTGGGGGGCCACCTGAGGGAAATCGGCTGGACCTTCCACTTCTTCAACCAGCTGCCG
AAGCTGATCGCGGAAAACATCGAGGGCAGCCTGGCGCGGGCGTTCAAGCCGCTGGGGATAAGCGAGTGGAACGAC
GTGTTCTGGGTGGCGCACCCGGGGAACTGGGGCATCATGGACGCCATCGAGACAAAGCTGGGGCTGGAACAGGGG
AAGCTCGCCACGGCGCGGCACGTCTTCAGCGAGTACGGAAACATGCAGAGCGCCACCGTGTACTTCGTGATGGAC
GAGGTGAGGAAGCGGTCGGCGGCAGAGGGGCGGGCCACCACCGGCGAAGGCCTGGAGTGGGGAGTGCTGTTTGGG
TTTGGCCCAGGCCTCACCATAGAAACTGTCGTGCTACGCAGTGTACCATTACCGACGACTGAGAATCTTTATTTT
CAG

Figure S2. Full sequence of wild-type (wt) potato virus X (PVX; GenBank accession number MT799816) and its derived recombinant viruses PVX-mCherry, PVX-CURS3 and PVX-CCoAOMT-1. In recombinant PVX clones, heterologous sequences are transcribed from PVX coat protein (CP) promoter, and a deleted version of PVX CP, lacking the 29 initial codons, is transcribed from a heterologous promoter derived from bamboo mosaic virus (BaMV) CP. **PVX CP promoter** with an ATG-AGG mutation to abolish start codon is underlined. **BaMV CP promoter** is in brown. cDNAs corresponding to **mCherry**, *C. longa* **curcumin synthase 3** (CURS3) and *Nicotiana tabacum* **caffeoyl-coenzyme A (CoA)/5-hydroxyferuloyl-CoA 3/5-O methyltransferase** (CCoAOMT-1) are coloured on dark red, blue and purple, respectively. Flanking position of insertions are on blue background.

>PVX-wt
GAAAACTAAACCATACACCACCAACACAACCAAACCCACCACGCCCAATTGTTACACACCCGCTTGAAAAAGAAA
GTTTAACAAATGGCCAAGGTGCGCGAGGTTTACCAATCTTTTACAGACTCCACCACAAAAACTCTCATCCAAGAT
GAGGCTTATAGAAACATTCGCCCCATCATGGAAAAACACAAACTAGCTAACCCTTACGCTCAAACGGTTGAAGCG
GCTAATGATCTAGAGGGGTTCGGCATAGCCACCAATCCCTATAGCATTGAATTGCATACACATGCAGCCGCTAAG
ACCATAGAGAATAAACTTCTAGAGGTGCTTGGTTCCATCCTACCACAAGAACCTGTTACATTTATGTTTCTTAAA
CCCAGAAAGCTAAACTACATGAGAAGAAACCCGCGGATCAAGGACATTTTCCAAAATGTTGCCATTGAACCAAGA
GACGTAGCCAGGTACCCCAAGGAAACAATAATTGACAAACTCACAGAGATCACAACGGAAACAGCATACATTAGT
GACACTCTGCACTTCTTGGATCCGAGCTACATAGTGGAGACATTCCAAAACTGCCCAAAATTGCAAACATTGTAT
GCGACCTTAGTTCTCCCCGTTGAGGCAGCCTTTAAAATGGAAAGCACTCACCCGAACATATACAGCCTCAAATAC
TTCGGAGATGGTTTCCAGTATATACCAGGCAACCATGGTGGCGGGGCATACCATCATGAATTCGCTCATCTACAA
TGGCTCAAAGTGGGAAAGATCAAGTGGAGGGACCCCAAGGATAGCTTTCTCGGACATCTCAATTACACGACTGAG
CAGGTTGAGATGCACACAGTGACAGTACAGTTGCAGGAATCGTTCGCGGCAAACCACTTGTACTGCATCAGGAGA
GGAGACTTGCTCACACCGGAGGTGCGCACTTTCGGCCAACCTGACAGGTACGTGATTCCACCACAGATCTTCCTC
CCAAAAGTTCACAACTGCAAGAAGCCGATTCTCAAGAAAACTATGATGCAGCTCTTCTTGTATGTTAGGACAGTC
AAGGTCGCAAAAAATTGTGACATTTTTGCCAAAGTCAGACAATTAATTAAATCATCTGACTTGGACAAATACTCT
GCTGTGGAACTGGTTTACTTAGTAAGCTACATGGAGTTCCTTGCCGATTTACAAGCTACCACCTGCTTCTCAGAC
ACACTTTCTGGTGGCTTGCTAACAAAGACCCTTGCACCGGTGAGGGCTTGGATACAAGAGAAAAAGATGCAGCTG
TTTGGTCTTGAGGACTACGCGAAGTTAGTCAAAGCAGTTGATTTCCACCCGGTGGATTTTTCTTTCAAAGTGGAA
ACTTGGGACTTCAGATTCCACCCCTTGCAAGCGTGGAAAGCCTTCCGACCAAGGGAAGTGTCGGATGTAGAGGAA
ATGGAAAGTTTGTTCTCAGATGGGGACCTGCTTGATTGCTTCACAAGAATGCCAGCTTATGCGGTAAACGCAGAG
GAAGATTTAGCTGCAATCAGGAAAACGCCCGAGATGGATGTCGGTCAAGAAGTTAAAGAGCCTGCAGGAGACAGA
AATCAATACTCAAACCCTGCAGAAACTTTCCTCAACAAGCTCCACAGGAAACACAGTAGGGAGGTGAAACACCAG
GCCGCAAAGAAAGCTAAACGCCTAGCTGAAATCCAGGAGTCAATGAGAGCTGAAGGTGATGCCGAACCAAATGAA

ATAAGCGGGACGATGGGGGCAATACCCAGCAACGCCGAACTTCCTGGCACGAATGATGCCAGACAAGAACTCACA
CTCCCAACCACTAAACCTGTCCCTGCAAGGTGGGAAGATGCTTCATTCACAGATTCTAGTGTGGAAGAGGAGCAG
GTTAAACTCCTTGGAAAAGAAACCGTTGAAACAGCGACGCAACAAGTCATCGAAGGACTTCCTTGGAAACACTGG
ATTCCTCAATTAAATGCTGTTGGATTCAAGGCGCTGGAAATTCAGAGGGATAGGAGTGGAACAATGATCATGCCC
ATCACAGAAATGGTCTCCGGGCTGGAAAAAGAGGACTTCCCTGAAGGAACTCCAAAAGAGTTGGCACGAGAATTG
TTCGCTATGAACAGAAGCCCTGCCACCATCCCTTTGGACCTGCTTAGAGCCAGAGACTACGGCAGTGATGTAAAG
AACAAGAGAATTGGTGCCATCACAAAGACACAGGCAACGAGTTGGGGCGAATACTTGACAGGAAAGATAGAAAGC
TTAACTGAGAGGAAAGTTGCGACTTGTGTCATTCATGGAGCTGGAGGTTCTGGAAAAAGTCATGCCATCCAGAAG
GCATTGAGAGAAATTGGCAAGGGCTCGGACATCACTGTAGTCCTGCCGACCAATGAACTGCGGCTAGATTGGAGT
AAGAAAGTGCCTAACACTGAGCCCTATATGTTCAAGACCTCTGAAAAGGCGTTAATTGGGGGAACAGGCAGCATA
GTCATCTTTGACGATTACTCAAAACTTCCTCCCGGTTACATAGAAGCCTTAGTCTGTTTCTACTCTAAAATCAAG
CTAATCATTCTAACAGGAGATAGCAGACAAAGCGTCTACCATGAAACTGCTGAGGACGCCTCCATCAGGCATTTG
GGACCAGCAACAGAGTACTTCTCAAAATACTGCCGATACTATCTCAATGCCACACACCGCAACAAGAAAGATCTT
GCGAACATGCTTGGTGTCTACAGTGAGAGAACGGGAGTCACCGAAATCAGCATGAGCGCCGAGTTCTTAGAAGGA
ATCCCAACTTTGGTACCCTCGGATGAGAAGAGAAAGCTGTACATGGGCACCGGGAGGAATGACACGTTCACATAC
GCTGGATGCCAGGGGCTAACTAAGCCGAAGGTACAAATAGTGTTGGACCACAACACCCAAGTGTGTAGCGCGAAT
GTGATGTACACGGCACTTTCTAGAGCCACCGATAGGATTCACTTCGTGAACACAAGTGCAAATTCCTCTGCCTTC
TGGGAAAAGTTGGACAGCACCCCTTACCTCAAGACTTTCCTATCAGTGGTGAGAGAACAAGCACTCAGGGAGTAC
GAGCCGGCAGAGGCAGAGCCAATTCAAGAGCCTGAGCCCCAGACACACATGTGTGTCGAGAATGAGGAGTCCGTG
CTAGAAGAGTACAAAGAGGAACTCTTGGAAAAGTTTGACAGAGAGATCCACTCTGAATCCCATGGTCATTCAAAC
TGTGTCCAAACTGAAGACACAACCATTCAGTTGTTTTCGCATCAACAAGCAAAAGATGAGACCCTCCTCTGGGCG
ACTATAGATGCGCGGCTCAAGACCAGCAATCAAGAAACAAACTTCCGAGAATTCCTGAGCAAGAAGGACATTGGG
GACGTTCTGTTTTTAAACTACCAAAAAGCTATGGGTTTACCCAAAGAGCGTATTCCTTTTTCCCAAGAGGTCTGG
GAAGCTTGTGCCCACGAAGTACAAAGCAAGTACCTCAGCAAGTCAAAGTGCAACTTGATCAATGGGACTGTGAGA
CAGAGCCCAGACTTCGATGAAAATAAGATTATGGTATTCCTCAAGTCGCAGTGGGTCACAAAGGTGGAAAAACTA
GGTCTACCCAAGATTAAGCCAGGTCAAACCATAGCAGCCTTTTACCAGCAGACTGTGATGCTTTTTGGAACTATG
GCTAGGTACATGCGATGGTTCAGACAGGCTTTCCAGCCAAAAGAAGTCTTCATAAACTGTGAGACCACGCCAGAT
GACATGTCTGCATGGGCCTTGAACAACTGGAATTTCAGCAGACCTAGCTTGGCTAATGACTACACAGCTTTCGAC
CAGTCTCAGGATGGAGCCATGTTGCAATTTGAGGTGCTCAAAGCCAAACACCACTGCATACCAGAGGAAATCATT
CAGGCATACATAGATATTAAGACTAATGCACAGATTTTCCTAGGCACGTTATCAATTATGCGCCTGACTGGTGAA
GGTCCCACTTTTGATGCAAACACTGAGTGCAACATAGCTTACACCCATACAAAGTTTGACATCCCAGCCGGAACT
GCTCAAGTTTATGCAGGAGACGACTCCGCACTGGACTGTGTTCCAGAAGTGAAGCATAGTTTCCACAGGCTTGAG
GACAAATTACTCCTAAAGTCAAAGCCTGTAATCACGCAGCAAAAGAAGGGCAGTTGGCCTGAGTTTTGTGGTTGG
CTGATCACACCAAAAGGGGTGATGAAAGACCCAATTAAGCTCCATGTTAGCTTAAAATTGGCTGAAGCTAAGGGT
GAACTCAAGAAATGTCAAGATTCCTATGAAATTGATCTGAGTTATGCCTATGACCACAAGGACTCTCTGCATGAC
TTGTTCGATGAGAAACAGTGTCAGGCACACACACTCACTTGCAGAACACTAATCAAGTCAGGGAGAGGCACTGTC
TCACTTTCCCGCCTCAGAAACTTTCTTTAACCGTTAAGTTACCTTAGAGATTTGAATAAGATGGATATTCTCATC
AGTAGTTTGAAAAGTTTAGGTTATTCTAGGACTTCCAAATCTTTAGATTCAGGACCTTTGGTAGTACATGCAGTA
GCCGGAGCCGGTAAGTCCACAGCCCTAAGGAAGTTGATCCTCAGACACCCAACATTCACCGTGCATACACTCGGT
GTCCCTGACAAGGTGAGTATCAGAACTAGAGGCATACAGAAGCCAGGACCTATTCCTGAGGGCAACTTCGCAATC
CTCGATGAGTATACTTTGGACAACACCACAAGGAACTCATACCAGGCACTTTTTGCTGACCCTTATCAGGCACCG
GAGTTTAGCCTAGAGCCCCACTTCTACTTGGAAACATCATTTCGAGTTCCGAGGAAAGTGGCAGATTTGATAGCT
GGCTGTGGCTTCGATTTCGAGACCAACTCACCGGAAGAAGGGCACTTAGAGATCACTGGCATATTCAAAGGGCCC
CTACTCGGAAAGGTGATAGCCATTGATGAGGAGTCTGAGACAACACTGTCCAGGCATGGTGTTGAGTTTGTTAAG
CCCTGCCAAGTGACGGGACTTGAGTTCAAAGTAGTCACTATTGTGTCTGCCGCACCAATAGAGGAAATTGGCCAG
TCCACAGCTTTCTACAACGCTATCACCAGGTCAAAGGGATTGACATATGTCCGCGCAGGGCCATAGGCTGACCGC
TCCGGTCAATTCTGAAAAAGTGTACATAGTATTAGGTCTATCATTTGCTTTAGTTTCAATTACCTTTCTGCTTTC
TAGAAATAGCTTACCCCACGTCGGTGACAACATTCACAGCTTGCCACACGGAGGAGCTTACAGAGACGGCACCAA
AGCAATCTTGTACAACTCCCCAAATCTAGGGTCACGAGTGAGTCTACACAACGGAAAGAACGCAGCATTTGCTGC
CGTTTTGCTACTGACTTTGCTGATCTATGGAAGTAAATACATATCTCAACGCAATCATACTTGTGCTTGTGGTAA
CAATCATAGCAGTCATTAGCACTTCCTTAGTGAGGACTGAACCTTGTGTCATCAAGATTACTGGGGAATCAATCA
CAGTGTTGGCTTGCAAACTAGATGCAGAAACCATAAGGGCCATTGCCGATCTCAAGCCACTCTCCGTTGAACGGT
TAAGTTTCCATTGATACTCGAAAGATGTCAGCACCAGCTAGCACAACACAGCCCATAGGGTCAACTACCTCAACT
ACCACAAAAACTGCAGGCGCAACTCCTGCCACAGCTTCAGGCCTGTTCACTATCCCGGATGGGGATTTCTTTAGT
ACAGCCCGTGCCATAGTAGCCAGCAATGCTGTCGCAACAAATGAGGACCTCAGCAAGATTGAGGCTATTTGGAAG
GACATGAAGGTGCCCACAGACACTATGGCACAGGCTGCTTGGGACTTAGTCAGACACTGTGCTGATGTAGGATCA
TCCGCTCAAACAGAAATGATAGATACAGGTCCCTATTCCAACGGCATCAGCAGAGCTAGACTGGCAGCAGCAATT
AAAGAGGTGTGCACACTTAGGCAATTTTGCATGAAGTATGCCCCAGTGGTATGGAACTGGATGTTAACTAACAAC
AGTCCACCTGCTAACTGGCAAGCACAAGGTTTCAAGCCTGAGCACAAATTCGCTGCATTCGACTTCTTCAATGGA
GTCACCAACCCAGCTGCCATCATGCCCAAAGAGGGGCTCATCCGGCCACCGTCTGAAGCTGAAATGAATGCTGCC
CAAACTGCTGCCTTTGTGAAGATTACAAAGGCCAGGGCACAATCCAACGACTTTGCCAGCCTAGATGCAGCTGTC

ACTCGAGGTCGTATCACTGGAACAACAACCGCTGAGGCTGTTGTCACTCTACCACCACCATAACTACGTCTACAT
AACCGACGCCTACCCCAGTTTCATAGTATTTTCTGGTTTGATTGTATGAATAATATAAATAAAAAAAAAAAA

>PVX-mCherry (insert between A5585 and T5737 of PVX-wt)
AGGGCCATTGCCGATCTCAAGCCACTCTCCGTTGAACGGTTAAGTTTCCATTGATACTCGAAAGAGGTCAGCACC
AGCTAGCATGGTTAGCAAAGGCGAGGAGGATAACATGGCCATCATCAAGGAGTTCATGCGCTTCAAGGTGCACAT
GGAGGGCTCCGTGAACGGCCACGAGTTCGAGATCGAGGGCGAGGGCGAGGGCCGCCCCTACGAGGGCACCCAGAC
CGCCAAGCTGAAGGTGACCAAGGGTGGCCCCCTGCCCTTCGCCTGGGACATCCTGTCCCCTCAGTTCATGTACGG
CTCCAAGGCCTACGTGAAGCACCCCGCCGACATCCCCGACTACTTGAAGCTGTCCTTCCCCGAGGGCTTCAAGTG
GGAGCGCGTGATGAACTTCGAGGACGGCGGCGTGGTGACCGTGACCCAGGACTCCTCCCTGCAGGACGGCGAGTT
CATCTACAAGGTGAAGCTGCGCGGCACCAACTTCCCCTCCGACGGCCCCGTAATGCAGAAGAAGACCATGGGCTG
GGAGGCCTCCTCCGAGCGGATGTACCCCGAGGACGGCGCCCTGAAGGGCGAGATCAAGCAGAGGCTGAAGCTGAA
GGACGGCGGCCACTACGACGCTGAGGTCAAGACCACCTACAAGGCCAAGAAGCCCGTGCAGCTGCCCGGCGCCTA
CAACGTCAACATCAAGTTGGACATCACCTCCCACAACGAGGACTACACCATCGTGGAACAGTACGAACGCGCCGA
GGGCCGCCACTCCACCGGCGGCATGGATGAGCTGTATAAGTAGGGTTTGTTAAGTTTCCCTTTTTACTCGAAAGA
TG

>PVX-CURS3 (insert between A5585 and T5737 of PVX-wt)
AGGGCCATTGCCGATCTCAAGCCACTCTCCGTTGAACGGTTAAGTTTCCATTGATACTCGAAAGAGGTCAGCACC
AGCTAGCATGGGCAGCCTGCAGGCAATGCGCAGGGCACAGCGGGCTCAAGGCCCGGCCACCATCATGGCTGTCGG
CACCTCCAACCCGCCTAACCTCTACGAGCAGACCTCCTACCCCGACTTCTATTTCCGCGTCACCAACTCCGACCA
CAAGCACGAGCTCAAGAACAAATTCCGTGTTATCTGTGAGAAGACGAAGGTGAAAAGACGGTACTTGCACTTGAC
GGAGGAGATCCTGAAGCAGAGGCCCAAGCTCTGCTCCTACATGGAGCCCTCCTTCGACGATCGGCAGGACATCGT
GGTGGAGGAGATACCAAAGCTGGCGAAGGAGGCGGCGGAGAAGGCGATCAAGGAGTGGGGCCGCCCCAAGTCGGA
GATCACCCACTTGGTGTTCTGCTCCATCAGCGGTATCGACATGCCCGGCGCCGATTACCGCCTCGCCACCCTCCT
CGGCCTCCCCCTGTCCGTCAACCGCCTCATGCTCTACAGCCAGGCCTGCCACATGGGCGCGCAGATGCTGCGCAT
AGCCAAGGACCTCGCGGAGAACAACCGGGGCGCGCGCGTCCTGGCCGTATCCTGCGAAATCACTGTGCTCAGCTT
CCGCGGTCCGGACGCGGGCGACTTCGAGGCCCTCGCGTGTCAGGCCGGCTTCGGCGACGGTGCCGCTGCCGTCGT
CGTCGGGGCCGACCCCCTCCCGGGCGTCGAGAGGCCCATCTACGAGATCGCGGCGGCGATGCAGGAAACGGTGCC
GGAGAGCGAGAGGGCGGTGGGGGGCCACCTGAGGGAAATCGGCTGGACCTTCCACTTCTTCAACCAGCTGCCGAA
GCTGATCGCGGAAAACATCGAGGGCAGCCTGGCGCGGGCGTTCAAGCCGCTGGGGATAAGCGAGTGGAACGACGT
GTTCTGGGTGGCGCACCCGGGGAACTGGGGCATCATGGACGCCATCGAGACAAAGCTGGGGCTGGAACAGGGGAA
GCTCGCCACGGCGCGGCACGTCTTCAGCGAGTACGGAAACATGCAGAGCGCCACCGTGTACTTCGTGATGGACGA
GGTGAGGAAGCGGTCGGCGGCAGAGGGGCGGGCCACCACCGGCGAAGGCCTGGAGTGGGGAGTGCTGTTTGGGTT
TGGCCCAGGCCTCACCATAGAAACTGTCGTGCTACGCAGTGTACCATTACCGTAGGGTTTGTTAAGTTTCCCTTT
TTACTCGAAAGATG

>PVX-CCoAOMT-1 (insert between A5585 and T5737 of PVX-wt)
AGGGCCATTGCCGATCTCAAGCCACTCTCCGTTGAACGGTTAAGTTTCCATTGATACTCGAAAGAGGTCAGCACC
AGCTAGCATGGCAACCAATGGAAGACATCAAGAAGTTGGACACAAGAGTCTTTTGCAAAGTGATGCCCTTTATCA
GTACATTCTTGAAACAAGCGTGTACCCAAGAGAGCCTGAGCCCATGAAAGAGCTAAGAGAGATCACCGCAAAACA
CCCCTGGAACCTCATGACCACCTCTGCCGATGAAGGGCAATTCTTGAGCATGCTTATCAAACTCATTAATGCCAA
GAACACAATGGAGATTGGTGTTTTTACTGGTTACTCTCTGCTTGCTACTGCCATGGCTCTTCCCGATGATGGCAA
GATTCTAGCTATGGATATTAACCGGGAAAACTACGAGATTGGTCTTCCAGTGATTGAAAAGGCTGGACTAGCTCA
CAAAATTGAATTCAAAGAAGGCCCTGCACTTCCCGTTCTTGATCAAATGATTGAAGATGGAAAATACCATGGATC
ATATGATTTCATATTTGTAGACGCTGACAAAGACAACTACTTGAATTATCACAAGAGATTAATCGACTTGGTCAA
AATTGGTGGACTAATTGGGTATGATAACACCCTATGGAATGGATCAGTGGTTGCACCACCTGATGCACCTCTTAG
GAAATACGTTAGGTATTATAGAGATTTCGTATTGGAACTCAACAAGGCTTTGGCTGCTGATTCAAGAATCGAAAT
TTGCCAGCTACCTGTTGGTGACGGCATCACCCTTTGCCGCCGCATTAGTTAGGGTTTGTTAAGTTTCCCTTTTTA
CTCGAAAGATG

CHAPTER 3

Poduction of potyvirus-derived nanoparticles decorated with a nanobody in biofactory plants

CHAPTER 3

Production of Potyvirus-Derived Nanoparticles Decorated with a Nanobody in Biofactory Plants

Maricarmen Martí, Fernando Merwaiss, Anamarija Butković, and José-Antonio Daròs*

Instituto de Biología Molecular y Celular de Plantas (Consejo Superior de Investigaciones Científicas – Universitat Politècnica de València), 46022 Valencia, Spain

Adapted from the article published in 2022 at:
Frontiers in Bioengineering and Biotechnology, 10: 877363.
DOI: 10.3389/fbioe.2022.877363

https://doi.org/10.3389/fbioe.2022.877363

Author contributions: All authors contributed to conceive the project. M.M., F.M. and A.B. performed the experiments. All authors analysed the data. M.M., F.M. and J.-A.D. wrote the manuscript. All authors reviewed and approved the manuscript.

ABSTRACT

Viral nanoparticles (VNPs) have recently attracted attention for their use as building blocks for novel materials to support a range of functions of potential interest in nanotechnology and medicine. Viral capsids are ideal for presenting small epitopes by inserting them at an appropriate site on the selected coat protein (CP). VNPs presenting antibodies on their surfaces are considered highly promising tools for therapeutic and diagnostic purposes. Due to their size, nanobodies are an interesting alternative to classic antibodies for surface presentation. Nanobodies are the variable domains of heavy-chain (VHH) antibodies from animals belonging to the family Camelidae, which have several properties that make them attractive therapeutic molecules, such as their small size, simple structure, and high affinity and specificity. In this work, we have produced genetically encoded VNPs derived from two different potyviruses—the largest group of RNA viruses that infect plants—decorated with nanobodies. We have created a VNP derived from zucchini yellow mosaic virus (ZYMV) decorated with a nanobody against the green fluorescent protein (GFP) in zucchini (*Cucurbita pepo*) plants. As reported for other viruses, the expression of ZYMV-derived VNPs decorated with this nanobody was only made possible by including a picornavirus 2A splicing peptide between the fused proteins, which resulted in a mixed population of unmodified and decorated CPs. We have also produced tobacco etch virus (TEV)-derived VNPs in *Nicotiana benthamiana* plants decorated with the same nanobody against GFP. Strikingly, in this case, VNPs could be assembled by direct fusion of the nanobody to the viral CP with no 2A splicing involved, likely resulting in fully decorated VNPs. For both expression systems, correct assembly and purification of the recombinant VNPs was confirmed by transmission electron microscope; the functionality of the CP-fused nanobody was assessed by western blot and binding assays. In sum, here we report the production of genetically encoded plant-derived VNPs decorated with a nanobody. This system may be an attractive alternative for the sustainable production in plants of nanobody-containing nanomaterials for diagnostic and therapeutic purposes.

***Keywords*:** viral nanoparticle, VNP, plant virus, nanobody, potyvirus, zucchini yellow mosaic virus, tobacco etch virus.

1. INTRODUCTION

Nanotechnology is a rapidly expanding research area focused on the utilization of nanoscale particles for a broad range of applications. Numerous platforms have been developed to produce nanomaterials, ranging from chemical synthesis to repurposing bionanomaterials such as those derived from viral particles, known as viral nanoparticles (VNPs). These are virus-based formulations that can be used as building blocks for novel materials to support a range of functions of potential interest in medicine and nanotechnology, including vaccine platforms, targeted bioimaging and drug delivery (Steinmetz and Manchester, 2016; Steele et al., 2017; Chung et al., 2020; Rybicki, 2020). VNPs are receiving increasing attention due to their outstanding structural characteristics and easy functionalization (compared to synthetic nanoparticles). The advantages of VNPs include their ability to self-assemble with precise symmetry and polyvalency, their stability under a wide range of conditions, and their biocompatibility and biodegradability.

In particular, plant-derived VNPs provide unique nanoscale scaffolds for biotechnology applications in many areas (Marsian and Lomonossoff, 2016; Alemzadeh et al., 2018; Shukla et al., 2020a; Chung et al., 2021). Plant VNPs are attractive due to their desirable properties, including high yields and the rapid and scalable production that can be achieved in the laboratory or in molecular farming approaches, in which plants are used as VNP production factories (Lomonossoff and D'Aoust, 2016; Tusé et al., 2020). Furthermore, they present the advantage of being non-infectious in mammals—and thus inherently safe. Several plant viruses, both spherical and rod-shaped, have already been successfully deployed in the production of VNPs as scaffolds to support the display of peptides genetically encoded or chemically conjugated to structural viral proteins. Research in this area has focused on the development of plant viruses carrying antigenic epitopes from human or animal pathogens, with the aim of developing novel recombinant vaccines or diagnostic reagents (González-Gamboa et al., 2017; Chung et al., 2021; Peyret et al., 2021;

Stander et al., 2021). The most widely used plant viruses for nanotechnology approaches are cowpea mosaic virus (CPMV) (Sainsbury et al., 2010; Beatty and Lewis, 2019; Ortega-Rivera et al., 2021), tobacco mosaic virus (TMV) (Röder et al., 2017; Lomonossoff and Wege, 2018), and potato virus X (PVX) (Lico et al., 2015; Le et al., 2019; Röder et al., 2019; Shukla et al., 2020b).

Viral genome engineering is the preferred strategy for modifying VNPs when the aim is to display small peptides. In particular, viral capsids are ideal for presenting epitopes by inserting them at an appropriate site on the selected viral coat protein (CP) (Cruz et al., 1996; Dickmeis et al., 2015; Röder et al., 2017). Although this CP-based decoration approach often results in the production of assembled particles, large cargoes may also produce reduced yield or defective particles. However, by incorporating wild-type subunits to produce mosaic particles, this problem can be alleviated (Cruz et al., 1996; Smolenska et al., 1998; Castells-Graells et al., 2018). This can be achieved by including the well-known picornavirus 2A splicing peptide between the fused proteins, utilizing the so-called overcoat strategy, which results in a mixed population of wild-type and modified proteins via a ribosomal co-translational skip mechanism.

Monoclonal antibodies (mAbs) represent a major class of biopharmaceutical products for therapeutic and diagnostic applications, with growing demand worldwide (Donini and Marusic, 2019; Chen, 2022). Plants have long been considered advantageous platforms for large-scale production of antibodies, because they constitute an inexpensive, efficient, and safe alternative system (Giritch et al., 2006; Juarez et al., 2016; Edgue et al., 2017). In addition to full-size mAbs, smaller antibody fragments capable of antigen binding are also actively studied and employed in medicine and research (Yusibov et al., 2016; Julve Parreño et al., 2018; Satheeshkumar, 2020; Malaquias et al., 2021; Wang et al., 2021). An interesting new alternative to mAbs are nanobodies (Muyldermans, 2013). These are the variable domain of heavy-chain (VHH) antibodies from animals belonging to the family *Camelidae* (Figure 1A), which have several properties that make them attractive therapeutic molecules. With molecular masses of 12–15 kDa, nanobodies are the smallest currently known antigen-binding proteins. Despite their small sizes,

nanobodies bind their epitopes with high specificity and strong affinity (Muyldermans, 2013; Mitchell and Colwell, 2018; Wang et al., 2021).

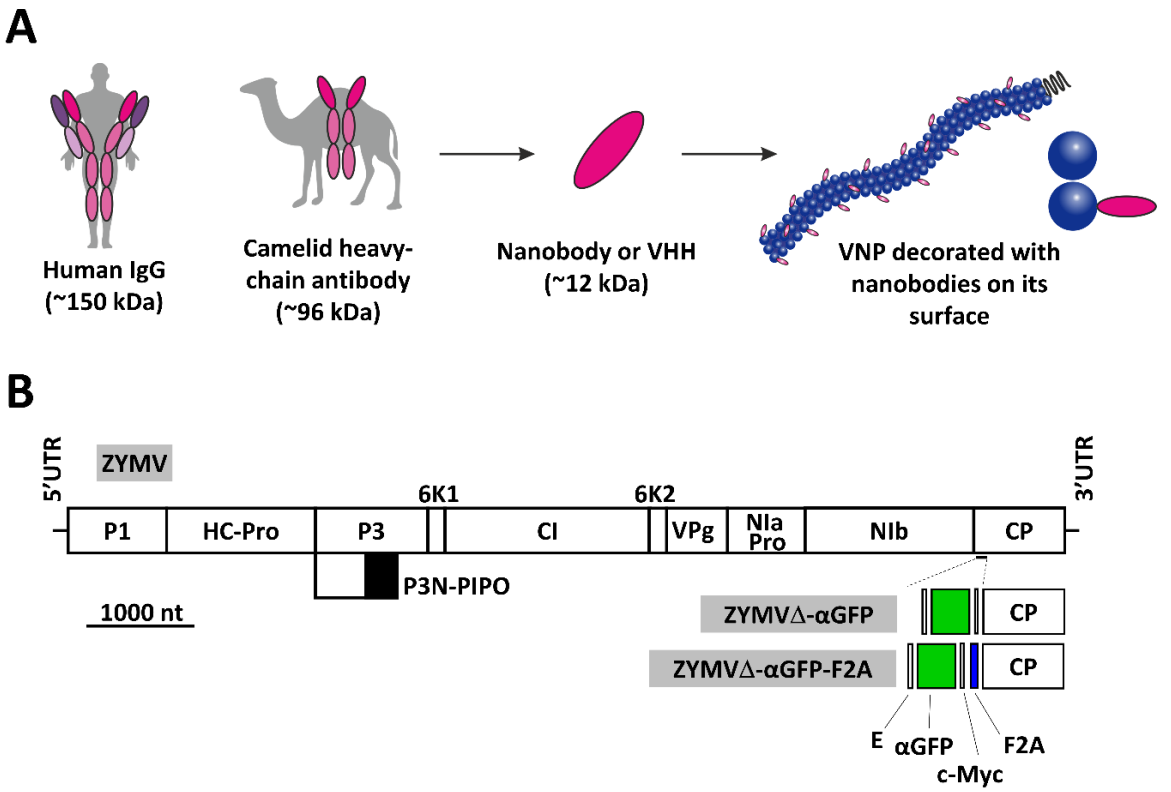

Figure 1. Production of potyvirus nanoparticles decorated with a nanobody in biofactory plants. **(A)** Schematic comparison of a conventional human antibody and a camelid heavy-chain antibody, from which single-domain antibodies or nanobodies are derived. A potyvirus virion partially decorated with nanobodies in its surface is also schematized. **(B)** Schematic representation of the ZYMV genome indicating the position where a heterologous sequence coding for an anti-GFP nanobody (αGFP) flanked with E and c-Myc epitopes was inserted, along with picornavirus F2A peptide. Lines represent ZYMV 5' and 3' UTRs; boxes represent P1, HC-Pro, P3, P3N-PIPO, 6K1, CI, 6K2, VPg, NIaPro, NIb, and CP cistrons, as indicated. Scale bar corresponds to 1000 nt.

Zucchini yellow mosaic virus (ZYMV) and tobacco etch virus (TEV) are two representative members of the genus *Potyvirus* within the family *Potyviridae,* the largest group of plant-infecting RNA viruses. They are flexuous rod-shaped viruses about 750 nm in length with a positive single-stranded RNA genome of approximately 10 kb (Revers and García, 2015). Several features make potyviruses appealing as expression vectors. Their expression via a polyprotein processed into a series of mature gene products facilitates production of heterologous proteins in an amount equimolar to the rest of the viral proteins. If the heterologous proteins are inserted

flanked by the specific processing sites of a viral protease, they can be efficiently released from the polyprotein from a single vector (Kelloniemi et al., 2008; Bedoya et al., 2010; Cordero et al., 2018). The elongated nature of the virion allows for accommodating substantial amounts of foreign genetic material, as well as an extended surface for increased peptide exposure. Remarkably, some potyviruses have already been used as nanoscaffolds for short antigenic peptide presentation, yielding increased immunogenicity (Fernández-Fernández et al., 2002; Manuel-Cabrera et al., 2016; González-Gamboa et al., 2017; Yuste-Calvo et al., 2019). In addition, previous studies have shown that replacing the 33 amino-terminal amino acids of the ZYMV CP with a c-Myc tag does not affect the infectivity of the virus or its movement through the host plant (Arazi et al., 2001a).

We have previously reported the use of potyviral vectors for expressing heterologous proteins in plants, and even an entire biosynthetic pathway (Bedoya et al., 2010, 2012; Majer et al., 2015, 2017; Cordero et al., 2018; Martí et al., 2020; Houhou et al., 2022). In this study, we report the production of genetically encoded viral nanoparticles derived from ZYMV and TEV as nanoscaffolds for nanobody presentation. A picornavirus 2A peptide that mediates cleavage was used to modulate the degree of nanobody decoration on nanoparticles. More importantly, these recombinant virions carrying a nanobody against green fluorescent protein (GFP) were able to bind their antigen efficiently, demonstrating that these nanobodies were functional.

2. MATERIALS AND METHODS

2.1. Plasmid construction

Plasmid pGZYMV (Majer et al., 2017) contains the cDNA of an infectious wild-type (wt) variant of ZYMV (GenBank accession number KX499498), flanked by the cauliflower mosaic virus (CaMV) 35S promoter and terminator in a binary vector that derives from pCLEAN-G181 (Thole et al., 2007) (Figure 1B and Supplementary Figure S1). Derivatives from pGZYMV were constructed using standard molecular biology techniques, including polymerase chain reaction (PCR) amplification with the high-

fidelity Phusion DNA polymerase (Thermo Scientific), DNA digestion with restriction enzymes followed by DNA ligation with T4 DNA ligase (Thermo Scientific), and Gibson assembly of DNA fragments (Gibson et al., 2009) using the NEBuilder HiFi DNA assembly master mix (New England Biolabs). pGZYMVΔ contains a ZYMV variant with a deletion from positions 8551 to 8640 of KX499498, corresponding to codons 4–33 of viral CP (Figure 1B and Supplementary Figure S1, ZYMVΔ). In pGZYMVΔ-αGFP, codons deleted from ZYMV CP were replaced by an anti-green fluorescent protein (αGFP) nanobody (Salema et al., 2013) flanked by E and c-Myc epitopes (Figure 1B and Supplementary Figure S1, ZYMVΔ-αGFP). In pGZYMVΔ-αGFP-F2A, a cDNA corresponding to foot-and-mouth disease virus 2A self-cleavage peptide (F2A) (Kim et al., 2011) was inserted between the αGFP and the deleted version of the CP (CPΔ) coding regions. The resulting viral recombinant clone was named ZYMVΔ-αGFP-F2A (Figure 1B and Supplementary Figure S1).

Plasmid pGTEVa (Bedoya et al., 2012) contains the cDNA of an infectious TEV variant with the GenBank accession number DQ986288 (G273A, A1119G), flanked by the CaMV 35S promoter and terminator in a binary vector derived from pCLEAN-G181. In pGTEV-αGFP, the αGFP nanobody cDNA, flanked by E and c-Myc epitopes, was inserted at the 5' end of CP cistron. The three initial codons of TEV CP, including silent mutations, were duplicated to mediate NIaPro proteolytic processing. In pGTEV-αGFP-F2A, the cDNA corresponding to picornavirus F2A was inserted between the αGFP and the viral CP (Supplementary Figure S2).

Plasmid pEGFPSt contains the coding region of the enhanced GFP with a carboxy-terminal Twin-Strep tag (Schmidt et al., 2013) under the control of the bacteriophage T7 promoter and terminator for expression in Escherichia coli (Supplementary Figure S3).

2.2 Plant Inoculation

Seeds of zucchini plants (*Cucurbita pepo* L. cv. MU-CU-16, accession BGV004370 from Centro de Conservación y Mejora de la Agrodiversidad Valenciana, Universitat Politècnica de València) were kept in darkness at 37ºC for 2 days and moved to a growth chamber at 25ºC with a 16/8 h day/night cycle to promote germination.

Seedlings were sown into individual pots and maintained in a greenhouse at 25ºC with a 16/8 h day/night cycle. The strain C58C1 of *Agrobacterium tumefaciens*, carrying the helper plasmid pCLEAN-S48 (Thole et al., 2007), was transformed with the plasmids containing the different ZYMV and TEV viral clones mentioned above. Transformed bacteria were selected in plates with 50 µg/ml rifampicin, 50 µg/ml kanamycin, and 7.5 µg/ml tetracycline. Individual colonies of the different clones were further grown for 24 h at 28ºC in liquid media up to an optical density at 600 nm (OD600) of 0.5 to 1. Cells were harvested by centrifugation, resuspended in agroinoculation solution (10 mM MES-NaOH [pH 5.6], 10 mM MgCl2, and 150 µM acetosyringone) at OD600 of 0.5; the culture was further incubated for 2 h at 28ºC. With a needleless syringe, cultures corresponding to ZYMV clones were used to infiltrate one cotyledon and one true leaf from 2-week old zucchini plants. After agroinoculation, plants were kept in a growth chamber at 25ºC under a 12 h day/night photoperiod with an average photon flux density of 240 $\mu mol \cdot m^{-2} \cdot s^{-1}$. Aliquots of symptomatic tissues from upper leaves and the equivalent tissues from mock-inoculated controls were harvested at 21 days post-inoculation (dpi), frozen in liquid nitrogen, and stored at -80ºC until use.

Nicotiana benthamiana plants were grown at 25°C under a 16/8 h day/night cycle in growth chambers. Fully expanded upper leaves from plants 4–6 weeks old were used for agroinoculation, based on the protocol described above using A. tumefaciens cultures corresponding to the TEV clones. Immediately following infiltration, plants were watered and transferred to a growth chamber under a 12-h day/night and 25ºC cycle. Aliquots of symptomatic tissues from upper leaves and the equivalent tissues from mock-inoculated controls were harvested at 14 dpi, frozen in liquid nitrogen, and stored at -80ºC until use.

2.3 RT-PCR Analysis of the Viral Progeny

Total RNA was purified from leaf tissue aliquots using silica-gel columns (Zymo Research) (Uranga et al., 2021a). For ZYMV analysis, aliquots of the RNA preparations were subjected to reverse transcription (RT) using the RevertAid reverse transcriptase (Thermo Scientific) and primer PI (5'-AGGCTTGCAAACGGAGTCTAA-3'). Aliquots of the RT products were subjected to PCR amplification using the high-fidelity Phusion

DNA polymerase and primers PII (5'-TGTAATGCTCCAATCAGGCACT-3') and PIII (5'-CTGCATTGTATTCACACCTAGT-3'), which are homologous and complementary, respectively, to sequences flanking the ZYMV CP cistron. For TEV analysis, reverse transcription was completed using primer PIV (5'-TCATAACCCAAGTTCCGTTC-3'), while PCR amplification was performed with primers PV (5'-CATCTGTGCATCAATGATCGAA-3') and PVI (5'-GTGTGGCTCGAGCATTTGACAA-3'). PCR products were separated via electrophoresis in 1% (w/v) agarose gels that were subsequently stained with 1% (w/v) ethidium bromide.

2.4 Western Blot Analysis

Aliquots of frozen tissue (approximately 50 mg) were ground with a mill (Star-Beater, VWR) using a 4-mm diameter steel ball for 1 min at 30 s^{-1}. Three volumes of protein extraction buffer (60 mM Tris-HCl [pH 6.8], 2% [w/v] sodium dodecyl sulfate [SDS], 100 mM dithiothreitol [DTT], 10% [v/v] glycerol, 0.01% [w/v] bromophenol blue) were added. Samples were thoroughly vortexed, incubated for 5 min at 100ºC, and clarified with centrifugation for 5 min. Aliquots of the supernatants were separated via SDS-polyacrylamide gel electrophoresis (PAGE) in 12.5% (w/v) polyacrylamide gels. Proteins were electro-blotted to polyvinylidene difluoride (PVDF) membranes for 1 h. Membranes were blocked in 5% (w/v) non-fat milk in washing buffer (10 mM Tris-HCl [pH 7.5], 154 mM NaCl, 0.1% [w/v] Nonidet NP-40) for 1 h and were then incubated overnight at 4ºC with various antibodies in blocking solution at 1:10,000 dilutions. Membranes were washed three times with washing buffer prior to detection. ZYMV CP and TEV CP were detected using polyclonal antibodies (Bioreba) conjugated to alkaline phosphatase (AP). cMyc and E epitopes were detected using monoclonal antibodies (Thermo Scientific) conjugated to AP and horseradish peroxidase (HRP), respectively. AP and HRP were finally revealed using CSPD (Roche) and SuperSignal West Pico PLUS chemiluminescent (Thermo Scientific) substrates, respectively. Images were recorded using an Amersham ImageQuant 800 (Cytiva).

2.5 Expression in Escherichia coli of Recombinant GFP and Purification

E. coli BL21(DE3)pLysS were electroporated with pEGFPSt, and transformed bacteria were selected in lysogenic broth (LB) plates containing 50 µg/ml ampicillin and 34 µg/ml chloramphenicol. A single colony was further grown at 37ºC in 250 ml of LB liquid media containing the same antibiotics up to an OD600 of 0.6. Isopropyl β-D-1-thiogalactopyranoside (IPTG) was added to 0.4 mM, with culturing being continued for 3 h at the same temperature. Cells were pelleted at 7700 x g for 15 min, washed with water, pelleted again, and finally resuspended in 7.5 ml of water with a protease inhibitor cocktail (complete; Roche). Bacteria were frozen and kept at -80ºC until protein purification. The cell preparation was thawed and 1 ml of 1 M Tris-HCl (pH 8.0), 1 ml 10% (v/v) Nonidet-P40, 20 µl 0.5 M EDTA (pH 8.0), 200 µl 0.5 M DTT, 125 U benzonase (Millipore), and 10 mg lysozyme were added; this mix was incubated for 45 min at 4ºC with gentle agitation. KCl (0.11 g) was then added, and the mix was further incubated for 15 min. Finally, 50 µl 1 M MgCl2 were added, and the preparation was brought to a final volume of 10 ml. This mix was then centrifuged at 84,500 x g at 4ºC for 30 min; the supernatant was filtered using a 0.45 µm syringe filter.

Recombinant GFP with a carboxy-terminal TST was purified using affinity chromatography in native conditions with a 1 ml Strep-Tactin XT superflow column (IBA). Protein purification was conducted using an AKTA Prime Plus liquid chromatography system (GE Healthcare) at 4˚C and a flow rate of 1 ml/min. The column was equilibrated with 10 ml of chromatography buffer (100 mM Tris-HCl [pH 8.0], 150 mM KCl, 1 mM EDTA, 5 mM MgCl2, 10 mM DTT, and 1% [v/v] Nonidet P40) before loading the protein extract. This column was then washed with 20 ml of chromatography buffer, and the recombinant GFP was finally eluted in 50 mM biotin in chromatography buffer with collection of 1-ml fractions. Purified protein fractions were analyzed via SDS-polyacrylamide gel electrophoresis (SDS-PAGE; 12.5% [w/v] polyacrylamide, 0.05% [w/v] SDS), followed by Coomassie blue staining. Bovine serum albumin standards were also run in the gel to quantify the GFP amount in each fraction.

2.6 Virion Purification

Aliquots of symptomatic leaf tissue (0.5 g) were homogenized using a Polytron (Kinematica) in the presence of 1 ml of cold extraction buffer (0.5 M boric acid [pH 8.0], 1% [w/v] polyvinylpyrrolidone [PVP] 40, and 100 mM 2-mercaptoethanol). Next, 0.25 ml chloroform and 0.25 ml CCl4 were added, and grinding continued. The mix was clarified via centrifugation for 15 min; the supernatant was recovered. While stirring the preparation on ice, we added 154 µl of a 40% (w/v) polyethylene glycol (PEG) 6000, 17.5% (w/v) NaCl solution. Stirring was maintained for 15 min. The mix was centrifuged for 5 min at 16 000 x g, and the supernatant was discarded. Sediment was resuspended by gentle agitation with a magnetic stir bar in 100 µl of 50 mM boric acid [pH 8.0], 5 mM EDTA, 0.25% (w/v) Triton X-100, and 25% (v/v) glycerol. Preparations were stored at -80ºC until use.

2.7 Electron Microscopy Analysis

Virion preparations were stained with 2% (w/v) phosphotungstic acid (PTA; pH 7.0), using the drop technique. The grid (carbon film coated only, 200 mesh, EMS) was layered on a 10 µl sample drop and incubated for 15 min. Grids were then washed with water, stained with 2% (w/v) PTA for 3 min, and dried at room temperature. Virion preparations were examined with a JEM-1400Flash (120 kV) electron microscope (JEOL).

3. RESULTS

3.1 Plant-Based Production of ZYMV Nanoparticles Decorated with Anti-GFP Nanobodies.

Previous work has shown that a ZYMV clone with a deletion corresponding to the 33 amino-terminal codons of the viral CP is infectious and that some heterologous sequences, notably c-Myc and 6xHis tags, can be fused to the amino-terminal end of this deleted version of CP without substantially impacting the infectivity and stability of

the resulting recombinant clone (Arazi et al., 2001a). We wondered whether ZYMV would still support the expression of a substantially larger moiety, such as a nanobody, fused to the deleted version of CP to produce decorated nanoparticles. To examine this, we prepared a ZYMV recombinant clone in which CP codons from +4 to +33 (ZYMVΔ) were replaced by the cDNA of a nanobody specifically recognizing GFP (Salema et al., 2013) (ZYMVΔ-αGFP; Figure 1B and Supplementary Figure S1). αGFP nanobody was tagged with flanking c-Myc and E epitopes to facilitate detection (Figure 1B and Supplementary Figure S1). We maintained the first three codons of ZYMV CP to assure efficient NIaPro-mediated processing of the recombinant CP from the viral polyprotein (Adams et al., 2005). Since we foresaw potential limitations on the infectivity of a recombinant ZYMV fully decorated with the nanobody, we also prepared a derivative clone in which a picornavirus splicing domain—namely F2A (Kim et al., 2011)—was inserted between the nanobody and the CP to produce partially decorated viral nanoparticles (ZYMVΔ-αGFP-F2A; Figure 1B and Supplementary Figure S1).

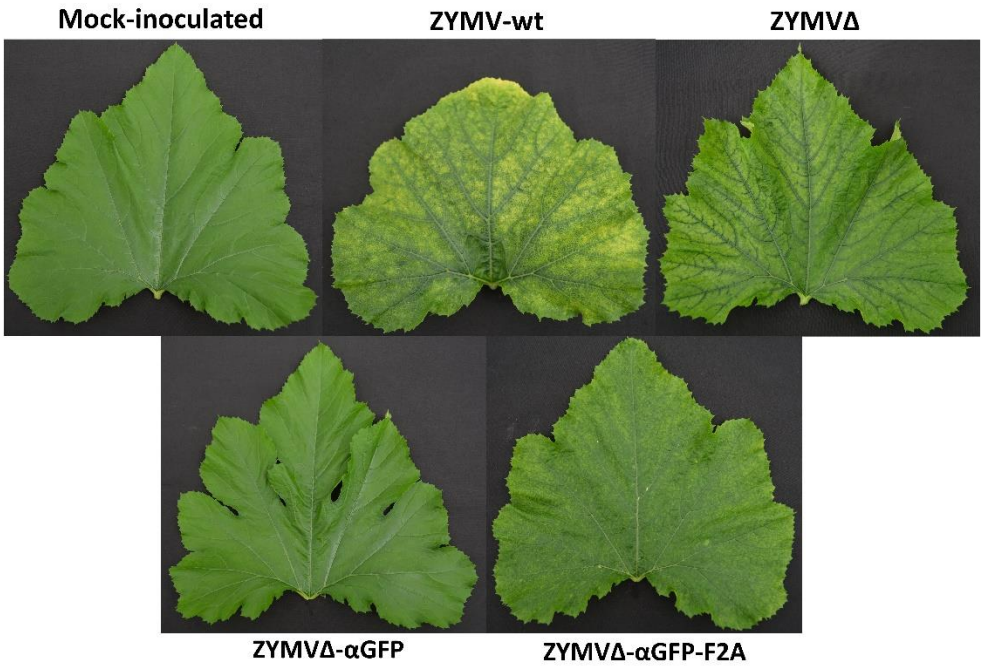

Figure 2. Pictures of representative upper leaves from zucchini plants mock-inoculated and agroinoculated with ZYMV-wt, ZYMVΔ, ZYMVΔ-αGFP, and ZYMVΔ-αGFP-F2A, as indicated, taken at 21 dpi.

Zucchini plants were agroinoculated with ZYMV-wt and the various recombinant clones. Upper leaves of plants inoculated with ZYMV-wt showed typical symptoms of

infection at 14 dpi. Similar symptoms, although milder, were observed in plants inoculated with ZYMVΔ. The symptoms in plants inoculated with ZYMVΔ-αGFP-F2A were particularly mild, while plants inoculated with ZYMVΔ-αGFP showed no apparent symptoms of infection (Figure 2).

We then investigated viral ZYMV infection and the presence of the heterologous sequences corresponding to the αGFP nanobody in the viral progenies at 21 dpi, using RT-PCR amplification followed by electrophoretic analysis. RT-PCR products likely corresponding to the presence of full-length CP (850 bp) and the CPΔ (760 bp) were amplified from control plants inoculated with ZYMV-wt and ZYMVΔ, respectively (Figure 3A, lanes 4 and 5). Although they carried the nanobody sequence in the infectious clone, plants inoculated with ZYMVΔ-αGFP exhibited a slight band with the same position as that in ZYMVΔ (Figure 3A, lane 6), probably arising from a progeny that lost the exogenous sequence. Conversely, plants inoculated with ZYMVΔ-αGFP-F2A successfully produced a band whose position matched that expected for a recombinant clone maintaining the αGFP insert (1279 bp; Figure 3A, lane 7, gray arrowhead). Next, from equivalent tissue aliquots from upper leaves harvested at 21 dpi, the presence of ZYMV CP and the αGFP nanobody was assessed using western blot analysis with a polyclonal antibody against ZYMV CP and a monoclonal antibody against the c-Myc tag, respectively. Reaction with the anti-ZYMV CP antibody produced a single band in the lane corresponding to the plant inoculated with ZYMV-wt (Figure 3B, lane 2, black arrowhead). The position of this band, in comparison to those of protein size standards, suggests that it arose from ZYMV-wt CP. Lanes corresponding to plants inoculated with ZYMVΔ, and ZYMVΔ-αGFP-F2A showed bands with lower positions in the membrane, suggesting that they arose from the deleted version of ZYMV CP (Figure 3B, lanes 3, and 5, white arrowhead). Interestingly, a second intense band in the upper part of the membrane was also observed in the lane corresponding to a plant inoculated with ZYMVΔ-αGFP-F2A (Figure 3B, lane 5, gray arrowhead). A comparison with protein size standards suggests that it arose from a fusion between the deleted version of CP and the αGFP nanobody. No bands were observed in the lanes corresponding to the mock-inoculated plant and the plant inoculated with ZYMVΔ-αGFP (Figure 3B, lanes 1 and 4). Accordingly, reaction with the anti-c-Myc antibody exclusively produced bands in the lane corresponding to the

plant inoculated with ZYMVΔ-αGFP-F2A (Figure 3C). The positions of the most intense bands in the membrane suggest detection of the αGFP-F2A-CPΔ fusion (Figure 3C, lane 5, gray arrowhead) and the free αGFP nanobody resulting from the F2A activity (Figure 3C, lane 5, striped arrowhead).

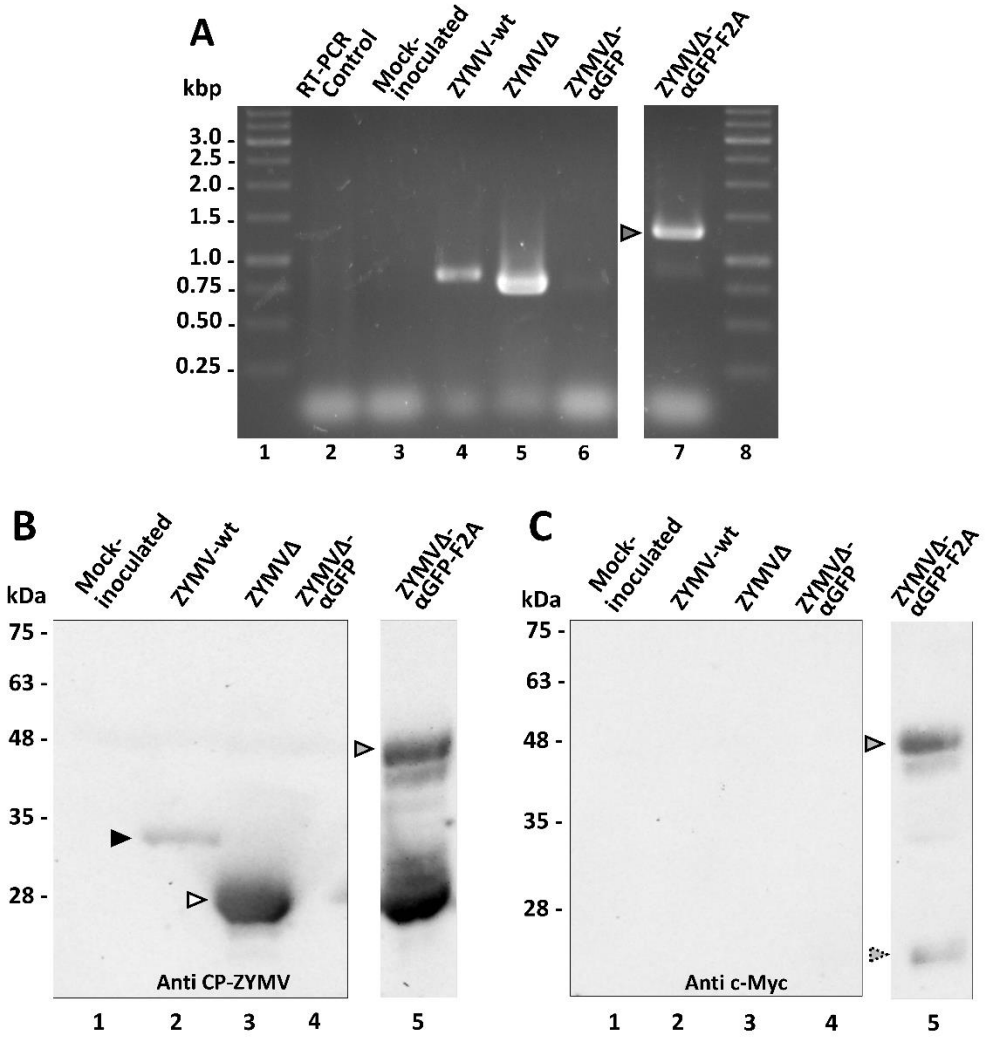

Figure 3. Analysis of zucchini tissues from plants inoculated with various ZYMV-derived recombinant clones at 21 dpi. **(A)** RT-PCR analysis of the progeny of recombinant ZYMV inoculated into zucchini plants. Representative samples from triplicate-inoculated plants are shown. Amplification products corresponding to the ZYMV CP region were separated via electrophoresis in an agarose gel, which was stained with ethidium bromide. Lanes 1 and 8, DNA marker ladder with sizes (in kbp) in the left; lane 2, RT-PCR control with no RNA added; lane 3, mock-inoculated plant; lanes 4 to 7, plants agroinoculated with ZYMV-wt, ZYMVΔ, ZYMVΔ-αGFP, and ZYMVΔ-αGFP-F2A, respectively. **(B and C)** Western blot analyses of protein extracts using an antibody against **(B)** ZYMV CP and **(C)** the c-Myc epitope fused to the αGFP nanobody. Proteins were separated by SDS-PAGE and transferred to a membrane. Lane 1, mock-inoculated plant; lanes 2 to 5, plants agroinoculated with ZYMV-wt, ZYMVΔ, ZYMVΔ-αGFP, and ZYMVΔ-αGFP-F2A, respectively. The positions and sizes of protein standards are indicated on the left. Black and white arrowheads indicate the positions of ZYMV

CP and CPΔ, respectively. Gray and stripped arrowheads indicates the position of the αGFP-F2A-CPΔ fusion and free αGFP, respectively.

Together, these findings suggest that agroinoculation of the different ZYMV recombinant clones yielded infected plants. However, only ZYMVΔ-αGFP-F2A, which contains a picornavirus 2A self-cleavage domain —likely resulting in a partially nanobody-decorated viral nanoparticle—produced a substantial amount of αGFP-F2A-CPΔ fusion in infected plants.

3.2 GFP-Binding Activity of Nanoparticles Derived from ZYMVΔ-F2A-αGFP

Virions were next purified from zucchini plants agroinoculated with ZYMV-wt, ZYMVΔ, and ZYMVΔ-αGFP-F2A at 21 dpi. Transmission electron microscope (TEM) analysis of virion preparations showed the presence in all cases of the elongated viral nanoparticles, with a length of approximately 750 nm expected for ZYMV (Figure 4A). Next, we separated the virion preparations by SDS-PAGE and transferred the proteins to PVDF membranes that were incubated with recombinant GFP. After washing the membranes, binding of GFP was detected by using an anti-GFP antibody or by directly analyzing the green fluorescence. When an anti-GFP antibody was used to detect the presence of GFP (Figure 4B), bands were observed in a position of the membrane corresponding to the expected migration of the αGFP-F2A-CPΔ fusion capsomers.

When analyzing the membrane with a fluorescence stereomicroscope, intense green fluorescent signals at exactly the same position were observed (Figure 4C). We observed no such reaction bands or fluorescent signals in the lanes where ZYMVΔ virions were separated. Finally, aliquots of the virion preparations were directly spotted onto PVDF membranes that were also incubated with recombinant GFP. After washing the membranes, binding of GFP was detected again—either indirectly by reaction with an anti-GFP antibody or directly using a fluorescence stereomicroscope. In contrast to spots containing nanoparticles purified from plants inoculated with ZYMVΔ, those corresponding to ZYMVΔ-αGFP-F2A showed strong reaction with the anti-GFP antibody (Figure 4D), along with intense green fluorescence (Figure 4E). Overall, these results strongly suggest that zucchini plants infected with recombinant ZYMVΔ-αGFP-F2A accumulate viral nanoparticles partially decorated with an αGFP nanobody, due to

the conditional activity of picornaviral F2A peptide, and that these ZYMV-derived nanoparticles exhibit specific GFP-binding activity.

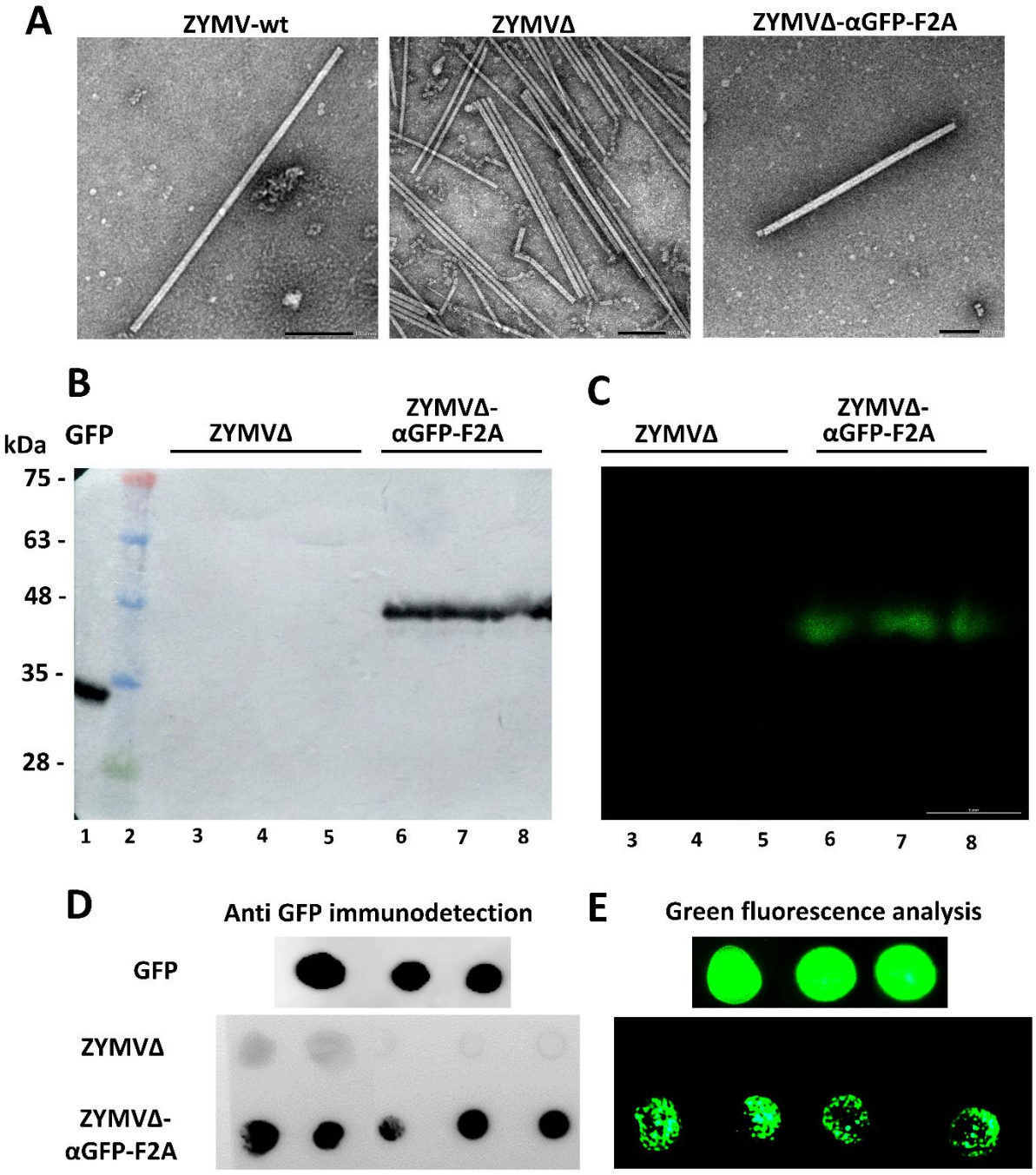

Figure 4. Antigen-binding capacity of ZYMV VNPs. **(A)** TEM micrographs of purified ZYMV-wt, ZYMVΔ, and ZYMVΔ-αGFP-F2A virions, as indicated. Scale bar is 100 nm. **(B and C)** GFP-binding properties of ZYMV αGFP-F2A-CPΔ capsomers. Virion preparations from zucchini plants infected with ZYMVΔ and ZYMVΔ-αGFP-F2A were separated by SDS-PAGE in triplicate, and the proteins were transferred to a membrane. The membranes were incubated with recombinant GFP and washed; GFP was revealed by **(B)** reaction with a specific antibody or **(C)** by directly imaging the green fluorescence. Lane 1, recombinant GFP; lane 2, protein standards with sizes in kDa on the left; lanes 3 to 8, virion preparations from plants infected with ZYMVΔ (lanes 3 to 5) or ZYMVΔ-αGFP-F2A (lanes 6 to 8). **(D and E)** Dot-blot analysis of

the GFP-binding activity of ZYMVΔ-αGFP-F2A virions. Aliquots of virion preparations from plants infected with ZYMVΔ and ZYMVΔ-αGFP-F2A, as indicated, were spotted on membranes that were incubated with recombinant GFP, and GFP detected with a specific antibody **(D)**, or the fluorescence directly analyzed using a stereomicroscope **(E)**. Membranes in which aliquots of recombinant GFP were spotted were used as a positive control.

3.3 Plant-Based Production of TEV Nanoparticles Decorated with Anti-GFP Nanobodies

We next explored whether the same concept could be extended to TEV, another potyvirus frequently used for expressing heterologous proteins in plants of *N. benthamiana*, the preferred production platform in molecular farming (Peyret and Lomonossoff, 2015; Bally et al., 2018; Goulet et al., 2019). To this end, we cloned a cDNA coding for the αGFP nanobody fused to the 5' end of the viral CP cistron (Figure 5A). In this case, unlike with ZYMV, we inserted the exogenous sequence without deleting any subsequent region of the CP coding sequence. In addition to the viral clone with the directly fused nanobody, we also built a derived viral clone including the self-cleaving F2A domain, based on the results obtained with ZYMV. *N. benthamiana* plants were agroinoculated with TEV-wt and the different recombinant clones (TEV-αGFP and TEV-αGFP-F2A).

Upper leaves of plants inoculated with TEV-wt showed typical symptoms of infection at 7 dpi, while plants inoculated with TEV-αGFP-F2A showed similar symptoms just 2 days later. Strikingly, unlike the results with ZYMV, the TEV-αGFP clone carrying the αGFP directly fused to the CP developed infection symptoms in the upper leaves at 11 dpi (Figure 5B). To analyze the outcome of the infection for each viral clone, we collected tissue from infected upper leaves at 14 dpi and evaluated the presence of the heterologous sequence corresponding to the αGFP nanobody in the viral progenies, using RT-PCR amplification followed by electrophoretic analysis. As expected, a 500-bp RT-PCR product was amplified from plants inoculated with TEV-wt (Figure 5C, lane 2). Accordingly, plants inoculated with TEV-αGFP and TEV-αGFP-F2A produced bands whose positions matched those expected for recombinant clones containing the αGFP fused sequence, without or with F2A, respectively (953 and 1028 bp; Figure 5C, lanes 3 and 4).

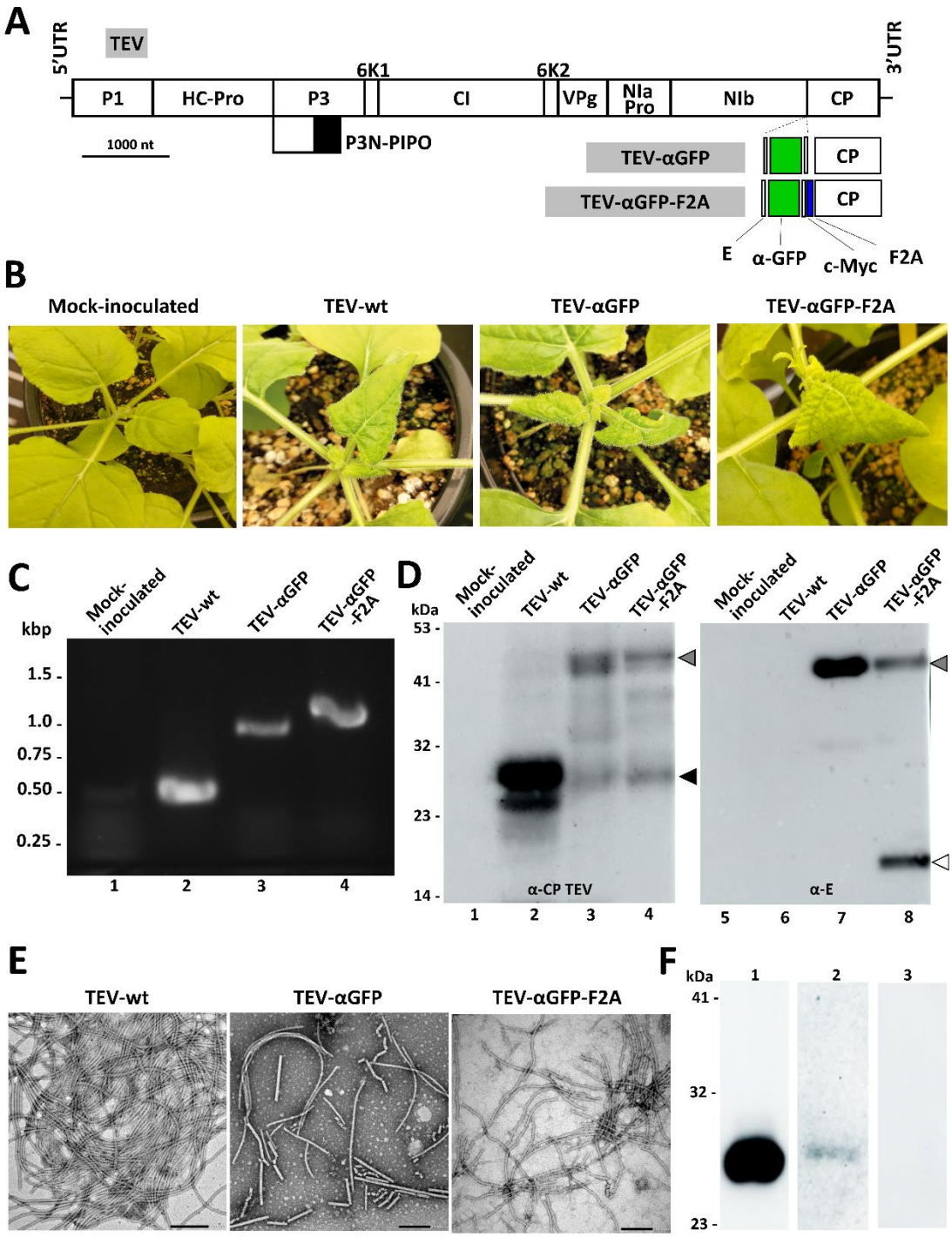

Figure 5. Production of TEV-derived nanoparticles decorated with a nanobody in biofactory plants. **(A)** Schematic representation of the TEV genome indicating the position where a heterologous sequence coding for an αGFP flanked with E and c-Myc epitopes was inserted with or without the picornavirus F2A peptide. Lines represent the TEV 5' and 3' UTRs; boxes represent the P1, HC-Pro, P3, P3N-PIPO, 6K1, CI, 6K2, VPg, NIaPro, NIb, and CP cistrons, as indicated. Scale bar corresponds to 1000 nt. **(B)** Pictures of representative upper leaves from *N. benthamiana* plants agroinoculated with TEV-wt, TEV-αGFP, and TEV-αGFP-F2A, as indicated, taken at 14 dpi. **(C)** RT-PCR analysis of the progeny of recombinant TEV inoculated into *N. benthamiana* plants. Representative samples from triplicate-inoculated plants are shown. Amplification products around the TEV CP region were separated by electrophoresis in an agarose gel, which was stained with ethidium bromide. DNA marker ladder with sizes (in

kbp) on the left; lane 1, mock-inoculated plant; lanes 2 to 4, plants agroinoculated with TEV-wt TEV-αGFP, and TEVΔ-αGFP-F2A, respectively. **(D)** Western blot analyses of protein extracts using antibodies against TEV CP (left panel) and the E epitope fused to the αGFP nanobody (right panel). Proteins were separated by SDS-PAGE and transferred to a membrane. Lane 1 and 5, mock-inoculated plant; lanes 2 and 6, plant agroinoculated with TEV-wt; lanes 3 and 7, plant agroinoculated with TEVΔ-αGFP; lanes 4 and 8, plant agroinoculated with TEVΔ-αGFP-F2A. The positions and sizes of protein standards are indicated on the left. Arrowheads indicates the positions of TEV CP (black), free αGFP (white), and the αGFP-F2A-CP fusion (gray). **(E)** TEM micrographs of purified TEV-wt, TEV-αGFP, and TEV-αGFP-F2A virions, as indicated. Scale bar indicates 200 nm. **(F)** Assays to evaluate the antigen-binding capacity of the TEV-derived VNP, with nanobodies against GFP by western blot. GFP was separated by SDS-PAGE by triplicate, and the proteins were transferred to a membrane. The first lane was incubated with a commercial anti GFP antibody conjugated to HRP; the second lane was incubated with virion preparations from plants infected with TEV-αGFP-F2A and a secondary α-E-HRP; the third lane was incubated only with the α-E-HRP antibody.

We next analyzed the accumulation of the CP and the fused αGFP by western blot assays, using a polyclonal antibody against TEV CP and a monoclonal antibody against the E tag, respectively. Reaction with the anti-TEV CP antibody produced a single band corresponding to the expected size (30 kDa), which was observed in the lane corresponding to the plant inoculated with TEV-wt (Figure 5D, lane 2, black arrowhead), while the plant inoculated with TEV-αGFP-F2A showed two bands with similar intensity whose sizes corresponded to the fused αGFP-F2A-CP (48 kDa) and the free CP (Figure 5D, lane 4, gray and black arrowheads, respectively). Interestingly, a similar two-band pattern was observed for the plant inoculated with TEV-αGFP, although the intensity of the fused-CP band (46 kDa) was stronger (Figure 5D, lane 3). This result, although striking, could reflect the presence of a small subpopulation of viral progeny that lost the inserted sequence or the partial in vivo proteolytic cleavage of the inserted polypeptide extension. Reaction with the anti-E antibody showed the presence of a band arising from a protein of the expected size for the αGFP and CPΔ fusion in the lanes corresponding to plants inoculated with TEV-αGFP and TEV-αGFP-F2A (Figure 5D, lanes 7 and 8, gray arrowhead). As expected, free αGFP nanobody was detected only in the last lane, as a result of the activity of the F2A peptide (Figure 5D, lane 8, white arrowhead).

Next, VNPs were purified from *N. benthamiana* plants agroinoculated with TEV-wt, TEV-αGFP, and TEV-αGFP-F2A at 14 dpi. TEV-wt VNPs were obtained with an estimated yield of 50 mg per kg of fresh infected tissue; recombinant VNPs yield decreased to around 5 and 10 mg per kg for TEV-αGFP and TEV-αGFP-F2A,

respectively. TEM analysis of virion preparations shows the presence in all cases of the elongated and flexuous viral nanoparticles, with a length of approximately 750 nm expected for TEV (Figure 5E). To finally analyze the functionality of the nanobodies, we ran an aliquot of purified recombinant GFP by SDS-PAGE and performed a western blot assay using the VNPs derived from TEV-αGFP-F2A as a primary antibody. The presence of the VNPs interacting with GFP in the transferred membrane was revealed using an anti-E antibody conjugated to HRP (Figure 5F, lane 2). As a positive control, we detected the presence of GFP with a commercial anti-GFP antibody conjugated to HRP (Figure 5F, lane 1), while the negative control lane was incubated only with anti-E-HRP (Figure 5F, lane 3). We successfully detected GFP using our αGFP-decorated VNP derived from TEV, showing that the CP-fused nanobodies are functional after virion assembly. These results indicate that agroinoculation of TEV recombinant clones coding for a CP-fused αGFP nanobody resulted in infections and the efficient production of VNPs carrying functional recombinant nanobodies.

4. DISCUSSION

Plant viruses-derived VNPs have been engineered to be used as vaccines or diagnostic reagents (Lico et al., 2015; Rybicki, 2020; Chung et al., 2021) as well to be used as carriers for drug delivery, targeted bioimaging and cancer immunotherapies (Shukla and Steinmetz, 2016; Chung et al., 2020). In these applications, virion shape plays a key role. For instance, elongated virions better accommodate large amounts of foreign genetic material; due to their higher aspect ratio, an elongated shape may present ligands more effectively than spherical counterparts. Furthermore, in clinical applications, rod filamentous viruses have better passive tumor homing, deeper tissue penetration, and more possibilities to resist immune detection and macrophage uptake than spherical counterparts (Bruckman et al., 2014; Shukla et al., 2015, 2020a). Strikingly, limited attention has been paid to potyviruses, the largest group of plant filamentous viruses. Nevertheless, viruses of this type are amenable to nanotechnology, as shown by recent reports on their genetic modification to expose epitopes on their surface, suggesting than these viruses may also have potential

biomedical applications (Sánchez et al., 2013; Yuste-Calvo et al., 2019; Frías-Sánchez et al., 2021).

Nanobodies have arisen in several fields, garnering outstanding interest as targeting molecules for bioimaging probes in cancer treatment and research (Oliveira et al., 2013), as therapeutics and diagnostic reagents against human diseases and pathogens (De Meyer et al., 2014; Wang et al., 2016, 2020), or in agriculture to mitigate the adverse effects of pesticide use (Ghannam et al., 2015; De Coninck et al., 2017; Hemmer et al., 2018). Nevertheless, nanobodies face several constraints: due to their small sizes, they are quickly eliminated from the bloodstream, and in some circumstances, their benefits must be enhanced by combined administration with other treatments (Salvador et al., 2019). The aim of this study was to produce genetically encoded VNPs derived from potyviruses as an alternative platform for nanobody display in plant biofactories. In this regard, the use of spherical VLPs for nanobody display has been reported by means of assembling recombinant fused capsids (Peyret et al., 2015). In contrast, in this study, we have functionalized the CP subunits of ZYMV and TEV to obtain flexuous rod-shaped biomaterials for nanobody presentation via genetic fusion. A nanobody against GFP was chosen as a proof of concept.

ZYMV is an important pathogen of cucurbits that reduces yields in some of the most important crops worldwide, such as squash, melon, or cucumbers (Gal-On, 2007; Simmons et al., 2013). So far, ZYMV has been used in biotechnology to produce antiviral and antitumor proteins or metabolites (Arazi et al., 2001b, 2002; Cordero et al., 2017; Majer et al., 2017), or to fortify zucchini fruits with carotenoids (Houhou et al., 2022). Furthermore, zucchini plants may be suitable biofactories due to their rapid growth rate and capacity for high biomass production over a short period of time, thereby facilitating production of a high amount of the desired product. By introducing selected epitopes at an appropriate position on the viral CP, VNPs are ideal scaffolds for their presentation. It has been reported that the ZYMV CP amino-terminal end is not necessary for infection and can even be partially replaced by a non-viral sequence (Arazi et al., 2001a). We decided to generate this shorter CP harboring a nanobody for its presentation. Potyvirus CP deletions and insertion of heterologous sequences at the carboxy-terminal end are unlikely to be viable due to the presence of RNA elements required for genome amplification in this region of the genome (Haldeman-Cahill et al.,

1998). First, we confirmed that having a truncated CP with thirty fewer amino acids from its amino terminal end was not an impediment for infection (Figure 2 and Figure 3). Conversely, the direct fusion of the nanobody to CP did not result in plants with infection symptoms. Although several peptides have been successfully presented in this way in other systems, the size of peptide fusions remains a limiting factor that can impair virus assembly. Thus far, the maximum epitope sequences that have been displayed as direct CP fusions on the particle surface have been 60 and 113 amino acid residues in length, respectively (Uhde-Holzem et al., 2016; Röder et al., 2018). In contrast, our αGFP nanobody flanked by the E and c-Myc tags consisted of 148 amino acids. In order to display larger sequences, the 2A splicing peptide from picornaviruses can be inserted between the polypeptide of interest and the CP (Uhde-Holzem et al., 2010; Kim et al., 2011; Dickmeis et al., 2015). Different picornaviral 2A peptides showed different cleavage efficiency in vivo in different cell lines and organisms (Kim et al., 2011). In this way, by using different 2A peptides, the degree of decoration of the viral nanoparticles can be modulated, thereby increasing the chances of obtaining viable viruses that accumulate at optimal concentrations. Among the different picornavirus 2A peptides, F2A exhibits less efficient *in vivo* cleavage (Kim et al., 2011); therefore a higher degree of VNP decoration is expected. Despite the expected outcome of not obtaining satisfactory results with the direct fusion of the nanobody to the CP, the addition of a 2A peptide allowed us to obtain partially decorated ZYMV VNPs. After purification, the morphology of ZYMVΔ-αGFP-F2A VNPs was assessed via TEM, and no differences were found between these and the ZYMVΔ or ZYMV-wt VNPs (Figure 4A). Later, we evaluated the binding efficacy of the ZYMVΔ-αGFP-F2A VNP to its antigen. Interestingly, we proved that these VNPs can bind GFP successfully (Figure 4), suggesting that potyvirus-derived nanoparticles were decorated with functional multivalent nanobodies.

Next, TEV was tested as a source of scaffolds for nanobody presentation. This potyvirus was chosen because it has traditionally been used as a model for RNA viruses research (Bedoya et al., 2012) and because we have extensively exploited it as a biotechnological tool previously (Bedoya and Daròs, 2010; Majer et al., 2017; Martí et al., 2020; Uranga et al., 2021b). Furthermore, in contrast to most of the ZYMV strains (Gal-On, 2007; Cordero et al., 2017), TEV much more effectively infects *N.*

benthamiana, which can be grown at high density in a matter of weeks and is the workhorse plant for excellence in plant molecular farming (Peyret and Lomonossoff, 2015). Interestingly, in this case, assembly was not compromised by the direct fusion of the nanobody to the TEV CP (Figure 5). Despite TEV-αGFP not carrying the F2A peptide, a slight band with a size corresponding to the free CP was also detected by Western blot in some samples (Figure 5D). On the one hand, this could reflect the presence of a small subpopulation in the viral progeny that lost the inserted sequence. On the other hand, free CP could also result from *in vivo* cleavage of some of protruding nanobodies, as previously proposed for PVX-derived VNPs (Röder et al., 2018). To shed some light on this, future work on time-course analysis of viral vector progeny would inform about insert stability and would help to optimize harvest time. All in all, although it may facilitate virus amplification and probably increase the viral load in the plant, the inclusion of the F2A peptide does not seem to be a necessary requirement for assembly of TEV-derived VNPs decorated with nanobodies.

The results presented in this study should allow us to extend and develop a set of plant VNPs for nanobody presentation. In order to avoid severe off-target effects of systemic drugs in medicine, several efforts are being made to develop targeted therapy using VNPs, in which drugs are either delivered specifically to tumor cells or activated specifically within them (Chung et al., 2020; Shukla et al., 2020a; Thuenemann et al., 2021). Therefore, further attempts in this area will involve the presentation of nanobodies with medicinal value. In addition, nanobodies presented on multivalent nanoparticles could improve the diagnosis and treatment of diseases. In summary, we report on genetically encoded potyvirus-derived VNPs used as scaffolds for nanobody presentation. This study sets the framework for the development of new tools derived from plant VNPs as nanomaterials useful in medicine or in other fields, according to the nanobodies of interest used.

DATA AVAILABILITY STATEMENT

The original contributions presented in the study are included in the article/supplementary material, further inquiries can be directed to the corresponding author/s.

FUNDING

This research was supported by grant PID2020-114691RB-I00 from the Ministerio de Ciencia e Innovación (Spain; co-financed by the European Region Development Fund) through the Agencia Estatal de Investigación. M.M. is the recipient of a predoctoral contract (FPU16/05294) from the Ministerio de Educación, Cultura y Deporte (Spain).

ACKNOWLEDGEMENTS

We thank Dr. Luis Ángel Fernández (CNB, CSIC, Madrid, Spain) for kindly providing us the αGFP nanobody cDNA.

CONFLICT OF INTEREST

The authors declare that the research was conducted in the absence of any commercial or financial relationships that could be construed as a potential conflict of interest.

REFERENCES

Adams, M.J., Antoniw, J.F., Beaudoin, F., 2005. Overview and analysis of the polyprotein cleavage sites in the family Potyviridae . Mol. Plant Pathol. 6, 471–487.

Alemzadeh, E., Dehshahri, A., Izadpanah, K., Ahmadi, F., 2018. Plant virus nanoparticles: Novel and robust nanocarriers for drug delivery and imaging. Colloids Surfaces B Biointerfaces 167, 20–27. https://doi.org/10.1016/j.colsurfb.2018.03.026

Arazi, T., Shiboleth, Y.M., Gal-On, A., 2001a. A nonviral peptide can replace the entire N terminus of zucchini yellow mosaic potyvirus coat protein and permits viral systemic infection. J. Virol. 75, 6329–6336. https://doi.org/10.1128/JVI.75.14.6329-6336.2001

Arazi, T., Shiboleth, Y.M., Lee Huang, P., Huang, P.L., Zhang, L., Lee-Huang, S., Gal-On, A., 2002. Production of antiviral and antitumor proteins MAP30 and GAP31 in cucurbits using the plant virus vector ZYMV-AGII. Biochem. Biophys. Res. Commun. 292, 441–448. https://doi.org/10.1006/bbrc.2002.6653

Arazi, T., Slutsky, S.G., Shiboleth, Y.M., Wang, Y., Rubinstein, M., Barak, S., Yang, J., Gal-On, A., 2001b. Engineering zucchini yellow mosaic potyvirus as a non-pathogenic vector for expression of heterologous proteins in cucurbits. J. Biotechnol. 87, 67–82. https://doi.org/10.1016/S0168-1656(01)00229-2

Bally, J., Jung, H., Mortimer, C., Naim, F., Philips, J.G., Hellens, R., Bombarely, A., Goodin, M.M., Waterhouse, P.M., 2018. The Rise and Rise of Nicotiana benthamiana : A Plant for All Reasons.

Beatty, P.H., Lewis, J.D., 2019. Cowpea mosaic virus nanoparticles for cancer imaging and therapy. Adv.

Drug Deliv. Rev. 145, 130–144. https://doi.org/10.1016/j.addr.2019.04.005
Bedoya, L., Martínez, F., Rubio, L., Daròs, J.A., 2010. Simultaneous equimolar expression of multiple proteins in plants from a disarmed potyvirus vector. J. Biotechnol. 150, 268–275. https://doi.org/10.1016/j.jbiotec.2010.08.006
Bedoya, L.C., Daròs, J.A., 2010. Stability of Tobacco etch virus infectious clones in plasmid vectors. Virus Res. 149, 234–240. https://doi.org/10.1016/j.virusres.2010.02.004
Bedoya, L.C., Martínez, F., Orzáez, D., Daròs, J.A., 2012. Visual tracking of plant virus infection and movement using a reporter MYB transcription factor that activates anthocyanin biosynthesis. Plant Physiol. 158, 1130–1138. https://doi.org/10.1104/pp.111.192922
Bruckman, M.A., Randolph, L.N., VanMeter, A., Hern, S., Shoffstall, A.J., Taurog, R.E., Steinmetz, N.F., 2014. Biodistribution, pharmacokinetics, and blood compatibility of native and PEGylated tobacco mosaic virus nano-rods and -spheres in mice. Virology 449, 163–173. https://doi.org/10.1016/j.virol.2013.10.035
Castells-Graells, R., Lomonossoff, G.P., Saunders, K., 2018. Production of mosaic turnip crinkle virus-like particles derived by coinfiltration of wild-type and modified forms of virus coat protein in plants. Methods Mol. Biol. 1776, 3–17. https://doi.org/10.1007/978-1-4939-7808-3_1
Chen, Q., 2022. Development of plant-made monoclonal antibodies against viral infections. Curr. Opin. Virol. 52, 148–160. https://doi.org/10.1016/j.coviro.2021.12.005
Chung, Y.H., Cai, H., Steinmetz, N.F., 2020. Viral nanoparticles for drug delivery, imaging, immunotherapy, and theranostic applications. Adv. Drug Deliv. Rev. 156, 214–235.
Chung, Y.H., Church, D., Koellhoffer, E.C., Osota, E., Shukla, S., Rybicki, E.P., Pokorski, J.K., Steinmetz, N.F., 2021. Integrating plant molecular farming and materials research for next-generation vaccines. Nat. Rev. Mater. https://doi.org/10.1038/s41578-021-00399-5
Cordero, T., Cerdan, L., Carbonell, A., Katsarou, K., Kalantidis, K., Daròs, J.A., 2017. Dicer-like 4 is involved in restricting the systemic movement of zucchini yellow mosaic virus in nicotiana benthamiana. Mol. Plant-Microbe Interact. 30, 63–71. https://doi.org/10.1094/MPMI-11-16-0239-R
Cordero, T., Rosado, A., Majer, E., Jaramillo, A., Rodrigo, G., Daròs, J.A., 2018. Boolean Computation in Plants Using Post-translational Genetic Control and a Visual Output Signal. ACS Synth. Biol. 7, 2322–2330. https://doi.org/10.1021/acssynbio.8b00214
Cruz, S.S., Chapman, S., Roberts, A.G., Roberts, I.M., Prior, D.A.M., Oparka, K.J., 1996. Assembly and movement of a plant virus carrying a green fluorescent protein overcoat. Proc. Natl. Acad. Sci. U. S. A. 93, 6286–6290. https://doi.org/10.1073/pnas.93.13.6286
De Coninck, B., Verheesen, P., Vos, C.M., Van Daele, I., De Bolle, M.F., Vieira, J. V., Peferoen, M., Cammue, B.P.A., Thevissen, K., 2017. Fungal glucosylceramide-specific camelid single domain antibodies are characterized by broad spectrum antifungal activity. Front. Microbiol. 8, 1–10. https://doi.org/10.3389/fmicb.2017.01059
De Meyer, T., Muyldermans, S., Depicker, A., 2014. Nanobody-based products as research and diagnostic tools. Trends Biotechnol. 32, 263–270. https://doi.org/10.1016/j.tibtech.2014.03.001
Dickmeis, C., Honickel, M.M.A., Fischer, R., Commandeur, U., 2015. Production of hybrid chimeric PVX particles using a combination of TMV and PVX-based expression vectors. Front. Bioeng. Biotechnol. 3, 1–12. https://doi.org/10.3389/fbioe.2015.00189
Donini, M., Marusic, C., 2019. Current state-of-the-art in plant-based antibody production systems. Biotechnol. Lett. 41, 335–346. https://doi.org/10.1007/s10529-019-02651-z
Edgue, G., Twyman, R.M., Beiss, V., Fischer, R., Sack, M., 2017. Antibodies from plants for bionanomaterials. Wiley Interdiscip. Rev. Nanomedicine Nanobiotechnology 9. https://doi.org/10.1002/wnan.1462
Fernandez, M.R., Martínez-torrecuadrada, J.L., Roncal, F., Domínguez, E., García, J.A., 2002. Identification of Immunogenic Hot Spots within Plum Pox Potyvirus Capsid Protein for Efficient Antigen Presentation 76, 12646–12653. https://doi.org/10.1128/JVI.76.24.12646
Frías-Sánchez, A.I., Quevedo-Moreno, D.A., Samandari, M., Tavares-Negrete, J.A., Sánchez-Rodríguez,

V.H., González-Gamboa, I., Ponz, F., Alvarez, M.M., Trujillo-De Santiago, G., 2021. Biofabrication of muscle fibers enhanced with plant viral nanoparticles using surface chaotic flows. Biofabrication 13. https://doi.org/10.1088/1758-5090/abd9d7

Gal-On, A., 2007. Zucchini yellow mosaic virus: Insect transmission and pathogenicity - The tails of two proteins: Pathogen profile. Mol. Plant Pathol. 8, 139–150. https://doi.org/10.1111/j.1364-3703.2007.00381.x

Ghannam, A., Kumari, S., Muyldermans, S., Abbady, A.Q., 2015. Camelid nanobodies with high affinity for broad bean mottle virus: a possible promising tool to immunomodulate plant resistance against viruses. Plant Mol. Biol. 87, 355–369. https://doi.org/10.1007/s11103-015-0282-5

Gibson, D.G., Young, L., Chuang, R.-Y., Venter, J.C., Hutchison III, C.A., Smith, H.O., 2009. Enzymatic assembly of DNA molecules up to several hundred kilobases. Nat. Methods 6, 343–345. https://doi.org/10.1038/nmeth.1318

Giritch, A., Marillonnet, S., Engler, C., Van Eldik, G., Botterman, J., Klimyuk, V., Gleba, Y., 2006. Rapid high-yield expression of full-size IgG antibodies in plants coinfected with noncompeting viral vectros. Proc. Natl. Acad. Sci. U. S. A. 103, 14701–14706. https://doi.org/10.1073/pnas.0606631103

González-Gamboa, I., Manrique, P., Manrique, P., Ponz, F., 2017. Plant-made potyvirus-like particles used for log-increasing antibody sensing capacity. J. Biotechnol. 254, 17–24. https://doi.org/10.1016/j.jbiotec.2017.06.014

Goulet, M.C., Gaudreau, L., Gagné, M., Maltais, A.M., Laliberté, A.C., Éthier, G., Bechtold, N., Martel, M., D'Aoust, M.A., Gosselin, A., Pepin, S., Michaud, D., 2019. Production of biopharmaceuticals in Nicotiana benthamiana—axillary stem growth as a key determinant of total protein yield. Front. Plant Sci. 10, 735. https://doi.org/10.3389/fpls.2019.00735

Haldeman-Cahill, R., Daròs, J.-A., Carrington, J.C., 1998. Secondary Structures in the Capsid Protein Coding Sequence and 3′ Nontranslated Region Involved in Amplification of the Tobacco Etch Virus Genome. J. Virol. 72, 4072–4079. https://doi.org/10.1128/jvi.72.5.4072-4079.1998

Hemmer, C., Djennane, S., Ackerer, L., Hleibieh, K., Marmonier, A., Gersch, S., Garcia, S., Vigne, E., Komar, V., Perrin, M., Gertz, C., Belval, L., Berthold, F., Monsion, B., Schmitt-Keichinger, C., Lemaire, O., Lorber, B., Gutiérrez, C., Muyldermans, S., Demangeat, G., Ritzenthaler, C., 2018. Nanobody-mediated resistance to Grapevine fanleaf virus in plants. Plant Biotechnol. J. 16, 660–671. https://doi.org/10.1111/pbi.12819

Houhou, F., Martí, M., Cordero, T., Aragonés, V., Sáez, C., Cebolla-Cornejo, J., Castro, A.P., Rodríguez-Concepción, M., Picó, B., Daròs, J., 2022. Carotenoid fortification of zucchini fruits using a viral RNA vector. Biotechnol. J. 2100328. https://doi.org/10.1002/biot.202100328

Juarez, P., Virdi, V., Depicker, A., Orzaez, D., 2016. Biomanufacturing of protective antibodies and other therapeutics in edible plant tissues for oral applications. Plant Biotechnol. J. 14, 1791–1799. https://doi.org/10.1111/pbi.12541

Julve Parreño, J., Huet, E., Fernández-del-Carmen, A., Segura, A., Micol, V., Gandia, A., Pan, W., Albaladejo, I., Forment, J., Pla, D., Wigdorovitz, A., Calvete, J., Gutierrez, J., Granell, A., Orzaez, D., 2018. A synthetic biology approach for consistent production of plant-made recombinant polyclonal antibodies against snake venom toxins. Plant Biotechnol. J. 16, 727–736. https://doi.org/10.1111/pbi.12823

Kelloniemi, J., Mäkinen, K., Valkonen, J.P.T., 2008. Three heterologous proteins simultaneously expressed from a chimeric potyvirus: Infectivity, stability and the correlation of genome and virion lengths. Virus Res. 135, 282–291. https://doi.org/10.1016/j.virusres.2008.04.006

Kim, J.H., Lee, S.R., Li, L.H., Park, H.J., Park, J.H., Lee, K.Y., Kim, M.K., Shin, B.A., Choi, S.Y., 2011. High cleavage efficiency of a 2A peptide derived from porcine teschovirus-1 in human cell lines, zebrafish and mice. PLoS One 6, 1–8. https://doi.org/10.1371/journal.pone.0018556

Le, D.H.T., Commandeur, U., Steinmetz, N.F., 2019. Presentation and delivery of tumor necrosis factor-related apoptosis-inducing ligand via elongated plant viral nanoparticle enhances antitumor

efficacy. ACS Nano 13, 2501–2510. https://doi.org/10.1021/acsnano.8b09462
Lico, C., Benvenuto, E., Baschieri, S., 2015. The two-faced potato virus X: From plant pathogen to smart nanoparticle. Front. Plant Sci. 6, 1–8. https://doi.org/10.3389/fpls.2015.01009
Lomonossoff, G.P. and, Wege, C., 2020. TMV Particles: The Journey From Fundamental Studies to Bionanotechnology Applications. Adv. Virus Res. 102.
Lomonossoff, G.P., D'Aoust, M.A., 2016. Plant-produced biopharmaceuticals: A case of technical developments driving clinical deployment. Science (80-.). https://doi.org/10.1126/science.aaf6638
Maia Malaquias, A., Carlos Marques, L., Pereira, S.S., Freitas, C. De, Maranh, A.Q., Stabeli, R.G., Orlando, E., Tramontina, P., Izabel, M., Guedes, F., Freire, C., Fernandes, C., 2021. A review of plant-based expression systems as a platform for single-domain recombinant antibody production. Int. J. Biol. Macromol. 193, 1130–1137. https://doi.org/10.1016/j.ijbiomac.2021.10.126
Majer, E., Llorente, B., Rodríguez-Concepción, M., Daròs, J.A., 2017. Rewiring carotenoid biosynthesis in plants using a viral vector. Sci. Rep. 7, 1–10. https://doi.org/10.1038/srep41645
Majer, E., Navarro, J.A., Daròs, J.A., 2015. A potyvirus vector efficiently targets recombinant proteins to chloroplasts, mitochondria and nuclei in plant cells when expressed at the amino terminus of the polyprotein. Biotechnol. J. 10, 1792–1802. https://doi.org/10.1002/biot.201500042
Manuel-cabrera, C.A., Vallejo-cardona, A.A., Padilla-camberos, E., Hernández-gutiérrez, R., Herrera-rodríguez, S.E., Gutiérrez-ortega, A., 2016. Self-assembly of hexahistidine-tagged tobacco etch virus capsid protein into microfilaments that induce IgG2-specific response against a soluble porcine reproductive and respiratory syndrome virus chimeric protein. Virol. J. 1–6. https://doi.org/10.1186/s12985-016-0651-y
Marsian, J., Lomonossoff, G.P., 2016. Molecular pharming-VLPs made in plants. Curr. Opin. Biotechnol. 37, 201–206. https://doi.org/10.1016/j.copbio.2015.12.007
Martí, M., Diretto, G., Aragonés, V., Frusciante, S., Ahrazem, O., Gómez-Gómez, L., Daròs, J.A., 2020. Efficient production of saffron crocins and picrocrocin in Nicotiana benthamiana using a virus-driven system. Metab. Eng. 61, 238–250. https://doi.org/10.1016/j.ymben.2020.06.009
Mitchell, L.S., Colwell, L.J., 2018. Comparative analysis of nanobody sequence and structure data 697–706. https://doi.org/10.1002/prot.25497
Muyldermans, S., 2013. Nanobodies: Natural Single-Domain Antibodies. Annu. Rev. Biochem. 82, 775–797. https://doi.org/10.1146/annurev-biochem-063011-092449
Oliveira, S., Heukers, R., Sornkom, J., Kok, R.J., Van Bergen En Henegouwen, P.M.P., 2013. Targeting tumors with nanobodies for cancer imaging and therapy. J. Control. Release 172, 607–617. https://doi.org/10.1016/j.jconrel.2013.08.298
Ortega-Rivera, O.A., Shukla, S., Shin, M.D., Chen, A., Beiss, V., Moreno-Gonzalez, M.A., Zheng, Y., Clark, A.E., Carlin, A.F., Pokorski, J.K., Steinmetz, N.F., 2021. Cowpea Mosaic Virus Nanoparticle Vaccine Candidates Displaying Peptide Epitopes Can Neutralize the Severe Acute Respiratory Syndrome Coronavirus. ACS Infect. Dis. 7, 3096–3110. https://doi.org/10.1021/acsinfecdis.1c00410
Peyret, H., Gehin, A., Thuenemann, E.C., Blond, D., El Turabi, A., Beales, L., Clarke, D., Gilbert, R.J.C., Fry, E.E., Stuart, D.I., Holmes, K., Stonehouse, N.J., Whelan, M., Rosenberg, W., Lomonossoff, G.P., Rowlands, D.J., 2015. Tandem fusion of hepatitis B core antigen allows assembly of virus-like particles in bacteria and plants with enhanced capacity to accommodate foreign proteins. PLoS One 10, 1–20. https://doi.org/10.1371/journal.pone.0120751
Peyret, H., Lomonossoff, G.P., 2015. When plant virology met Agrobacterium: The rise of the deconstructed clones. Plant Biotechnol. J. 13, 1121–1135. https://doi.org/10.1111/pbi.12412
Peyret, H., Steele, J.F.C., Jung, J.W., Thuenemann, E.C., Meshcheriakova, Y., Lomonossoff, G.P., 2021. Producing vaccines against enveloped viruses in plants: Making the impossible, difficult. Vaccines 9. https://doi.org/10.3390/vaccines9070780
Revers, F., García, J.A., 2015. Molecular biology of potyviruses. Adv. Virus Res. 92, 101–199. https://doi.org/10.1016/bs.aivir.2014.11.006
Röder, J., Dickmeis, C., Commandeur, U., 2019. Small, smaller, nano: New applications for potato virus

X in nanotechnology. Front. Plant Sci. https://doi.org/10.3389/fpls.2019.00158

Röder, J., Dickmeis, C., Fischer, R., Commandeur, U., 2018. Systemic Infection of Nicotiana benthamiana with Potato virus X Nanoparticles Presenting a Fluorescent iLOV Polypeptide Fused Directly to the Coat Protein. Biomed Res. Int. 2018. https://doi.org/10.1155/2018/9328671

Röder, J., Fischer, R., Commandeur, U., 2017. Adoption of the 2A Ribosomal skip principle to tobacco mosaic virus for peptide display. Front. Plant Sci. 8, 1–11. https://doi.org/10.3389/fpls.2017.01125

Rybicki, E.P., 2020. Plant molecular farming of virus-like nanoparticles as vaccines and reagents. Wiley Interdiscip. Rev. Nanomedicine Nanobiotechnology 12, 1–22. https://doi.org/10.1002/wnan.1587

Sainsbury, F., Cañizares, M.C., Lomonossoff, G.P., 2010. Cowpea mosaic virus: The plant virus-based biotechnology workhorse. Annu. Rev. Phytopathol. 48, 437–455. https://doi.org/10.1146/annurev-phyto-073009-114242

Salema, V., Marín, E., Martínez-Arteaga, R., Ruano-Gallego, D., Fraile, S., Margolles, Y., Teira, X., Gutierrez, C., Bodelón, G., Fernández, L.A., 2013. Selection of single domain antibodies from immune libraries displayed on the surface of E. coli cells with two b-domains of opposite topologies. PLoS One 8, e75126. https://doi.org/10.1371/journal.pone.0075126

Salvador, J.P., Vilaplana, L., Marco, M.P., 2019. Nanobody: outstanding features for diagnostic and therapeutic applications. Anal. Bioanal. Chem. 411, 1703–1713. https://doi.org/10.1007/s00216-019-01633-4

Sánchez, F., Sáez, M., Lunello, P., Ponz, F., 2013. Plant viral elongated nanoparticles modified for log-increases of foreign peptide immunogenicity and specific antibody detection. J. Biotechnol. 168, 409–415. https://doi.org/10.1016/j.jbiotec.2013.09.002

Satheeshkumar, P.K., 2020. Expression of Single Chain Variable Fragment (scFv) Molecules in Plants : A Comprehensive Update. Mol. Biotechnol. 62, 151–167. https://doi.org/10.1007/s12033-020-00241-3

Schmidt, T.G., Batz, L., Bonet, L., Carl, U., Holzapfel, G., Kiem, K., Matulewicz, K., Niermeier, D., Schuchardt, I., Stanar, K., 2013. Development of the Twin-Strep-tag(R) and its application for purification of recombinant proteins from cell culture supernatants. Protein. Expr. Purif. 92, 54–61. https://doi.org/10.1016/j.pep.2013.08.021

Shukla, S., DiFranco, N.A., Wen, A.M., Commandeur, U., Steinmetz, N.F., 2015. To Target or Not to Target: Active vs. Passive Tumor Homing of Filamentous Nanoparticles Based on Potato virus X. Cell. Mol. Bioeng. 8, 433–444. https://doi.org/10.1007/s12195-015-0388-5

Shukla, S., Hu, H., Cai, H., Chan, S.K., Boone, C.E., Beiss, V., Chariou, P.L., Steinmetz, N.F., 2020a. Plant Viruses and Bacteriophage-Based Reagents for Diagnosis and Therapy. Annu. Rev. Virol. 7, 559–587. https://doi.org/10.1146/annurev-virology-010720-052252

Shukla, S., Roe, A.J., Liu, R., Veliz, F.A., Commandeur, U., Wald, D.N., Steinmetz, N.F., 2020b. Affinity of plant viral nanoparticle potato virus X (PVX) towards malignant B cells enables cancer drug delivery. Biomater. Sci. 8, 3935–3943. https://doi.org/10.1039/d0bm00683a

Shukla, S., Steinmetz, N.F., 2016. Emerging nanotechnologies for cancer immunotherapy. Exp. Biol. Med. 241, 1116–1126. https://doi.org/10.1177/1535370216647123

Simmons, H.E., Dunham, J.P., Zinn, K.E., Munkvold, G.P., Holmes, E.C., Stephenson, A.G., 2013. Zucchini yellow mosaic virus (ZYMV, Potyvirus): Vertical transmission, seed infection and cryptic infections. Virus Res. 176, 259–264. https://doi.org/10.1016/j.virusres.2013.06.016

Smolenska, L., Roberts, I.M., Learmonth, D., Porter, A.J., Harris, W.J., Wilson, T.M.A., Santa Cruz, S., 1998. Production of a functional single chain antibody attached to the surface of a plant virus. FEBS Lett. 441, 379–382. https://doi.org/10.1016/S0014-5793(98)01586-5

Stander, J., Chabeda, A., Rybicki, E.P., Meyers, A.E., 2021. A Plant-Produced Virus-Like Particle Displaying Envelope Protein Domain III Elicits an Immune Response Against West Nile Virus in Mice. Front. Plant Sci. 12, 1–12. https://doi.org/10.3389/fpls.2021.738619

Steele, J.F.C., Peyret, H., Saunders, K., Castells-Graells, R., Marsian, J., Meshcheriakova, Y., Lomonossoff, G.P., 2017. Synthetic plant virology for nanobiotechnology and nanomedicine. Wiley

Interdiscip. Rev. Nanomedicine Nanobiotechnology 9, 1–18. https://doi.org/10.1002/wnan.1447
Steinmetz, N.F., Manchester, M., 2016. Viral nanoparticles: Tools for materials science and biomedicine, in: Handbook of Clinical Nanomedicine: Nanoparticles, Imaging, Therapy and Clinical Applications. Pan Stanford Publishing Pte. Ltd., Singapore, pp. 641–656. https://doi.org/10.4032/9789814669214
Thole, V., Worland, B., Snape, J.W., Vain, P., 2007. The pCLEAN dual binary vector system for Agrobacterium-mediated plant transformation. Plant Physiol. 145, 1211–1219. https://doi.org/10.1104/pp.107.108563
Thuenemann, E.C., Le, D.H.T., Lomonossoff, G.P., Steinmetz, N.F., 2021. Bluetongue Virus Particles as Nanoreactors for Enzyme Delivery and Cancer Therapy. Mol. Pharm. 18, 1150–1156. https://doi.org/10.1021/acs.molpharmaceut.0c01053
Tusé, D., Mcdonald, K.A., Buyel, J.F., Buyel, J.F., 2020. The Emergency Response Capacity of Plant-Based Biopharmaceutical Manufacturing-What It Is and What It Could Be Screening of Product Candidates. Front. Plant Sci. 11. https://doi.org/10.3389/fpls.2020.594019
Uhde-holzem, K., Mcburney, M., Tiu, B.D.B., Advincula, R.C., Fischer, R., Commandeur, U., Steinmetz, N.F., 2016. Production of Immunoabsorbent Nanoparticles by Displaying Single-Domain Protein A on Potato Virus X a 231–241. https://doi.org/10.1002/mabi.201500280
Uhde-Holzem, K., Schlösser, V., Viazov, S., Fischer, R., Commandeur, U., 2010. Immunogenic properties of chimeric potato virus X particles displaying the hepatitis C virus hypervariable region I peptide R9. J. Virol. Methods 166, 12–20. https://doi.org/10.1016/j.jviromet.2010.01.017
Uranga, M., Aragonés, V., Selma, S., Vázquez-Vilar, M., Orzáez, D., Daròs, J.A., 2021a. Efficient Cas9 multiplex editing using unspaced sgRNA arrays engineering in a Potato virus X vector. Plant J. 106, 555–565. https://doi.org/10.1111/tpj.15164
Uranga, M., Vazquez-Vilar, M., Orzáez, Di., Daròs, J.A., 2021b. CRISPR-Cas12a Genome Editing at the Whole-Plant Level Using Two Compatible RNA Virus Vectors. Cris. J. 4, 761–769. https://doi.org/10.1089/crispr.2021.0049
Wang, M., Gao, S., Zeng, W., Yang, Y., Ma, J., Wang, Y., 2020. Plant Virology Delivers Diverse Toolsets for Biotechnology. Viruses 12, 1–16. https://doi.org/10.3390/v12111338
Wang, W., Yuan, J., Jiang, C., 2021. Applications of nanobodies in plant science and biotechnology. Plant Mol. Biol. 105, 43–53. https://doi.org/10.1007/s11103-020-01082-z
Wang, Y., Fan, Z., Shao, L., Kong, X., Hou, X., Tian, D., Sun, Y., Xiao, Y., Yu, L., 2016. Nanobody-derived nanobiotechnology tool kits for diverse biomedical and biotechnology applications. Int. J. Nanomedicine 11, 3287–3303. https://doi.org/10.2147/IJN.S107194
Yusibov, V., Kushnir, N., Streatfield, S.J., 2016. Antibody Production in Plants and Green Algae. Annu. Rev. Plant Biol. 67, 669–701. https://doi.org/10.1146/annurev-arplant-043015-111812
Yuste-Calvo, C., López-Santalla, M., Zurita, L., Cruz-Fernández, C.F., Sánchez, F., Garín, M.I., Ponz, F., 2019. Elongated flexuous plant virus-derived nanoparticles functionalized for autoantibody detection. Nanomaterials 9, 1–13. https://doi.org/10.3390/nano9101438.

SUPPLEMENTARY MATERIAL

Figure S1. Nucleotide sequences of ZYMV-wt (GenBank accession number KX499498) and the derived recombinant viruses ZYMVΔ, -αGFP, and αGFP-F2A. The boundaries of viral cistrons are indicated on blue background. **Start** and **stop** codons are underlined. Heterologous sequences were inserted between nucleotide positions **8550** and **8642** (underlined). cDNAs corresponding to the anti-green fluorescent protein (αGFP) nanobody, and picornavirus **F2A** peptides are in green and blue, respectively.

>ZYMV-wt
AAATTAAAACAAATCACAAAGACTACAGAAATCAACGAACAAACAAACGAATTTTAAACCGTGTTAACAAACAAG
CAATTTATAATTCGCACAGCATCAAGAATTTCTGCAATCATTTTGTTTATTTTAGACACAACAATGGCCTCAGTT
ATGATTGGTTCAATCTCCGTACCCATCGCACAGCCTGCGCAGTGTGCAAACACCCAAGCGAGCAACCGGGTTAAC
GTAGTGGCACCTGGCCACATGGCAACATGCCCACCATCATTGAAAACGCACACATACTACATGCATGAGTCTAAG
AAGTTGATAAATTCAGATAAAAGCAATGAAATTTTGAACAATTTCTTTAACACTGATGAGATGAAATTCGCGCTC
ACTAGGAATGAAATGAGTAAGGTGAAAAAGGGTCCGAATGGGAGGGTAGTTCTTCGCAAACCGAGCAAGCAGCGG
GTTTTCGCTCGGATCGAGCAGGATGAGGCAGCACGCAAGGAAGAAGCTGTTTTCCTTGCAGGAAATTATGATGGT
TCGATCACAAATCTAGTGAGTGTTCTTCCATCTGAAATGACTCGCGATGTTGATGCGAGTTTGCGATCACCATTT
TACAAGCGCACATATAAGAAGGACAGAAAGAAAGTGGCGCAAAAGCAAATCGCGCAGGCACCACTTAACAGCTTG
TGCACACGTGTTCTTAAAATTGCGCGCAATAGAAACATCCCTGTTGAGATAATTGGCAACAAGAAAGCAAGACAT
ACACTTACCTTCAAGAGGTTTAGGGGATGTTTTGTTGGAAAGGTGTCAGTTGCACATGAGGAAGGACGAATGCAA
CACACTGAGATATCATACGAGCAGTTTGAATGGATTCTACAAGCTATTTGTCGGGTTACTTATACAGAGCGAATT
CGTGAGGAAGACATTAAACCAGGTTGTAGTGGGTGGGTGTTAGGCACTGATCATACATTGACCAAGAGATATTCA
AGATTGCCACATCTGGTAATTCGAGGTAGAGATGATGACGGGATTGTGAACGCGCTGGAACCGGTGTTATTTTAC
AGCGAAGTTGACCACTATTCGTCGCAACCGGAAGTTCAGTTCTTCCAAGGATGGCGACGAATGTTCGACAAGTTT
AGACCCAGTCCAGATCATGTGTGCAAAGTTGATCACAACAATGAGGAGTGTGGTGAGTTAGCAGCAATCTTTTGT
CAGGCTTTGTTCCCAGTAGTGAAATTATCGTGCCAAACATGCAGAGAAAAGCTTAGTAGAGTTAGCTTCGAGGAA
TTCAAAGATTCTTTGAATACAAACTTTATTATCCATAAGGACGAATGGGATAGTTTCAAAGAGGGCTCTCATTAC
GATAATATTTTCAAATTAATTAAAGTAGCAACACAGGTAACTCAGAATCTCAAGCTCTCATCTGAAGTAATGAAG
TTAGTTCAGAACCACACAAGCACTCACATGAAGCAAATACAAGATATCAACAAGGCGCTCATGAAAGGTTCATTG
GTTACGCAAGACGAATTGGACTTGGCTTTGAAACAGCTTCTAGAAATGACTCAGTGGTTTAAGAACCACATGCAC
CTGACTGGTGAAGAAGCATTGAAGATGTTCAGAAACAAGCGCTCTAGCAAGGCTATGATAAATCCTAACCTTTTA
TGTGATAACCAGTTGGACAAAAATGGAAACTTTGTCTGGGGAGAAAGAGGATATCATTCCAAGCGATTATTCAAG
AACTTCTTTGAGGAAGTTATACCAAGTGAAGGATATACGAAATACGTAGTGCGAAACTTCCCAAATGGTACTCGT
AAGTTGGCCATAGGCTCATTGATCGTACCACTCAACTTGGATAGGGCACGCACTGCACTCCTTGGAGAGAGTATT
GAGAAGAAGCCACTCACATCAGCATGTGTCTCCCAACAGAATGGAAATTATATACACTCATGCTGCTGTGTGACG
ATGGATGATGGAACTCCGATGTACTCAGAGCTTAAGAGCCCGACGAAGAGACATCTAGTTATAGGAGCTTCTGGT
GATCCAAAGTACATTGATTTACCAGCATCTGAGGCAGAACGCATGTATATAGCAAAGGAAGGTTATTGCTATCTT
AACATTTTTCTCGCAATGCTTGTGAATGTTAATGAGAACGAGGCAAAGGATTTCACCAAAATGATTCGTGATGTT
TTGATCCCTATGCTTGGGCAATGGCCTTCGTTGATGGATGTCGCGACTGCAGCATACATTTTAGGTGTATTCCAT
CCTGAAACGCGATGCGCTGAATTACCTAGGATTCTTGTTGACCATGCTACGCAAACCATGCATGTCATTGATTCA
TATGGATCATTAACTGTTGGTTATCACGTGCTCAAGGCCGGAACTGTCAATCATTTAATTCAATTTGCCTCAAAT
GATCTGCAGAGCGAGATGAAGCATTACAGAGTCGGCGGAACGCCAACACAGCGCATAAAACTTGAGGAGCAATTG
ATTAAAGGAATCTTCAAACCAAAACTTATGATGCAGCTCTTGCACGATGACCCATACATATTATTGCTTGGCATG
ATCTCACCCACCATTCTTGTGCACATGTATAGGATGCGTCATTTTGAGCGAGGTATTGAAATATGGATTAAGAGA
GATCATGAAATTGGAAAGATTTTCGTCATATTGGAACAGCTCACACGGAAGGTTGCTCTGGCTGAAGTTCTTGTT
GATCAGCTCGATTTGATAAGTGAAGCTTCACCACATTTACTTGAAATCATGAAGGGTTGTCAAGATAATCAAAGG
GCGTATGTACCTGCGCTGGATCTGTTAACGATACAAGTAGAGCGTGAGTTTTCAAATAAAGAACTTAAAACCAAT
GGCTATCCAGATTTGCAGCAAACGTTGTTTGATATGAGAGAAAAAATGTATGCAAAGCAGTTGCACAGTTCATGG
CAAGAGCTAAGCTTGCTGGAAAAATCTTGTGTAACCGTGCGATTGAAGCAATTCTCGATTTTTACGGAAAGAAAT
TTAATCCAGCGAGCAAAAGAAGGAAAGCGCACATCTTCGCTACAATTTGTTCACGAGTGCTTTATCACGACCCGA
GTACATGCGAAGAGCATTCGCGATGCAGGCGTGCGCAAGCTAAATGAGGCTCTCGTTGGAACTTGTAAGTTCTTT
TTCTCTTGTGGTTTCAAGATTTTTGCGCGGTGTTACAGCGACATTATATACCTTGTGAACGTGTGTTTGGTATTC
TCTTTGGTGTTACAAATGTCTAATACTGTGCGCAACATGATAGCGGCGACAAGGGAAGAAAAGGAGAGAGCGATG
GCAAATAAAGCTGATGAAAATGAAAGGACGTTAATGCACATGTACCACATTTTCAGTAAGAAGCAGGATGAAGCG
CCCATATATAACGACTTTCTTGAACATGTTCGCAATGTAAGACCAGATCTTGAGGAAACCCTCTTGTACATGGCT
GGTGCAGAGGTTGTTGCAACACAGGCCAAGTCAGCGGTTCAGATTCAGTTCGAGAAGATTATAGCTGTATTGGCG

CTGCTCACTATGTGCTTTGACGCCGAAAGAAGTGATGCCATTTTCAAGATTTTGACAAAGCTCAAAACAGTTTTT
GGCACGGTTGGAGAAACGGTCCGACTTCAAGGACTTGAAGATATTGAGAGCTTGGAAGACGATAAGAGACTCACA
ATTGACTTTGATATTAACACGAATGAGGCTCAATCGTCGACAACGTTTGATGTTCATTTTGATGATTGGTGGAAT
CGGCAGCTACAGCAAAATCGCACAGTTCCACATTATAGGACCACAGGTAAATTCCTCGAATTCACCAGAAGCACT
GCAGCTTTTGTGGCTAATGAAATAGCATCATCAAGTGAAGGAGAATTTTTAGTTAGAGGAGCAGTGGGTTCTGGA
AAATCAACGAGCTTGCCTGCGCATCTTTCCAAGAAGGGTAAAGTATTACTACTCGAACCCACACGCCCTTTGGCG
GAGAATGTCAGTAGACAGTTGGCAGGCGATCCTTTTTTCCAAAACGTCACACTCAGAATGAGAGGGCTAAATTGC
TTTGGTTCAAGTAACATTACAGTGATGACGAGTGGATTTGCTTTTCACTACTATGTTAATAATCCACACCAATTA
ATGGAATTTGACTTTATTATCATAGACGAATGCCATGTTACGGACAGTGCGACTATAGCTTTCAATTGCGCACTT
AAGGAGTATAATTTTGCTGGCAAATTGATTAAAGTATCTGCAACGCCGCCAGGGAGGGAGTGTGATTTCGATACG
CAATTCGCGGTGAAAGTCAAAACGGAGGACCACCTTTCATTCCATGCATTCGTTGGCGCACAGAAGACTGGTTCA
AACGCTGATATGGTTCAGCATGGCAATAACATACTTGTGTATGTTGCAAGTTATAACGAAGTAGACATGCTTTCC
AAATTACTCACTGAGCGACAATTTTCAGTGACGAAGGTAGATGGGCGAACAATGCAACTTGGGAAAACTACCATT
GAAACGCATGGCACTAGTCAAAAGCCTCATTTCATAGTAGCCACAAACATCATTGAGAATGGAGTGACGTTGGAT
GTCGAATGTGTTGTTGATTTTGGGCTAAAAGTGGTCGCAGAATTAGACAGCGAAAATCGGTGTGTGCGCTACAAC
AAGAAATCAGTTAGTTATGGAGAAAGGATTCAGCGGCTAGGGAGAGTGGGGAGATCTAAGCCTGGAACTGCATTG
CGTATAGGGCACACAGAAAAAGGCATCGAGAACATTCCCGAATTCATTGCCACAGAAGCAGCAGCCTTATCATTT
GCATATGGGCTTCCAGTCACCACGCATGGGGTTTCCACAAATATACTCGGAAAGTGCACAGTTAAACAGATGAGA
TGTGCTTTGAATTTTGAGTTAACTCCTTTCTTTACCACTCATTTAATTCGCCATGATGGTAGCATGCACCCACTG
ATACACGAAGAACTGAAACAATTTAAACTCAGGGACTCAGAAATGGTGCTCAACAAGGTTGCATTACCTCACCAA
TTTGTGAGTCAATGGTTGGATCAAAGTGAGTATGAACGCATTGGAGTGCACGTTCAATGCCATGAGAGCACACGC
ATACCTTTTTACACAAATGGAGTGCCTGATAAAGTCTATGAGAAAATTTGGAAGTGCATACAAGAAAACAAGAAT
GATGCGGTTTTTGGTAAGCTTTCAAGTGCTTGTTCGACTAAGGTTAGTTATACACTCAGCACTGATCCAGCAGCA
TTACCCAGAACTATTGCAATCATCGACCACCTGCTTGCCGAGGAAATGATGAAGCGGAATCACTTCGACACGATC
AGCTCAGCTGTAACGGGCTATTCATTTTCCCTCGCTGGAATTGCTGATTCTTTTAGGAAAAGGTATATGCGCGAT
TACACAGCGCATAACATTGCAATTCTCCAACAAGCACGTGCCCAGCTGCTCGAATTCAATAGTAAAAATGTGAAC
ATCAACAACCTGTCCGATCTGGAAGGAATTGGAGTTATTAAGTCGGTGGTGTTGCAAAGTAAGCAAGAGGTCAGC
AACTTCCTAGGACTTCGCGGTAAATGGGATGGGCGGAAATTTGCGAATGATGTGATATTGGCGATCATGACACTC
TTAGGAGGTGGATGGTTCATGTGGGAATACTTCACGAAAAAGATCAATGAACCCGTGCGCGTTGAAAGCAAGAAA
CGGCGATCTCAAAAGTTGAAATTCAGGGATGCGTACGATAGGAAAGTCGGACGTGAGATTTTTGGCGATGATGAC
ACAATTGGGCGCACTTTTGGCGAAGCTTACACGAAGAGAGGAAAGGTCAAAGGAAACAACAGCACAAAAGGAATG
GGACGGAAAACTCGCAATTTTGTGCATTTATATGGTGTGGAGCCTGAGAATTACAGCTTTATTAGATTTGTGGAC
CCTCTCACTGGCCATACATTGGACGAAAGCACCCATACAGACATTTCGTTAGTGCAGGAGGAGTTTGGAAGTATT
AGAGAGAAATTTCTGGAGAATGATTTAATCTCGAGGCAGTCTATTATTAACAAACCCGGTATTCAAGCATATTTT
ATGGGCAAGGGCACCGAAGAAGCACTCAAAGTTGATTTGACTCCTCATGTACCATTGCTTCTGTGCAGAAACACC
AATGCCATTGCGGGGTATCCAGAGAGAGAAAATGAGTTGAGACAAACCGGCACACCAGTTAAGGTTTCTTTTAAA
GACGTGCCAGAGAAAAACGAACATGTCGAGTTGGAGAGCAAATCCATCTACAAAGGAGTGCGCGATTACAATGGC
ATTTCAACAATCGTCTGTCAATTAACGAACGATTCTGATGGCCTCAAGGAGACTATGTATGGTATTGGCTACGGG
CCGATAATCATTACTAATGGGCACCTCTTCAGGAAAAACAATGGTACACTTCTAGTCAGGTCTTGGCATGGTGAA
TTCACTGTTAAAAATACCACAACGCTCAAAGTGCATTTCATAGAAGGGAAGGATGTTGTTTTAGTGCGTATGCCA
AAGGACTTTCCACCGTTCAAAAGCAACGCTTCTTTTAGAGCGCCAAAACGCGAGGAACGAGCATGCTTGGTTGGA
ACAAATTTTCAAGAGAAGAGTCTCCGCTCCACTGTTTCAGAATCTTCAATGACAATACCTGAAGGAACTGGCTCA
TATTGGATTCATTGGATTTCAACCAATGAAGGGGACTGCGGATTACCCATGGTTTCAACAACGGATGGTAAGATA
ATTGGAGTTCATGGTTTGGCTTCCACAGTCTCATCTAAGAATTATTTTGTCCCATTCACTGATGATTTTATAGCC
ACGCATTTGAGCAAGCTTGATGATCTCACATGGACTCAGCATTGGCTATGGCAACCTAGCAAAATCGCGTGGGGA
ACGCTCAACTTAGTTGATGAACAACCAGGGCCTGAATTTCGTATTTCAAATCTAGTCAAGGATTTGTTCACTTCT
GGTGTTGAAACACAGAGCAAGCGGGAAAGATGGGTCTACGAAAGCTGTGAAGGGAACCTTCGAGCTGTTGGAACT
GCGCAATCAGCGTTAGTCACCAAACATGTTGTCAAGGGCAAGTGTTCTTTCTTCGAAGAATATTTGCAAACACAC
GCAGAAGCGAGCGCCTATTTCAGACCCTTAATGGGAGAGTACCAGCCGAGCAAGTTGAACAAAGAGGCCTTCAAA
AAGGATTTCTTTAAATACAACAAACCCGTCACTGTTAATCAATTGGATCATGATAAATTTTTAGAAGCAGTGGAT
GGGGTTATACGTATGATGTGTGACTTTGAGTTCAATGAATGCCGATTCATTACAGATCCCGAGGAAATTTACAAC
TCTCTGAACATGAAAGCAGCAATTGGAGCCCAATATAGAGGAAAGAAGAAAGAATATTTTGAAGGGCTAGATGAT
TTTGATCGAGAGCGACTATTATTTCAAAGTTGTGAAAGGTTGTTTAATGGCTATAAAGGTTTGTGGAATGGATCT
TTAAAGGCTGAGCTCAGGCCGCTTGAGAAAGTCAGGGCTAACAAAACACGAACTTTTACAGCAGCGCCAATTGAT
ACATTGCTTGGAGCTAAAGTTTGCGTGGATGATTTCAATAATGAATTTTACAGCAAAAATCTCAAGTGTCCATGG
ACGGTTGGCATGACAAAATTTTATGGTGGTTGGGATAAATTGATGAGATCGTTACCTGATGGTTGGTTATACTGT
CATGCTGATGGATCACAGTTTGACAGTTCATTAACCCCAGCTCTATTGAATGCAGTTCTTATAATCAGGTCTTTT
TACATGGAAGATTGGTGGGTTGGCCAAGAGATGCTCGAAAATCTCTATGCTGAGATTGTGTACACTCCAATTCTT
GCTCCGGATGGAACAATTTTCAAGAAATTTAGAGGTAACAACAGTGGGCAACCCTCAACAGTGGTGGATAACACA
CTAATGGTTGTGATCTCTATTTACTATGCGTGCATGAAGTTTGGGTGGAATTGCGAGGAAATTGAGAATAAACTT
GTCTTCTTTGCAAATGGAGATGACCTGATACTTGCAGTCAGAGATGAAGACAGCGGCTTACTTGATAACATGTCA

TCCTCTTTTTCCGAACTTGGACTGAATTACGATTTTTCGGAACGCACGCACAAAAGAGAAGATCTTTGGTTCATG
TCCCACCAGGCAATGTTAATTGATGGAATGTACATCCCAAAACTTGAGAAAGAGAGAATTGTTTCAATTCTAGAA
TGGGATAGAAGTAAGGAAATAATGCACCGAACAGAGGCTATTTGCGCTGCAATGATTGAAGCATGGGGACACACC
GAGCTTTTACAAGAAATCAGAAAGTTTTACCTGTGGTTCGTTGAAAAGGAAGAAGTGCGAGAATTGGCTGCCCTC
GGAAAAGCTCCATACATAGCTGAGACAGCTCTTCGTAAGTTATACACTGACAAGGGAGCGGATACGAGTGAACTG
GCACGCTATCTACGAGCCCTCCATCAAGATATCTTCTTTGAACAAGGAGACACTGTAATGCTCCAATCAGGCACT
CAGCCAACTGTGGCAGACGCTGGGGCTACAAAGAAAGACAAAGAAGATGACAAAGGGAAAAACAAGGATGTTTCA
GGCTCCGGCTCAGGTGAGAAAACGATAGCAGCTGTCACAAAGGACAAGGATGTGAATGCTGGTTCTCATGGGAAG
ATCGTGCCGCGTCTTTCAAAGATCACAAAGAAAATGTCACTGCCACGCGTGAAAGGAAATGTGATACTCGATATC
GATCATTTGCTGGAATATAAACCGGATCAAATCGAGTTGTACAACACACGAGCGTCTCATCAGCAATTCGCTTCC
TGGTTTAACCAAGTTAAAACAGAATATGATCTGAATGAGCAACAGATGGGAGTTGTAATGAATGGTTTCATGGTT
TGGTGTATTGAAAATGGCACCTCACCCGACATTAATGGAGTGTGGGTTATGATGGACGGAAATGAGCAAGTTGAA
TATCCTTTGAAACCAATAGTTGAAAATGCAAAGCCAACGCTGCGGCAAATAATGCATCATTTTTCAGATGCAGCG
GAGGCATACATAGAGATGAGAAATGCAGAGGCACCATACATGCCGAGGTATGGTTTGCTTCGAAACCTACGGGAT
AGGAGTTTGGCACGATATGCTTTCGATTTCTATGAAGTCAATTCTAAAACTCCTGAAAGAGCCCGTGAAGCTGTT
GCGCAAATGAAAGCAGCAGCTCTTAGCAATGTTTCTTCAAGGTTGTTTGGCCTTGATGGAAATGTTGCCACTACT
AGCGAAGACACTGAACGGCACACTGCACGTGATGTTAATAGAAACATGCACACCTTACTAGGTGTGAATACAATG
CAGTAAAGGGTAGGTCGCCTACCTAGGTTATTGTTTCGCTGCCGACGTAATTCTAATATTTACCGCTTTATTTGA
TATCTTTAAATTTCTAGAGTGGGCTTCCCACCCTTAAAGCGTAAAGTTTATGTTAGTTGTCCAGGAGTGCCGTAG
TCCTGTCGGAAGCTTTAGTGTGAGCCTCTCACGAATAAGCTCGAGATTAGACTCCGTTTGCAAGCCTAAAAAAAA
AAAAAAAAAAAAAAAAAAAAAAAAAAAAAAAAAAAAAA

>ZYMVΔ (deletion from positions 8551 to 8640 of ZYMV-wt)

>ZYMVΔ-αGFP (insert between positions 8550 and 8641 of ZYMV-wt),
GGTGCGCCGGTGCCGTATCCGGATCCGCTGGAACCGgcccagccggccATGGCTCAGGTGCAGCTGGTGGAGTCT
GGGGGAGCCTTGGTGCAGCCGGGGGGGTCTCTGAGACTCTCCTGTGCAGCCTCTGGATTCCCCGTCAATCGCTAT
AGTATGAGGTGGTACCGCCAGGCTCCAGGGAAGGAGCGCGAGTGGGTCGCGGGTATGAGTAGTGCTGGTGATCGT
TCAAGTTATGAAGACTCCGTGAAGGGCCGATTCACCATCTCCAGAGACGACGCCAGGAATACGGTGTATCTGCAA
ATGAACAGCCTGAAACCTGAGGACACGGCCGTGTATTACTGTAATGTCAATGTGGGCTTTGAGTACTGGGGCCAG
GGGACCCAGGTCACCGTCTCCTCAgcggccgccGAACAAAAACTCATCTCAGAAGAGGATgcagctgca

αGFP nanobody in green, **E** and **c-Myc** epitopes on yellow and blue background, respectively, and spacers in blue.

>ZYMVΔ-αGFP-F2A (insert between positions 8550 and 8641 of ZYMV-wt)
GGTGCGCCGGTGCCGTATCCGGATCCGCTGGAACCGgcccagccggccATGGCTCAGGTGCAGCTGGTGGAGTCT
GGGGGAGCCTTGGTGCAGCCGGGGGGGTCTCTGAGACTCTCCTGTGCAGCCTCTGGATTCCCCGTCAATCGCTAT
AGTATGAGGTGGTACCGCCAGGCTCCAGGGAAGGAGCGCGAGTGGGTCGCGGGTATGAGTAGTGCTGGTGATCGT
TCAAGTTATGAAGACTCCGTGAAGGGCCGATTCACCATCTCCAGAGACGACGCCAGGAATACGGTGTATCTGCAA
ATGAACAGCCTGAAACCTGAGGACACGGCCGTGTATTACTGTAATGTCAATGTGGGCTTTGAGTACTGGGGCCAG
GGGACCCAGGTCACCGTCTCCTCAgcggccgccGAACAAAAACTCATCTCAGAAGAGGATgcagctgcaGGAAGC
GGAGTGAAACAGACTTTGAATTTTGACCTTCTCAAGTTGGCGGGAGACGTGGAGTCCAACCCTGGACCT

αGFP nanobody in green, **F2A** peptide in blue (splicing position underlined), **E** and **c-Myc** epitopes on yellow and blue background, respectively, and spacers in blue.

Figure S2. Nucleotide sequences of TEV-wt (GenBank accession number DQ986288, including silent mutations **G273A** and A1119G in red) and the derived recombinant viruses TEV-αGFP, and TEV-αGFP-F2A. The boundaries of viral cistrons are indicated on blue background. **Start** and **stop** codons are underlined. Heterologous sequences were inserted between nucleotide positions **8517** and **8518** (underlined). cDNAs corresponding to the anti-green fluorescent protein (αGFP) nanobody, and picornavirus **F2A** peptides are in green and blue, respectively.

>TEV-wt (DQ986288, G273A, A1119G); cistrons boundaries are indicated on blue background; start and stop codons are underlined

AAAATAACAAATCTCAACACAACATATACAAAACAAACGAATCTCAAGCAATCAAGCATTCTACTTCTATTGCAG
CAATTTAAATCATTTCTTTTAAAGCAAAAGCAATTTTCTGAAAATTTTCACCATTTACGAACGATAGCCATGGCA
CTCATCTTTGGCACAGTCAACGCTAACATCCTGAAGGAAGTGTTCGGTGGAGCTCGTATGGCTTGCGTTACCAGC
GCACATATGGCTGGAGCGAATGGAAGCATTTTGAAGAAGGCAGAAGAAACCTCTCGTGCAATCATGCACAAACCA
GTGATCTTCGGAGAAGACTACATTACCGAGGCAGACTTGCCTTACACACCACTCCATTTAGAGGTCGATGCTGAA
ATGGAGCGGATGTATTATCTTGGTCGTCGCGCGCTCACCCATGGCAAGAGACGCAAAGTTTCTGTGAATAACAAG
AGGAACAGGAGAAGGAAAGTGGCCAAAACGTACGTGGGGCGTGATTCCATTGTTGAGAAGATTGTAGTGCCCCAC
ACCGAGAGAAAGGTTGATACCACAGCAGCAGTGGAAGACATTTGCAATGAAGCTACCACTCAACTTGTGCATAAT
AGTATGCCAAAGCGTAAGAAGCAGAAAAACTTCTTGCCCGCCACTTCACTAAGTAACGTGTATGCCCAAACTTGG
AGCATAGTGCGCAAACGCCATATGCAGGTGGAGATCATTAGCAAGAAGAGCGTCCGAGCGAGGGTCAAGAGATTT
GAGGGCTCGGTGCAATTGTTCGCAAGTGTGCGTCACATGTATGGCGAGAGGAAAAGGGTGGACTTACGTATTGAC
AACTGGCAGCAAGAGACACTTCTAGACCTTGCTAAAAGATTTAAGAATGAGAGAGTGGATCAATCGAAGCTCACT
TTTGGTTCAAGTGGCCTAGTTTTGAGGCAAGGCTCGTACGGACCTGCGCATTGGTATCGACATGGTATGTTCATT
GTACGCGGTCGGTCGGATGGGATGTTGGTGGATGCTCGTGCGAAGGTAACGTTCGCTGTTTGTCACTCAATGACA
CATTATAGCGACAAATCAATCTCTGAGGCATTCTTCATACCATACTCTAAGAAATTCTTGGAGTTGAGGCCAGAT
GGAATCTCCCATGAGTGTACAAGAGGAGTATCAGTTGAGCGGTGCGGTGAGGTGGCTGCAATCCTGACACAAGCA
CTTTCACCGTGTGGTAAGATCACATGCAAACGTTGCATGGTTGAAACACCTGACATTGTTGAGGGTGAGTCGGGA
GACAGTGTCACCAACCAAGGTAAGCTCCTAGCAATGCTGAAAGAACAGTATCCAGATTTCCCAATGGCCGAGAAA
CTACTCACAAGGTTTTTGCAACAGAAATCACTAGTAAATACAAATTTGACAGCCTGCGTGAGCGTCAAACAACTC
ATTGGTGACCGCAAACAAGCTCCATTCACACACGTACTGGCTGTCAGCGAAATTCTGTTTAAAGGCAATAAACTA
ACAGGGGCCGATCTCGAAGAGGCAAGCACACATATGCTTGAAATAGCAAGGTTCTTGAACAATCGCACTGAAAAT
ATGCGCATTGGCCACCTTGGTTCTTTCAGAAATAAAATCTCATCGAAGGCCCATGTGAATAACGCACTCATGTGT
GATAATCAACTTGATCAGAATGGGAATTTTATTTGGGGACTAAGGGGTGCACACGCAAAGAGGTTTCTTAAAGGA
TTTTTCACTGAGATTGACCCAAATGAAGGATACGATAAGTATGTTATCAGGAAACATATCAGGGGTAGCAGAAAG
CTAGCAATTGGCAATTTGATAATGTCAACTGACTTCCAGACGCTCAGGCAACAAATTCAAGGCGAAACTATTGAG
CGTAAAGAAATTGGGAATCACTGCATTTCAATGCGGAATGGTAATTACGTGTACCCATGTTGTTGTGTTACTCTT
GAAGATGGTAAGGCTCAATATTCGGATCTAAAGCATCCAACGAAGAGACATCTGGTCATTGGCAACTCTGGCGAT
TCAAAGTACCTAGACCTTCCAGTTCTCAATGAAGAGAAAATGTATATAGCTAATGAAGGTTATTGCTACATGAAC
ATTTTCTTTGCTCTACTAGTGAATGTCAAGGAAGAGGATGCAAAGGACTTCACCAAGTTTATAAGGGACACAATT
GTTCCAAAGCTTGGAGCGTGGCCAACAATGCAAGATGTTGCAACTGCATGCTACTTACTTTCCATTCTTTACCCA
GATGTCCTGAGTGCTGAATTACCCAGAATTTTGGTTGATCATGACAACAAAACAATGCATGTTTTGGATTCGTAT
GGGTCTAGAACGACAGGATACCACATGTTGAAAATGAACACAACATCCCAGCTAATTGAATTCGTTCATTCAGGT
TTGGAATCCGAAATGAAAACTTACAATGTTGGAGGGATGAACCGAGATATGGTCACACAAGGTGCAATTGAGATG
TTGATCAAGTCCATATACAAACCACATCTCATGAAGCAGTTACTTGAGGAGGAGCCATACATAATTGTCCTGGCA
ATAGTCTCCCCTTCAATTTTAATTGCCATGTACAACTCTGGAACTTTTGAGCAGGCGTTACAAATGTGGTTGCCA
AATACAATGAGGTTAGCTAACCTCGCTGCCATCTTGTCAGCCTTGGCGCAAAAGTTAACTTTGGCAGACTTGTTC
GTCCAGCAGCGTAATTTGATTAATGAGTATGCGCAGGTAATTTTGGACAATCTGATTGACGGTGTCAGGGTTAAC
CATTCGCTATCCCTAGCAATGGAAATTGTTACTATTAAGCTGGCCACCCAAGAGATGGACATGGCGTTGAGGGAA
GGTGGCTATGCTGTGACCTCTGAAAAGGTGCATGAAATGTTGGAAAAAAACTATGTAAAGGCTTTGAAGGATGCA
TGGGACGAATTAACTTGGTTGGAAAAATTCTCCGCAATCAGGCATTCAAGAAAGCTCTTGAAATTTGGGCGAAAG
CCTTTAATCATGAAAAACACCGTAGATTGCGGCGGACATATAGACTTGTCTGTGAAATCGCTTTTCAAGTTCCAC
TTGGAACTCCTGAAGGGAACCATCTCAAGAGCCGTAAATGGTGGTGCAAGAAAGGTAAGAGTAGCGAAGAATGCC
ATGACAAAAGGGGTTTTTCTCAAAATCTACAGCATGCTTCCTGACGTCTACAAGTTTATCACAGTCTCGAGTGTC
CTTTCCTTGTTGTTGACATTCTTATTTCAAATTGACTGCATGATAAGGGCACACCGAGAGGCGAAGGTTGCTGCA
CAGTTGCAGAAAGAGAGCGAGTGGGACAATATCATCAATAGAACTTTCCAGTATTCTAAGCTTGAAAATCCTATT
GGCTATCGCTCTACAGCGGAGGAAAGACTCCAATCAGAACACCCCGAGGCTTTCGAGTACTACAAGTTTTGCATT
GGAAAGGAAGACCTCGTTGAACAGGCAAAACAACCGGAGATAGCATACTTTGAAAAGATTATAGCTTTCATCACA
CTTGTATTAATGGCTTTTGACGCTGAGCGGAGTGATGGAGTGTTCAAGATACTCAATAAGTTCAAAGGAATACTG
AGCTCAACGGAGAGGGAGATCATCTACACGCAGAGTTTGGATGATTACGTTACAACCTTTGATGACAATATGACA
ATCAACCTCGAGTTGAATATGGATGAACTCCACAAGACGAGCCTTCCTGGAGTCACTTTTAAGCAATGGTGGAAC
AACCAAATCAGCCGAGGCAACGTGAAGCCACATTATAGAACTGAGGGGCACTTCATGGAGTTTACCAGAGATACT
GCGGCATCGGTTGCCAGCGAGATATCACACTCACCCGCAAGAGATTTTCTTGTGAGAGGTGCTGTTGGATCTGGA
AAATCCACAGGACTTCCATACCATTTATCAAAGAGAGGGAGAGTGTTAATGCTTGAGCCTACCAGACCACTCACA
GATAACGTGCACAAGCAACTGAGAAGTGAACCATTTAACTGCTTCCCAACTTTGAGGATGAGAGGGAAGTCAACT
TTTGGGTCATCACCGATTACAGTCATGACTAGTGGATTCGCTTTACACCATTTTGCACGAAACATAGCTGAGGTA
AAAACATACGATTTTGTCATAATTGATGAATGTCATGTGAATGATGCTTCTGCTATAGCGTTTAGGAATCTACTG
TTTGAACATGAATTTGAAGGAAAAGTCCTCAAAGTGTCAGCCACACCACCAGGTAGAGAAGTTGAATTCACAACT
CAGTTTCCCGTGAAACTCAAGATAGAAGAGGCTCTTAGCTTTCAGGAATTTGTAAGTTTACAAGGGACAGGTGCC
AACGCCGATGTGATTAGTTGTGGCGACAACATACTAGTATATGTTGCTAGCTACAATGATGTTGATAGTCTTGGC

AAGCTCCTTGTGCAAAAGGGATACAAAGTGTCGAAGATTGATGGAAGAACAATGAAGAGTGGAGGAACTGAAATA
ATCACTGAAGGTACTTCAGTGAAAAAGCATTTCATAGTCGCAACTAATATTATTGAGAATGGTGTAACCATTGAC
ATTGATGTAGTTGTGGATTTTGGGACTAAGGTTGTACCAGTTTTGGATGTGGACAATAGAGCGGTGCAGTACAAC
AAAACTGTGGTGAGTTATGGGGAGCGCATCCAAAGACTCGGTAGAGTTGGGCGACACAAGGAAGGAGTAGCACTT
CGAATTGGCCAAACAAATAAAACACTGGTTGAAATTCCAGAAATGGTTGCCACTGAAGCTGCCTTTCTATGCTTC
ATGTACAATTTGCCAGTGACAACACAGAGTGTTTCAACCACACTGCTGGAAAATGCCACATTATTACAAGCTAGA
ACTATGGCACAGTTTGAGCTATCATATTTTTACACAATTAATTTTGTGCGATTTGATGGTAGTATGCATCCAGTC
ATACATGACAAGCTGAAGCGCTTTAAGCTACACACTTGTGAGACATTCCTCAATAAGTTGGCGATCCCAAATAAA
GGCTTATCCTCTTGGCTTACGAGTGGAGAGTATAAGCGACTTGGTTACATAGCAGAGGATGCTGGCATAAGAATC
CCATTCGTGTGCAAAGAAATTCCAGACTCCTTGCATGAGGAAATTTGGCACATTGTAGTCGCCCATAAAGGTGAC
TCGGGTATTGGGAGGCTCACTAGCGTACAGGCAGCAAAGGTTGTTTATACTCTGCAAACGGATGTGCACTCAATT
GCGAGGACTCTAGCATGCATCAATAGACTCATAGCACATGAACAAATGAAGCAGAGTCATTTTGAAGCCGCAACT
GGGAGAGCATTTTCCTTCACAAATTACTCAATACAAAGCATATTTGACACGCTGAAAGCAAATTATGCTACAAAG
CATACGAAAGAAAATATTGCAGTGCTTCAGCAGGCAAAAGATCAATTGCTAGAGTTTTCGAACCTAGCAAAGGAT
CAAGATGTCACGGGTATCATCCAAGACTTCAATCACCTGGAAACTATCTATCTCCAATCAGATAGCGAAGTGGCT
AAGCATCTGAAGCTTAAAAGTCACTGGAATAAAAGCCAAATCACTAGGGACATCATAATAGCTTTGTCTGTGTTA
ATTGGTGGTGGATGGATGCTTGCAACGTACTTCAAGGACAAGTTCAATGAACCAGTCTATTTCCAAGGGAAGAAG
AATCAGAAGCACAAGCTTAAGATGAGAGAGGCGCGTGGGGCTAGAGGGCAATATGAGGTTGCAGCGGAGCCAGAG
GCGCTAGAACATTACTTTGGAAGCGCATATAATAACAAAGGAAAGCGCAAGGGCACCACGAGAGGAATGGGTGCA
AAGTCTCGGAAATTCATAAACATGTATGGGTTTGATCCAACTGATTTTTCATACATTAGGTTTGTGGATCCATTG
ACAGGTCACACTATTGATGAGTCCACAAACGCACCTATTGATTTAGTGCAGCATGAGTTTGGAAAGGTTAGAACA
CGCATGTTAATTGACGATGAGATAGAGCCTCAAAGTCTTAGCACCCACACCACAATCCATGCTTATTTGGTGAAT
AGTGGCACGAAGAAAGTTCTTAAGGTTGATTTAACACCACACTCGTCGCTACGTGCGAGTGAGAAATCAACAGCA
ATAATGGGATTTCCTGAAAGGGAGAATGAATTGCGTCAAACCGGCATGGCAGTGCCAGTGGCTTATGATCAATTG
CCACCAAAGAGTGAGGACTTGACGTTTGAAGGAGAAAGCTTGTTTAAGGGACCACGTGATTACAACCCGATATCG
AGCACCATTTGTCACTTGACGAATGAATCTGATGGGCACACAACATCGTTGTATGGTATTGGATTTGGTCCCTTC
ATCATTACAAACAAGCACTTGTTTAGAAGAAATAATGGAACACTGTTGGTCCAATCACTACATGGTGTATTCAAG
GTCAAGAACACCACGACTTTGCAACAACACCTCATTGATGGGAGGGACATGATAATTATTCGCATGCCTAAGGAT
TTCCCACCATTTCCTCAAAAGCTGAAATTTAGAGAGCCACAAAGGGAAGAGCGCATATGTCTTGTGACAACCAAC
TTCCAAACTAAGAGCATGTCTAGCATGGTGTCAGACACTAGTTGCACATTCCCTTCATCTGATGGCATATTCTGG
AAGCATTGGATTCAAACCAAGGATGGGCAGTGTGGCAGTCCATTAGTATCAACTAGAGATGGGTTCATTGTTGGT
ATACACTCAGCATCGAATTTCACCAACACAAACAATTATTTCACAAGCGTGCCGAAAAACTTCATGGAATTGTTG
ACAAATCAGGAGGCGCAGCAGTGGGTTAGTGGTTGGCGATTAAATGCTGACTCAGTATTGTGGGGGGGCCATAAA
GTTTTCATGAGCAAACCTGAAGAGCCTTTTCAGCCAGTTAAGGAAGCGACTCAACTCATGAGTGAATTGGTGTAC
TCGCAAGGGGAGAAGAGGAAATGGGTCGTGGAAGCACTGTCAGGGAACTTGAGGCCAGTGGCTGAGTGTCCCAGT
CAGTTAGTCACAAAGCATGTGGTTAAAGGAAAGTGTCCCCTCTTTGAGCTCTACTTGCAGTTGAATCCAGAAAAG
GAAGCATATTTTAAACCGATGATGGGAGCATATAAGCCAAGTCGACTTAATAGAGAGGCGTTCCTCAAGGACATT
CTAAAATATGCTAGTGAAATTGAGATTGGGAATGTGGATTGTGACTTGCTGGAGCTTGCAATAAGCATGCTCATC
ACAAAGCTCAAGGCGTTAGGATTCCCAACTGTGAACTACATCACTGACCCAGAGGAAATTTTTAGTGCATTGAAT
ATGAAAGCAGCTATGGGAGCACTATACAAAGGCAAGAAGAAAGAAGCTCTCAGCGAGCTCACACTAGATGAGCAG
GAGGCAATGCTCAAAGCAAGTTGCCTGCGACTGTATACGGGAAAGCTGGGAATTTGGAATGGCTCATTGAAAGCA
GAGTTGCGTCCAATTGAGAAGGTTGAAAACAACAAAACGCGAACTTTCACAGCAGCACCAATAGACACTCTTCTT
GCTGGTAAAGTTTGCGTGGATGATTTCAACAATCAATTTTATGATCTCAACATAAAGGCACCATGGACAGTTGGT
ATGACTAAGTTTTATCAGGGGTGGAATGAATTGATGGAGGCTTTACCAAGTGGGTGGGTGTATTGTGACGCTGAT
GGTTCGCAATTCGACAGTTCCTTGACTCCATTCCTCATTAATGCTGTATTGAAAGTGCGACTTGCCTTCATGGAG
GAATGGGATATTGGTGAGCAAATGCTGCGAAATTTGTACACTGAGATAGTGTATACACCAATCCTCACACCGGAT
GGTACTATCATTAAGAAGCATAAAGGCAACAATAGCGGGCAACCTTCAACAGTGGTGGACAACACACTCATGGTC
ATTATTGCAATGTTATACACATGTGAGAAGTGTGGAATCAACAAGGAAGAGATTGTGTATTACGTCAATGGCGAT
GACCTATTGATTGCCATTCACCCAGATAAAGCTGAGAGGTTGAGTGGATTCAAAGAATCTTTCGGAGAGTTGGGC
CTGAAATATGAATTTGACTGCACCACCAGGGACAAGACACAGTTGTGGTTCATGTCACACAGGGCTTTGGAGAGG
GATGGCATGTATATACCAAAGCTAGAAGAAGAAAGGATTGTTTCTATTTTGGAATGGGACAGATCCAAAGAGCCG
TCACATAGGCTTGAAGCCATCTGTGCATCAATGATCGAAGCATGGGGTTATGACAAGCTGGTTGAAGAAATCCGC
AATTTCTATGCATGGGTTTTGGAACAAGCGCCGTATTCACAGCTTGCAGAAGAAGGAAAGGCGCCATATCTGGCT
GAGACTGCGCTTAAGTTTTTGTACACATCTCAGCACGGAACAAACTCTGAGATAGAAGAGTATTTAAAAGTGTTG
TATGATTACGATATTCCAACGACTGAGAATCTTTATTTTCAGAGTGGCACTGTGGGTGCTGGTGTTGACGCTGGT
AAGAAGAAAGATCAAAAGGATGATAAAGTCGCTGAGCAGGCTTCAAAGGATAGGGATGTTAATGCTGGAACTTCA
GGAACATTCTCAGTTCCACGAATAAATGCTATGGCCACAAAACTTCAATATCCAAGGATGAGGGGAGAGGTGGTT
GTAAACTTGAATCACCTTTTAGGATACAAGCCACAGCAAATTGATTTGTCAAATGCTCGAGCCACACATGAGCAG
TTTGCCGCGTGGCATCAGGCAGTGATGACAGCCTATGGAGTGAATGAAGAGCAAATGAAAATATTGCTAAATGGA
TTTATGGTGTGGTGCATAGAAAATGGGACTTCCCCAAATTTGAACGGAACTTGGGTTATGATGGATGGTGAGGAG
CAAGTTTCATACCCGCTGAAACCAATGGTTGAAAACGCGCAGCCAACACTGAGGCAAATTATGACACACTTCAGT

GACCTGGCTGAAGCGTATATTGAGATGAGGAATAGGGAGCGACCATACATGCCTAGGTATGGTCTACAGAGAAAC
ATTACAGACATGAGTTTGTCACGCTATGCGTTCGACTTCTATGAGCTAACTTCAAAAACACCTGTTAGAGCGAGG
GAGGCGCATATGCAAATGAAAGCTGCTGCAGTACGAAACAGTGGAACTAGGTTATTTGGTCTTGATGGCAACGTG
GGTACTGCAGAGGAAGACACTGAACGGCACACAGCGCACGATGTGAACCGTAACATGCACACACTATTAGGGGTC
CGCCAGTGATAGTTTCTGCGTGTCTTTGCTTTCCGCTTTTAAGCTTATTGTAATATATATGAATAGCTATTCACA
GTGGGACTTGGTCTTGTGTTGAATGGTATCTTATATGTTTTAATATGTCTTATTAGTCTCATTACTTAGGCGAAC
GACAAAGTGAGGTCACCTCGGTCTAATTCTCCTATGTAGTGCGAGAAAAAAAAAAAAAAAAAAAAAAAAAAAAA
AAAAAAAAAAAAAA

>TEV-αGFP (insert between possitions 8517 and 8518 of TEV-wt)
TCAGGTACAGGTGCGCCGGTGCCGTATCCGGATCCGCTGGAACCGgcccagccggccATGGCTCAGGTGCAGCTG
GTGGAGTCTGGGGGAGCCTTGGTGCAGCCGGGGGGGTCTCTGAGACTCTCCTGTGCAGCCTCTGGATTCCCCGTC
AATCGCTATAGTATGAGGTGGTACCGCCAGGCTCCAGGGAAGGAGCGCGAGTGGGTCGCGGGTATGAGTAGTGCT
GGTGATCGTTCAAGTTATGAAGACTCCGTGAAGGGCCGATTCACCATCTCCAGAGACGACGCCAGGAATACGGTG
TATCTGCAAATGAACAGCCTGAAACCTGAGGACACGGCCGTGTATTACTGTAATGTCAATGTGGGCTTTGAGTAC
TGGGGCCAGGGGACCCAGGTCACCGTCTCCTCAgcggccgccGAACAAAAACTCATCTCAGAAGAGGATgcagct
gca

Duplicated three initial codons (silent mutations) of TEV CP are in black. αGFP nanobody in green, **E** and **c-Myc** epitopes on yellow and blue background, respectively, and spacers in blue.

>TEV-αGFP-F2A (insert between possitions 8517 and 8518 of TEV-wt)
TCAGGTACAGGTGCGCCGGTGCCGTATCCGGATCCGCTGGAACCGgcccagccggccATGGCTCAGGTGCAGCTG
GTGGAGTCTGGGGGAGCCTTGGTGCAGCCGGGGGGGTCTCTGAGACTCTCCTGTGCAGCCTCTGGATTCCCCGTC
AATCGCTATAGTATGAGGTGGTACCGCCAGGCTCCAGGGAAGGAGCGCGAGTGGGTCGCGGGTATGAGTAGTGCT
GGTGATCGTTCAAGTTATGAAGACTCCGTGAAGGGCCGATTCACCATCTCCAGAGACGACGCCAGGAATACGGTG
TATCTGCAAATGAACAGCCTGAAACCTGAGGACACGGCCGTGTATTACTGTAATGTCAATGTGGGCTTTGAGTAC
TGGGGCCAGGGGACCCAGGTCACCGTCTCCTCAgcggccgccGAACAAAAACTCATCTCAGAAGAGGATgcagct
gcaGGAAGCGGAGTGAAACAGACTTTGAATTTTGACCTTCTCAAGTTGGCGGGAGACGTGGAGTCCAACCCTGGA
CCT

Duplicated three initial codons (silent mutations) of TEV CP are in black. αGFP nanobody in green, **F2A** peptide in blue (splicing position underlined), **E** and **c-Myc** epitopes on yellow and blue background, respectively, and spacers in blue.

Figure S3. Nucleotide sequence of the recombinant enhanced green fluorescent protein (eGFP) with the **Twin-Strep tag** (in red, spacers in grey) produced in *Escherichia coli*. **Start** and **stop** codons are underlined.

ATGGTGAGCAAGGGCGAGGAGCTGTTCACCGGGGTGGTGCCCATCCTGGTCGAGCTGGACGGCGACGTAAACGGC
CACAAGTTCAGCGTGTCCGGCGAGGGCGAGGGCGATGCCACCTACGGCAAGCTGACCCTGAAGTTCATCTGCACC
ACCGGCAAGCTGCCCGTGCCCTGGCCCACCCTCGTGACCACCCTGACCTACGGCGTGCAGTGCTTCAGCCGCTAC
CCCGACCACATGAAGCAGCACGACTTCTTCAAGTCCGCCATGCCCGAAGGCTACGTCCAGGAGCGCACCATCTTC
TTCAAGGACGACGGCAACTACAAGACCCGCGCCGAGGTGAAGTTCGAGGGCGACACCCTGGTGAACCGCATCGAG
CTGAAGGGCATCGACTTCAAGGAGGACGGCAACATCCTGGGGCACAAGCTGGAGTACAACTACAACAGCCACAAC
GTCTATATCATGGCCGACAAGCAGAAGAACGGCATCAAGGTGAACTTCAAGATCCGCCACAACATCGAGGACGGC
AGCGTGCAGCTCGCCGACCACTACCAGCAGAACACCCCCATCGGCGACGGCCCCGTGCTGCTGCCCGACAACCAC
TACCTGAGCACCCAGTCCGCCCTGAGCAAAGACCCCAACGAGAAGCGCGATCACATGGTCCTGCTGGAGTTCGTG
ACCGCCGCCGGGATCACTCTCGGCATGGACGAGCTGTACAAGAGCGCATGGAGTCATCCTCAATTCGAGAAAGGT
GGAGGTTCTGGCGGTGGATCGGGAGGTTCAGCGTGGAGCCACCCGCAGTTCGAAAAATCCGGATGA

GENERAL DISCUSSION

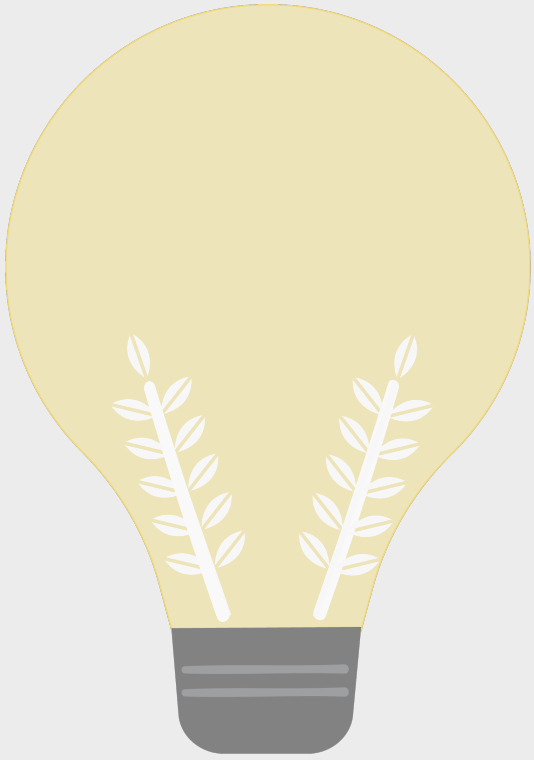

Photosynthetic organisms as plants are the mainstay of life on Earth, essential for humans directly providing food, shelter, feedstock or fuel, and also indirectly for their appreciated compounds (Jose et al., 2019). Plant biotechnology aims to improve agronomic traits. More recently, molecular farming has emerged by using plants as alternative platforms or 'biofactories' targeting the sustainable production of valuable compounds of pharmaceutical or industrial interest (Jose et al., 2019; Kumar et al., 2020; Majer et al., 2017; Mohammadinejad et al., 2019; Xu et al., 2012).

Transient expression by means of viral vectors avoids plant stable transformation, which is a work-intensive and time-consuming process, obtaining the product easily in just a few days in a highly scalable manner (Gleba et al., 2007; Molina-Hidalgo et al., 2021; Peyret and Lomonossoff, 2015). Plant viruses constitute a threat in agriculture as they are a major cause of global crop losses (Jones and Naidu, 2019), not only affecting economically but also socially (Jones, 2021). Despite having small genomes, these obligate parasites are able to synthetize massive amount of proteins after hijacking the host cell machinery (Balke and Zeltins, 2019). As a consequence, plant virologists have been inspired to take advantage of this unique feature of redirecting the biosynthetic capacity of the host cell (Balke and Zeltins, 2019) as the basis to fulfil numberless applications (Abrahamian et al., 2020; McGarry et al., 2017; Pasin et al., 2019; Sainsbury et al., 2010; Wang et al., 2020). Therefore, intensive viral research motivated by their devastating effects has led into generation of viral vectors engineered to transiently express heterologous proteins, enzymes, transcription factors, or used as scaffolds to present epitopes or deliver cargo (Hefferon, 2012; Sainsbury and Lomonossoff, 2014; Wang et al., 2020). The successful development of these viral vectors changed totally some of the negative perceptions of plant viruses (Dawson et al., 2015; Pogue et al., 2002).

What can viruses do for us? The 'make an ally from an enemy' tale

Plants constitute natural sources of a great number of specialized secondary metabolites (Mohammadinejad et al., 2019). Consequently, massive efforts have been made to understand their metabolic pathways, and many attempts have been undertaken to manipulate them using transgenic techniques to induce the production

of health-promoting compounds (Farré et al., 2014; Martin and Li, 2017; Torres-Montilla and Rodriguez-Concepcion, 2021). Viruses represent an attractive option to do this, even though some limitations arise. There are promising previous results with potyvirus-based expression vectors for the induction of compounds with antioxidant properties (Bedoya et al., 2010, 2012; Cordero et al., 2017b; Majer et al., 2017).

Based on these previous results, the first goal of this work aimed to produce specific carotenoids species by using a viral expression system. For this purpose, the cDNAs of carotenoid cleavage dioxygenase (CCD) enzymes from *Crocus sativus* (CsCCD2L) and *Buddleja davidii* (BdCCD4.1) were inserted into a TEV-based vector lacking the NIb cistron, and *N. benthamiana* used as biofactories (Chapter 1). Apocarotenoids present in saffron have been shown to have health-promoting properties, but its high cost derived from its scarcity and manual harvest hinder their use in the pharmaceutical sector. After metabolic analysis of symptomatic yellow tissue (Chapter 1, Fig. 2B), results showed that the only virus-driven expression of CsCCD2L was enough for the notable production of safranal, 0.2% of crocins and 0.8% of picrocrocin in leaf DW (Chapter 1, Fig. 5, 7A and 7B), in only 13 days. *Pantoea ananatis* crtB (PaCrtB), saffron β-carotene hydroxylase 2 (CsBCH2) (Ahrazem et al., 2016), as well as a non-carotenoid transporter, the saffron lipid transfer protein 1 (CsLTP1) (Wang et al., 2016a) were co-expressed with CsCCD2L to further improve the apocarotenoid content. CsCCD2/PaCrtB or CsCCD2/CsBCH2 co-expression led to an increase of crocins up to 1.9 and 1.6 fold, respectively, reaching 0.35% in leaves DW for the former (Chapter 1, Fig. 8C). Furthermore, knowing the presence of promiscuous orthologue enzymes present in *N. benthamiana* that allow the trigger of biosynthesis of distinct apocarotenoids by the expression of a single CCD, this system could be improved even more in the future. Namely, increasing the amount of the crocetin precursor, zeaxanthin, could boost the apocarotenoid biosynthesis (Diretto et al., 2019; Lagarde et al., 2000; Römer et al., 2002). This may be accomplished through the overexpression of early or late structural genes to increase the flux of the carotenoid pathway, as this work shows for the phytoene synthase (PSY in plants and crtB in *P. ananatis*) a rate-limiting enzyme of carotenoid biosynthesis pathway. Phytoene desaturase (PDS), z-carotene desaturase (ZDS) and carotene isomerase (CRTISO) have also been reported to have potential to improve carotenoid content and stress

tolerance (Li et al., 2020). A very recent study on transgenic tomato highlights the potential of CCD2L with a pair of glucosyltransferases (UGTs) for the apocarotenoid production in fruits. So far, this is the highest report on saffron apocarotenoids produced in heterologous systems, 14.5 and 2.9 mg/g DW of crocins and picrocrocin, respectively (Ahrazem et al., 2022). Therefore, UGTs could be also assessed using our viral system. Alternatively, interest has been turned out lately to the Orange protein and its interaction with PSY during carotenoid accumulation. Accordingly, the *Orange* (*OR*) gene could be assessed also to enhance carotenoid levels in future attempts (Osorio, 2019). *Arabidopsis thaliana OR* (*AtOR)* has been demonstrated to promote carotenoid accumulation by inducing the formation of carotenoid-sequestering plastoglobuli only when the carotenoid pool is limited. This was tested in transgenic corn lines where its expression led to a 32-fold increase in carotenoids with respect to the controls with no changes of the rest of the metabolic composition (Berman et al., 2017). This was also reported in sweet potato by increasing β-carotene levels 186-fold in their storage roots (Kim et al., 2021). Hence, these enzymes could be tested in the viral system to assess if they improve the amount of apocarotenoids produced. In addition, another possibility arises as alternative to transgenesis, editing of plant lines to have a knocked-out ZEP or LCY-ε, which oppose zeaxanthin accumulation, as well as editing the orthologue genes involved in the carotenoid pathway mimicking other well-known to enhance carotenoid accumulation as the *OR* gene (Endo et al., 2019). A VIGE technology has recently been developed to deliver CRISPR components enabling DNA-free genome editing at the whole-plant level through using viral vectors, thus avoiding stable transformation (Uranga et al., 2021a, 2021b). By means of two compatible RNA virus vectors, TEV and PVX, it was possible the expression of a Cas12a nuclease and the corresponding guide RNA, respectively (Uranga et al., 2021b). Consequently, this approach could be exploited to obtained *N. benthamiana* edited lines of great interest for molecular farming purposes, to potentially achieve higher accumulations of certain metabolites of interest.

Even though the quantity of apocarotenoids produced here are below those that accumulate in natural sources, this viral system still represents an attractive alternative for the sustainable production of valuable saffron apocarotenoids. Large amount of *N.*

benthamiana infected tissue can be easily and rapidly obtained with the virus-driven system after only two weeks in adult *N. benthamiana* plants, in contrast to the costly harvest of saffron stigmas or the low accumulation in *Buddleja* spp. flowers.

Considering these encouraging results after the tailored induction of carotenoids, in this work we wanted to go further in another fascinating metabolic pathway (Chapter 2). Curcuminoids, polyphenols from turmeric (*Curcuma longa* L.) rhizome, have gained great interest in the last years, especially curcumin as it seems to protect against the development of several human chronic diseases (Prasad et al., 2014; Salehi et al., 2019). However, metabolic engineering normally does not only require the action of one enzyme, but more in the same cell to achieve the production of a desired metabolite. Consequently, the next goal was to study the possibility of expressing more than one enzyme involved in the curcuminoid biosynthetic pathway in order to obtain turmeric metabolites. Derived from previous data, for the expression of turmeric curcuminoids at least two enzymes were required, *C. longa* diketide-CoA synthase 1 (DCS1) and curcumin synthase 3 (CURS3). Limited by the cargo capacity of viral vectors, the employment of two non-related viral vectors was initially proposed for the coordinated expression of more than one product needed in the same cell. The phenomenon known as viral exclusion has been documented since its discovery almost 90 years ago. Plants infected with a mild isolate of a virus prevent the infection against a more severe isolate from the same virus or related ones, but remain susceptible to more distant viruses (Sainsbury et al., 2012; Zhang et al., 2018b). This highly specific self-discriminatory circumstance on the same cells confers cross protection to host plants and hence has been used to manage many virus diseases in crops. Accordingly, when designing a system based on multiple viral vectors, viral exclusion is crucial and must be taken into consideration for the choice of the involved viruses. The dual system here developed was based on two compatible positive-stranded RNA viral species, TEV and PVX, non-phylogenetically related, belonging to different families and able to co-infect the same cells (Zhang et al., 2018a).

Once confirmed the possibility of using TEV and PVX efficiently at the same time in an experimental setup with fluorescent proteins (Chapter 2, Fig. 3), two curcuminoid enzymes were cloned in these viral vectors. Using a multigene engineering approach in *N. benthamiana* as biofactory once more, *C. longa* DCS1 and CURS3 were co-

expressed using TEV in combination with PVX. After 8 dpi, mild yellow coloration was revealed in plants inoculated with TEVΔN-DCS1 and PVX-CURS3. Metabolic analysis at 13 dpi demonstrated the induction of curcuminoids as curcumin, dihydrocurcumin, dihydro-demethoxycurcumin, demethoxycurcumin, dihydro-bisdemethoxycurcumin and bisdemethoxycurcumin (Chapter 2, Fig. 3). Sequential inoculation turned out to be more effective that co-inoculation in the curcumin production after its absolute quantification. Although the dual system was successful, higher yields of the appreciated curcumin were expected. For that reason, we went back to the TEV-based vector (Bedoya et al., 2010) used previously in some successful metabolic engineering approaches (Llorente et al., 2020; Majer et al., 2017; Martí et al., 2020). This technology aimed to make more room for exogenous sequences with the replacement of the viral NIb cistron (~1.6 kb), and to produce the heterologous protein in an amount equimolar to the other viral proteins. DCS1 and CURS3 are ~1.2 kb each, resulting in almost 2.4 kb of extra genetic information, which makes TEVΔNIb even more interesting. Using just one viral system, TEVΔN-DCS1-CURS3 was able to increase 2-fold the curcumin accumulation up to 12 µg/g DW in infected leaves compared to the dual viral complex. Then, trying to further increase the curcumin accumulation, the addition of another enzyme, *N. tabacum* CCoAOMT-1 expressed from PVX was evaluated, but contrary to our hypothesis, there was no improvement. After a time-course analysis, TEVΔN-DCS1-CURS3 allowed the maximum accumulation at 11 dpi with 22 ± 4 µg/g DW. Other heterologous systems that may have had better outcomes, as bacteria (Couto et al., 2017; Rodrigues et al., 2020) or yeast (Kan et al., 2019), face much higher costs than growing plants. Besides, natural curcumin from turmeric rhizomes also differs enormously from varieties and its extraction process makes it harder to obtain. In any case, the virus-based curcumin production process needs to be optimized to reach higher concentrations of curcumin. Furthermore, it has been reported that the curcuminoid production using caffeic acid O-methyltransferase (COMT), which converts caffeic acid to ferulic acid, is significantly higher than that using CCoAOMT, which converts caffeoyl-CoA to feruloyl-CoA. The highest production of curcumin has been obtained from ferulic acid using COMT, 1529 µM of curcuminoids (563 mg/L) (Rodrigues et al., 2020). Hence, the use of this enzyme in the viral system could improve the final outcome of this biosynthetic pathway. Heterologous curcuminoid

production in plants is still a challenging but attractive alternative to the complex extractions required from its natural source (Yixuan et al., 2021).

In conclusion, again, regardless the low amount of curcuminoids obtained, the virus-approach reported in this thesis may still be a reasonable source of valuable curcuminoids, as it involves easy and quick techniques to obtain practically constant and unlimited amounts of infected *N. benthamiana* tissues. In sum, results presented in Chapter 1 and Chapter 2 highlighted that the introduction of novel genes, and not necessarily the whole pathway, is enough to trigger the synthesis of specific compounds that normally are not produced in the plant cell, as previously anticipated (Arya et al., 2020). Apart from using relevant scientific plants as *N. benthamiana*, other agronomic crop plants could be also assessed.

Besides expressing proteins or rewiring the cell metabolism, viruses can also be used as scaffolds for nanoparticle production. Nanotechnology is a growing sector that has recently focused on viruses as building blocks for a great deal of applications, namely production of vaccine candidates, targeted imaging or drug delivery (Chung et al., 2021; Lico et al., 2015; Rybicki, 2020). If inserted in a suitable place on the virus CP, capsids can turn into excellent epitope presenting systems. Potential applications derived from antibody exposure can be fulfilled, but the smaller nanobodies are growing in the market as promising therapeutic and diagnostic tools. The last objective of this thesis was to produce genetically encoded potyvirus VNPs for nanobody display in plant biofactories as an alternative platform for bionanomaterials (Chapter 3).

Nanobodies display exceptional advantages in research, as diagnostics or therapeutics against human diseases or in agricultural application. In addition, the effect of nanobodies might be further improved if combined with other treatments (De Coninck et al., 2017; Oliveira et al., 2013; Salvador et al., 2019; Wang et al., 2020). Elongated virions, as those of potyviruses, may have some advantages respect to icosahedral counterparts in medical applications. In fact, a growing number of results suggests that anisotropic materials with high aspect ratios (length/width) might be more suitable for drug delivery. More specifically, higher peptide display, larger contact surface area, better tissue penetration and chance to better resist immune detection outstand as the main advantages from elongated nanoparticles. These characteristics lead to a more efficient display and interaction between the functional modules and the

targeted receptors, increasing the success possibilities in terms of diagnosis or treatment in medicine (Bruckman et al., 2014; González-Gamboa et al., 2017; Le et al., 2019a; Shukla et al., 2015). This is the reason why VNPs derived from the potyvirus ZYMV were functionalized with a nanobody via genetic fusion and produced in zucchini plants. A picornavirus 2A splicing peptide (F2A) between the fused proteins was absolutely necessary to generate a VNP with a mixed population of decorated and wt CPs (ZYMVΔ-αGFP-F2A) (Chapter 3, Fig. 3). The beneficial effect of 2A peptides to produce plant virus-derived nanoparticles was previously reported (Dickmeis et al., 2015; Kim et al., 2011; Uhde-Holzem et al., 2010). *N. benthamiana* is the preferred production platform in plant molecular farming (Goulet et al., 2019; Peyret and Lomonossoff, 2015). To explore this host, a second potyvirus, TEV, was chosen (Chapter 3, Fig. 5). Contrary to ZYMV, fully-decorated TEV VNPs were remarkably assembled without the need of a 2A peptide by direct fusion of the nanobody to the CP. As a proof of concept, both systems presented nanobodies against the green fluorescent protein (GFP) by means of a truncated ZYMV CP, as previously reported (Arazi et al., 2001a), or a full-lentth TEV CP.

The correct assembly of VNPs and binding efficacy was confirmed (Chapter 3, Figs. 4 and 5). Improving yield of VNP production, as well as demonstrating the decoration by immunodetection in TEM analyses, will be objectives for the future. In this work the modification of two potyviruses by genetic engineering was achieved for the display of a 117 residue epitope as direct CP fusion, the maximum ever reported so far to our knowledge without impairing virus assembly (Röder et al., 2018; Uhde-holzem et al., 2016). Successful results suggest that these potyvirus-derived nanoparticles can be used as presentation scaffold for other functional nanobodies and even multifunctional features. Specifically in medicine, several efforts are being made to avoid off-target effects in cancer treatment (Chung et al., 2020; Thuenemann et al., 2021); VNPs may contribute to the target delivery or imaging in cancer treatment and research. In sum, these genetically encoded nanomaterials as scaffolds for nanobody presentation may represent a mighty tool to be far exploited in several fields.

So now… what is next? The bright future of plant viruses in biotechnology

Nowadays, there is no doubt that remarkable advancements have been undertaken in biotechnology. This will be an essential discipline to face the long-term global challenges as the burden of climate change or the need to feed an ever-growing population. Transgenesis, or more recently genome editing, have emerged to obtain plants more productive, providing healthier food, and more resistant to abiotic or biotic stresses. In the sight of a climate change scenario, we need plants to produce not as currently they are producing but even more. Besides, there is also needed a reduction in the use of pesticides or fertilizers which contaminate animals and the environment. Consequently, biotechnology can help to achieve those goals.

Considerable efforts have been taken to increase the nutritional content of the food we eat or to obtain proteins and compounds of nutraceutical, pharmaceutical or industrial interest in a sustainable and easy manner. In particular, plant viruses have been long studied as they are responsible for nearly half of all plant diseases causing enormous losses in agriculture. As addressed in this work, they can also be conveniently employed for many beneficial applications (Abrahamian et al., 2020; Pasin et al., 2019; Wang et al., 2020). The work shown in this thesis tries to harness some viral vectors for the tailored rewirement of plant metabolism obtaining metabolites of interest and for their use as scaffolds for nanobody presentation. Achievements serve as illustration about what can be potentially done with this alternative technology in the future.

Products made in plants offer numerable advantages over their synthetic counterparts (Arya et al., 2020; Chouhan et al., 2017), and viral vector can help to reach those goals. In chapters 1 and 2, defective TEV clones were used, which lack the NIb cistron, the RNA-dependent RNA polymerase, known for being able to be supplemented in trans (Bedoya et al., 2010; Li and Carrington, 1995). Therefore, these viral vectors are unable to replicate autonomously in wild-type plants. They only replicate in transgenic *N. benthamiana* plants expressing this NIb, as a biosafety measure. In any case, and particularly for viral vectors that are infectious itself, these biotechnological tools must be used wisely only under authorised and controlled environments. This approach is not exempted from controversy, though. There may be

a debate in the society when it comes to the use of genetically altered full-competent plant viruses that can spread into the environment, as with other technologies as transgenesis or gene editing.

To sum up, ‘with great power comes great responsibility’, the convenient use of plant viruses can uncover fascinating applications that were never imagined before and ‘bring good out of bad’. Throughout this thesis we have seen how viruses can turn from foes to friends. The works presented here clearly reflect the versatility of plant viruses as biotechnological tools. Nevertheless, more extensive research still needs to be addressed in the plant virus biotechnology field to unravel novel goals with these little fellows.

CONCLUSIONS

1. The sole expression of an appropriate carotenoid cleavage dioxygenase (CCD) using a tobacco etch virus (TEV)-driven system in *Nicotiana benthamiana* plants is able to trigger the production of remarkable amounts of highly appreciated apocarotenoids, such as crocins and picrocrocin, in less than two weeks.

2. The expression of *Crocus sativus* CsCCD2L led to a higher apocarotenoid accumulation compared to the *Buddleja davidii* BdCCD4.1. An improvement of the apocarotenoid content was achieved when CsCCD2L was co-expressed with other carotenogenic enzymes using the same system, especially with *Pantoea ananatis* phytoene synthase (PaCrtB), but also with saffron β-carotene hydroxylase 2 (BCH2).

3. A multigene engineering strategy allowed the heterologous production of turmeric curcuminoids in adult *N. benthamiana* plants in less than two weeks. To achieve this, *Curcuma longa* diketide-CoA synthase 1 (DCS1) and curcumin synthase 3 (CURS3) were co-expressed using vectors derived from TEV alone or in combination with a second compatible vector derived from potato virus X (PVX).

4. Sequential inoculation of TEV and PVX vectors was more efficient than co-inoculation to produce turmeric polyphenols. DCS1 and CURS3 co-expression using a single TEV vector was even better, leading to a 2-fold increase in curcumin accumulation.

5. Genetically encoded viral nanoparticles (VNPs) derived from two different potyviruses presenting a nanobody on their surface were successfully produced. These VNPs could be used as building blocks in nanotechnology, or in medicine for diagnostic or therapeutic purposes.

6. Zucchini yellow mosaic virus (ZYMV)-derived VNPs needed a picornavirus 2A splicing peptide between the CP and the nanobody against the green fluorescent protein (GFP) to assemble, contrary to the VNPs derived from TEV. The morphology and functionality of both systems was confirmed.

7. The works here presented related with the virus-driven production of appreciated metabolites and the use of plant viruses as nanoparticles for many purposes; demonstrating that viruses, safely manipulated, can turn into powerful tools in biotechnology.

REFERENCES

REFERENCES

Abrahamian, P., Hammond, R.W., Hammond, J., 2020. Plant Virus-Derived Vectors: Applications in Agricultural and Medical Biotechnology. Annu. Rev. Virol. 7, 513–535. https://doi.org/10.1146/annurev-virology-010720-054958

Agrawal, S., Karcher, D., Ruf, S., Erban, A., Hertle, A.P., Kopka, J., Bock, R., 2022. Riboswitch-mediated inducible expression of an astaxanthin biosynthetic operon in plastids. Plant Physiol. 188, 637–652. https://doi.org/10.1093/plphys/kiab428

Ahrazem, O., Diretto, G., Rambla, J.L., Rubio-moraga, Á., Lobato, M., Frusciante, S., Argandoña, J., Presa, S., Granell, A., Gómez-Gómez, L., 2022. Engineering high levels of saffron apocarotenoids in tomato. Hortic. Res. uhac074. https://doi.org/10.1093/hr/uhac074

Ahrazem, O., Rubio-Moraga, A., Berman, J., Capell, T., Christou, P., Zhu, C., Gómez-Gómez, L., 2016. The carotenoid cleavage dioxygenase CCD2 catalysing the synthesis of crocetin in spring crocuses and saffron is a plastidial enzyme. New Phytol. 209, 650–663. https://doi.org/10.1111/nph.13609

Akter, J., Hossain, M.A., Takara, K., Islam, M.Z., Hou, D.X., 2019. Antioxidant activity of different species and varieties of turmeric (Curcuma spp): Isolation of active compounds. Comp. Biochem. Physiol. Part - C Toxicol. Pharmacol. 215, 9–17. https://doi.org/10.1016/j.cbpc.2018.09.002

Albuquerque, B.R., Heleno, S.A. 8., Oliveira, M.B.P.P., Barros, L., Ferreira, I.C.F.R., 2021. Phenolic compounds: Current industrial applications, limitations and future challenges. Food Funct. 12, 14–29. https://doi.org/10.1039/d0fo02324h

Alemzadeh, E., Dehshahri, A., Izadpanah, K., Ahmadi, F., 2018. Plant virus nanoparticles: Novel and robust nanocarriers for drug delivery and imaging. Colloids Surfaces B Biointerfaces 167, 20–27. https://doi.org/10.1016/j.colsurfb.2018.03.026

Altunay, B., Morgenroth, A., Beheshti, M., Vogg, A., Wong, N.C.L., Ting, H.H., Biersack, H.J., Stickeler, E., Mottaghy, F.M., 2021. HER2-directed antibodies, affibodies and nanobodies as drug-delivery vehicles in breast cancer with a specific focus on radioimmunotherapy and radioimmunoimaging. Eur. J. Nucl. Med. Mol. Imaging 48, 1371–1389. https://doi.org/10.1007/s00259-020-05094-1

Arazi, T., Shiboleth, Y.M., Gal-On, A., 2001a. A Nonviral Peptide Can Replace the Entire N Terminus of Zucchini Yellow Mosaic Potyvirus Coat Protein and Permits Viral Systemic Infection. J. Virol. 75, 6329–6336. https://doi.org/10.1128/jvi.75.14.6329-6336.2001

Arazi, T., Slutsky, S.G., Shiboleth, Y.M., Wang, Y., Rubinstein, M., Barak, S., Yang, J., Gal-On, A., 2001b. Engineering zucchini yellow mosaic potyvirus as a non-pathogenic vector for expression of heterologous proteins in cucurbits. J. Biotechnol. 87, 67–82. https://doi.org/10.1016/S0168-1656(01)00229-2

Arias, D., Arenas-M, A., Flores-Ortiz, C., Peirano, C., Handford, M., Stange, C., 2021. Daucus carota DcPSY2 and DcLCYB1 as Tools for Carotenoid Metabolic Engineering to Improve the Nutritional Value of Fruits. Front. Plant Sci. 12, 1–15. https://doi.org/10.3389/fpls.2021.677553

Arya, S.S., Rookes, J.E., Cahill, D.M., Lenka, S.K., 2020. Next-generation metabolic engineering approaches towards development of plant cell suspension cultures as specialized metabolite producing biofactories. Biotechnol. Adv. 45, 107635. https://doi.org/10.1016/j.biotechadv.2020.107635

Ashrafizadeh, M., Rafiei, H., Mohammadinejad, R., Afshar, E.G., Farkhondeh, T., Samarghandian, S., 2020. Potential therapeutic effects of curcumin mediated by JAK/STAT signaling pathway: A review. Phyther. Res. 34, 1745–1760. https://doi.org/10.1002/ptr.6642

Bailon Calderon, H., Yaniro Coronel, V.O., Cáceres Rey, O.A., Colque Alave, E.G., Leiva Duran, W.J., Padilla Rojas, C., Montejo Arevalo, H., García Neyra, D., Galarza Pérez, M., Bonilla, C., Tintaya, B., Ricciardi, G., Smiejkowska, N., Romão, E., Vincke, C., Lévano, J., Celys, M., Lomonte, B., Muyldermans, S., 2020. Development of Nanobodies Against Hemorrhagic and Myotoxic

Components of Bothrops atrox Snake Venom. Front. Immunol. 11, 1–12. https://doi.org/10.3389/fimmu.2020.00655

Balke, I., Zeltins, A., 2019. Use of plant viruses and virus-like particles for the creation of novel vaccines. Adv. Drug Deliv. Rev. 145, 119–129. https://doi.org/10.1016/j.addr.2018.08.007

Bawa, A.S., Anilakumar, K.R., 2013. Genetically modified foods: Safety, risks and public concerns - A review. J. Food Sci. Technol. 50, 1035–1046. https://doi.org/10.1007/s13197-012-0899-1

Beauchemin, C., Bougie, V., Laliberté, J.F., 2005. Simultaneous production of two foreign proteins from a potyvirus-based vector. Virus Res. 112, 1–8. https://doi.org/10.1016/j.virusres.2005.03.001

Bedoya, L., Martínez, F., Rubio, L., Daròs, J.A., 2010. Simultaneous equimolar expression of multiple proteins in plants from a disarmed potyvirus vector. J. Biotechnol. 150, 268–275. https://doi.org/10.1016/j.jbiotec.2010.08.006

Bedoya, L.C., Daròs, J.A., 2010. Stability of Tobacco etch virus infectious clones in plasmid vectors. Virus Res. 149, 234–240. https://doi.org/10.1016/j.virusres.2010.02.004

Bedoya, L.C., Martínez, F., Orzáez, D., Daròs, J.A., 2012. Visual tracking of plant virus infection and movement using a reporter MYB transcription factor that activates anthocyanin biosynthesis. Plant Physiol. 158, 1130–1138. https://doi.org/10.1104/pp.111.192922

Berardi, A., Evans, D.J., Baldelli Bombelli, F., Lomonossoff, G.P., 2018. Stability of plant virus-based nanocarriers in gastrointestinal fluids. Nanoscale 10, 1667–1679. https://doi.org/10.1039/c7nr07182e

Berman, J., Zorrilla-López, U., Medina, V., Farré, G., Sandmann, G., Capell, T., Christou, P., Zhu, C., 2017. The Arabidopsis ORANGE (AtOR) gene promotes carotenoid accumulation in transgenic corn hybrids derived from parental lines with limited carotenoid pools. Plant Cell Rep. 36, 933–945. https://doi.org/10.1007/s00299-017-2126-z

Bisht, K., Wagner, K.H., Bulmer, A.C., 2010. Curcumin, resveratrol and flavonoids as anti-inflammatory, cyto- and DNA-protective dietary compounds. Toxicology 278, 88–100. https://doi.org/10.1016/j.tox.2009.11.008

Blancquaert, D., Van Daele, J., Strobbe, S., Kiekens, F., Storozhenko, S., De Steur, H., Gellynck, X., Lambert, W., Stove, C., Van Der Straeten, D., 2015. Improving folate (Vitamin B 9) stability in biofortified rice through metabolic engineering. Nat. Biotechnol. 33, 1076–1078. https://doi.org/10.1038/nbt.3358

Bonet, M.L., Canas, J.A., Ribot, J., Palou, A., 2016. Carotenoids in adipose tissue biology and obesity, Sub-Cellular Biochemistry. https://doi.org/10.1007/978-3-319-39126-7_15

Bonning, B.C., Pal, N., Liu, S., Wang, Z., Sivakumar, S., Dixon, P.M., King, G.F., Miller, W.A., 2014. Toxin delivery by the coat protein of an aphid-vectored plant virus provides plant resistance to aphids. Nat. Biotechnol. 32, 102–105. https://doi.org/10.1038/nbt.2753

Bruckman, M.A., Czapar, A.E., VanMeter, A., Randolph, L.N., Steinmetz, N.F., 2016. Tobacco mosaic virus-based protein nanoparticles and nanorods for chemotherapy delivery targeting breast cancer. J. Control. Release 231, 103–113. https://doi.org/10.1016/j.jconrel.2016.02.045

Bruckman, M.A., Hern, S., Jiang, K., Flask, C.A., Yu, X., Steinmetz, N.F., 2013. Tobacco mosaic virus rods and spheres as supramolecular high-relaxivity MRI contrast agents. J. Mater. Chem. B 1, 1482–1490. https://doi.org/10.1039/c3tb00461a

Bruckman, M.A., Randolph, L.N., VanMeter, A., Hern, S., Shoffstall, A.J., Taurog, R.E., Steinmetz, N.F., 2014. Biodistribution, pharmacokinetics, and blood compatibility of native and PEGylated tobacco mosaic virus nano-rods and -spheres in mice. Virology 449, 163–173. https://doi.org/10.1016/j.virol.2013.10.035

Butelli, E., Titta, L., Giorgio, M., Mock, H.P., Matros, A., Peterek, S., Schijlen, E.G.W.M., Hall, R.D., Bovy, A.G., Luo, J., Martin, C., 2008. Enrichment of tomato fruit with health-promoting anthocyanins by expression of select transcription factors. Nat. Biotechnol. 26, 1301–1308. https://doi.org/10.1038/nbt.1506

Buyel, J.F., 2019. Plant molecular farming – Integration and exploitation of side streams to achieve

sustainable biomanufacturing. Front. Plant Sci. 9, 1–17. https://doi.org/10.3389/fpls.2018.01893
Cai, H., Shukla, S., Steinmetz, N.F., 2020. The Antitumor Efficacy of CpG Oligonucleotides is Improved by Encapsulation in Plant Virus-Like Particles. Adv. Funct. Mater. 30, 1–11. https://doi.org/10.1002/adfm.201908743
Cai, H., Shukla, S., Wang, C., Masarapu, H., Steinmetz, N.F., 2019. Heterologous Prime-Boost Enhances the Antitumor Immune Response Elicited by Plant-Virus-Based Cancer Vaccine. J. Am. Chem. Soc. 141, 6509–6518. https://doi.org/10.1021/jacs.9b01523
Cao, J., Guenther, R.H., Sit, T.L., Lommel, S.A., Opperman, C.H., Willoughby, J.A., 2015. Development of abamectin loaded plant virus nanoparticles for efficacious plant parasitic nematode control. ACS Appl. Mater. Interfaces 7, 9546–9553. https://doi.org/10.1021/acsami.5b00940
Capell, T., Twyman, R.M., Armario-Najera, V., Ma, J.K.C., Schillberg, S., Christou, P., 2020. Potential Applications of Plant Biotechnology against SARS-CoV-2. Trends Plant Sci. 25, 635–643. https://doi.org/10.1016/j.tplants.2020.04.009
Carrington, J.C., Haldeman, R., Dolja, V. V, Restrepo-Hartwig, M.A., 1993. Internal cleavage and trans-proteolytic activities of the VPg-proteinase (NIa) of tobacco etch potyvirus in vivo. J. Virol. 67, 6995–7000. https://doi.org/10.1128/jvi.67.12.6995-7000.1993
Chilton, M.D., Drummond, M.H., Merlo, D.J., Sciaky, D., Montoya, A.L., Gordon, M.P., Nester, E.W., 1977. Stable incorporation of plasmid DNA into higher plant cells: the molecular basis of crown gall tumorigenesis. Cell 11, 263–271. https://doi.org/10.1016/0092-8674(77)90043-5
Chouhan, S., Sharma, K., Zha, J., Guleria, S., Koffas, M.A.G., 2017. Recent advances in the recombinant biosynthesis of polyphenols. Front. Microbiol. 8. https://doi.org/10.3389/fmicb.2017.02259
Chung, Y.H., Cai, H., Steinmetz, N.F., 2020. Viral nanoparticles for drug delivery, imaging, immunotherapy, and theranostic applications. Adv. Drug Deliv. Rev. 156, 214–235.
Chung, Y.H., Church, D., Koellhoffer, E.C., Steinmetz, N.F., 2021. Integrating plant molecular farming and materials research for next- generation vaccines. Nat. Rev. Mater. https://doi.org/10.1038/s41578-021-00399-5
Cordero, T., Cerdan, L., Carbonell, A., Katsarou, K., Kalantidis, K., Daròs, J.A., 2017a. Dicer-like 4 is involved in restricting the systemic movement of zucchini yellow mosaic virus in nicotiana benthamiana. Mol. Plant-Microbe Interact. 30, 63–71. https://doi.org/10.1094/MPMI-11-16-0239-R
Cordero, T., Mohamed, M.A., López-Moya, J.J., Daròs, J.A., 2017b. A recombinant Potato virus Y infectious clone tagged with the Rosea1 visual marker (PVY-Ros1) facilitates the analysis of viral infectivity and allows the production of large amounts of anthocyanins in plants. Front. Microbiol. 8, 1–11. https://doi.org/10.3389/fmicb.2017.00611
Couto, M.R., Rodrigues, J.L., Rodrigues, L.R., 2017. Optimization of fermentation conditions for the production of curcumin by engineered Escherichia coli. J. R. Soc. Interface 14, 1–8. https://doi.org/10.1098/rsif.2017.0470
Czapar, A.E., Zheng, Y.R., Riddell, I.A., Shukla, S., Awuah, S.G., Lippard, S.J., Steinmetz, N.F., 2016. Tobacco Mosaic Virus Delivery of Phenanthriplatin for Cancer therapy. ACS Nano 10, 4119–4126. https://doi.org/10.1021/acsnano.5b07360
Daniell, H., Streatfield, S.J., Wycoff, K., 2001. Medical molecular farming: Production of antibodies, biopharmaceuticals and edible vaccines in plants. Trends Plant Sci. 6, 219–226. https://doi.org/10.1016/S1360-1385(01)01922-7
Das, P., Adak, S., Lahiri Majumder, A., 2020. Genetic Manipulation for Improved Nutritional Quality in Rice. Front. Genet. 11, 1–19. https://doi.org/10.3389/fgene.2020.00776
Dawson, W.O., Bar-Joseph, M., Garnsey, S.M., Moreno, P., 2015. Citrus Tristeza Virus: Making an Ally from an Enemy. Annu. Rev. Phytopathol. 53, 137–155. https://doi.org/10.1146/annurev-phyto-080614-120012
de Araújo, F.F., de Paulo Farias, D., Neri-Numa, I.A., Pastore, G.M., 2021. Polyphenols and their applications: An approach in food chemistry and innovation potential. Food Chem. 338, 127535. https://doi.org/10.1016/j.foodchem.2020.127535

REFERENCES

De Coninck, B., Verheesen, P., Vos, C.M., Van Daele, I., De Bolle, M.F., Vieira, J. V., Peferoen, M., Cammue, B.P.A., Thevissen, K., 2017. Fungal glucosylceramide-specific camelid single domain antibodies are characterized by broad spectrum antifungal activity. Front. Microbiol. 8, 1–10. https://doi.org/10.3389/fmicb.2017.01059

De Meyer, T., Muyldermans, S., Depicker, A., 2014. Nanobody-based products as research and diagnostic tools. Trends Biotechnol. 32, 263–270. https://doi.org/10.1016/j.tibtech.2014.03.001

Demurtas, O.C., Frusciante, S., Ferrante, P., Diretto, G., Azad, N.H., Pietrella, M., Aprea, G., Taddei, A.R., Romano, E., Mi, J., Al-Babili, S., Frigerio, L., Giuliano, G., 2018. Candidate enzymes for saffron crocin biosynthesis are localized in multiple cellular compartments. Plant Physiol. 177, 990–1006. https://doi.org/10.1104/pp.17.01815

Dickmeis, C., Honickel, M.M.A., Fischer, R., Commandeur, U., 2015. Production of hybrid chimeric PVX particles using a combination of TMV and PVX-based expression vectors. Front. Bioeng. Biotechnol. 3, 1–12. https://doi.org/10.3389/fbioe.2015.00189

Diego-Martin, B., González, B., Vazquez-Vilar, M., Selma, S., Mateos-Fernández, R., Gianoglio, S., Fernández-del-Carmen, A., Orzáez, D., 2020. Pilot Production of SARS-CoV-2 Related Proteins in Plants: A Proof of Concept for Rapid Repurposing of Indoor Farms Into Biomanufacturing Facilities. Front. Plant Sci. 11. https://doi.org/10.3389/fpls.2020.612781

Dietrich, C., Maiss, E., 2003. Fluorescent labelling reveals spatial separation of potyvirus populations in mixed infected Nicotiana benthamiana plants. J. Gen. Virol. 84, 2871–2876. https://doi.org/10.1099/vir.0.19245-0

Diretto, G., Ahrazem, O., Rubio-Moraga, Á., Fiore, A., Sevi, F., Argandoña, J., Gómez-Gómez, L., 2019. UGT709G1: a novel uridine diphosphate glycosyltransferase involved in the biosynthesis of picrocrocin, the precursor of safranal in saffron (Crocus sativus). New Phytol. 224, 725–740. https://doi.org/10.1111/nph.16079

Diretto, G., Al-Babili, S., Tavazza, R., Papacchioli, V., Beyer, P., Giuliano, G., 2007. Metabolic engineering of potato carotenoid content through tuber-specific overexpression of a bacterial mini-pathway. PLoS One 2, e350. https://doi.org/10.1371/journal.pone.0000350

Edgar, R., Taylor, J., Lin, V., Altman, T., Barbera, P., Meleshko, D., Lohr, D., Novakovsky, G., Buchfink, B., Al-Shayeb, B., Banfield, J., de la Peña, M., Korobeynikov, A., Chikhi, R., Babaian, A., 2022. Petabase-scale sequence alignment catalyses viral discovery. Nature 602, 142–147. https://doi.org/10.1038/s41586-021-04332-2

Edgue, G., Twyman, R.M., Beiss, V., Fischer, R., Sack, M., 2017. Antibodies from plants for bionanomaterials. Wiley Interdiscip. Rev. Nanomedicine Nanobiotechnology 9. https://doi.org/10.1002/wnan.1462

Endo, A., Saika, H., Takemura, M., Misawa, N., Toki, S., 2019. A novel approach to carotenoid accumulation in rice callus by mimicking the cauliflower Orange mutation via genome editing. Rice 12, 1–5. https://doi.org/10.1186/s12284-019-0345-3

Esfandiari, N., Arzanani, M.K., Soleimani, M., Kohi-Habibi, M., Svendsen, W.E., 2016. A new application of plant virus nanoparticles as drug delivery in breast cancer. Tumor Biol. 37, 1229–1236. https://doi.org/10.1007/s13277-015-3867-3

Farré, G., Blancquaert, D., Capell, T., Van Der Straeten, D., Christou, P., Zhu, C., 2014. Engineering complex metabolic pathways in plants. Annu. Rev. Plant Biol. 65, 187–223. https://doi.org/10.1146/annurev-arplant-050213-035825

Fernández-Fernández, M.R., Mouriño, M., Rivera, J., Rodríguez, F., Plana-Durán, J., García, J.A., 2001. Protection of rabbits against rabbit hemorrhagic disease virus by immunization with the VP60 protein expressed in plants with a potyvirus-based vector. Virology 280, 283–291. https://doi.org/10.1006/viro.2000.0762

Fischer, R., Buyel, J.F., 2020. Molecular farming – The slope of enlightenment. Biotechnol. Adv. 40, 107519. https://doi.org/10.1016/j.biotechadv.2020.107519

Fischer, R., Schillberg, S., Hellwig, S., Twyman, R.M., Drossard, J., 2012. GMP issues for recombinant

plant-derived pharmaceutical proteins. Biotechnol. Adv. 30, 434–439. https://doi.org/10.1016/j.biotechadv.2011.08.007

Fresquet-Corrales, S., Roque, E., Sarrión-Perdigones, A., Rochina, M., López-Gresa, M.P., Díaz-Mula, H.M., Bellés, J.M., Tomás-Barberán, F., Beltrán, J.P., Cañas, L.A., 2017. Metabolic engineering to simultaneously activate anthocyanin and proanthocyanidin biosynthetic pathways in Nicotiana spp. PLoS One 12, 1–23. https://doi.org/10.1371/journal.pone.0184839

Frías-Sánchez, A.I., Quevedo-Moreno, D.A., Samandari, M., Tavares-Negrete, J.A., Sánchez-Rodríguez, V.H., González-Gamboa, I., Ponz, F., Alvarez, M.M., Trujillo-De Santiago, G., 2021. Biofabrication of muscle fibers enhanced with plant viral nanoparticles using surface chaotic flows. Biofabrication 13. https://doi.org/10.1088/1758-5090/abd9d7

Frusciante, S., Demurtas, O.C., Sulli, M., Mini, P., Aprea, G., Diretto, G., Karcher, D., Bock, R., Giuliano, G., 2022. Heterologous expression of Bixa orellana cleavage dioxygenase 4–3 drives crocin but not bixin biosynthesis . Plant Physiol. 188, 1469–1482. https://doi.org/10.1093/plphys/kiab583

Fuentes, S., Gibbs, A.J., Hajizadeh, M., Perez, A., Adams, I.P., Fribourg, C.E., Kreuze, J., Fox, A., Boonham, N., Jones, R.A.C., 2021. The phylogeography of potato virus x shows the fingerprints of its human vector. Viruses 13. https://doi.org/10.3390/v13040644

Gadhave, K.R., Gautam, S., Rasmussen, D.A., Srinivasan, R., 2020. Aphid Transmission of Potyvirus : The Largest Plant-infecting RNA virus genus. Viruses 12, 1–22.

Ghosh, S., Banerjee, S., Sil, P.C., 2015. The beneficial role of curcumin on inflammation, diabetes and neurodegenerative disease: A recent update. Food Chem. Toxicol. 83, 111–124. https://doi.org/10.1016/j.fct.2015.05.022

Gleba, Y., Klimyuk, V., Marillonnet, S., 2007. Viral vectors for the expression of proteins in plants. Curr. Opin. Biotechnol. 18, 134–141. https://doi.org/10.1016/j.copbio.2007.03.002

Gleba, Y., Marillonnet, S., Klimyuk, V., 2004. Engineering viral expression vectors for plants: The “full virus” and the “deconstructed virus” strategies. Curr. Opin. Plant Biol. 7, 182–188. https://doi.org/10.1016/j.pbi.2004.01.003

González-Gamboa, I., Manrique, P., Manrique, P., Ponz, F., 2017. Plant-made potyvirus-like particles used for log-increasing antibody sensing capacity. J. Biotechnol. 254, 17–24. https://doi.org/10.1016/j.jbiotec.2017.06.014

Goulet, M., Gaudreau, L., Gagné, M., Maltais, A., Michaud, D., 2019. Production of Biopharmaceuticals in Nicotiana benthamiana — Axillary Stem Growth as a Key Determinant of Total Protein Yield 10. https://doi.org/10.3389/fpls.2019.00735

Grützner, R., Schubert, R., Horn, C., Yang, C., Vogt, T., Marillonnet, S., 2021. Engineering Betalain Biosynthesis in Tomato for High Level Betanin Production in Fruits. Front. Plant Sci. 12, 1–17. https://doi.org/10.3389/fpls.2021.682443

Harada, H., Maoka, T., Osawa, A., Hattan, J.I., Kanamoto, H., Shindo, K., Otomatsu, T., Misawa, N., 2014. Construction of transplastomic lettuce (Lactuca sativa) dominantly producing astaxanthin fatty acid esters and detailed chemical analysis of generated carotenoids. Transgenic Res. 23, 303–315. https://doi.org/10.1007/s11248-013-9750-3

Harmsen, M.M., De Haard, H.J., 2007. Properties, production, and applications of camelid single-domain antibody fragments. Appl. Microbiol. Biotechnol. 77, 13–22. https://doi.org/10.1007/s00253-007-1142-2

He, M., He, C.Q., Ding, N.Z., 2022. Evolution of Potato virus X. Mol. Phylogenet. Evol. 167, 107336. https://doi.org/10.1016/j.ympev.2021.107336

Hefferon, K., 2017. Plant virus expression vectors: A powerhouse for global health. Biomedicines 5. https://doi.org/10.3390/biomedicines5030044

Hefferon, K.L., 2012. Plant virus expression vectors set the stage as production platforms for biopharmaceutical proteins. Virology 433, 1–6. https://doi.org/10.1016/j.virol.2012.06.012

Hemmer, C., Djennane, S., Ackerer, L., Hleibieh, K., Marmonier, A., Gersch, S., Garcia, S., Vigne, E., Komar, V., Perrin, M., Gertz, C., Belval, L., Berthold, F., Monsion, B., Schmitt-Keichinger, C.,

Lemaire, O., Lorber, B., Gutiérrez, C., Muyldermans, S., Demangeat, G., Ritzenthaler, C., 2018. Nanobody-mediated resistance to Grapevine fanleaf virus in plants. Plant Biotechnol. J. 16, 660–671. https://doi.org/10.1111/pbi.12819

Hu, G., Batool, Z., Cai, Z., Liu, Y., Ma, M., Sheng, L., Jin, Y., 2021. Production of self-assembling acylated ovalbumin nanogels as stable delivery vehicles for curcumin. Food Chem. 355, 129635. https://doi.org/10.1016/j.foodchem.2021.129635

Huang, J.C., Zhong, Y.J., Liu, J., Sandmann, G., Chen, F., 2013. Metabolic engineering of tomato for high-yield production of astaxanthin. Metab. Eng. 17, 59–67. https://doi.org/10.1016/j.ymben.2013.02.005

Hwang, H.-H., Yu, M., Lai, E.-M., 2017. Agrobacterium -Mediated Plant Transformation: Biology and Applications . Arab. B. 15, e0186. https://doi.org/10.1199/tab.0186

Islam, B. ul, Suhail, M., Khan, M.K., Zughaibi, T.A., Alserihi, R.F., Zaidi, S.K., Tabrez, S., 2021. Polyphenols as anticancer agents: Toxicological concern to healthy cells. Phyther. Res. 35, 6063–6079. https://doi.org/10.1002/ptr.7216

Jones, R.A.C., 2021. Global plant virus disease pandemics and epidemics. Plants 10, 1–41. https://doi.org/10.3390/plants10020233

Jones, R.A.C., Naidu, R.A., 2019. Global Dimensions of Plant Virus Diseases: Current Status and Future Perspectives. Annu. Rev. Virol. 6, 387–409. https://doi.org/10.1146/annurev-virology-092818-015606

Jose, S.B., Wu, C.H., Kamoun, S., 2019. Overcoming plant blindness in science, education, and society. Plants People Planet 1, 169–172. https://doi.org/10.1002/ppp3.51

Jovčevska, I., Muyldermans, S., 2020. The Therapeutic Potential of Nanobodies. BioDrugs 34, 11–26. https://doi.org/10.1007/s40259-019-00392-z

Kan, E., Katsuyama, Y., Maruyama, J.I., Tamano, K., Koyama, Y., Ohnishi, Y., 2019. Production of the plant polyketide curcumin in Aspergillus oryzae: Strengthening malonyl-CoA supply for yield improvement. Biosci. Biotechnol. Biochem. 83, 1372–1381. https://doi.org/10.1080/09168451.2019.1606699

Kang, L., Park, S.C., Ji, C.Y., Kim, H.S., Lee, H.S., Kwak, S.S., 2017. Metabolic engineering of carotenoids in transgenic sweetpotato. Breed. Sci. 67, 27–34. https://doi.org/10.1270/jsbbs.16118

Katsuyama, Y., Kita, T., Funa, N., Horinouchi, S., 2009. Curcuminoid biosynthesis by two type III polyketide synthases in the herb Curcuma longa. J. Biol. Chem. 284, 11160–11170. https://doi.org/10.1074/jbc.M900070200

Kaur, Navneet, Alok, A., Shivani, Kumar, P., Kaur, Navjot, Awasthi, P., Chaturvedi, S., Pandey, P., Pandey, A., Pandey, A.K., Tiwari, S., 2020. CRISPR/Cas9 directed editing of lycopene epsilon-cyclase modulates metabolic flux for β-carotene biosynthesis in banana fruit. Metab. Eng. 59, 76–86. https://doi.org/10.1016/j.ymben.2020.01.008

Kelloniemi, J., Mäkinen, K., Valkonen, J.P.T., 2008. Three heterologous proteins simultaneously expressed from a chimeric potyvirus: Infectivity, stability and the correlation of genome and virion lengths. Virus Res. 135, 282–291. https://doi.org/10.1016/j.virusres.2008.04.006

Khakhar, A., Voytas, D.F., 2021. RNA Viral Vectors for Accelerating Plant Synthetic Biology. Front. Plant Sci. 12. https://doi.org/10.3389/fpls.2021.668580

Kim, D., Lee, Y., Dreher, T.W., Cho, T.J., 2018. Empty Turnip yellow mosaic virus capsids as delivery vehicles to mammalian cells. Virus Res. 252, 13–21. https://doi.org/10.1016/j.virusres.2018.05.004

Kim, J.H., Lee, S.R., Li, L.H., Park, H.J., Park, J.H., Lee, K.Y., Kim, M.K., Shin, B.A., Choi, S.Y., 2011. High cleavage efficiency of a 2A peptide derived from porcine teschovirus-1 in human cell lines, zebrafish and mice. PLoS One 6, 1–8. https://doi.org/10.1371/journal.pone.0018556

Kim, S.E., Lee, C.J., Park, S.U., Lim, Y.H., Park, W.S., Kim, H.J., Ahn, M.J., Kwak, S.S., Kim, H.S., 2021. Overexpression of the golden snp-carrying orange gene enhances carotenoid accumulation and heat stress tolerance in sweetpotato plants. Antioxidants 10, 1–14. https://doi.org/10.3390/antiox10010051

Koenig, P.A., Das, H., Liu, H., Kümmerer, B.M., Gohr, F.N., Jenster, L.M., Schiffelers, L.D.J., Tesfamariam, Y.M., Uchima, M., Wuerth, J.D., Gatterdam, K., Ruetalo, N., Christensen, M.H., Fandrey, C.I., Normann, S., Tödtmann, J.M.P., Pritzl, S., Hanke, L., Boos, J., Yuan, M., Zhu, X., Schmid-Burgk, J.L., Kato, H., Schindler, M., Wilson, I.A., Geyer, M., Ludwig, K.U., Hällberg, B.M., Wu, N.C., Schmidt, F.I., 2021. Structure-guided multivalent nanobodies block SARS-CoV-2 infection and suppress mutational escape. Science (80-.). 371. https://doi.org/10.1126/science.abe6230

Kumar, K., Gambhir, G., Dass, A., Tripathi, A.K., Singh, A., Jha, A.K., Yadava, P., Choudhary, M., Rakshit, S., 2020. Genetically modified crops: current status and future prospects. Planta 251, 1–27. https://doi.org/10.1007/s00425-020-03372-8

Lagarde, D., Beuf, L., Vermaas, W., 2000. Increased production of zeaxanthin and other pigments by application of genetic engineering techniques to Synechocystis sp. strain PCC 6803. Appl. Environ. Microbiol. 66, 64–72. https://doi.org/10.1128/AEM.66.1.64-72.2000

Le, D.H.T., Commandeur, U., Steinmetz, N.F., 2019a. Presentation and delivery of tumor necrosis factor-related apoptosis-inducing ligand via elongated plant viral nanoparticle enhances antitumor efficacy. ACS Nano 13, 2501–2510. https://doi.org/10.1021/acsnano.8b09462

Le, D.H.T., Méndez-López, E., Wang, C., Commandeur, U., Aranda, M.A., Steinmetz, N.F., 2019b. Biodistribution of Filamentous Plant Virus Nanoparticles: Pepino Mosaic Virus versus Potato Virus X. Biomacromolecules 20, 469–477. https://doi.org/10.1021/acs.biomac.8b01365

Lee, K.L., Murray, A.A., Le, D.H.T., Sheen, M.R., Shukla, S., Commandeur, U., Fiering, S., Steinmetz, N.F., 2017. Combination of Plant Virus Nanoparticle-Based in Situ Vaccination with Chemotherapy Potentiates Antitumor Response. Nano Lett. 17, 4019–4028. https://doi.org/10.1021/acs.nanolett.7b00107

Lefeuvre, P., Martin, D.P., Elena, S.F., Shepherd, D.N., Roumagnac, P., Varsani, A., 2019. Evolution and ecology of plant viruses. Nat. Rev. Microbiol. 17, 632–644. https://doi.org/10.1038/s41579-019-0232-3

Li, C., Ji, J., Wang, G., Li, Z., Wang, Y., Fan, Y., 2020. Over-Expression of LcPDS, LcZDS, and LcCRTISO, Genes From Wolfberry for Carotenoid Biosynthesis, Enhanced Carotenoid Accumulation, and Salt Tolerance in Tobacco. Front. Plant Sci. 11, 1–12. https://doi.org/10.3389/fpls.2020.00119

Li, X.H., Carrington, J.C., 1995. Complementation of tobacco etch potyvirus mutants by active RNA polymerase expressed in transgenic cells. Proc. Natl. Acad. Sci. U. S. A. 92, 457–461. https://doi.org/10.1073/pnas.92.2.457

Lico, C., Benvenuto, E., Baschieri, S., 2015. The two-faced potato virus X: From plant pathogen to smart nanoparticle. Front. Plant Sci. 6, 1–8. https://doi.org/10.3389/fpls.2015.01009

Lindbo, J.A., 2007. TRBO: A high-efficiency tobacco mosaic virus RNA-based overexpression vector. Plant Physiol. 145, 1232–1240. https://doi.org/10.1104/pp.107.106377

Liu, X., Li, S., Yang, W., Mu, B., Jiao, Y., Zhou, X., Zhang, C., Fan, Y., Chen, R., 2018. Synthesis of seed-specific bidirectional promoters for metabolic engineering of anthocyanin-rich maize. Plant Cell Physiol. 59, 1942–1955. https://doi.org/10.1093/pcp/pcy110

Liu, X., Ma, X., Wang, H., Li, S., Yang, W., Nugroho, R.D., Luo, L., Zhou, X., Tang, C., Fan, Y., Zhao, Q., Zhang, J., Chen, R., 2021. Metabolic engineering of astaxanthin-rich maize and its use in the production of biofortified eggs. Plant Biotechnol. J. 19, 1812–1823. https://doi.org/10.1111/pbi.13593

Llorente, B., Torres-Montilla, S., Morelli, L., Florez-Sarasa, I., Matus, J.T., Ezquerro, M., D'Andrea, L., Houhou, F., Majer, E., Picó, B., Cebolla, J., Troncoso, A., Fernie, A.R., Daròs, J.A., Rodriguez-Concepcion, M., 2020. Synthetic conversion of leaf chloroplasts into carotenoid-rich plastids reveals mechanistic basis of natural chromoplast development. Proc. Natl. Acad. Sci. U. S. A. 117, 21796–21803. https://doi.org/10.1073/pnas.2004405117

Lu, R.M., Hwang, Y.C., Liu, I.J., Lee, C.C., Tsai, H.Z., Li, H.J., Wu, H.C., 2020. Development of therapeutic antibodies for the treatment of diseases. J. Biomed. Sci. 27, 1–30. https://doi.org/10.1186/s12929-019-0592-z

REFERENCES

Ma, J.K.C., Drake, P.M.W., Christou, P., 2003. The production of recombinant pharmaceutical proteins in plants. Nat. Rev. Genet. 4, 794–805. https://doi.org/10.1038/nrg1177

Ma, X., Zhang, X., Liu, H., Li, Z., 2020. Highly efficient DNA-free plant genome editing using virally delivered CRISPR–Cas9. Nat. Plants 6, 773–779. https://doi.org/10.1038/s41477-020-0704-5

Majer, E., Llorente, B., Rodríguez-Concepción, M., Daròs, J.A., 2017. Rewiring carotenoid biosynthesis in plants using a viral vector. Sci. Rep. 7, 1–10. https://doi.org/10.1038/srep41645

Majer, E., Navarro, J.A., Daròs, J.A., 2015. A potyvirus vector efficiently targets recombinant proteins to chloroplasts, mitochondria and nuclei in plant cells when expressed at the amino terminus of the polyprotein. Biotechnol. J. 10, 1792–1802. https://doi.org/10.1002/biot.201500042

Mäkinen, K., 2020. Plant susceptibility genes as a source for potyvirus resistance. Ann. Appl. Biol. 176, 122–129. https://doi.org/10.1111/aab.12562

Mandal, S., 2016. Curcumin, a Promising Anti-Cancer Therapeutic: It'S Bioactivity and Development of Drug Delivery Vehicles. Int. J. Drug Res. Tech. Int. J. Drug Res. Technol. 6, 43–57. https://doi.org/10.1016/j.jconrel.2015.04.025

Mann, V., Harker, M., Pecker, I., Hirschberg, J., 2000. Metabolic engineering of astaxanthin 18.

Mardanova, E.S., Blokhina, E.A., Tsybalova, L.M., Peyret, H., Lomonossoff, G.P., Ravin, N. V., 2017. Efficient transient expression of recombinant proteins in plants by the novel pEff vector based on the genome of potato virus X. Front. Plant Sci. 8, 1–8. https://doi.org/10.3389/fpls.2017.00247

Margolin, E.A., Strasser, R., Chapman, R., Williamson, A.L., Rybicki, E.P., Meyers, A.E., 2020. Engineering the Plant Secretory Pathway for the Production of Next-Generation Pharmaceuticals. Trends Biotechnol. 38, 1034–1044. https://doi.org/10.1016/j.tibtech.2020.03.004

Marillonnet, S., Giritch, A., Gils, M., Kandzia, R., Klimyuk, V., Gleba, Y., 2004. In planta engineering of viral RNA replicons: Efficient assembly by recombination of DNA modules delivered by Agrobacterium. May 101, 6852–6857.

Marsian, J., Lomonossoff, G.P., 2016. Molecular pharming-VLPs made in plants. Curr. Opin. Biotechnol. 37, 201–206. https://doi.org/10.1016/j.copbio.2015.12.007

Martí, M., Diretto, G., Aragonés, V., Frusciante, S., Ahrazem, O., Gómez-Gómez, L., Daròs, J.A., 2020. Efficient production of saffron crocins and picrocrocin in Nicotiana benthamiana using a virus-driven system. Metab. Eng. 61, 238–250. https://doi.org/10.1016/j.ymben.2020.06.009

Martin, C., Li, J., 2017. Medicine is not health care, food is health care: plant metabolic engineering, diet and human health. New Phytol. 216, 699–719. https://doi.org/10.1111/nph.14730

McGarry, R.C., Klocko, A.L., Pang, M., Strauss, S.H., Ayre, B.G., 2017. Virus-induced flowering: An application of reproductive biology to benefit plant research and breeding1[OPEN]. Plant Physiol. 173, 47–55. https://doi.org/10.1104/pp.16.01336

Mohammadinejad, R., Shavandi, A., Raie, D.S., Sangeetha, J., Soleimani, M., Shokrian Hajibehzad, S., Thangadurai, D., Hospet, R., Popoola, J.O., Arzani, A., Gómez-Lim, M.A., Iravani, S., Varma, R.S., 2019. Plant molecular farming: Production of metallic nanoparticles and therapeutic proteins using green factories. Green Chem. 21, 1845–1865. https://doi.org/10.1039/c9gc00335e

Molina-Hidalgo, F.J., Vazquez-Vilar, M., D'Andrea, L., Demurtas, O.C., Fraser, P., Giuliano, G., Bock, R., Orzáez, D., Goossens, A., 2021. Engineering Metabolism in Nicotiana Species: A Promising Future. Trends Biotechnol. 39, 901–913. https://doi.org/10.1016/j.tibtech.2020.11.012

Mortimer, C.L., Dugdale, B., Dale, J.L., 2015. Updates in inducible transgene expression using viral vectors: From transient to stable expression. Curr. Opin. Biotechnol. 32, 85–92. https://doi.org/10.1016/j.copbio.2014.11.009

Muyldermans, S., 2021. Applications of Nanobodies. Annu. Rev. Anim. Biosci. 9, 401–421. https://doi.org/10.1146/annurev-animal-021419-083831

Nogueira, M., Enfissi, E.M.A., Welsch, R., Beyer, P., Zurbriggen, M.D., Fraser, P.D., 2019. Construction of a fusion enzyme for astaxanthin formation and its characterisation in microbial and plant hosts: A new tool for engineering ketocarotenoids. Metab. Eng. 52, 243–252. https://doi.org/10.1016/j.ymben.2018.12.006

Nowicka, B., Trela-Makowej, A., Latowski, D., Strzalka, K., Szymańska, R., 2021. Antioxidant and signaling role of plastid-derived isoprenoid quinones and chromanols. Int. J. Mol. Sci. 22, 1–25. https://doi.org/10.3390/ijms22062950

Oliveira, S., Heukers, R., Sornkom, J., Kok, R.J., Van Bergen En Henegouwen, P.M.P., 2013. Targeting tumors with nanobodies for cancer imaging and therapy. J. Control. Release 172, 607–617. https://doi.org/10.1016/j.jconrel.2013.08.298

Ortega-Rivera, O.A., Shukla, S., Shin, M.D., Chen, A., Beiss, V., Moreno-Gonzalez, M.A., Zheng, Y., Clark, A.E., Carlin, A.F., Pokorski, J.K., Steinmetz, N.F., 2021. Cowpea Mosaic Virus Nanoparticle Vaccine Candidates Displaying Peptide Epitopes Can Neutralize the Severe Acute Respiratory Syndrome Coronavirus. ACS Infect. Dis. 7, 3096–3110. https://doi.org/10.1021/acsinfecdis.1c00410

Osorio, C.E., 2019. The Role of Orange Gene in Carotenoid Accumulation: Manipulating Chromoplasts Toward a Colored Future. Front. Plant Sci. 10. https://doi.org/10.3389/fpls.2019.01235

Otero-Muras, I., Carbonell, P., 2021. Automated engineering of synthetic metabolic pathways for efficient biomanufacturing. Metab. Eng. 63, 61–80. https://doi.org/10.1016/j.ymben.2020.11.012

Paine, J.A., Shipton, C.A., Chaggar, S., Howells, R.M., Kennedy, M.J., Vernon, G., Wright, S.Y., Hinchliffe, E., Adams, J.L., Silverstone, A.L., Drake, R., 2005. Improving the nutritional value of Golden Rice through increased pro-vitamin A content. Nat. Biotechnol. 23, 482–487. https://doi.org/10.1038/nbt1082

Pandey, K.B., Rizvi, S.I., 2009. Plant polyphenols as dietary antioxidants in human health and disease. Oxid. Med. Cell. Longev. 2, 270–278. https://doi.org/10.4161/oxim.2.5.9498

Pasin, F., Menzel, W., Daròs, J.A., 2019. Harnessed viruses in the age of metagenomics and synthetic biology: an update on infectious clone assembly and biotechnologies of plant viruses. Plant Biotechnol. J. 17, 1010–1026. https://doi.org/10.1111/pbi.13084

Peyret, H., Groppelli, E., Clark, D., Eckersley, N., Planche, T., Ma, J., Lomonossoff, G.P., 2022. Production and use of encapsidated RNA mimics as positive control reagents for SARS-CoV-2 RT-qPCR diagnostics. J. Virol. Methods 300, 114372. https://doi.org/10.1016/j.jviromet.2021.114372

Peyret, H., Lomonossoff, G.P., 2015. When plant virology met Agrobacterium: The rise of the deconstructed clones. Plant Biotechnol. J. 13, 1121–1135. https://doi.org/10.1111/pbi.12412

Pitek, A.S., Jameson, S.A., Veliz, F.A., Shukla, S., Steinmetz, N.F., 2016. Serum albumin “camouflage” of plant virus based nanoparticles prevents their antibody recognition and enhances pharmacokinetics. Biomaterials 89, 89–97. https://doi.org/10.1016/j.biomaterials.2016.02.032

Pitek, A.S., Park, J., Wang, Y., Gao, H., Hu, H., Simon, D.I., Steinmetz, N.F., 2018. Delivery of thrombolytic therapy using rod-shaped plant viral nanoparticles decreases the risk of hemorrhage. Nanoscale 10, 16547–16555. https://doi.org/10.1039/c8nr02861c

Pogue, G.P., Lindbo, J.A., Garger, S.J., Fitzmaurice, W.P., 2002. Making an ally from an enemy: Plant virology and the new agriculture. Annu. Rev. Phytopathol. 40, 45–74. https://doi.org/10.1146/annurev.phyto.40.021102.150133

Polturak, G., Grossman, N., Vela-Corcia, D., Dong, Y., Nudel, A., Pliner, M., Levy, M., Rogachev, I., Aharoni, A., 2017. Engineered gray mold resistance, antioxidant capacity, and pigmentation in betalain-producing crops and ornamentals. Proc. Natl. Acad. Sci. U. S. A. 114, 9062–9067. https://doi.org/10.1073/pnas.1707176114

Prasad, S., Gupta, S.C., Tyagi, A.K., Aggarwal, B.B., 2014. Curcumin, a component of golden spice: From bedside to bench and back. Biotechnol. Adv. 32, 1053–1064. https://doi.org/10.1016/j.biotechadv.2014.04.004

Rashidian, M., Ploegh, H., 2020. Nanobodies as non-invasive imaging tools. Immuno-Oncology Technol. 7, 2–14. https://doi.org/10.1016/j.iotech.2020.07.001

Revers, F., García, J.A., 2015. Molecular biology of potyviruses. Adv. Virus Res. 92, 101–199. https://doi.org/10.1016/bs.aivir.2014.11.006

Röder, J., Dickmeis, C., Fischer, R., Commandeur, U., 2018. Systemic Infection of Nicotiana benthamiana with Potato virus X Nanoparticles Presenting a Fluorescent iLOV Polypeptide Fused Directly to the

Coat Protein. Biomed Res. Int. 2018. https://doi.org/10.1155/2018/9328671

Rodrigues, J.L., Gomes, D., Rodrigues, L.R., 2020. A Combinatorial Approach to Optimize the Production of Curcuminoids From Tyrosine in Escherichia coli. Front. Bioeng. Biotechnol. 8, 1–15. https://doi.org/10.3389/fbioe.2020.00059

Rodrigues, J.L., Prather, K.L.J., Kluskens, L.D., Rodrigues, L.R., 2015. Heterologous Production of Curcuminoids. Microbiol. Mol. Biol. Rev. 79, 39–60. https://doi.org/10.1128/mmbr.00031-14

Römer, S., Lübeck, J., Kauder, F., Steiger, S., Adomat, C., Sandmann, G., 2002. Genetic engineering of a zeaxanthin-rich potato by antisense inactivation and co-suppression of carotenoid epoxidation. Metab. Eng. 4, 263–272. https://doi.org/10.1006/mben.2002.0234

Roossinck, M.J., 2012. Plant virus metagenomics: Biodiversity and ecology. Annu. Rev. Genet. 46, 359–369. https://doi.org/10.1146/annurev-genet-110711-155600

Roossinck, M.J., 2008. Mutant Clouds and Bottleneck Events in Plant Virus Evolution, Second Edi. ed, Origin and Evolution of Viruses. Elsevier Ltd. https://doi.org/10.1016/B978-0-12-374153-0.00012-6

Roossinck, M.J., Martin, D.P., Roumagnac, P., 2015. Plant virus metagenomics: Advances in virus discovery. Phytopathology 105, 716–727. https://doi.org/10.1094/PHYTO-12-14-0356-RVW

Rybicki, E.P., 2020. Plant molecular farming of virus-like nanoparticles as vaccines and reagents. Wiley Interdiscip. Rev. Nanomedicine Nanobiotechnology 12, 1–22. https://doi.org/10.1002/wnan.1587

Sack, M., Hofbauer, A., Fischer, R., Stoger, E., 2015. The increasing value of plant-made proteins. Curr. Opin. Biotechnol. 32, 163–170. https://doi.org/10.1016/j.copbio.2014.12.008

Sainsbury, F., 2020. Innovation in plant-based transient protein expression for infectious disease prevention and preparedness. Curr. Opin. Biotechnol. 61, 110–115. https://doi.org/10.1016/j.copbio.2019.11.002

Sainsbury, F., Cañizares, M.C., Lomonossoff, G.P., 2010. Cowpea mosaic virus: The plant virus-based biotechnology workhorse. Annu. Rev. Phytopathol. 48, 437–455. https://doi.org/10.1146/annurev-phyto-073009-114242

Sainsbury, F., Lomonossoff, G.P., 2014. Transient expressions of synthetic biology in plants. Curr. Opin. Plant Biol. 19, 1–7. https://doi.org/10.1016/j.pbi.2014.02.003

Sainsbury, F., Saxena, P., Geisler, K., Osbourn, A., Lomonossoff, G.P., 2012. Using a virus-derived system to manipulate plant natural product biosynthetic pathways, 1st ed, Methods in Enzymology. Elsevier Inc. https://doi.org/10.1016/B978-0-12-404634-4.00009-7

Salehi, B., Stojanović-Radić, Z., Matejić, J., Sharifi-Rad, M., Anil Kumar, N. V., Martins, N., Sharifi-Rad, J., 2019. The therapeutic potential of curcumin: A review of clinical trials. Eur. J. Med. Chem. 163, 527–545. https://doi.org/10.1016/j.ejmech.2018.12.016

Salehiabar, M., Nosrati, H., Javani, E., Aliakbarzadeh, F., Kheiri Manjili, H., Davaran, S., Danafar, H., 2018. Production of biological nanoparticles from bovine serum albumin as controlled release carrier for curcumin delivery. Int. J. Biol. Macromol. 115, 83–89. https://doi.org/10.1016/j.ijbiomac.2018.04.043

Salema, V., Fernández, L.Á., 2017. Escherichia coli surface display for the selection of nanobodies. Microb. Biotechnol. 10, 1468–1484. https://doi.org/10.1111/1751-7915.12819

Salema, V., Mañas, C., Cerdán, L., Piñero-Lambea, C., Marín, E., Roovers, R.C., Van Bergen en Henegouwen, P.M.P., Fernández, L.Á., 2016. High affinity nanobodies against human epidermal growth factor receptor selected on cells by E. coli display. MAbs 8, 1286–1301. https://doi.org/10.1080/19420862.2016.1216742

Salvador, J.P., Vilaplana, L., Marco, M.P., 2019. Nanobody: outstanding features for diagnostic and therapeutic applications. Anal. Bioanal. Chem. 411, 1703–1713. https://doi.org/10.1007/s00216-019-01633-4

Sanfaçon, H., 2017. Grand challenge in plant virology: Understanding the impact of plant viruses in model plants, in agricultural crops, and in complex ecosystems. Front. Microbiol. 8, 2013–2016. https://doi.org/10.3389/fmicb.2017.00860

Saxena, P., Hsieh, Y.C., Alvarado, V.Y., Sainsbury, F., Saunders, K., Lomonossoff, G.P., Scholthof, H.B., 2011. Improved foreign gene expression in plants using a virus-encoded suppressor of rna silencing modified to be developmentally harmless. Plant Biotechnol. J. 9, 703–712. https://doi.org/10.1111/j.1467-7652.2010.00574.x

Schillberg, S., Fischer, R., Emans, N., 2003. "Molecular farming" of antibodies in plants. Naturwissenschaften 90, 145–155. https://doi.org/10.1007/s00114-002-0400-5

Scholthof, K.B.G., Adkins, S., Czosnek, H., Palukaitis, P., Jacquot, E., Hohn, T., Hohn, B., Saunders, K., Candresse, T., Ahlquist, P., Hemenway, C., Foster, G.D., 2011. Top 10 plant viruses in molecular plant pathology. Mol. Plant Pathol. 12, 938–954. https://doi.org/10.1111/j.1364-3703.2011.00752.x

Shanmugaraj, B., Bulaon, C.J.I., Phoolcharoen, W., 2020. Plant molecular farming: A viable platform for recombinant biopharmaceutical production. Plants 9, 1–19. https://doi.org/10.3390/plants9070842

Sharifi, J., Khirehgesh, M.R., Safari, F., Akbari, B., 2021. EGFR and anti-EGFR nanobodies: review and update. J. Drug Target. 29, 387–402. https://doi.org/10.1080/1061186X.2020.1853756

Shukla, S., DiFranco, N.A., Wen, A.M., Commandeur, U., Steinmetz, N.F., 2015. To Target or Not to Target: Active vs. Passive Tumor Homing of Filamentous Nanoparticles Based on Potato virus X. Cell. Mol. Bioeng. 8, 433–444. https://doi.org/10.1007/s12195-015-0388-5

Shukla, S., Hu, H., Cai, H., Chan, S.K., Boone, C.E., Beiss, V., Chariou, P.L., Steinmetz, N.F., 2020a. Plant Viruses and Bacteriophage-Based Reagents for Diagnosis and Therapy. Annu. Rev. Virol. 7, 559–587. https://doi.org/10.1146/annurev-virology-010720-052252

Shukla, S., Roe, A.J., Liu, R., Veliz, F.A., Commandeur, U., Wald, D.N., Steinmetz, N.F., 2020b. Affinity of plant viral nanoparticle potato virus X (PVX) towards malignant B cells enables cancer drug delivery. Biomater. Sci. 8, 3935–3943. https://doi.org/10.1039/d0bm00683a

Stanić, Z., 2017. Curcumin, a Compound from Natural Sources, a True Scientific Challenge – A Review. Plant Foods Hum. Nutr. 72, 1–12. https://doi.org/10.1007/s11130-016-0590-1

Steele, J.F.C., Peyret, H., Saunders, K., Castells-Graells, R., Marsian, J., Meshcheriakova, Y., Lomonossoff, G.P., 2017. Synthetic plant virology for nanobiotechnology and nanomedicine. Wiley Interdiscip. Rev. Nanomedicine Nanobiotechnology 9, 1–18. https://doi.org/10.1002/wnan.1447

Steinmetz, N.F., Cho, C.-F., Ablack, A., Lewis, J.D., Manchester, M., 2011. Cowpea mosaic virus nanoparticles target surface vimentin on cancer cells. Nanomedicine 6, 351–364. https://doi.org/10.2217/nnm.10.136.Cowpea

Sun, D., Sang, Z., Kim, Y.J., Xiang, Y., Cohen, T., Belford, A.K., Huet, A., Conway, J.F., Sun, J., Taylor, D.J., Schneidman-Duhovny, D., Zhang, C., Huang, W., Shi, Y., 2021. Potent neutralizing nanobodies resist convergent circulating variants of SARS-CoV-2 by targeting diverse and conserved epitopes. Nat. Commun. 12, 1–14. https://doi.org/10.1038/s41467-021-24963-3

Those, S., Rnas, B., 2012. Potyviridae. Virus Taxon. 1069–1089. https://doi.org/10.1016/b978-0-12-384684-6.00093-8

Thuenemann, E.C., Le, D.H.T., Lomonossoff, G.P., Steinmetz, N.F., 2021. Bluetongue Virus Particles as Nanoreactors for Enzyme Delivery and Cancer Therapy. Mol. Pharm. 18, 1150–1156. https://doi.org/10.1021/acs.molpharmaceut.0c01053

Tian, Y.S., Wang, B., Peng, R.H., Xu, J., Li, T., Fu, X.Y., Xiong, A.S., Gao, J.J., Yao, Q.H., 2019. Enhancing carotenoid biosynthesis in rice endosperm by metabolic engineering. Plant Biotechnol. J. 17, 849–851. https://doi.org/10.1111/pbi.13059

Topp, E., Irwin, R., McAllister, T., Lessard, M., Joensuu, J.J., Kolotilin, I., Conrad, U., Stöger, E., Mor, T., Warzecha, H., Hall, J.C., McLean, M.D., Cox, E., Devriendt, B., Potter, A., Depicker, A., Virdi, V., Holbrook, L., Doshi, K., Dussault, M., Friendship, R., Yarosh, O., Yoo, H.S., MacDonald, J., Menassa, R., 2016. The case for plant-made veterinary immunotherapeutics. Biotechnol. Adv. 34, 597–604. https://doi.org/10.1016/j.biotechadv.2016.02.007

Torres-Montilla, S., Rodriguez-Concepcion, M., 2021. Making extra room for carotenoids in plant cells: New opportunities for biofortification. Prog. Lipid Res. 84, 101128. https://doi.org/10.1016/j.plipres.2021.101128

REFERENCES

Tschofen, M., Knopp, D., Hood, E., Stöger, E., 2016. Plant Molecular Farming: Much More than Medicines. Annu. Rev. Anal. Chem. 9, 271–294. https://doi.org/10.1146/annurev-anchem-071015-041706

Tsekoa, T.L., Singh, A.A., Buthelezi, S.G., 2020. Molecular farming for therapies and vaccines in Africa. Curr. Opin. Biotechnol. 61, 89–95. https://doi.org/10.1016/j.copbio.2019.11.005

Uhde-holzem, K., Mcburney, M., Tiu, B.D.B., Advincula, R.C., Fischer, R., Commandeur, U., Steinmetz, N.F., 2016. Production of Immunoabsorbent Nanoparticles by Displaying Single-Domain Protein A on Potato Virus X a 231–241. https://doi.org/10.1002/mabi.201500280

Uhde-Holzem, K., Schlösser, V., Viazov, S., Fischer, R., Commandeur, U., 2010. Immunogenic properties of chimeric potato virus X particles displaying the hepatitis C virus hypervariable region I peptide R9. J. Virol. Methods 166, 12–20. https://doi.org/10.1016/j.jviromet.2010.01.017

Uranga, M., Aragonés, V., Selma, S., Vázquez-Vilar, M., Orzáez, D., Daròs, J.A., 2021a. Efficient Cas9 multiplex editing using unspaced sgRNA arrays engineering in a Potato virus X vector. Plant J. 106, 555–565. https://doi.org/10.1111/tpj.15164

Uranga, M., Vazquez-Vilar, M., Orzáez, Di., Daròs, J.A., 2021b. CRISPR-Cas12a Genome Editing at the Whole-Plant Level Using Two Compatible RNA Virus Vectors. Cris. J. 4, 761–769. https://doi.org/10.1089/crispr.2021.0049

Venkataraman, S., Hefferon, K., 2021. Application of plant viruses in biotechnology, medicine, and human health. Viruses 13. https://doi.org/10.3390/v13091697

Walker, P.J., Siddell, S.G., Lefkowitz, E.J., Mushegian, A.R., Adriaenssens, E.M., Alfenas-Zerbini, P., Davison, A.J., Dempsey, D.M., Dutilh, B.E., García, M.L., Harrach, B., Harrison, R.L., Hendrickson, R.C., Junglen, S., Knowles, N.J., Krupovic, M., Kuhn, J.H., Lambert, A.J., Łobocka, M., Nibert, M.L., Oksanen, H.M., Orton, R.J., Robertson, D.L., Rubino, L., Sabanadzovic, S., Simmonds, P., Smith, D.B., Suzuki, N., Van Dooerslaer, K., Vandamme, A.M., Varsani, A., Zerbini, F.M., 2021. Changes to virus taxonomy and to the International Code of Virus Classification and Nomenclature ratified by the International Committee on Taxonomy of Viruses (2021). Arch. Virol. 166, 2633–2648. https://doi.org/10.1007/s00705-021-05156-1

Wang, B., Kashkooli, A.B., Sallets, A., Ting, H.M., de Ruijter, N.C.A., Olofsson, L., Brodelius, P., Pottier, M., Boutry, M., Bouwmeester, H., van der Krol, A.R., 2016a. Transient production of artemisinin in Nicotiana benthamiana is boosted by a specific lipid transfer protein from A. annua. Metab. Eng. 38, 159–169. https://doi.org/10.1016/j.ymben.2016.07.004

Wang, M., Gao, S., Zeng, W., Yang, Y., Ma, J., Wang, Y., 2020. Plant Virology Delivers Diverse Toolsets for Biotechnology. Viruses 12, 1–16. https://doi.org/10.3390/v12111338

Wang, W., Yuan, J., Jiang, C., 2021. Applications of nanobodies in plant science and biotechnology. Plant Mol. Biol. 105, 43–53. https://doi.org/10.1007/s11103-020-01082-z

Wang, Y., Fan, Z., Shao, L., Kong, X., Hou, X., Tian, D., Sun, Y., Xiao, Y., Yu, L., 2016b. Nanobody-derived nanobiotechnology tool kits for diverse biomedical and biotechnology applications. Int. J. Nanomedicine 11, 3287–3303. https://doi.org/10.2147/IJN.S107194

Wen, A.M., Steinmetz, N.F., 2016. Design of virus-based nanomaterials for medicine, biotechnology, and energy. Chem. Soc. Rev. 45, 4074–4126. https://doi.org/10.1039/c5cs00287g

Wicki, A., Witzigmann, D., Balasubramanian, V., Huwyler, J., 2015. Nanomedicine in cancer therapy: Challenges, opportunities, and clinical applications. J. Control. Release 200, 138–157. https://doi.org/10.1016/j.jconrel.2014.12.030

Williams, L., Jurado, S., Llorente, F., Romualdo, A., González, S., Saconne, A., Bronchalo, I., Martínez-Cortes, M., Pérez-Gómez, B., Ponz, F., Jiménez-Clavero, M.Á., Lunello, P., 2021. The C-Terminal Half of SARS-CoV-2 Nucleocapsid Protein, Industrially Produced in Plants, Is Valid as Antigen in COVID-19 Serological Tests. Front. Plant Sci. 12, 1–10. https://doi.org/10.3389/fpls.2021.699665

Wylie, S.J., Adams, M., Chalam, C., Kreuze, J., López-Moya, J.J., Ohshima, K., Praveen, S., Rabenstein, F., Stenger, D., Wang, A., Zerbini, F.M., 2017. ICTV virus taxonomy profile: Potyviridae. J. Gen. Virol. 98, 352–354. https://doi.org/10.1099/jgv.0.000740

Xu, J., Dolan, M.C., Medrano, G., Cramer, C.L., Weathers, P.J., 2012. Green factory: Plants as bioproduction platforms for recombinant proteins. Biotechnol. Adv. 30, 1171–1184. https://doi.org/10.1016/j.biotechadv.2011.08.020

Yang, X., Li, Y., Wang, A., 2021. Research Advances in Potyviruses: From the Laboratory Bench to the Field. Annu. Rev. Phytopathol. 59, 1–29. https://doi.org/10.1146/annurev-phyto-020620-114550

Ye, X., Beyer, P., 2000. Engineering the provitamin A (β-carotene) biosynthetic pathway into (carotenoid-free) rice endosperm. Science (80-.). 287, 303–305. https://doi.org/10.1126/science.287.5451.303

Yildiz, I., Lee, K.L., Chen, K., Shukla, S., Steinmetz, N.F., 2013. Infusion of imaging and therapeutic molecules into the plant virus-based carrier cowpea mosaic virus: Cargo-loading and delivery. J. Control. Release 172, 568–578. https://doi.org/10.1016/j.jconrel.2013.04.023

Yixuan, L., Qaria, M.A., Sivasamy, S., Jianzhong, S., Daochen, Z., 2021. Curcumin production and bioavailability: A comprehensive review of curcumin extraction, synthesis, biotransformation and delivery systems. Ind. Crops Prod. 172, 114050. https://doi.org/10.1016/j.indcrop.2021.114050

Yusibov, V., Kushnir, N., Streatfield, S.J., 2016. Antibody Production in Plants and Green Algae. Annu. Rev. Plant Biol. 67, 669–701. https://doi.org/10.1146/annurev-arplant-043015-111812

Yuste-Calvo, C., González-Gamboa, I., Pacios, L.F., Sánchez, F., Ponz, F., 2019a. Structure-Based Multifunctionalization of Flexuous Elongated Viral Nanoparticles. ACS Omega 4, 5019–5028. https://doi.org/10.1021/acsomega.8b02760

Yuste-Calvo, C., López-Santalla, M., Zurita, L., Cruz-Fernández, C.F., Sánchez, F., Garín, M.I., Ponz, F., 2019b. Elongated flexuous plant virus-derived nanoparticles functionalized for autoantibody detection. Nanomaterials 9, 1–13. https://doi.org/10.3390/nano9101438

Zaidi, S.S. e. A., Mahas, A., Vanderschuren, H., Mahfouz, M.M., 2020. Engineering crops of the future: CRISPR approaches to develop climate-resilient and disease-resistant plants. Genome Biol. 21, 1–19. https://doi.org/10.1186/s13059-020-02204-y

Zhang, X.F., Zhang, S., Guo, Q., Sun, R., Wei, T., Qu, F., 2018a. A new mechanistic model for viral cross protection and superinfection exclusion. Front. Plant Sci. 9, 1–9. https://doi.org/10.3389/fpls.2018.00040

Zhang, Y., Butelli, E., Alseekh, S., Tohge, T., Rallapalli, G., Luo, J., Kawar, P.G., Hill, L., Santino, A., Fernie, A.R., Martin, C., 2015. Multi-level engineering facilitates the production of phenylpropanoid compounds in tomato. Nat. Commun. 6, 1–11. https://doi.org/10.1038/ncomms9635

Zhang, Y., Dong, Y., Zhou, J., Li, X., Wang, F., 2018b. Application of plant viruses as a biotemplate for nanomaterial fabrication. Molecules 23. https://doi.org/10.3390/molecules23092311

Zheng, J., Cheng, J., Zheng, S., Feng, Q., Xiao, X., 2018. Curcumin, a polyphenolic curcuminoid with its protective effects and molecular mechanisms in diabetes and diabetic cardiomyopathy. Front. Pharmacol. 9, 1–10. https://doi.org/10.3389/fphar.2018.00472

Zheng, X., Kuijer, H.N.J., Al-Babili, S., 2021. Carotenoid Biofortification of Crops in the CRISPR Era. Trends Biotechnol. 39, 857–860. https://doi.org/10.1016/j.tibtech.2020.12.003

Zhu, Q., Yu, S., Zeng, D., Liu, H., Wang, H., Yang, Z., Xie, X., Shen, R., Tan, J., Li, H., Zhao, X., Zhang, Q., Chen, Y., Guo, J., Chen, L., Liu, Y.G., 2017. Development of “Purple Endosperm Rice” by Engineering Anthocyanin Biosynthesis in the Endosperm with a High-Efficiency Transgene Stacking System. Mol. Plant 10, 918–929. https://doi.org/10.1016/j.molp.2017.05.008

Zia-ul-haq, M., 2021. Carotenoids: Structure and Function in the Human Body, Carotenoids: Structure and Function in the Human Body. https://doi.org/10.1007/978-3-030-46459-2

ACKNOWLEDGEMENTS

—

AGRADECIMIENTOS

ACKNOWLEDGEMENTS / AGRADECIMIENTOS

Este apartado personal de la tesis me permite hacer un pequeño homenaje a toda esa gente buena que tengo a mi alrededor, y con esta excusa maravillosa, simplemente comienzo. Pero tranquilidad, voy a ser breve, de verdad.

En primer lugar, quería agradecer a mi director de tesis, José Antonio, la ayuda que me ha brindado estos años, y como no, me quedo con esa forma de trabajar tan metódica. Al formar parte del IBMCP he podido disfrutar de experiencias buenísimas tanto a nivel laboral como personal, y me quedo con esto. También quiero agradecer a mi tutor Carmelo que siempre me haya ayudado con alegría a llevar los trámites de la UPV, así como las clases de docencia que tanto voy a echar de menos.

Bueno, este es el momento en el que pongo el gorrito de mamá pitufa y me pongo reflexiva. Para todos los que me conozcáis, además de haber descubierto mi amor por los audios, no os sorprenderá saber que unas líneas aquí se me quedan tremendamente cortas para agradecer a todo el mundo que quisiera como considero os merecéis. Con cada persona me viene nombrar muchísimos recuerdos buenos (sabéis que lo que más me gustaría es escribir otra introducción con todas esas anécdotas… pero me voy a contener, así es).

¿Por dónde empezar en el IBMCP? Hemos sido muchísimas personas viéndonos todos los días compartiendo penas y alegrías. Debo agradecer mi experiencia en el IBMCP a Beltrán, Tere, Vero, Miry, Fakhri, Anamarija, Samaneh, Lucio, María, Alessandra, Mireia, Javi, Fernando, Enrique, Arcadio, Marcelo y Thais. Me quedo con tantas cosas buenas: esos paseos a Siberia a por primers; esas jornadas de trasplantes codo con codo para acabar rápido; esos almuerzos en el tranvía; ese tráfico de recetas de otros países; esos días de musicote; esos días de lluvia y de chubasquero improvisado con bolsas de basura para la bici o esas escaleras ya nuestras. Y cómo no, esos memes de westerns fallidos; esas miradas de “nos tomamos algo dulce hoy, ¿verdad?”; esa canción del 7 de septiembre; por esa definición de Mami Carmen; ese compañerismo para compartir la fruta; la divulgación del 11F; esos días en los que parecía que Valencia fuera Venecia o esas excursiones como a la Albufera o a cenar como gente de bien. Hemos hecho que seamos como una gran familia.

También me gustaría destacar el amor que transmite Marisol, así como su ayuda en el confocal. Como no, debo mencionar mi parte favorita, ir al invernadero, donde Toni siempre estaba tan atento con su música alegre para que fuera todo más ameno. O esos cruces con nuestra vecina Carmen cuando me preguntaba si no tenía frío en invierno al ir en tirantes y la bata, esos intercambios de chocolate 99% con Alberto, o esas explicaciones sobre bioinformática de Marcos que daba gusto escuchar. Así es como debe ser trabajar en ciencia, tanto si te salen las cosas como si no, disfrutando lo que hacemos. Grazie mille per tutto a Gianfranco, Sarah, Maria, Olivia e Giuseppe per avermi accolto nell' ENEA. I wanted to thank also to George, Hadrien, Keith, Eva, Sachin, Yulia and Yae-Wan for the good times at the JIC (whisky included).

Otra parte fundamental en mi vida en Valencia han sido mis compañeras de piso, que se han convertido en mis amigas, Sofía, Alice, Marta y Laura. Por esas cenas en el chahipiso, las misiones y los vídeos para el canal, muchas gracias por todo, considero no podría haber tenido más suerte al conoceros y estar así de feliz. También gracias al último fichaje, Andrés, por esas largas charlas con todas en la replaceta. A mis amigas Alexandra y Lary por esos paseos a nuestro querido San Julián (Serra Grossa, lo más bonito de Alicante, viva Alicante) y las escapadas exprés que nos faltan por hacer. A Lola, que aunque estemos lejos, estamos siempre ahí, ya sea en la feria de navidad o con los caballos en Norwich. Al mejor mentor posible, Miguel, por esos consejos y esa calma que transmites. También agradezco a mi familia caudetana por todo lo bonito con ellos, incluidos como no, a Revuelo y Valiente. Y disculpadme si dejo a alguien en el tintero, en general gracias a todos los que aunque sea cruzando una sonrisa o un buenos días, habéis hecho que sea más bonito el día.

Finalmente quiero agradecer a mi familia por estar conmigo. A mi mami por momentos como cuando le explico curiosidades de ciencia y me escucha con tanta ilusión como cuando le explicaba sobre Descartes. A mi Tete Luis por abarcar más de lo que puede con ese instinto protector. A mi Tete Fran porque cuando hace falta aparece como el coche fantástico. Y a mi padre por momentos al lado de la lumbre y esos viajes para ver terreno.

Y acabo con el DNA es una molécula que siempre me ha gustado, incluso antes de entender bien qué era. Le doy muchos sentidos, pero la connotación que le voy a dar aquí es de flexibilidad, resiliencia… Os quiero a tod@s mucho. ¡A ser feliz!

“What we know is a drop,
what we don’t know is an ocean”

Isaac Newton

"Science and everyday life cannot
and should not be separated"

Rosalind Franklin

"Yo no quiero cuotas, no quiero que a las mujeres se nos dé nada por el hecho de ser mujeres.

Que se nos dé si lo valemos, pero que NO se nos quite por el hecho de serlo"

Margarita Salas

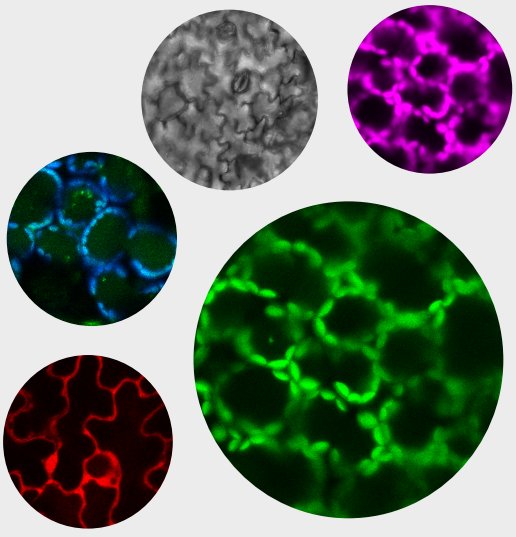

UNIVERSITAT
POLITÈCNICA
DE VALÈNCIA